

**Evaluation of *in vitro* and *in vivo* radioprotection and  
cytotoxic activities by novel selenium compounds**

*By*

**Prachi Verma**

**LIFE01201204009**

**BHABHA ATOMIC RESEARCH CENTRE, MUMBAI**

*A thesis submitted to the*

*Board of Studies in Life Sciences*

*In partial fulfillment of requirements for the Degree of*

**DOCTOR OF PHILOSOPHY**

*of*

**HOMI BHABHA NATIONAL INSTITUTE**

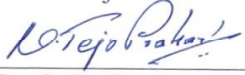
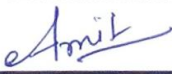


**October, 2017**

# Homi Bhabha National Institute

## Recommendations of the Viva Voce Committee

As members of the Viva Voce Committee, we certify that we have read the dissertation prepared by **Prachi Verma** entitled “**Evaluation of *in vitro* and *in vivo* radioprotection and cytotoxic activities by novel selenium compounds**” and recommend that it may be accepted as fulfilling the thesis requirement for the award of Degree of Doctor of Philosophy.

Chairman – Dr. P. S. Variyar	Date:16/02/2018
	
Convener – Dr. K. I. Priyadarsini	Date:16/02/2018
	
Examiner – Dr. N. Tejo Prakash	Date:16/02/2018
	
Member 1- Dr. S. K. Sandur	Date:16/02/2018
	
Member 2- Dr. M. Subramanian	Date:16/02/2018
	
Technical Advisor – Dr. Amit Kunwar	Date:16/02/2018
	

Final approval and acceptance of this thesis is contingent upon the candidate's submission of the final copies of the thesis to HBNI.

I/We hereby certify that I/we have read this thesis prepared under my/our direction and recommend that it may be accepted as fulfilling the thesis requirement.

**Date:** 16/02/2018

**Place:** BARC, Mumbai

  
(Guide)

## **STATEMENT BY AUTHOR**

This dissertation has been submitted in partial fulfillment of requirements for an advanced degree at Homi Bhabha National Institute (HBNI) and is deposited in the Library to be made available to borrowers under rules of the HBNI.

Brief quotations from this dissertation are allowable without special permission, provided that accurate acknowledgement of source is made. Requests for permission for extended quotation from or reproduction of this manuscript in whole or in part may be granted by the Competent Authority of HBNI when in his or her judgment the proposed use of the material is in the interests of scholarship. In all other instances, however, permission must be obtained from the author.

Prachi Verma

## **DECLARATION**

I, hereby declare that the investigation presented in the thesis has been carried out by me. The work is original and has not been submitted earlier as a whole or in part for a degree / diploma at this or any other Institution / University.

Prachi Verma

## List of Publications arising from the thesis

### Journal

1. Alkyl chain modulated cytotoxicity and antioxidant activity of bioinspired amphiphilic selenolanes

**Prachi Verma**, Amit Kunwar, Kenta Arai, Michio Iwaoka, K. Indira Priyadarsini  
*Toxicology Research*, **2016**, *5*, 434 - 445.

2. Dihydroxyselenolane (DHS) supplementation improves survival following whole body irradiation (WBI) by suppressing tissue-specific inflammatory responses

Amit Kunwar\*, **Prachi Verma\***, Michio Iwaoka, K. Indira Priyadarsini. (**\*Joint first authors**)

*Mutation Research*, **2016**, *807*, 33 – 46.

3. Mechanism of radioprotection by dihydroxy-1-selenolane (DHS): effect of fatty acid conjugation and role of glutathione peroxidase (GPx)

**Prachi Verma**, Amit Kunwar, Kenta Arai, Michio Iwaoka, K. Indira Priyadarsini  
*Biochimie*, **2018**, *144*, 122-133.

### Conferences

1. Dihydroxy Selenolane, a glutathione peroxidase mimic as a radioprotector and an anti-inflammatory agent

**Prachi Verma**, Amit Kunwar, Michio Iwaoka, K. Indira Priyadarsini.

23<sup>rd</sup> Annual Meeting of Society for Redox Biology and Medicine (SFRBM), San Francisco, 16 November 2016.

*Free Radical Biology and Medicine*, **2016**, *100*, S113.

2. Comparative cytotoxicity and antioxidant evaluation of biologically active fatty acid conjugates of water soluble selenolanes in cells

A. Kunwar, **Prachi Verma**, K. I. Priyadarsini, K. Arai, M. Iwaoka

Global Advances in Selenium Research from Theory to Application (eBook), Proceedings of the 4<sup>th</sup> International conference on selenium in the environment and human health 2015, Chapter 23, Pages: 49 - 50.

3. Radioprotection studies by small water-soluble, GPx active cyclic selenium compound

**Prachi Verma**, Amit Kunwar, M. Iwaoka, K. I. Priyadarsini

International Conference of Radiation Biology, New Delhi, 11 November 2014.

4. Dihydroxyselenolane (DHS) in radiation induced oxidative stress in Chinese Hamster Ovary Cells

**Prachi Verma**, Amit Kunwar, M. Iwaoka, K. I. Priyadarsini

National Research Scholars Meet in Life Sciences, Mumbai, 17 December 2015.

5. Radioprotective effect of dihydroxyselenolane (DHS) in cellular and mice model systems

**Prachi Verma**, Amit Kunwar, M. Iwaoka, K. I. Priyadarsini

SFRR-India, "International Conference on Translational Research in Ionizing Radiation, Free Radicals, Antioxidants and Functional Food", Kalyani, 7 January 2016.

6. Radioprotective effect of an organoselenium dihydroxy selenolane (DHS) in cellular model systems

**Prachi Verma**, Amit Kunwar, M. Iwaoka, K. I. Priyadarsini

SFRR-India "Basic and Applied Aspects of Health Management Using Radiation, Antioxidants and Nutraceuticals", Mumbai, 9 January, 2017.

7. Radioprotective activity of dihydroxyselenolane: Mechanism of action and role of glutathione peroxidase

**Prachi Verma**, Amit Kunwar, Kenta Arai, M. Iwaoka, K. I. Priyadarsini.

Symposium on Selenium Chemistry and Biology, Mumbai, India, 9 November, 2017.

**(ACS Best Poster Award)**

## **Others**

1. Effect of low-dose selenium supplementation on the genotoxicity, tissue injury and survival of mice exposed to acute whole body irradiation

**Prachi Verma**, Amit Kunwar, K. Indira Priyadarsini

*Biological Trace Element Research*, **2017**, *179*, 130 – 139.

2. Cellular evaluation of diselenonicotinamide (DSNA) as a radioprotector against cell death and DNA damage

Raghuraman\*, **Prachi Verma\***, A. Kunwar, P.P. Phadnis, V.K. Jain, K.I. Priyadarsini

**(\*Equal contribution)**

*Metallomics*, **2017**, *9*, 715 - 725.

Prachi Verma

*Dedicated*  
*to my loving*  
*parents*

## ACKNOWLEDGEMENT

*As I am closer to the completion of my PhD, I would like to thank several individuals for their constant support and contribution without which this thesis would not have been possible.*

*Firstly, I wish to express my deep sense of gratitude to my research guide Dr. K. Indira Priyadarsini, Head, Chemistry Division, Bhabha Atomic research Centre, for her motivating words, peerless guidance, valuable advice and continuous encouragement. I am truly privileged to work under her mentorship. I am thankful to her for critically reviewing my work and being a constant source of inspiration.*

*I am greatly indebted to my research supervisor Dr. Amit Kunwar. His scientific ideas, intellect, wisdom, practical approach and expert planning helped me a lot to carry out the research work and in bringing this thesis into good shape. His teachings will always help me to excel in my life. I am privileged to work with you sir.*

*I am thankful to Dr. P. D. Naik, Associate Director, Chemistry group and Head, RPC Division for providing all the necessary laboratory facilities and support during the tenure of my research work, I convey my special thanks to Bioscience group, Bhabha Atomic research Centre, Mumbai for providing chemicals and lab facility whenever required.*

*I would like to extend my gratitude to Dr. P. S. Variyar, Dr. S. K. Sandur, Dr. M. Subramanian and Dr. M. G. R. Rajan for critically reviewing my research work and providing valuable suggestions.*

*I extend my sincere thanks to Dr. M. Iwaoaka, Tokai University, Japan, for providing DHS and other selenium compounds which is the backbone of this thesis.*

*It gives me immense pleasure to acknowledge Dr. Hema Rajaram, Dean, Life Sciences for helping me in every possible way. I am thankful to you Mam for your empathy, support and advice.*

*I express my sincere thanks to Dr. Beena G. Singh with whom I did my first experiment. Your words always boosted my energy and confidence. I also owe my heartfelt thanks to Dr. Atanu Barik,*

*for giving me an insight and understanding of lab work, Your valuable suggestions and positive attitude will always help me throughout my life. I owe my thanks to Dr. Vishal Kapoor for teaching, motivating and helping me to reach at this point of my life. I extend my special thanks to Dr. Deepak Sharma for teaching me the basic handling of cell culture.*

*With the depth of my heart, I would like to thank my lab mates Pavitra, Shaikat, Rupali, Ram, Vishwa and Shruti for helping and understanding me during my difficult times. Special thanks to Pavitra with whom I started my PhD journey. Her selfless and friendly nature helped me a lot during my research work, I am grateful to you all for making this journey joyful and memorable.*

*I owe my special thanks to my beloved friends Usha, Pooja, Rahul, Mahesh, Gautam, Neha and Prashant for taking care, supporting and motivating me. I would be not sitting and writing this thesis if you all were not there during my ill health. I am thankful to Meenakshi and Parvati for their help and motivation. I will always remember our funny talks. My special thanks to Satyam for never letting me alone and standing always by my side. His support and understanding helped me a lot during my tough times.*

*I would like to thank all project trainees Manobala, Chetna, Lopamudra, Rinny, Raghu, Indranil, Vara Sir and Naman for their help, support and making a joyful environment in the lab.*

*I am overwhelmed to thank my parents for their motivation and unconditional support. Their trust and belief kept me going through my tough times. It is only because of their sacrifices and blessing, I have reached to this point of my life.*

*Words won't be able to express my thanks to my brother Siddhartha. His bountiful love, care and affection provided me with the strength of completing my work,*

*Finally, I am thankful to Homi Bhabha National Institute and Department of Atomic Energy for providing funds required to carry out this work,*

*October, 2017*

*Prachi Verma*

	<b>TABLE OF CONTENTS</b>	<b>PAGE NO.</b>
	<b>SYNOPSIS</b>	<b>i</b>
	<b>LIST OF ABBREVIATIONS</b>	<b>xiii</b>
	<b>LIST OF SCHEMES</b>	<b>xviii</b>
	<b>LIST OF TABLES</b>	<b>xix</b>
	<b>LIST OF FIGURES</b>	<b>xx</b>
	<b>CHAPTER 1: INTRODUCTION</b>	<b>1</b>
1.1	Radiation	2
1.2	Radiobiology	3
1.3	Interaction of radiation with cells	3
1.3.1	Damage to lipids	4
1.3.2	Damage to proteins	5
1.3.3	Damage to deoxyribonucleic acid (DNA)	6
1.4	Cellular defense mechanisms	7
1.4.1	Antioxidants	8
1.4.2	Repair mechanisms	8
1.4.2.1	Cell cycle	8
1.4.2.2	DNA damage response	10
1.4.2.3	DNA repair	11
1.5	Oxidative stress	13
1.6	Cellular response to radiation	14
1.6.1	Cell survival curve	15
1.6.2	Acute radiation syndromes	16
1.6.3	Chronic radiation syndromes	17
1.7	Radiation protection	18

1.7.1	Radioprotectors	19
1.7.2	Strategies to develop radioprotectors	20
1.7.2.1	Sulfhydryl compounds as radioprotectors	20
1.7.2.2	Other radioprotectors	21
1.7.3	Limitations of existing radioprotectors	22
1.8	Selenium	23
1.8.1	Selenium as a micronutrient	24
1.8.2	Selenium metabolism	25
1.8.3	Selenoproteins	26
1.8.3.1	TrxR	26
1.8.3.2	Deiodinases	27
1.8.3.3	SelenoP	27
1.8.3.4	GPx	28
1.8.4	Catalytic mechanism of selenium containing GPx	30
1.8.5	Selenium as radioprotectors	30
1.8.5.1	Organoselenium compounds as radioprotectors	31
1.8.5.2	Mechanisms of action of selenium compounds	33
1.8.6	Dihydroxyselenolane (DHS)	34
1.9	Rationale and objectives of the thesis	36
	<b>CHAPTER 2: MATERIALS AND METHODS</b>	<b>38</b>
2.1	Chemicals	39
2.2	Instruments	40
2.3	Animal maintenance	41
2.4	Maintenance of cell lines	42
2.5	Radiation source and irradiation	42

2.6	Methods for evaluating <i>in vivo</i> parameters	44
2.6.1	Bronchoalveolar lavage fluid (BALF) collection and analysis	44
2.6.2	Estimation of cytokines like IL-6 and TNF- $\alpha$ in serum	45
2.6.3	Splenocytes preparation, spleen index and cellularity	45
2.6.4	Endogenous spleen colony formation assay	45
2.6.5	Hematocount	46
2.6.6	Histopathological study	46
2.7	Methods of cytotoxicity studies in cells	46
2.7.1	MTT assay	46
2.7.2	Clonogenic assay	47
2.7.3	Estimation of apoptosis by DNA ladder assay	48
2.7.4	Estimation of apoptosis and cell cycle distribution by PI staining	48
2.7.5	Characterization of cell death by Annexin V-PI staining	49
2.7.6	Estimation of mitochondrial membrane potential (MMP)	49
2.7.7	Estimation of LDH release from cells	50
2.7.8	Measurement of membrane fluidity	50
2.8	Methods of biochemical assays in cell lysate and tissue homogenate	51
2.8.1	Preparation of tissue homogenate and cell lysate	51
2.8.2	Estimation of protein content	51
2.8.3	Estimation of GPx activity	52
2.8.4	Estimation of ROS	52
2.8.5	Estimation of GSH and GSSG	53
2.8.6	Estimation of lipid peroxidation	54
2.8.7	Estimation of protein carbonylation	54

2.9	Methods for genotoxicity assessment in cells	<b>55</b>
2.9.1	Estimation of DNA damage by alkaline single cell gel electrophoresis	<b>55</b>
2.9.2	Micronuclei assay	<b>56</b>
2.9.3	$\gamma$ -H2AX assay	<b>56</b>
2.10	Gene expression analysis in cells and tissues by RT-PCR	<b>57</b>
<b>CHAPTER 3: RADIOPROTECTIVE EFFECT OF DHS AGAINST WHOLE BODY IRRADIATION IN MICE</b>		<b>59</b>
3.1	Introduction	<b>60</b>
3.2	Materials and Methods	<b>61</b>
3.3	Results	<b>62</b>
3.3.1	Dosage optimization of DHS to improve the 30 day post irradiation survival	<b>62</b>
3.3.2	Effect of DHS and SeM on the 30 day post irradiation survival	<b>64</b>
3.3.3	Effect of DHS and SeM on the radiation induced genotoxicity	<b>65</b>
3.3.4	Effect of DHS and SeM on the radiation induced hematopoietic toxicity	<b>67</b>
3.3.5	Effect of DHS and SeM on the radiation induced intestinal toxicity and inflammatory responses	<b>71</b>
3.3.6	Effect of DHS and SeM on the radiation induced oxidative damage and inflammatory responses in the lung	<b>75</b>

3.3.7	Effect of DHS and SeM on the radiation induced systemic inflammation	80
3.3.8	Effect of DHS and SeM on hepatic architecture	81
3.3.9	Effect of DHS and SeM on <i>SelenoP-1</i> expression in the liver	83
3.3.10	Effect of DHS and SeM on total GPx activity	84
3.3.11	Effect of DHS and SeM on the tissue specific expressions of GPx isoforms	85
3.4	Discussion	88
3.5	Summary	93
<b>CHAPTER 4: EFFECT OF ALKYL CHAIN LENGTH ON THE CELLULAR UPTAKE AND ANTIOXIDANT ACTIVITY OF DHS AND MAS</b>		<b>94</b>
4.1	Introduction	95
4.2	Materials and Methods	96
4.3	Results	97
4.3.1	Effect of DHS, MAS and their fatty acid / alkyl derivatives on cytotoxicity in CHO cells	97
4.3.2	Effect of DHS, MAS and their fatty acid / alkyl derivatives on LDH release in CHO cells	99
4.3.3	Characterization of cell death by DHS, MAS and their fatty acid / alkyl derivatives in CHO cells	101
4.3.4	Effect of DHS, MAS and their fatty acid / alkyl derivatives on MMP in CHO cells	103
4.3.5	Effect of DHS, MAS and their fatty acid / alkyl derivatives on plasma membrane fluidity in CHO cells	105

4.3.6	Effect of alkyl chain length on the uptake of DHS and MAS derivatives in CHO cells	107
4.3.7	Effect of alkyl chain length on the self-aggregation properties of DHS and MAS derivatives	110
4.3.8	Effect of DHS, MAS and their C <sub>6</sub> derivatives on the antioxidant activity in CHO cells	112
4.4	Discussion	115
4.5	Summary	119
<b>CHAPTER 5: COMPARATIVE RADIOPROTECTIVE ACTIVITY OF DHS AND DHS-C<sub>6</sub> IN CELLS AND THEIR MECHANISM OF ACTION</b>		<b>120</b>
5.1	Introduction	121
5.2	Materials and Methods	122
5.3	Results	123
5.3.1	Effect of DHS pre-treatment on toxicity in CHO cells by clonogenic assay	123
5.3.2	Effect of DHS pre-treatment on the radiation induced cell death in CHO cells	124
5.3.3	Comparative effect of DHS and DHS-C <sub>6</sub> pre-treatment on the radiation induced cell death in CHO cells	125
5.3.4	Effect of DHS and DHS-C <sub>6</sub> treatment on GPx level in CHO cells	127
5.3.5	Effect of DHS and DHS-C <sub>6</sub> pre-treatment on the radiation induced G2/M arrest in CHO cells	130

5.3.6	Effect of DHS and DHS-C <sub>6</sub> pre-treatment on the radiation induced DNA damage in CHO cells	132
5.3.7	Effect of DHS and DHS-C <sub>6</sub> pre-treatment on DNA repair kinetics in CHO cells following radiation exposure	134
5.3.8	Effect of DHS and DHS-C <sub>6</sub> pre-treatment on DNA repair and cell cycle checkpoint pathways in CHO cells following radiation exposure	137
5.3.9	Effect of DHS and DHS-C <sub>6</sub> pre-treatment on the radiation induced oxidative stress in CHO cells	142
5.3.10	Effect of DHS and DHS-C <sub>6</sub> pre-treatment on <i>SelenoP-1</i> expression in CHO cells	144
5.3.11	Effect of DHS and DHS-C <sub>6</sub> pre-treatment on the radiation induced apoptosis in splenic lymphocytes and CHO cells	145
5.4	Discussion	148
5.5	Summary	151
	<b>CHAPTER 6: SUMMARY AND FUTURE SCOPE</b>	<b>152</b>
	<b>REFERENCES</b>	<b>158</b>
	<b>REPRINTS OF PUBLISHE PAPERS</b>	

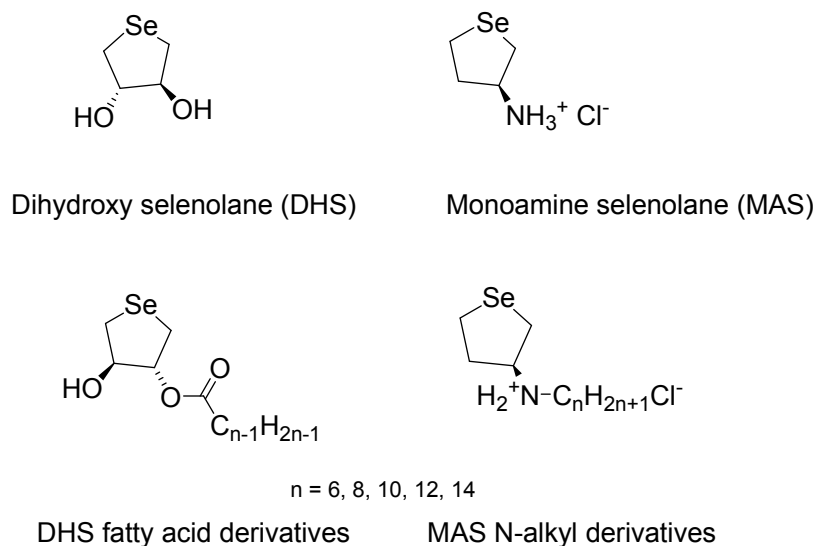
## SYNOPSIS

Unwanted exposure to ionizing radiation depending on its type, energy and absorbed dose can induce serious health hazards ranging from mutation, radiation syndromes, cancer and even to death.<sup>1</sup> In cells, ionizing radiation causes radiolysis of water, the major cellular component, leading to generation of free radicals like hydroxyl radical ( $\bullet\text{OH}$ ), superoxide radical ( $\text{O}_2^{\bullet-}$ ), peroxy radical ( $\text{ROO}^\bullet$ ) collectively termed as reactive oxygen species (ROS).<sup>2,3</sup> ROS cause oxidation of biomolecules resulting in disturbance of the redox homeostasis of cells which may ultimately lead to cell death.<sup>4</sup> Therefore there is a need for development of agents, termed as radioprotectors that can reduce radiation induced toxicity to normal cells.<sup>5</sup> After extensive research on various natural and synthetic compounds, sulfur compounds were reported to possess potential radioprotective activity due to their good free radical scavenging ability. The most effective sulfur compound identified till date for radioprotection is amifostine which is an aminothiols. This has been approved clinically to reduce radiation induced xerostomia in case of head and neck cancer patients.<sup>6</sup> But amifostine has certain limitations and exhibits considerable toxicity at the radioprotective dose. This warranted search for more effective and non-toxic drugs.<sup>7</sup>

Most of the initial research on sulfur compounds concluded that an ideal radioprotector should be able to donate electrons to ROS easily. Selenium and sulfur belong to the same group of the chalcogens with similar chemical properties. Selenium can scavenge free radicals more easily as compared to sulfur due to its higher nucleophilicity and lower ionization potential. Thus selenium compounds are anticipated to be better radioprotectors than the analogous sulfur compounds.<sup>8</sup> This led to a world-wide research to evaluate the radioprotective ability of inorganic and organic selenium compounds from natural as well as synthetic origins. Till date, an inorganic selenium compound, sodium selenite has been

tested in clinic to prevent radiation induced damage while organic selenium compounds are still under pre-clinical stage of evaluation. One selenium compound 3, 3'-diselenodipropionic acid (DSePA), developed from our group has shown promising results and is under preclinical stage for development as a lung radioprotector.

Having inspired by the outcomes of research with DSePA, we have examined in this thesis a water soluble cyclic organoselenium compound, trans-3,4-dihydroxyselenolane (DHS) for its radioprotective activity.<sup>9</sup> Further we have also explored the fatty acid / alkyl derivatives of DHS and a structurally similar monoamine selenolane (MAS) of variable chain length as a strategy to design a pro-drug to achieve required hydrophobicity such that it can increase uptake in cells. The chemical structures of DHS, MAS and their fatty acid / alkyl derivatives used in the present study are presented in Scheme 1.



*Scheme 1: Chemical structures of DHS, MAS and their fatty acid / alkyl derivatives*

## **Organization of the thesis:**

The work carried out in the present thesis is divided into six chapters:

- (1)** Introduction and Review of literature.
- (2)** Materials and Methods.
- (3)** Radioprotective effects of DHS against whole body irradiation (WBI) in mice model system.
- (4)** Effect of alkyl chain length on the cellular uptake and antioxidant activity of DHS and MAS.
- (5)** Comparative radioprotective activity of DHS and DHS-C<sub>6</sub> in cells and their mechanism of their action.
- (6)** Summary and future scope.

## **Chapter 1: Introduction and review of literature**

This is an introductory chapter and describes the literature related to the present thesis work. These include preliminary concepts on radiation biology, deleterious effect of radiation in terms of damage to biomolecules like lipids, proteins and DNA, details of DNA damage response, intracellular antioxidants, oxidative stress and signaling pathways. The chapter also describes in detail the need for radioprotectors, their classification and history of development. A brief overview of the importance of selenium in biology, its toxicity / essentiality, selenoproteins and the current status of research on selenium based radioprotectors is also discussed. At the end of the chapter details about the selenium compounds studied in the present thesis are included.

## **Chapter 2: Materials and Methods**

This chapter gives details about chemicals, instruments and methodologies used for the research work carried out in the thesis. The compound DHS, MAS and their fatty acid / alkyl derivatives were synthesized by Prof. Michio Iwaoka at Tokai University, Japan. The *in vivo* radioprotection studies were done in BALB/c mice with strict adherence to the ethical guidelines laid down by the institutional animal ethics committee of BARC. For cellular studies, Chinese Hamster Ovary (CHO) cells obtained from Radiation Physics and Advisory Division, BARC were used. The irradiation of mice and cells were performed using a <sup>60</sup>Co Bhabhatron  $\gamma$ -source (Department of Atomic Energy, India) with a dose rate of 1 Gy / min as estimated by Fricke dosimeter. All the biochemical and molecular assays in cells and tissues were performed following standard methods as reported in literature. The anti-genotoxic effect of test compounds were investigated by micronuclei,  $\gamma$ -H2AX and comet assay. The mechanism of action was investigated by performing the pharmacological inhibition experiments. The statistical analysis of the data was done by student's t test, one-way ANOVA of Origin software (version 6.0.0). The P values < 0.05 were considered as statistically significant.

## **Chapter 3: Radioprotective effects of DHS against whole body irradiation (WBI) in mice model system**

This chapter gives details regarding the *in vivo* radioprotective activity of DHS against WBI to an absorbed dose of 8 Gy in BALB/c mice. DHS was administered intraperitoneally (ip) under three different treatment regimes. In the first experiment, single dose of DHS was administered 30 minutes prior to radiation exposure. In the second experiment, DHS was administered for 5 consecutive days prior to radiation exposure and in the third experiment, DHS was administered not only for 5 consecutive days prior to

irradiation but also during the post irradiation period for three times a week until the end of the experiment. The results indicated that DHS offered best protection under the third treatment condition. DHS at the lowest tested dose of 2 mg/kg body weight showed 40 % improvement in 30 day survival of mice. Increasing the dosage up to 50 mg/kg body weight did not increase the protection suggesting saturation. This dosage and treatment schedule was employed for further studies. Radiation exposure causes tissue injury leading to hematopoietic and gastrointestinal syndrome.<sup>10,11</sup> The effect of DHS supplementation on the organ specific toxicity and inflammatory responses in BALB/c mice exposed to WBI was monitored in terms of biochemical / histological changes at 10 and 30 day post irradiation as the median survival time of radiation treated group was 10 day. The results indicated that supplementation with DHS did not protect against radiation induced acute (10 day) hematopoietic and gastrointestinal damage assessed in terms of spleen parameters (index, cellularity and colony forming units), hematocount and villi structure but showed restoration of the above parameters in mice surviving till 30 day post irradiation. Interestingly DHS treated mice ameliorated the radiation induced acute oxidative damage parameters like lipid peroxidation and inflammatory response marked by an increase in the expression of pro-inflammatory cytokines like *Icam-1*, *Ccl-2* and *iNos-2* in lung and intestine. In line with these results, DHS administration also reduced the radiation induced DNA damage in peripheral leukocytes as monitored by comet assay. Further, DHS was evaluated for its ability to modulate the expression of a selenoenzyme like GPx in lungs, spleen and intestine. DHS supplementation caused tissue specific induction of all three GPx isoforms (*GPx 1*, *GPx 2* and *GPx 4*) in different tissue on 10 and 30 day leading to an overall increase in GPx activity. DHS also showed higher level of another antioxidant enzyme *SelenoP-1* at both time points which might contribute to its ability to reduce radiation induced systemic inflammation. Throughout the studies, DHS was compared with

a standard organoselenium compound, selenomethionine (SeM) which is not only a major dietary source of selenium to humans but has also been evaluated for radioprotection.<sup>12</sup> Additionally, DHS and SeM being cyclic and linear selenium compounds respectively, such studies are useful to understand the importance of structure if any in their radioprotective activities. The results indicated that DHS is as good as SeM in improving survival. Most of the biochemical and histological parameters were comparable, except that SeM did not alter the expression of *GPx 4*. Thus in conclusion survival advantage offered by DHS and SeM may be attributed to the suppression of radiation induced inflammatory responses and antioxidant effects mediated through GPx. One of the limitations of linear organoselenium compounds like SeM is its metabolic instability. Compared to linear ones, cyclic organoselenium are considered to be metabolically stable and thus are expected to exhibit higher antioxidant effects. Since DHS is highly water soluble, may be poorly bio-available therefore in the next chapter, DHS and a series of its lipophilic derivatives were evaluated for bio-availability employing a cellular model. Subsequently the effect of these derivatives on the induction of antioxidant selenoprotein like GPx was also investigated for their probable exploration as radioprotective agents.

#### **Chapter 4: Effect of alkyl chain length on the cellular uptake and antioxidant activity of DHS and MAS**

Attaching a fatty acid / alkyl group as a lipophilic unit with a pharmacologically important hydrophilic moiety is an effective approach to increase its bioavailability.<sup>13,14</sup> Accordingly, a series of lipophilic derivatives of DHS and a structurally related molecule, MAS, were synthesized by attaching fatty acids or alkyl groups of variable chain length (C<sub>6</sub> - C<sub>14</sub>). All these derivatives were evaluated for cytotoxicity, uptake and antioxidant activity in CHO cells and the results are discussed in this chapter. The aim of this work is to

identify the most effective compounds that can be further evaluated for radioprotection. The cytotoxicity studies at various time points (24 -72 h) indicated that the parent compounds DHS and MAS were non-toxic, however the cytotoxicity of their fatty acid / alkyl derivatives increased with an increasing concentration (1 - 50  $\mu$ M) and chain length ( $C_6$  -  $C_{14}$ ). The cytotoxicity of DHS and MAS derivatives were in the following order  $C_6 < C_8 < C_{10} \sim C_{12} > C_{14}$ . Among the DHS and MAS derivatives, the former showed significantly lesser cytotoxicity than the latter at each chain length and treatment concentration. The mechanistic investigation revealed that the higher ( $\geq C_8$ ) fatty acid / alkyl derivatives of DHS and MAS led to cell death by necrosis caused by cytolysis or membrane disintegration as evidenced by the acute mitochondrial depolarization, propidium iodide staining and leakage of intracellular protein LDH. Since plasma membrane disruption is also marked by the changes in its fluidity, the effect of the long ( $>C_8$ ) chain derivatives of DHS and MAS on membrane disruption was revalidated by measuring the fluidity parameter in terms of an anisotropy value of a fluorophore, DPH, known to be localized in the plasma membrane.<sup>15</sup> Our results indicated that treatment with parent compounds (DHS and MAS) at 25  $\mu$ M did not affect the anisotropy value of DPH even after 4 h of their addition to cells, whereas ( $>C_8$ ) derivatives of DHS and MAS at identical concentration showed time dependant decrease in anisotropy. Further DHS and MAS derivatives with long alkyl chain, being amphiphilic in nature may aggregate causing non-linear relationship between chain length and cytotoxic effect. Indeed our results indicated that the higher ( $\geq C_{12}$ ) fatty acid / alkyl derivatives of DHS and MAS formed aggregates as a function of concentration. Due to this, there was lower availability of free molecules to interact with the cell membrane causing lesser cytotoxicity at longer chain length. Subsequently, the cellular uptake of DHS, MAS and their non toxic derivatives like DHS- $C_6$  and MAS- $C_6$  was examined. The results indicated that the  $C_6$  derivatives

improved the uptake of the parent compound by ~ 2.5-fold. Further, treatments with DHS-C<sub>6</sub> and MAS-C<sub>6</sub> showed significantly higher induction of antioxidant selenoenzymes such as *GPx 1* and *TrxR 1* both at mRNA and activity levels as compared to the respective parent compounds. Additionally, these derivatives also provided better protection against the AAPH induced lipid peroxidation and protein oxidation than the parent compounds. In conclusion C<sub>6</sub> derivatives of DHS and MAS are better than the parent compounds in terms of bio-availability exhibiting antioxidant effects in the cell. The study also provided evidence for the importance of hydrophilic-lipophilic balance (HLB) in regulating cytotoxicity as well as bioavailability. Based on these studies, in the next chapter we have performed radioprotection studies of DHS-C<sub>6</sub> and compared with DHS. Due to chemical instability and slightly higher toxicity of MAS-C<sub>6</sub> it was not taken up for further studies.

## **Chapter 5: Comparative radioprotective activity of DHS and DHS-C<sub>6</sub> in cells and their mechanism of action**

This chapter describes the comparative radioprotective effects of DHS and DHS-C<sub>6</sub> against  $\gamma$ -irradiation using cellular model system. Attempts were also made to understand their mechanism of actions. CHO cells being a model cellular system for radiation-related research was used for this purpose. These cells were treated with DHS in the concentration range of 1-100  $\mu$ M for 16 h, exposed to  $\gamma$ -radiation to an absorbed dose of 4 Gy and evaluated for cell survival by clonogenic assay. Results showed that DHS pre-treatment prevented the radiation induced cell death in a concentration dependant manner up to 25  $\mu$ M and increase in concentration to 100  $\mu$ M showed saturation effect. Further to examine, how increased cellular uptake can influence the radioprotective activity, studies were performed with DHS-C<sub>6</sub>. The results revealed that at an identical concentration of 25  $\mu$ M, DHS-C<sub>6</sub> pre-treatment offered significantly higher protection (40 %) against the radiation

(4 Gy) induced cell death as compared to the parent compound DHS. The radiation dose response of DHS and DHS-C<sub>6</sub> was evaluated by estimating the survival fraction as a function of the increasing absorbed dose (1-12 Gy) through clonogenic assay. From this study, dose modification factor (DMF) for DHS and DHS-C<sub>6</sub> was estimated to be 1.14 and 1.24 respectively. Notably treatment with both DHS and DHS-C<sub>6</sub> significantly increased GPx activity in cells by ~ 2.5 fold. Anticipating the role of GPx in radioprotection, our investigations revealed that addition of mercaptosuccinic acid, a pharmacological inhibitor of GPx abrogated the DHS mediated improvement in survival fraction against radiation exposure. Since CHO cells undergo radiation induced cell death through mitotic catastrophe mediated through G2 / M cell cycle arrest and chromosomal aberration, it was anticipated that radioprotective effect of DHS might be related to its effect on cell cycle arrest and DNA damage / repair. Therefore to address this issue, CHO cells treated with DHS and/or mercaptosuccinic acid were exposed to radiation and cell cycle analysis was performed using propidium iodide. The results showed that treatment with DHS resulted in shift of cells from radiation induced G2/M arrest to G1 and the presence of mercaptosuccinic acid reversed this effect. Further to study the role of DHS in DNA repair, comet assay was performed at 0, 15, 30 and 60 minutes following radiation exposure. The results indicated that DHS and DHS-C<sub>6</sub> pre-treatment led to faster repair of DNA compared to radiation control. At 30 minutes, there was a decrease in all four comet parameters (percent DNA tail, tail moment, tail length and olive tail moment) by 41 %, 36 %, 35 %, and 46 % respectively in DHS and by 57 %, 50 %, 52 %, and 66 % respectively in DHS-C<sub>6</sub> treated group compared to radiation control. The radioprotective effect of DHS against radiation induced DNA damage was also evidenced by  $\gamma$ -H2AX and micronuclei assays. Interestingly, addition of mercaptosuccinic acid abrogated the DHS mediated DNA repair monitored through comet,  $\gamma$ -H2AX and micronuclei assays. Further inhibitors of DNA

damage response proteins like check point kinase 1 (CHK 1) and DNA-protein kinase (DNA-PK) although abrogated the radioprotective effect of DHS or DHS-C<sub>6</sub> separately, did not show additive effect in combination with GPx inhibitor. All these results together thus confirmed that DHS or DHS-C<sub>6</sub> induced GPx levels in CHO cells, facilitated DNA repair through modulating DNA damage response signaling against radiation exposure and responsible for the observed radioprotective effect. Having understood the radioprotective action of DHS and DHS-C<sub>6</sub> in CHO cells, it was important to evaluate the effect of these compounds in radiosensitive cells like lymphocytes. Notably treatment with DHS or DHS-C<sub>6</sub> did not protect lymphocytes from radiation exposure. Lymphocytes undergo transient G1 arrest and apoptosis after radiation exposure suggesting the inability of above compounds in preventing the radiation induced early apoptosis. In conclusion, present study gains significance in view of the fact that late-responding normal tissue cells involved in chronic syndromes undergo delayed mitotic death following radiation exposure. Therefore DHS-C<sub>6</sub> a lipophilic derivative of DHS showing protection against radiation induced mitotic death can be a model compound for *in vivo* evaluation as selenium based radioprotector to reduce radiation toxicities in late-responding normal cells.

## **Chapter 6: Summary and future scope**

1. DHS, a water soluble, non-toxic organoselenium compound when administered at a dosage of 2 mg/kg body weight for 5 consecutive days prior to radiation exposure and three times a week post WBI of 8 Gy improved 30 day survival of mice by 40 %. Radioprotective activity of DHS was found to be associated with GPx induction, reduction of lipid peroxidation and inflammation in the radiosensitive organs. The protection offered by DHS was comparable to that by a natural dietary organoselenium compound SeM.

2. The fatty acid / alkyl conjugation of DHS and MAS (>C<sub>8</sub>) improved the ability of DHS and MAS to incorporate in the cells but at the same time induced toxicity by necrosis in CHO cells. An optimum chain length derivative, DHS-C<sub>6</sub> and MAS-C<sub>6</sub> showed the right hydrophilic-lipophilic balance to increase the availability as well as antioxidant activity in cells.
3. DHS and DHS-C<sub>6</sub> protected CHO cells from radiation induced mitotic death with DMF of 1.14 and 1.24 respectively. It prevented radiation induced DNA damage by augmenting DNA repair in a GPx dependant manner.
4. As DHS and DHS-C<sub>6</sub> led to induction of GPx at mRNA and activity levels, the tissue specific role of GPx in their radioprotective activities needs to be investigated in future.
5. The ability of DHS and DHS-C<sub>6</sub> to prevent radiation induced inflammatory responses and mitotic death in late-responding cells warrant future experiments to explore them against chronic syndromes.

## References

1. K. Kamiya, K. Ozasa, S. Akiba, O. Niwa, K. Kodama, N. Takamura, E. K. Zaharieva, Y. Kimura, R. Wakeford, *Lancet*, 2015, **386**, 469-478.
2. C. von Sonntag, *The chemical basis of radiation biology*, 1987.
3. J. K. Tak, J. W. Park, *Free Radic. Biol. Med.*, 2009, **46**, 1177-85.
4. P. A. Riley, *Int. J. Radiat. Biol.*, 1994, **65**, 27-33.
5. J. F. Weiss, M. G. Simic, *Pharmacol. Ther.*, 1998, **39**, 1-2.
6. C. N. Andreassen, C. Grau, J. C. Lindegaard, *Semin. Radiat. Oncol.*, 2008, **13**, 62-72.

7. P. E. Brown, *Nature*, 1967, **213**, 363-364.
8. L. A. Wessjohann, A. Schneider, M. Abbas, W. Brandt, *Biol. Chem.*, 2007, **388**, 997-1006.
9. M. Iwaoka, T. Takahashi, S. Tomoda, *Heteroat. Chem.*, 2001, **12**, 293-299.
10. A. L. Carsten, In: Response of different species to total body irradiation, 1984, 59-86.
11. K. E. Carr, S. P. Hume, R. Ettarh, E. A. Carr, S. McCollough, In: Radiation and the Gastrointestinal Tract, 1995, 113-128.
12. J. F. Weiss, R. L. Hoover, K. S. Kumar, *Free Radic. Res. Commun.*, 1987, **3**, 33-38.
13. K. Arai, K. Moriai, A. Ogawa, M. Iwaoka, *Chem. Asian J.*, 2014, **12**, 3464-3471.
14. M. Iwaoka, A. Katakura, J. Mishima, Y. Ishihara, A. Kunwar, K. I. Priyadarsini, *Molecules*, 2015, **20**, 12364-12375.
15. M. Shinitzky, Y. Barenholzb, *Biochim. Biophys. Acta*, 1987, **515**, 367-394.

## **LIST OF ABBREVIATIONS**

LET	Linear energy transfer
Gy	Gray
ROS	Reactive oxygen species
RNS	Reactive nitrogen species
PUFA	Polyunsaturated fatty acids
LOOH	Lipid hydroperoxide
MDA	Malondialdehyde
DNA	Deoxyribonucleic acid
SSB	Single strand break
DSB	Double strand break
MN	Micronuclei
GPx	Glutathione peroxidase
SOD	Superoxide dismutase
TrxR	Thioredoxin reductases
Trx	Thioredoxin
CAT	Catalase
H <sub>2</sub> O <sub>2</sub>	Hydrogen peroxide
GSH	Glutathione
CDK	Cyclin dependent protein kinase
CHK	Checkpoint kinase
ATM	Ataxia-telangiectasia-mutated
ATR	(ATM- and Rad3-Related) kinase
NHEJ	Non homologous end joining

HR	Homologous recombination
DNA-PK	DNA protein kinase
XRCC4	X-ray repair cross-complementing protein 4
RPA	Replication protein A
RIP1 / RIP3	Receptor interacting proteins 1 and 3
$W_R$	Radiation weighing factor
$W_T$	Tissue weighing factor
LQ	Linear quadratic model
ARS	Acute radiation syndromes
WBI	Whole body irradiation
CRS	Chronic radiation syndromes
iNos-2	Nitric oxide synthase 2
Ccl-2	Chemokine (C-C motif) ligand 2
ICAM-1	Intracellular adhesion molecule 1
VCAM-1	Vascular adhesion molecule 1
IL	Interleukin
TGF- $\beta$	Transforming growth factor beta
ECM	Extracellular matrix protein
ICRP	International commission on radiological protection
ALARA	As low as reasonably achievable
DMF	Dose modifying factor
bFGF	Basic fibroblast growth factor
KGF	Keratinocyte growth factor
EPO	Erythropoietin
SelenoP	Selenoprotein P

DIO	Iodothyronine deiodinase
SeM	Selenomethionine
SeC	Selenocysteine
MRE	Metal responsive element
COX2	Cyclooxygenase 2
PGE <sub>2</sub>	Prostaglandin
DSePA	Diselenodipropionic acid
CHO	Chinese Hamster Ovary
DHS	Dihydroxyselenolane
AAPH	2, 2'-azobis (2-amidinopropane) dihydrochloride
TAS	Total antioxidant status
MAS	Monoamine selenolane
TCA	Trichloroacetic acid
DNPH	2,2'-dinitrophenyl hydrazine
TBA	Thiobarbituric acid
DMSO	Dimethyl sulfoxide
PMSF	Phenylmethylsulphonyl fluoride
LMPA	Low melting point agarose
HMPA	High melting point agarose
EtBr	Ethidium bromide
DCFDA	2,7 dichlorodihydro fluorescein-diacetate
NADPH	$\beta$ -nicotinamide adenine dinucleotide 2'-phosphate reduced tetrasodium salt hydrate
GR	Glutathione reductase
CuOOH	Cumene hydroperoxide

PI	Propidium iodide
MS	Mercaptosuccinic acid
BSA	Bovine serum albumin
DEPC	Diethyl pyrocarbonate
HPO <sub>3</sub>	Metaphosphoric acid
OPT	O-phthaldialdehyde
NEM	N-ethylmaleimide
NaOH	Sodium hydroxide
JC-1	5, 5', 6, 6'-tetrachloro-1,1',3,3'-tetraethylbenzimidazolo- carbocyanine iodide
LDH	Lactate dehydrogenase
DMEM	Dulbecco modified eagle medium
RPMI-1640	Roswell park memorial institute medium-1640
FCS	Fetal calf serum
UCN-01	7-hydroxy staurosporine
PV1091	7-nitro-1H-indole-2-carboxylic acid {4-[1- (guanidinohydrazone)-ethyl]-phenyl}-amide)
NU7026	2-(Morpholin-4-yl)-benzo[h]chomen-4-one
RT-PCR	Real time-polymerase chain reaction
RBC	Red blood cells
PBS	Phosphate buffered saline
HSCs	Hematopoietic stem cells
MTT	[3-(4,5-Dimethylthiazol-2-yl)-2,5-Diphenyltetrazolium Bromide
PS	Phosphatidylserine

DPH	1,6-diphenyl-1,3,5-hexatriene
BHT	Butylated hydroxy toluene
4HNE	4 hydroxynonenal
ip	Intraperitoneal
b.wt	Body weight
BALF	Bronchoalveolar lavage Fluid
TDNA	Tail DNA
OTM	Olive tail moment
Csf-3	Colony stimulating factor -3
CFU	Colony forming unit
WBC	White blood cells
TNF- $\alpha$	Tumor necrosis factor alpha
HLB	Hydrophobic-lipophilic balance

<u>LIST OF SCHEMES</u>	<b>PAGE NO.</b>
<b>Scheme 1.1</b>	<b>4</b>
Radiolysis of water	
<b>Scheme 1.2</b>	<b>7</b>
Radiation induced DNA damage	
<b>Scheme 1.3</b>	<b>11</b>
DNA damage response	
<b>Scheme 1.4</b>	<b>26</b>
<i>In vivo</i> metabolism of selenium	
<b>Scheme 1.5</b>	<b>30</b>
Catalytic cycle of glutathione peroxidase	
<b>Scheme 1.6</b>	<b>34</b>
Role of selenium in DNA repair	
<b>Scheme 1.7</b>	<b>36</b>
Chemical structures of DHS, MAS and their fatty acid / alkyl chain derivatives	
<b>Scheme 2.1</b>	<b>42</b>
Decay of <sup>60</sup> Co	
<b>Scheme 6.1</b>	<b>156</b>
Proposed model for the radioprotective effect of DHS / DHS-C <sub>6</sub>	

**LIST OF TABLES**

**PAGE NO.**

<b>Table 1.1</b>	<b>22</b>
List of promising radioprotectors	
<b>Table 2.1</b>	<b>58</b>
List of primers	
<b>Table 3.1</b>	<b>71</b>
Hematocount under different treatment conditions	
<b>Table 3.2</b>	<b>77</b>
Count of immune cell types in BALF cell under different treatment conditions	

## LIST OF FIGURES

## PAGE NO.

### **Fig. 1.1**

**15**

Shape of cell survival curves.

### **Fig. 3.1**

**63**

Kalpan-Meier survival curve representing the effect of DHS (2 - 50 mg/kg b.wt) administration (ip) on 30 day survival of mice exposed to WBI of 8 Gy. (A) Single ip administration of DHS at 30 minutes prior to radiation exposure. (B) DHS was administered for five consecutive days and 30 minutes after the last dose, mice were irradiated (C) DHS was administered for five consecutive days prior to irradiation and continued during the post irradiation period for three times per week till 30 days.

### **Fig 3.2**

**65**

(A) Comparative effect of DHS (2 mg/kg b.wt) and SeM (2 mg/kg b.wt) administration (ip) on the 30 day survival of mice exposed to WBI at an absorbed dose of 8 Gy. Both drugs were administered for five consecutive days prior to irradiation and continued during the post irradiation period for three times a week till the end of experiment. (B) Relative change in body weight for different treatment groups plotted as a function of time in days.

### **Fig 3.3**

**66**

Effect of DHS (2 mg/kg b.wt ) and SeM (2 mg/kg b.wt) administration (ip) on the radiation (5 Gy) induced DNA strand breaks in peripheral lymphocytes as assayed by comet assay. DHS and SeM were given for five consecutive days prior to irradiation and peripheral blood was drawn at 15 and 60 minutes post irradiation from the tail vein of mice. The blood containing peripheral lymphocytes were subjected to single cell gel electrophoresis. (A) Bar graphs shows % TDNA and OTM in various treatment groups.

(B) Representative fluorescent images show nuclei stained with SYBR Green-II dye 15 minutes post irradiation under different treatment groups following electrophoresis.

**Fig 3.4**

**68**

Bar graph shows effect of DHS (2 mg/kg b.wt) and SeM (2 mg/kg b.wt) supplementation (ip) on (A) spleen index (spleen weight/body weight) and (B) spleen cellularity against WBI of 8 Gy.

**Fig 3.5**

**69**

(A) Bar graph shows effect of DHS (2 mg/kg b.wt) and SeM (2 mg/kg b.wt) supplementation (ip) on spleen colonies against WBI of 8 Gy. (B) Images of spleen colonies under different treatment conditions. The spleen colony forming assay was performed only at 10 day post irradiation. (C) mRNA expression of *Csf-3* as monitored by RT-PCR. The expression of above genes in different treatment groups was normalized against the sham control group and the relative expression changes have been plotted. Actin expression was used as internal control.

**Fig 3.6**

**72**

Bar graph shows the effect of DHS (2 mg/kg b.wt) and SeM (2 mg/kg b.wt) supplementation (ip) on microvilli height against WBI of 8 Gy.

**Fig 3.7**

**73**

Effect of DHS (2 mg/kg b.wt) and SeM (2 mg/kg b.wt) supplementation (ip) on the radiation (8 Gy) induced intestinal toxicity. Images of representative tissue section of jejunum excised from the mice of the various groups and stained with hematoxylin and eosin.

**Fig 3.8**

**74**

Effect of DHS (2 mg/kg b.wt) and SeM (2 mg kg b.wt) supplementation (ip) on the radiation (8 Gy) induced intestinal inflammatory responses. (A) Level of lipid

peroxidation in the jejunum excised from the mice of various groups. (B), (C) and (D) mRNA expressions of *Icam-1*, *Ccl-2* and *iNOS-2* respectively as monitored by RT-PCR. The expression of above genes in different treatment groups was normalized against the sham control group and the relative expression changes have been plotted. Actin expression was used as internal control.

**Fig 3.9**

75

Effect of DHS (2 mg/kg b.wt) and SeM (2 mg/kg b.wt) supplementation (ip) on the radiation (8 Gy) induced lung inflammatory responses. Bar graph shows the inflammatory scores under different treatment conditions.

**Fig 3.10**

76

Representative tissue section of right lung stained with hematoxylin and eosin shows the effect of DHS (2 mg/kg b.wt) and SeM (2 mg/kg b.wt) supplementation (ip) on the radiation (8 Gy) induced lung damage.

**Fig 3.11**

78

Effect of DHS (2 mg/kg b.wt) and SeM (2 mg/kg b.wt) supplementation (ip) on the radiation (8 Gy) induced changes in the level of (A) lipid peroxidation and (B) BAL protein in lung.

**Fig 3.12**

79

Bar graph shows effect of DHS (2 mg/kg b.wt) and SeM (2 mg/kg b.wt) supplementation (ip) against WBI of 8 Gy on pro-inflammatory gene expression (A) *Icam-1* and (B) *Ccl-2* in the lung. The expression of above genes in different treatment groups was normalized against the sham control group and the relative expression changes have been plotted. Actin expression was used as internal control.

**Fig 3.13****81**

Bar graph shows effect of DHS (2 mg/kg b.wt) and SeM (2 mg/kg b.wt) supplementation (ip) on the radiation (8 Gy) induced systemic inflammation. Levels of (A) IL-6 & (B) TNF- $\alpha$  monitored in the serum using ELISA kit.

**Fig 3.14****82**

Representative tissue section stained with hematoxylin and eosin shows the effect of DHS (2 mg/kg b.wt) and SeM (2 mg/kg b.wt) supplementation (ip) on the radiation (8 Gy) induced changes in hepatic architecture.

**Fig 3.15****83**

Bar graph shows the effect of DHS (2 mg/kg b.wt) and SeM (2 mg/kg b.wt) supplementation (ip) on the counts of binucleate cells in liver tissue section.

**Fig 3.16****84**

Effect of DHS (2 mg/kg b.wt) and SeM (2 mg/kg b.wt) supplementation (ip) on mRNA expression of *SelenoP-1* in hepatic tissue against WBI of 8 Gy under different treatment conditions. The expression of gene in different treatment groups was normalized against the sham control group and the relative expression changes have been plotted. Actin expression was used as internal control.

**Fig 3.17****85**

Effect of DHS (2 mg/kg b.wt) and SeM (2 mg/kg b.wt) supplementation (ip) on the radiation (8 Gy) induced changes in total GPx activity in (A) lung, (B) intestine and (C) spleen.

**Fig 3.18****87**

Effect of DHS (2 mg/kg b.wt) and SeM (2 mg/kg b.wt) supplementation (ip) on the mRNA expression of *GPx 1*, *GPx 2* and *GPx 4* in lung, intestine and spleen against WBI of 8 Gy. The expression of gene in different treatment groups was normalized

against the sham control group and the relative expression changes have been plotted. Actin expression was used as internal control.

**Fig 4.1**

**98**

Cytotoxic effect of DHS, MAS and their derivatives ( $C_{6-14}$ ) in the concentration range of (1 - 50  $\mu$ M) by MTT assay at different time points (24, 48 and 72 h) after their addition to CHO cells. Cytotoxicity is expressed as percentage of the control cells (DMSO, 0.25 %).

**Fig 4.2**

**99**

Cytotoxic effect of free fatty acids ( $C_{6:0}$  to  $C_{12:0}$ ) in CHO cells. Cells were treated with increasing concentration of fatty acids for 72 h and the cytotoxicity was determined by MTT assay. Cytotoxicity is expressed as percentage of control cells (DMSO, 0.25 %)

**Fig 4.3**

**100**

Effect of DHS and MAS treatment on LDH activity in cell lysate. The control sample represents untreated cell lysate subjected to LDH determination.

**Fig 4.4**

**101**

Effect of treatments (25  $\mu$ M) with (A) DHS and its derivatives and (B) MAS and its derivatives on LDH release compared to control at 2, 4, 6 and 24 h after their addition to cells.

**Fig 4.5**

**102**

Characterization of cell death induced by the  $C_6$  and  $C_{14}$  derivatives of DHS and MAS by Annexin V-PI staining at 16 h after their addition to CHO cells. Representative dot plots acquired from flow cytometry shows distribution of cells under different treatment conditions.

**Fig 4.6****103**

Bar graph shows percentage (%) live, apoptotic and necrotic cells after treatment with C<sub>6</sub> and C<sub>14</sub> derivatives of DHS and MAS for 16 h in CHO cells by Annexin V- PI staining.

**Fig 4.7****104**

Bar graph shows the ratio of red ( $\lambda_{em} = 610$  nm) and green ( $\lambda_{em} = 535$  nm) fluorescence intensity of JC-1 staining at 2, 4 and 8 h after treatment with 25  $\mu$ M of C<sub>6</sub> and C<sub>14</sub> derivatives of DHS and MAS.

**Fig 4.8****105**

Representative photographs of red ( $\lambda_{em} = 610$  nm) and green ( $\lambda_{em} = 535$  nm) fluorescence emission of JC-1 staining at 8 h after treatment with 25  $\mu$ M of C<sub>6</sub> and C<sub>14</sub> derivatives of DHS and MAS.

**Fig 4.9****106**

(A & B) Effect of the treatment (25  $\mu$ M) with C<sub>6</sub> and C<sub>14</sub> derivatives of DHS and MAS respectively on plasma membrane fluidity measured as the change in the anisotropy value of a membrane bound fluorophore, DPH at 2 and 4 h after their addition to CHO cells,  $\lambda_{ex} = 365$  nm,  $\lambda_{em} = 430$  nm.

**Fig 4.10****108**

Effect of alkyl chain length (C<sub>6-14</sub>) on the uptake of DHS and MAS derivatives into membranes / cells following their addition to CHO cells at 25  $\mu$ M for an hour.

**Fig 4.11****109**

(A) Overlapped fluorescence spectra of CHO cells stained with a membrane bound fluorophore, DPH recorded soon after the addition of DHS-C<sub>14</sub> to the cell suspension in a time course manner (0 – 45 min). The excitation was performed at 365 nm. (B) Graph

shows the interaction / binding of DHS-C<sub>14</sub> with the plasma membrane monitored in terms of the changes in the fluorescence intensity ( $\lambda_{em} = 430$  nm) of DPH.

**Fig 4.12**

**110**

(A) Overlapped fluorescence spectra of CHO cells stained with a membrane bound fluorophore, DPH recorded soon after the addition of MAS-C<sub>14</sub> to the cell suspension in a time course manner (0 – 45 min). The excitation was performed at 365 nm. (B) Graph shows the interaction / binding of MAS-C<sub>14</sub> with the plasma membrane monitored in terms of the changes in the fluorescence intensity ( $\lambda_{em} = 430$  nm) of DPH.

**Fig 4.13**

**111**

Aggregation studies of fatty acid derivatives of DHS (C<sub>6-14</sub>) using fluorescence enhancement of a lipophilic fluorophore DPH. (A) Representative fluorescence spectra of DPH in 50  $\mu$ M aqueous solution of DHS (C<sub>6-14</sub>) containing 0.25 % DMSO. (B) Line graph shows enhancement in the fluorescence intensity of DPH by DHS (C<sub>6-14</sub>) at their increasing concentrations of 2 to 50  $\mu$ M.  $I_f$  – Fluorescence intensity in presence of selenium compounds.  $I_o$  - Fluorescence intensity in absence of selenium compounds.  $\lambda_{ex} = 365$  nm,  $\lambda_{em} = 430$  nm.

**Fig 4.14**

**112**

Aggregation studies of alkyl derivatives of MAS (C<sub>6-14</sub>) using fluorescence enhancement of a lipophilic fluorophore DPH. (A) Representative fluorescence spectra of DPH in 50  $\mu$ M aqueous solution of MAS (C<sub>6-14</sub>) containing 0.25 % DMSO. (B) Line graph shows enhancement in the fluorescence intensity of DPH by MAS (C<sub>6-14</sub>) in the increasing concentration (2 - 50  $\mu$ M).  $I_f$  – Fluorescence intensity in presence of selenium compounds.  $I_o$  - Fluorescence intensity in absence of selenium compounds.  $\lambda_{ex} = 365$  nm,  $\lambda_{em} = 430$  nm.

**Fig 4.15****114**

Effect of pre-treatment (25  $\mu$ M for 16 h) with DHS, MAS and their C<sub>6</sub> derivatives on (A) GPx activity and (B) expression of genes such as *GPx 1* and *GPx 4*. The expression of above genes in different treatment groups was normalized against control group and the relative expression changes have been plotted. Actin expression was used as internal control

**Fig 4.16****115**

Effect of pre-treatment (25  $\mu$ M for 16 h) with DHS, MAS and their C<sub>6</sub> derivatives against the AAPH (30 mM) induced lipid peroxidation and protein carbonylation estimated at 6 h post exposure by TBARS and DNPH assays respectively.

**Fig 5.1****123**

(A) Bar graph shows the cytotoxic effect of DHS in CHO cells by clonogenic assay. (B) Representative images show colonies of CHO cells. Cells were pre-treated with DHS in a concentration ranging from 0.1 - 100  $\mu$ M for 16 h, washed with 1X PBS, supplemented with fresh culture medium and cultured for 7 days to form colonies.

**Fig 5.2****125**

Bar graph shows the effect of the varying concentration (0.1 - 100  $\mu$ M) of DHS pre-treatment for 16 h on the survival fraction in CHO cells against  $\gamma$ -irradiation (4 Gy) as estimated by clonogenic assay.

**Fig 5.3****126**

Bar graph shows the effect of DHS and DHS-C<sub>6</sub> pre-treatment (25  $\mu$ M for 16 h) on survival fraction against radiation exposure of 4 Gy.

- Fig 5.4** **127**  
(A) Semi log plot shows radiation dose (1 - 12 Gy) response curve of DHS and DHS-C<sub>6</sub> pre-treatment (25 μM for 16 h) in CHO cells by clonogenic assay. (B) Representative images show colonies of CHO cells under different treatment conditions.
- Fig 5.5** **128**  
Effect of pre-treatment with DHS, DHS-C<sub>6</sub> (25 μM for 16 h) on GPx activity and its modulation by MS (10 mM for 2 h) in CHO cells.
- Fig 5.6** **129**  
(A & B) Effect of MS (10 mM) on radioprotective activity of DHS and DHS-C<sub>6</sub> (25 μM for 16 h) against radiation dose of 4 Gy and 11 Gy respectively in terms of survival fraction estimated by clonogenic assay in CHO cells. (C) Representative images shows colonies of CHO cells under different treatment conditions at 11 Gy.
- Fig 5.7** **131**  
(A & B) Representative figure and bar graph respectively shows distribution of cells in different phases of cell cycle (G1, S, and G2/M) at 48 h, 72 h and 96 h following radiation exposure of 4 Gy by PI staining in CHO cells. (C & D) Representative figure and bar graph respectively shows distribution of cells in different phases of cell cycle (G1, S and G2/M) at 96 h post irradiation (4 Gy) under different treatment conditions.
- Fig 5.8** **133**  
Effect of DHS and DHS-C<sub>6</sub> pre-treatment (25 μM for 16 h) on γ-H2AX foci after radiation (2 Gy) exposure in CHO cells. (A) Bar graph shows the number of radiation (2 Gy) induced γ-H2AX foci at 30 minutes post irradiation. (B) Representative fluorescent images under different treatment conditions in CHO cells.

- Fig 5.9** **134**  
Effect of DHS and DHS-C<sub>6</sub> pre-treatment (25 μM for 16 h) on radiation (4 Gy) induced micronuclei frequency in CHO cells. Bar graph shows counts of radiation (4 Gy) induced micronuclei under different treatment conditions
- Fig 5.10** **135**  
(A & B) Effect of DHS and DHS-C<sub>6</sub> pre-treatment (25 μM for 16 h) on DNA repair kinetics in CHO cells after radiation (4 Gy) exposure and its modulation by MS treatment (10 mM) in terms of % TDNA and OTM respectively. DNA repair was monitored by comet assay as a function of post irradiation time (0 - 60 minutes).
- Fig 5.11** **137**  
Representative fluorescent images of cells stained with SYBR-Green-II at 30 minutes post irradiation under different treatment conditions by comet assay.
- Fig 5.12** **138**  
(A & B) Effect of NU-7026 (10 μM) and MS (10 mM) on the radioprotective activity of DHS and DHS-C<sub>6</sub> pre-treatment at 25 μM for 16 h in CHO cells against radiation dose of 4 Gy and 11 Gy respectively by clonogenic assay. (C) Representative images show colonies of CHO cells under different treatment combinations.
- Fig 5.13** **140**  
(A & B) Effect of UCN-01 (25 nM) and MS (10 mM) on the radioprotective activity of DHS and DHS-C<sub>6</sub> pre-treatment at 25 μM for 16 h in CHO cells against radiation dose of 4 Gy and 11 Gy respectively by clonogenic assay. (C) Representative images show colonies of CHO cells under different treatment combinations.
- Fig 5.14** **141**  
(A & B) Effect of PV-1019 (400 nM) and MS (10 mM) on the radioprotective activity of DHS and DHS-C<sub>6</sub> pre-treatment at 25 μM for 16 h in CHO cells against radiation

dose of 4 Gy and 11 Gy respectively by clonogenic assay. (C) Representative images show colonies of CHO cells under different treatment combinations.

**Fig 5.15**

**143**

(A) Effect of DHS or DHS-C<sub>6</sub> pre-treatment (25 μM for 16 h) on intracellular ROS production at 30 minutes post irradiation (4 Gy) in CHO cells. (B) Representative images of DCFDA stained cells under different treatment conditions at 30 minutes post irradiation (4 Gy). (C) Effect of DHS and DHS-C<sub>6</sub> pre-treatment (25 μM for 16 h) on GSH/GSSG ratio at 6 h post γ-irradiation (4 Gy).

**Fig 5.16**

**144**

Effect of DHS and DHS-C<sub>6</sub> pre-treatment (25 μM for 16 h) on mRNA expressions of *SelenoP-1* in CHO cells at 6 h post irradiation (4 Gy) as estimated by RT-PCR. The expression of above genes in different treatment groups was normalized against control group and the relative expression changes have been plotted. Actin expression was used as internal control

**Fig 5.17**

**146**

Effect of DHS and DHS-C<sub>6</sub> pre-treatment (25 μM for 16 h) on the radiation (4 Gy) induced apoptosis in lymphocytes. (A) Representative figure showing pre-G1 population at 48 h post irradiation by PI staining. (B) Bar graph shows percentage (%) of cells in pre-G1 phase under different treatment conditions at 48 h post irradiation by PI staining.

**Fig 5.18**

**146**

Effect of DHS and DHS-C<sub>6</sub> pre-treatment (25 μM for 16 h) on the radiation (4 Gy) induced apoptosis in lymphocytes. (A) DNA ladder assay at 24 h post irradiation (4 Gy) under different treatment conditions. (B) Effect on MMP estimated as ratio of red

( $\lambda_{em} = 610$  nm) and green ( $\lambda_{em} = 535$  nm) fluorescence intensity of JC-1 staining at 18 h post irradiation under different treatment conditions.

**Fig 5.19**

**147**

Effect of DHS and DHS-C<sub>6</sub> pre-treatment (25  $\mu$ M for 16 h) on the radiation (15 Gy) induced apoptosis in CHO cells. (A) Representative figure shows pre-G1 population at 48 h post irradiation by PI staining. (B) Bar graph showing percentage (%) of cells in pre-G1 phase under different treatment conditions at 48 h post irradiation by PI staining.

# **Chapter 1**

## **Introduction and Review of Literature**

This chapter gives a brief introduction of all the important topics related to the present thesis work. These include preliminary concepts on radiation biology, deleterious effect of radiation on biomolecules, DNA damage response and various DNA repair pathways. The chapter also contains details on history and development of radioprotectors, importance of selenium, its toxicity / essentiality, selenoproteins and recent developments on selenium radioprotectors. At the end of the chapter details about the selenium compounds employed for the present thesis are included.

## 1.1. Radiation

Radiation is the form of energy emitted as particles or electromagnetic waves from a material or space. Depending on the energy of emitted particles or waves, radiation can be classified into either non-ionizing or ionizing<sup>1</sup>. While the low energy non ionizing radiations were known to be ubiquitously present in the universe, the concept of ionizing radiation emerged with the discovery of X-ray in 1895 by a German physicist William Conrad Roentgen<sup>2</sup>. In the course of performing experiments with cathode tube, he discovered that some invisible rays could pass through the screen used to block the light. He named these rays as X-rays to designate something unknown. This was followed by another milestone discovery in 1896 by Antoine Henrie Becquerel that unstable nuclei like uranium salts are capable of emitting similar radiation naturally which is termed as radioactivity<sup>3-5</sup>.

Nuclear radiation has played an important role in human lives ever since its discovery. While such radiations have been known to induce unwanted and sometimes irreversible changes to living beings, they became indispensable tools and revolutionized the field of medicine especially in the treatment and diagnosis of cancer<sup>6</sup>. As the name suggests ionizing radiations whether electromagnetic (X-rays,  $\gamma$ -rays) or particulate ( $\alpha$ - particles, beta particles etc) have enough energy to eject an electron from atom or molecule and responsible for most of the biological damage. The energy transferred by radiation per unit length of the track is termed as linear energy transfer (LET). It is expressed as kiloelectron volt per micrometer of the material (KeV/ $\mu$ m). Heavy charged particles have high LET as compared to electromagnetic rays. Exposure to radiation is defined as the measure of intensity of radiation field. The S.I unit of exposure is coulombs per kilogram (C/kg) i.e the quantity of X-ray or  $\gamma$  ray that

produces 1 coulomb of charge per kg of air. The amount of energy from a given radiation source, which is deposited in the material of given mass is termed as absorbed dose. The S.I unit of absorbed dose is Gray (Gy) which is equal to one joule of energy deposited in one kilogram of material (1 J/kg). The traditional unit of absorbed dose is Rad which is equal to 0.01 Gy<sup>7,8</sup>.

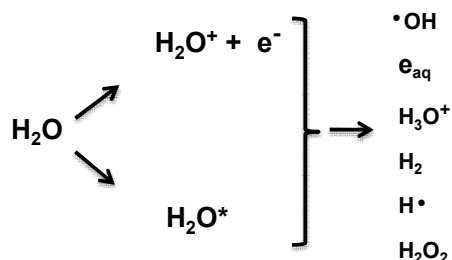
## **1.2. Radiobiology**

The first observed effect of radiation exposure on living organism came into light in 1895 when William Roentgen developed burns on exposure to X-rays. The first systematic experiment to demonstrate the biological effect of radiation exposure was performed by Becquerel in 1896, wherein he showed that radium (a radioactive element) caused skin erythema and ulcer. Later, radium was also found to be the cause of death of women working at US Radium dial painting factory. After the nuclear accident at Hiroshima and Nagasaki, 1945 several research laboratories initiated radiation biology to study the interaction of radiation with cells and living organism.<sup>9</sup>

## **1.3. Interaction of radiation with cells**

Ionizing radiation while interacting with cells causes primarily ionisation and excitation of bio-molecules. In general, two different types of effects are seen due to interaction of ionizing radiation with cells and are recognized as direct and indirect effects. In direct effect, the absorbed radiation causes direct damage of the biomolecules, initiating a chain of events leading to biological changes. This type of effect is mostly seen in high LET radiation ( $\alpha$  particles, neutrons, protons etc.). During indirect effect of radiation in cells, water being a major (70 %) constituent absorbs maximum radiation dose and undergoes ionisation and excitation (a process known as

radiolysis) producing highly reactive free radical species (Scheme. 1.1) like hydroxyl radical ( $\bullet\text{OH}$ ), hydrogen radical ( $\text{H}\bullet$ ), superoxide radical ( $\text{O}_2^{\bullet-}$ ) and peroxy radical ( $\text{ROO}\bullet$ )<sup>10-12</sup>. The indirect effect is mostly seen in low LET radiations (X-ray,  $\gamma$  ray) and accounts for 75 % of the total biological damage caused by radiation<sup>1</sup>. Radiolytically generated free radicals are termed as reactive oxygen species (ROS). ROS can damage biomolecules like lipids, proteins and DNA which is responsible for cell death, tissue injury and ultimately radiation syndromes<sup>10</sup>. The consequences of radiation effect to bio-molecules are described below.



*Scheme 1.1 Radiolysis of water*

### 1.3.1. Damage to lipids

Lipids are amphipathic molecules composed of fatty acids and glycerol or sterols. It is the constituent of cell membranes and plays an important role in signaling and energy storage. Lipid peroxidation is described as a process under which ROS generated during irradiation attack lipids containing carbon-carbon double bonds, especially polyunsaturated fatty acids (PUFAs). Lipid peroxidation consists of three steps: initiation, propagation and termination. During initiation, ROS abstracts hydrogen from a methylene group present in the lipid (LH) molecule resulting in the formation of lipid radical ( $\text{L}\bullet$ ).  $\text{L}\bullet$  as a carbon centered radical stabilizes itself by molecular rearrangement to form conjugated diene. In the propagation step, the lipid

radical reacts with oxygen present in the surrounding environment to form lipid peroxy radical ( $\text{LOO}^\bullet$ ). This radical is capable of abstracting a hydrogen atom from other lipid molecule producing new lipid radical ( $\text{L}^\bullet$ ) and lipid hydroperoxides ( $\text{LOOH}$ ). The peroxy radical generated will continue this chain reaction until the reaction is terminated by an agent capable of donating an electron to  $\text{LOO}^\bullet$ .<sup>13</sup> The primary products of lipid peroxidation are  $\text{LOOH}$  which is responsible for the formation of secondary products like malondialdehyde (MDA), propanal and 4 hydroxynonenal (4-HNE). MDA is mutagenic and generally used as a marker for the lipid peroxidation. The main consequences of lipid peroxidation are changes in membrane fluidity, formation of DNA-lipid adducts, modulation in cell signalling pathways, inflammation and cell death<sup>14</sup>.

### **1.3.2. Damage to proteins**

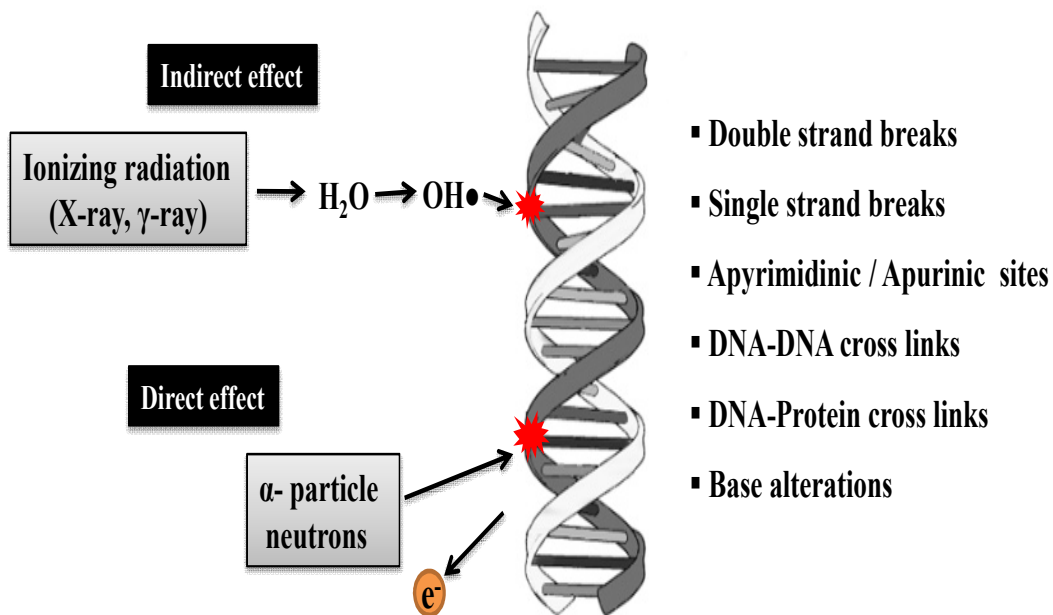
Proteins are one of the important targets for ROS mediated damage due to their abundance in the cell. Their diverse role as enzymes, transcription factors, growth hormones and cytokines accounts for their importance in the functioning of the cell. The sulfur containing amino acids like methionine and cysteine in a polypeptide chain are more susceptible to ROS mediated oxidation resulting in the formation of methionine sulfoxide and disulfides<sup>15</sup>. The major products of protein oxidation are carbonyls and aldehydes or ketones. The oxidative modification of proteins results in protein peroxidation, loss of secondary and tertiary structures, protein fragmentation, proteolytic degradation and protein-protein cross links. The consequences of protein damage are loss of enzymatic activity, changes in the cellular redox potential, inactivation / activation of transcription factors and altered signal transduction pathways<sup>16-18</sup>.

### 1.3.3. Damage to deoxyribonucleic acid (DNA)

DNA stores all the genetic information necessary for carrying out biological function. It is a double helical structure with two polynucleotide strands in anti-parallel direction. Each nucleotide is composed of a nitrogenous base, a deoxyribose sugar and a phosphate group. The nitrogenous bases of two chains are joined together by hydrogen bonds. Using DNA as a template, RNA strand is synthesized by a process called transcription. Each three bases of the RNA code for one amino acid. The process of synthesis of protein from RNA is termed as translation. The sequence of amino acid is crucial for the synthesis of a functional protein. If there is damage to the DNA integrity, it will lead to the loss of the genetic information required for the biological function. Any error in the DNA sequence will result in the transfer of incorrect information to the next generation, an event termed as mutation. Thus, DNA is the most critical target of radiation exposure. Among the ROS,  $\bullet\text{OH}$  radical is considered to be primarily responsible for most of the radiation induced DNA damage. It starts with hydrogen abstraction from the deoxyribose carbon or  $\bullet\text{OH}$  radical attack on the unsaturated electron rich bond of nitrogenous bases resulting in several changes including DNA strand breaks, abasic sites, base modification, DNA-DNA cross links and DNA-protein cross links (Scheme 1.2)<sup>10,12,19</sup>. Some of the products of base oxidation are 8-oxo guanosine (8-OHdG), thymine glycol, 5-methylcytosine etc. The reactivity of  $\bullet\text{OH}$  towards DNA moiety follows the order of pyrimidines > purines > deoxyribose<sup>20,21</sup>.

DNA strand breaks can be of two types: single strand breaks (SSBs) and double strand breaks (DSBs). If the break has occurred in one of the strands of DNA, it is termed as SSB. SSBs are repaired easily using opposite strand as a template. In contrast,

if the break happens in both the strands of DNA either opposite to one another or separated by few bases is termed as DSB. Unlike SSBs, DSBs cannot be repaired easily due to the lack of a template strand and is therefore the most lethal form of DNA damage. DSBs can lead to chromosomal aberrations<sup>21,22</sup>. The most common chromosomal aberrations are dicentrics, translocation, acentric fragments, rings and anaphase bridge. The acentric / chromosome fragments which are not incorporated in the daughter cell during cell division are termed as micronuclei (MN) as they are covered by nuclear membrane and identified as small nuclei in the dividing cells. The chromosomes which are not segregated during cell division due to microtubule or spindle failure can also form MN<sup>7,23</sup>.



*Scheme 1.2 Radiation induced DNA damage<sup>19</sup>*

#### 1.4. Cellular defense mechanisms

Every cell is equipped with endogenous defense mechanism to take care of the radiation induced oxidative damages. This includes antioxidants and a network of

interconnected repair pathways. A brief introduction of both is given in the below sections.

### **1.4.1. Antioxidants**

Antioxidants are the molecules which donate an electron to the free radicals and convert them to less reactive species. They maintain redox homeostasis in cells by balancing the concentration of oxidants and reductants. There are two types of antioxidants, enzymatic and non-enzymatic antioxidants<sup>24,25</sup>. Some of the enzymatic antioxidants are glutathione peroxidases (GPx), superoxide dismutase (SOD), thioredoxin reductases (TrxR) and catalase (CAT). GPx catalyses the conversion of organic hydroperoxides and hydrogen peroxide ( $H_2O_2$ ) to alcohol and water respectively. On the other hand, CAT specifically catalyses the conversion of  $H_2O_2$  to water. SOD is present in all aerobic organisms and converts highly reactive  $O_2^{\bullet-}$  to less reactive  $H_2O_2$  molecule. Some of the non-enzymatic antioxidants are glutathione (GSH), vitamin A, C, E, carotenoids, bilirubin etc. The mechanism of action of non-enzymatic antioxidants is either by free radical scavenging or by terminating the free radical chain reaction<sup>14,25</sup>.

### **1.4.2. Repair mechanisms**

#### **1.4.2.1. Cell cycle**

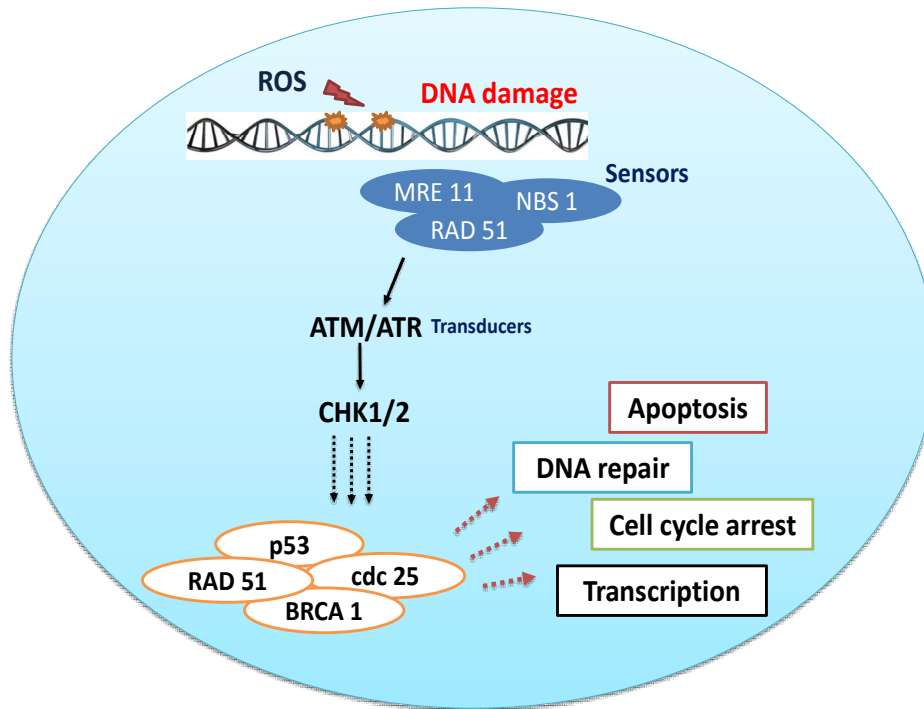
Cellular repair machinery takes care of the radiation induced DNA damage. Before going in to the detail of the repair process, a brief introduction of the cell division and checkpoint control is discussed. A eukaryotic cell passes through different steps namely G1, S, G2/M phases between two successive cell divisions. In G1 phase (first gap phase), cell prepares itself for cell division. In S phase (synthetic phases), cell

duplicates its DNA content. G2 is the second gap phase during which cell makes proteins which will be required for mitosis and cytokinesis. In M phase (mitotic phase), cytoplasm is divided into two parts with both carrying equal copies of DNA. Cell cycle is regulated by specific protein complexes termed as cyclin dependent protein kinases (CDKs). CDKs are serine-threonine kinases that phosphorylate proteins involved in DNA replication and cell cycle progression. There are four types of CDKs: CDK 1, 2, 4 and 6<sup>26,27</sup>. As the name suggests CDKs require specific cyclins to get activated. There are multiple cyclins depending on the stage of the cell cycle like cyclin D, E, A and B. All CDKs are present in equal amount throughout the cell cycle while the level of a cyclins varies with stages of cell cycle. The level of a particular cyclin - CDK complex drops as the cells move from one phase to the next phase and the cell cycle progresses. This is caused by the ubiquitin mediated degradation of the cyclins. D type of cyclins senses the external growth factor or mitogens and after binding with CDK 4 or CDK 6 regulates entry of cells in G1 phase. Cyclin E expression is maximal at the end of the G1 phase. It complexes with CDK 2 and favours G1/S phase transition. Cyclin E - CDK 2 complex can phosphorylate proteins which play a role in the process of DNA replication. Cyclin A binds to CDK 1/2 which regulates the completion of S phase, Cyclin B - CDK 1 regulates G2/M checkpoint and drives cells toward mitosis<sup>26-29</sup>. They can phosphorylate a large number of proteins like condensins which are responsible for chromosome condensation and others which regulate microtubule behavior and chromosome segregation. Therefore, the level of cyclins - CDKs determines the functioning and the fate the cell division. Cell cycle checkpoint monitors major events of the cell cycle like cell size, chromosome integrity and allows cell division to proceed only if DNA replication has occurred properly and all other

conditions are favorable. There are three known checkpoints, G1/S, G2/M and spindle checkpoint.

#### **1.4.2.2. DNA damage response**

For genomic integrity, cell has an inherent ability to detect initial DNA damage, and relay the signal to the effector molecules to evoke cellular responses including cell cycle arrest, DNA repair and apoptosis altogether termed as DNA damage response (DDR). Checkpoint kinase 1 (CHK 1) and checkpoint kinase 2 (CHK 2) are the key components of the DDR in mammalian cells<sup>30-32</sup>. They are structurally unrelated yet have similar function. Upon recognition of the DNA damage by sensor proteins Mre11, Rad 50, Nbs1 (MRN), it activates ATM (ataxia-telangiectasia-mutated) / ATR (ATM- and Rad3-Related) kinases which transduces signal to CHK 1/2. CHK 1 is primarily activated by ATR in response to SSBs while CHK 2 is activated by ATM in response to DSBs. Again, CHK 1 is active even during unperturbed cell cycle and gets further activated in response to DNA damage or stalled replication while CHK 2 gets activated specifically in response to DNA damage<sup>33</sup>. Upon activation, they pass the signal to a number of effectors like Cdc25A, Cdc25C, p53, Mdm2, BRCA1, Gadd45  $\alpha$  which can provoke cell cycle arrest for DNA repair or apoptosis depending on the severity of the damage. In brief, CHK 2 mediates phosphorylation of Cdc25C rendering it inactive. Cdc25C is required for the dephosphorylation and activation of the CDK. Thus CDK / Cyclin complex required for cell cycle progression from G2 to M phase is inhibited and cell cycle arrest occurs which is required for DNA repair<sup>30,31,34</sup>. The pathway for DNA damage response is represented in scheme 1.3.



*Scheme 1.3 DNA damage response<sup>33,35</sup>*

### 1.4.2.3. DNA repair

For efficient removal of any damaged DNA, cells have repair system like base excision repair, nucleotide excision repair, photoreactivation, non homologous end joining (NHEJ) and homologous recombination (HR). Although cells possess different types of repair systems, each is relatively specific for a certain type of DNA damage. For example, when there is a modification or loss of a small sequence of bases in DNA strand, excision repair occurs during which DNA glycosylases excise the damaged DNA, polymerases add the original DNA sequence using the undamaged strand as its template and the double helix is sealed by DNA ligase<sup>36</sup>. Ionizing radiation induced DSBs are generally repaired by NHEJ and HR pathways.

**NHEJ** is the major pathway of DSBs repair in eukaryotes. It does not require a homologous sequence and directly ligates the DNA strands using micro homologies in the overhangs of the broken DNA segment. It is error prone and not restricted to a particular phase of cell cycle. It comprises of three steps: DNA end binding, terminal end processing and ligation. The NHEJ pathway of DNA repair starts with the recognition and the binding of Ku heterodimers (Ku70/80) to the broken end of the DNA. Ku heterodimers forms a ring like structure encircling the duplex DNA to stabilize the overhangs. Ku acts as a scaffold for the recruitment of the catalytic machinery like DNA protein kinase (DNA-PKcs), X-ray repair cross-complementing protein 4 (XRCC4), DNA ligase IV of the NHEJ pathway. The next step is to make ends of the DNA ligatable. It is done with the help of end processing enzymes like artemis, werner, aprataxin etc. Artemis cleaves the end of the damaged DNA by its 5' and 3' endonuclease activity. Werner is a helicase and facilitates cleavage of the DNA with its 3' to 5' exonuclease activity. Aprataxin helps in ligation of the blunt ends by DNA ligase IV and repair the DSBs<sup>36,37</sup>.

**HR** pathway requires a homologous template for the synthesis of the broken end. HR is mostly predominant in cells during S phase. HR is the more efficient mechanism of cell repair and is less error prone. The first step in HR pathway is the resection of the 5' to 3' end to generate 3' single strand tail. The 3' ends are bound by replication protein A (RPA) to stabilize the structure and to facilitate the recruitment of the Rad 51 for homology search. After the homologous sequence is identified, Rad 51 mediates strand invasion wherein the damaged DNA invades the sister chromatid and form a four-way junction termed as 'Holliday Junction'. The junction is then resolved

either by dissolution or endonuclease activity resulting in error free joining of the DSBs<sup>38</sup>.

### **1.5. Oxidative stress**

When cell's endogenous antioxidant defense system and repair mechanism are unable to check the ROS induced damage to biomolecules, it results in a physiological condition termed as oxidative stress. Radiation also leads to oxidative stress in cells through ROS generation. In response to radiation induced oxidative stress, various signalling pathways like MAPK, JNK and p53 are activated which may lead to cell death<sup>39</sup>. An irradiated cell can undergo death by three different mechanisms as described below:

**Apoptosis** known as programmed cell death is considered to be the major mode of radiation induced cell death in radiosensitive cells. In response to irradiation, primarily the intrinsic pathway (mitochondrial release of cytochrome c and subsequent apoptosome formation) is activated to mediate apoptosis. However, depending on the absorbed dose and cell type other apoptotic pathways like the extrinsic pathway (death receptor-mediated caspase activation) or the membrane stress pathway (ceramide production and subsequent second messenger signalling) may also be activated. The intrinsic pathway is initiated by DNA damage triggering the activation of p53 and downstream signalling proteins like Bax, Bid, caspases and nucleases<sup>40</sup>.

**Necrosis** is characterized by the early rupture of the plasma membrane, dilatation of cytoplasmic organelles and uncontrolled release of cytoplasmic contents. Necrosis typically occurs from a higher magnitude of stress resulting from high dose radiation exposure. In contrast to apoptosis, necrosis is associated with increased

inflammation of the surrounding normal tissue. The molecular mechanism leading to necrotic cell death is not fully understood. It is presumed to occur due to energy (ATP) depletion resulting in cell swelling, mitochondrial permeability and activation of receptor interacting proteins 1 and 3 (RIP1 / RIP3)<sup>41</sup>.

**Mitotic catastrophe** also termed as reproductive death occurs due to the improper entry of cells in the mitosis without completion of S phase. It results due to lack of functional checkpoints, DNA repair and activation of p53. It is the prime mode of cell death induced by ionizing radiation in epithelial cells<sup>42</sup>.

### **1.6. Cellular response to radiation**

Cellular response to radiation varies depending on the cell type. For example, cells which are undifferentiated, immature and actively dividing (stem cells, lymphoid organs, reproductive organs, stomach mucosa, bone marrow, basal layer of skin and intestinal crypts) are radiosensitive whereas cells which are differentiated, mature and not actively dividing (brain, bone, pituitary and liver) are radioresistant<sup>43,44</sup>. The radiosensitivity of cells also depends on the phase of the cell cycle. S phase is the most radioresistant as the DNA strands are open for replication and easy for the repair enzymes to function. M phase is the most radiosensitive as the chromosomes are condensed and there is no checkpoint after this phase<sup>45</sup>. Moreover, an equal absorbed dose of different types of radiation does not produce the same biological effect. Radiation weighing factor ( $W_R$ ) defines the effectiveness per unit dose of a particular type of radiation. The absorbed dose multiplied with  $W_R$  gives equivalent dose and its S.I. unit is Sievert (Sv)<sup>7,46</sup>.

$$\text{Equivalent Dose} = \text{Absorbed Dose (Gy)} \times \text{Radiation weighing factor (} W_R \text{)} \quad (1.1)$$

The effect of radiation on biological system also depends on the radiosensitivity of tissues and organs. Thus, a new term effective dose is introduced which considers tissue sensitivity of different organs and is expressed as:

$$\text{Effective Dose} = \text{Equivalent dose} \times \text{Tissue weighing factor (W}_T\text{)} \quad (1.2)$$

The biological damage also depends on the dose rate of radiation. Dose rate is defined as the amount of radiation received by an individual in a particular span of time. High dose rate delivers large amount of radiation in a short span of time leading to acute damage<sup>7,46</sup>.

### 1.6.1. Cell survival curve

The cellular response to radiation dose is described by the cell survival curve which plots survival fraction on a log scale against radiation dose on a linear scale. The shape of the survival curve varies for high LET and low LET radiation as shown in figure 1.1. For high LET radiation like  $\alpha$  particles and neutrons, the curve is linear with survival function as an exponential function of the entire dose range. For low LET radiation like X or  $\gamma$  rays, the curve is linear at low dose, followed by a shoulder region and then becomes linear again at high dose (Fig 1.1 A).

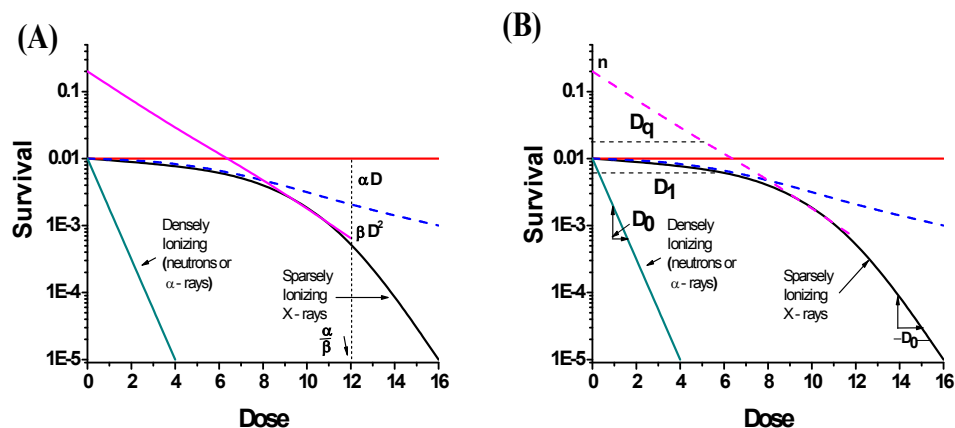


Figure 1.1 Shape of cell survival curves<sup>7</sup>

The linear quadratic model (LQ) is used to describe the shape of the cell survival curve. According to LQ, cell killing results from the chromosomal aberration (rings, dicentrics etc) which is caused due to DSBs. The DSBs can occur either by single event killing or two event killing. At low dose, there is a likelihood of single particle causing two breaks in the DNA strand and therefore the survival is proportional to the dose. At high dose, there is a more chance of different charged particles to produce two breaks in the DNA strand, therefore survival is proportional to the square of the dose (Fig 1.1 A) and expressed as,

$$S = e^{-(\alpha D + \beta D^2)} \quad (1.3)$$

Where S is the number of cell surviving, D is dose,  $\alpha$  and  $\beta$  are constants describing the initial slope and quadratic component of survival curve. Further, survival curve is used to estimate parameters like  $D_i$ ,  $D_0$  and n (Fig. 1.1 B). The  $D_i$  and  $D_0$  are the values of radiation absorbed dose required to reduce survival fraction from 1 to 0.37 and 0.1 to 0.037 respectively. The n known as the extrapolation number defines the shoulder width. It is obtained by extrapolating the exponential portion of the curve to the Y axis (survival fraction) and is indicative of cellular radiosensitivity<sup>7</sup>.

### 1.6.2. Acute radiation syndromes

As described in section 1.6.1, cellular damage is the first event that is considered to be the origin of organ and tissue damage resulting in acute and chronic syndrome. Acute radiation syndrome (ARS) occurs after whole body irradiation (WBI) with absorbed dose exceeding 1 Gy delivered at a relatively high dose rate<sup>47</sup>. There are basically three classes of ARS: **Hematopoietic syndrome** occurs at a dose ranging from 2 - 6 Gy<sup>48-50</sup>. The primary cause of death is the destruction of the lymphocytes, progenitor cells, bone marrow cells resulting in infection, poor wound healing,

hemorrhage and ultimately mortality within 30 days<sup>51,52</sup>. **Gastrointestinal syndrome** becomes visible at radiation dose ranging from 8 - 15 Gy. It results in denudation of villi, inflammation, loss of intestinal crypt cells and breakage of mucosal barrier. The clinically visible disorders of GI syndrome are dehydration, electrolyte imbalance, abdominal pain, diarrhoea, nausea, vomiting and ulcers. Death usually occurs within 2 weeks due to destructive and irreparable changes in the GI tract. **Cerebrovascular syndrome** (20 – 25 Gy) is characterized by damage to the non-dividing cells such as neurons. It usually results in loss of coordination, convulsions, respiratory distress, cerebral edema. Death occurs within 3 days as the damage is irreparable due to increased pressure in the cranial vault<sup>48,53–55</sup>.

### **1.6.3. Chronic radiation syndromes**

Chronic radiation syndrome (CRS) occurs in a time frame of 6 - 12 months after a long term exposure to radiation with low dose rate ( $< 0.1$  mGy/min)<sup>56</sup>. It is mostly seen in occupational workers who unknowingly are exposed to low dose of radiation. The mechanism leading to CRS is not clear but is suggested to be triggered by radiation induced oxidative stress causing a classical inflammatory response characterized by local leukocyte infiltration and disturbance in cytokine production. The clinical symptoms of CRS are skin atrophy, cataract, burns, cardiovascular disease, fibrosis and pneumonitis<sup>56</sup>. Some of the cytokine known to be upregulated in CRS are inducible nitric oxide synthase (iNos-2), chemokine (C-C motif) ligand 2 (Ccl-2), intracellular adhesion molecule (ICAM-1), vascular adhesion molecule (VCAM-1) among others. All these recruit monocytes, memory T cells and dendritic cells to the sites of inflammation. iNos-2 is responsible for the synthesis of nitric oxide (NO) which generates reactive nitrogen species (RNS) and ROS to kill invading pathogens. VCAM-

1 and ICAM-1 are adhesion molecules which increase the vascular permeability allowing the attachment of leukocytes to the endothelium and permit their subsequent transmigration into peripheral tissue<sup>57-59</sup>. Inflammatory process is amplified by the activation of resident mast cells both producing pro-inflammatory and pro-fibrosing mediators such as IL-1 $\beta$ , IL-6, IL-8, TNF- $\alpha$  and TGF- $\beta$ <sup>60-62</sup>. TGF- $\beta$  activates the production of extracellular matrix protein (ECM) and inhibits their degradation. In normal condition, they help in tissue repair and restore the normal tissue architecture. However, if the level of TGF- $\beta$  is uncontrollable it will lead to fibrosis and hamper tissue functioning<sup>63,64</sup>.

### **1.7. Radiation protection**

All living beings are continuously exposed to natural background radiation sources. This includes cosmic rays from outer space, terrestrial radiation from radioactive material present in the earth and internal radiation from the radioactive potassium-40 and carbon-14 present in the body. The average effective dose received from natural background is 2.4 mSv annually. People can get exposed to radiation by other means also which can be planned or unplanned. Radiation exposure during radiotherapy, medical diagnosis, space programme is termed as planned exposure whereas exposure during nuclear accidents and occupational activities is termed as unplanned exposure. For these exposures, dose limits have been set by international commission on radiological protection (ICRP) in order to ensure protection and safety of the individual. The justification of dose limit is that the radiation exposure of an occupation worker or general public should be limited to as low as reasonably achievable (ALARA). The dose limits for public exposure is 5 mSv in 5 years and for occupational worker it is 100 mSv in 5 years with a maximum of 50 mSv in a year.

Apart from these, additional safety measures like proper radiation shielding, rotation in the work hours and distant handling of radioactive material are followed in the nuclear establishments. In spite of all these regulations, there is a possibility of unwanted exposure. Therefore, to protect normal tissue from toxicities of unwanted radiation exposure, radioprotectors are employed<sup>7</sup>.

### **1.7.1. Radioprotectors**

Radioprotectors are agents designed to protect normal cells from radiation induced damages. These agents can also be used as adjuvants in radiotherapy if they can increase the tolerance of the normal cells without affecting or increasing the sensitivity of the tumor. The search for a radioprotector started six decades ago soon after the Second World War. An ideal radioprotector is one which is i) safe with no undesirable side effects, ii) easily administrable (oral) with rapid absorption and uniform distribution throughout the body, iii) chemically stable, iv) inexpensive and v) does not protect tumor<sup>65</sup>. The most reliable parameter to assess the efficacy of a radioprotector is the dose modifying factor (DMF)<sup>66,67</sup>. It is defined as the ratio of radiation absorbed dose required to affect a particular end point with and without radioprotector. In animal studies, the most commonly used end point is 30 day post irradiation survival. DMF varies depending on type and dose rate of radiation, biological end point and dosage, time and schedule of drug administration<sup>68-70</sup>. Radioprotectors can be classified into three types based on time of their administration<sup>71,72</sup>.

1. Prophylactic agent – They are given prior to radiation exposure and are useful during planned exposure such as radiotherapy.

2. Mitigators – They are given after the radiation exposure but before the development of the clinical symptoms of radiation induced damage to tissues.
3. Therapeutic agent – They are given after irradiation to treat the symptoms of radiation sickness in the individual.

### **1.7.2. Strategies to develop radioprotectors**

As radiation induced damage is mediated through generation of ROS, compounds which can scavenge ROS have been the first choice of researchers for evaluation as radioprotectors<sup>70</sup>. Accordingly, studies on free radical scavengers like GSH, flavonoids, vitamin A, C and E were reported to protect mice against radiation induced lethality. Endogenous antioxidants such as GPx, SOD and catalase were also reported to reduce the radiation induced mortality, hematopoietic syndrome and chromosomal damage in mice model system<sup>69,70</sup>. In the next section, thiols which are excellent free radical scavengers present in the cells are discussed in detail.

#### **1.7.2.1. Sulfhydryl compounds as radioprotectors**

Thiols (sulfur based compounds) present in the body can donate electron to the unstable molecules and convert them to less reactive species. The first study on the protective effect of a sulfur compound against ionizing radiation was performed half century ago by Patt et al. in 1949<sup>73</sup>. They reported that cysteine, a thiol amino acid, protected rats from a lethal dose of X-rays. This prompted department of Atomic Energy, USA to initiate an Antiradiation Drug Development Program at Walter Reed Army Institute of Research (WRAIR). Under this programme, more than 4000 sulfur compounds were screened for their ability to improve the survival of mice exposed to lethal dose of irradiation; among these the only compound WR-2721 later known as

amifostine showed promising result with acceptable toxicity<sup>74</sup>. After clinical trial in 1980, amifostine was approved by FDA for use as a protectant against radiation induced xerostomia in head and neck cancer patients. It was also found to protect against cisplatin induced nephrotoxicity, bleomycin-induced toxicity and toxicity induced by doxorubicin. Amifostine principally works by free radical scavenging and DNA repair<sup>75</sup>. Amifostine though approved clinically is not used as a general radioprotector due to its toxicity at the radioprotective dose warranting research for effective and non-toxic radioprotectors<sup>76</sup>. Accordingly, researchers have explored other strategies to develop radioprotective agents like growth factors, cytokines, interleukins and cell cycle modulators as discussed below<sup>65,77,78</sup>.

#### **1.7.2.2. Other radioprotectors**

Basic fibroblast growth factor (bFGF) has been shown to protect against radiation induced lethality by promoting recovery of all cell lineages and megakaryocytes of the irradiated mice. Similarly, keratinocyte growth factor (KGF) is a prophylactic and therapeutic agent that has been shown to facilitate DNA repair and scavenge ROS. KGF is also approved by FDA to treat radiation induced oral mucositis in cancer patients undergoing radiation and chemotherapy<sup>65,79,80</sup>. A large number of cytokines like IL-1, IL-3, IL-4, G-CSF, GM-CSF, erythropoietin (EPO) have been shown to accelerate bone marrow recovery after radiation exposure by increasing the proliferation of hematopoietic stem cells. Some of them like G-CSF, GM-CSF and IL-1 are approved by FDA to treat radiation induced myelosuppression in cancer patients<sup>65</sup>. Genistein, an isoflavone has also been shown to exhibit radioprotective effects through antioxidant action and by modulating cell cycle<sup>67</sup>. Genistein offered protection to normal cells while promoting G2/M cell cycle arrest in cancer cells<sup>69</sup>. The currently

available agents still under investigation to develop as a radioprotector is given in table

1.1.

*Table 1.1: List of promising radioprotectors*

<b>Compound</b>	<b>Mode of action</b>	<b>Beneficial use</b>
Amifostine	Protects form DNA damage, free radical scavenger	Approved by FDA to treat radiation induced xerostomia in head and neck cancer patients <sup>7,75</sup>
Genistein	Cell cycle modulator	Reduces pain / diarrhoea in patients undergoing radiotherapy of the abdomen <sup>78,77</sup>
KGF (Palifermin)	Growth factor	Approved by FDA to reduce mucositis in patients undergoing radiotherapy <sup>79,80</sup>
Halofuginone	TGF- $\beta$ inhibitor	Reduces fibrosis in patient undergoing radiotherapy <sup>71</sup>
G-CSF (Filgrastim)	Cytoprotectant	Approved by FDA for regeneration of neutrophils and platelets in patients undergoing radiotherapy <sup>82,83</sup>
Synthokine	IL-3 agonist	Reduces thrombocytopenia in patients undergoing radiotherapy <sup>84,85</sup>
IL-6	Cytokine	Therapeutic administration accelerates hematopoietic recovery, enhances regeneration of platelets after radiotherapy <sup>86</sup>
Tempol	Cytoprotectant, free radical quencher	Mitigate radiation induced acute injury <sup>86</sup>
Granisetron (Kytril)	Anti-emetic; 5-HT3 inhibitor	Approved by FDA for control of gastrointestinal disturbances in patients undergoing radiotherapy

### **1.7.3. Limitations of existing radioprotectors**

Unfortunately, none of the radioprotectors available till date possess all the properties of an ideal radioprotector. For example, the antioxidant radioprotectors provide protection by free radical scavenging for which they must be present in sufficient concentration inside each and every cell at the time of irradiation which may not be possible due to their poor bio-availability<sup>87,88</sup>. Additionally, most of them provide protection at low dose of radiation and have low DMF. All these are the major

drawbacks in the development of antioxidants as clinical radioprotectors. Further, cytokine radioprotectors help in recovery of hematopoietic stem cells by stimulating their regeneration in bone marrow and therefore are useful only in case of hematopoietic syndromes. Moreover, due to pleiotropic nature of cytokines, they can lead to undesirable side effects<sup>88</sup>. The other limitations of available radioprotectors are:

1. Unfavorable route of administration.
2. Lack of differential toxicity between normal and tumor cells.
3. Slow clearance of the metabolic products from the body.
4. High cost of treatment.

Therefore, the need of the hour is to develop an agent which can prevent from acute radiation syndrome and organ specific toxicity. In the present era, selenium compounds are gaining importance as radioprotective agents. The present thesis deals with the evaluation of selenium compounds as radioprotectors. Therefore, a brief introduction about selenium is given in subsequent sections.

## **1.8. Selenium**

Selenium was discovered by a Swedish Chemist Jons Jacob Berzelius in 1817 and named after the Greek Goddess of the moon Selene<sup>89</sup>. Selenium belongs to the 16<sup>th</sup> group of the periodic table or the group of chalcogens along with oxygen, sulfur, tellurium and polonium<sup>90</sup>. Its atomic number is 34 and atomic weight is 78.96. In 13<sup>th</sup> century, selenium toxicity was first observed by Marco polo in North West China. In 1856, Madison observed severe loss of weight, lack of hair, emaciation in horses grazing near Fort Randall in USA which was termed as alkali disease<sup>91,92-95</sup>. In 1934,

Franke and collaborators found selenium as the etiological agent of alkali disease<sup>96,97</sup>. Later in 1967, Magg and co-workers found that high dietary intake of selenium can lead to a disease termed as 'blind stagger' due to accumulation of selenium in the tissues<sup>98</sup>. This was characterized by impaired vision, lower appetite and shedding of hooves creating 'selenophobia' among people<sup>99</sup>. For the first time in 1957, Schwartz and Foltz demonstrated the nutritional essentiality of selenium in prokaryotes<sup>100</sup>. In the same year, selenium was found to be an essential nutrient for rats. Selenium deficiency was found to be linked to several diseases like white muscle disease in sheep, mulberry heart disease in swine, Keshan disease (heart disease) and Kashin-Beck disease (rheumatoid condition) in humans<sup>101-103</sup>. In 1973, selenium was reported to be present in some bacterial enzymes like formate dehydrogenase and glycine reductase<sup>104,105</sup>. It was also found to be present at the active site of the redox regulatory enzymes like GPx, TrxR, selenoprotein P (SelenoP) and iodothyronine deiodinase (DIO)<sup>106-110</sup>. Further studies indicated that selenium supplementation at supra-nutritional level prevented initiation of cancer in animals and human<sup>111</sup>. Due to the increasing evidences on selenium essentiality and toxicity, it started to be known as an 'essential poison' demanding strict regulation on the dietary levels of selenium<sup>99</sup>.

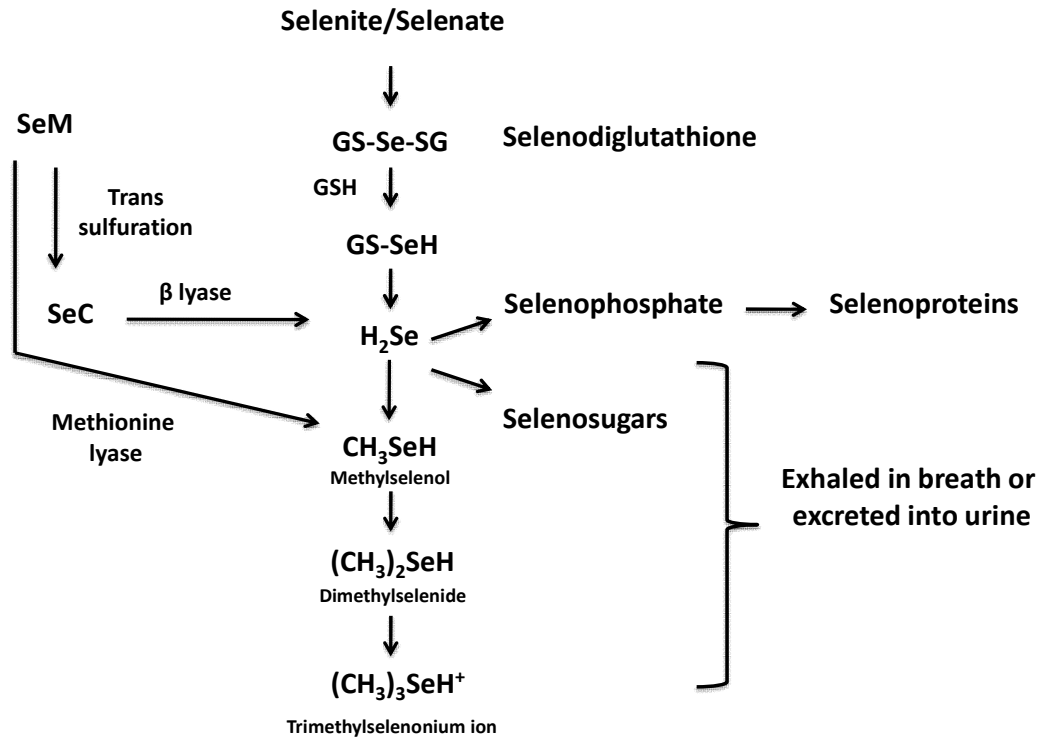
### **1.8.1. Selenium as a micronutrient**

Selenium is an essential micronutrient with a minimum daily requirement of 50 µg Se / per day<sup>101</sup>. The major source of selenium to animal is from diet i.e. plant and meat products. Some selenium rich foods are broccoli, mushrooms, radishes etc. Plants absorb selenium from soil which gets converted into organic forms like selenomethionine (SeM), selenocysteine (SeC) and methylselenocysteine<sup>112,113</sup>. Animals receive selenium from plants mainly in the form of SeM. In cells, SeM either

gets non-specifically incorporated into proteins in place of methionine or is metabolised to hydrogen selenide ( $\text{H}_2\text{Se}$ ) which gets incorporated into selenoproteins. The biosynthetic pathway for SeC is complex and requires several enzymatic steps. SeC tRNA is initially charged with serine by seryl-tRNA synthetase to form seryl-tRNA. The seryl moiety is converted to O-phosphoseryl-tRNA<sup>[Ser]Sec</sup> by a phosphokinase. SeC synthase (SecS) replaces oxygen in the O-phosphoseryl-tRNA<sup>[Ser]Sec</sup> by a selenium atom generating selenocysteyl-tRNA<sup>[Ser]Sec</sup>. The SeC tRNA is used in translating mRNA for selenoproteins. SeC is regarded as the 21<sup>st</sup> amino acid and has specific genetic codon UGA<sup>114-116</sup>. SeC is the only known amino acid in eukaryotes whose biosynthesis occurs on its tRNA.

### **1.8.2. Selenium metabolism**

Selenium whether organic (SeM, SeC etc) or inorganic (selenite, selenite etc) undergoes metabolism to produce selenoproteins or methylated selenium intermediates. Selenite ( $\text{Na}_2\text{SeO}_3$ ) and selenate ( $\text{Na}_2\text{SeO}_4$ ) form selenodiglutathione (GSSeSG) which undergoes reduction by thiols or NADPH dependant reductases to generate hydrogen selenide ( $\text{H}_2\text{Se}$ ). Selenophosphate synthetase converts  $\text{H}_2\text{Se}$  to selenophosphate which gets incorporated into selenoproteins.  $\text{H}_2\text{Se}$  can also undergo methylation using thiol S-methyltransferases to generate methylselenol and dimethylselenide which are exhaled via breath or excreted in the urine. Selenium is also excreted in the urine as trimethylselenonium ion and selenosugars. The methylated intermediates of selenium are considered to be non-toxic<sup>117</sup>. The pathway of selenium metabolism is given in scheme 1.4.



*Scheme 1.4 In vivo metabolism of selenium<sup>214</sup>*

### 1.8.3. Selenoproteins

The proteins which contain selenocysteine at the active site are termed as selenoproteins<sup>118</sup>. They are present in all classes of living beings including algae, bacteria, archaea, except plants and fungus. Till now 25 selenoproteins are known to be present in mammals having unique physiological functions<sup>119</sup>. The properties of some of the selenoproteins are listed below.

#### 1.8.3.1. TrxR

The classical thioredoxin (Trx) system consists of TrxR, NADPH and Trx. Trx R plays an important role in maintaining cellular redox homeostasis through its disulfide reductase activity. In mammalian cells, TrxR exists in three different isoforms: TrxR1 is cytosolic or nuclear. TrxR 2 is present in mitochondria and TrxR 3 or TGR

(thioredoxin-glutathione reductase) is testis specific. The main function of TrxR is to regenerate reduced Trx within cells<sup>120</sup>. Trx is critical for redox regulation of protein function and signalling. For example, it is required for the DNA binding of NF- $\kappa$ B, a transcription factor which controls the expression of cytokines and genes involved in regulation of cell growth and apoptosis<sup>121</sup>.

### **1.8.3.2. Deiodinases**

The iodothyronine deiodinases (DIO) is essential for thyroid hormone metabolism. There are three types of deiodinases (DIO 1, DIO 2 and DIO 3) which play an important role in the activation and deactivation of thyroid hormones. Deiodinases are homodimeric integral membrane proteins. DIO 1 and DIO 2 are present in plasma membrane whereas DIO 3 is located in endoplasmic reticulum membrane. They contain selenium in active site as selenocysteine. DIO 1 and DIO 2 catalyse the conversion of thyroxine (T4) to biologically active T3 hormone. DIO 3 inactivates T3 and prevents T4 activation. The thyroid hormone is essential for the development and differentiation of cells, regulation of basal metabolism and protein synthesis<sup>122</sup>.

### **1.8.3.3. SelenoP**

SelenoP is an extracellular glycoprotein and contains most of the selenium present in the plasma (“P” illustrates the plasma localization of this protein). It contains 10 SeC residues per polypeptide chain and accounts for 50 % of the total plasma selenium level. It is produced in the liver and then secreted in the plasma and therefore considered to be the source of selenium supply for most tissues. Some of the *in vitro* studies have shown that incubation of rat serum with mercuric chloride (HgCl<sub>2</sub>) resulted in formation of Hg-SelenoP complex. This suggested that SelenoP might have a role in heavy metal detoxification. This assumption is also supported by the presence

of a metal responsive element (MRE) in murine SelenoP promoter. Another important function of SelenoP is to act as an antioxidant. Some literature reports indicate that administration of SelenoP protects tissues from oxidative injury and subsequent inflammation<sup>123,124</sup>.

#### **1.8.3.4. GPx**

GPx is a family of isozymes that protects biomembranes and other cellular components from oxidative damage. It catalyses the reduction of H<sub>2</sub>O<sub>2</sub> and organic hydroperoxides to water or corresponding alcohols using GSH as the reductant. Till now, 8 different GPx isoforms (GPx 1 - GPx 8) have been identified in mammals. Among these, GPx 1-4 and GPx 6 are selenoproteins containing SeC at its active site. GPx 6 is a selenoprotein in human but not in rats and mice. The other three GPx isoforms GPx - 5, 7 and 8 are selenium independent and do not require SeC for catalytic activity. GPx 5, 7 and 8 with cysteine at its active site exhibit low GPx activity<sup>125</sup>. Here only selenium containing GPxs are explained in detail.

**GPx 1** was the first selenoprotein identified in 1973 by Flohe et al<sup>126</sup>. It is a homotetramer ubiquitously present in the cytosol and mitochondria and accounts for 90 % of total GPx present in the cell. GPx 1 is involved in preventing the harmful accumulation of intracellular H<sub>2</sub>O<sub>2</sub>. The genetic deletion of GPx 1 in mice model leads to lethality in embryonic stage suggesting it to be an essential antioxidant enzyme. GPx 1 has also been shown to play a role in cancer prevention by preventing oxidative DNA modification in the initiation phase of cancer development<sup>127</sup>.

**GPx 2** is mainly expressed in the intestine and therefore called as gastrointestinal GPx (GPx-GI). GPx 2 is a homotetramer closely related to GPx 1. It protects intestinal

epithelium from absorption of the food borne hydroperoxides. GPx 2 is mainly found in the crypt cells of the colon where intestinal stem cells reside. Wnt signalling pathway controls the growth and differentiation of intestinal stem cells. Interestingly the same signalling pathways also regulate the expression of GPx 2 suggesting biosynthesis of GPx 2 via Wnt pathway may have a role in the self renewal of the intestinal epithelial cells and maintenance of mucosal lining<sup>128</sup>. GPx 2 also suppresses cyclooxygenase 2 (COX2) expressions and subsequent prostaglandin (PGE<sub>2</sub>) production and therefore is expected to play anti-inflammatory role<sup>129</sup>.

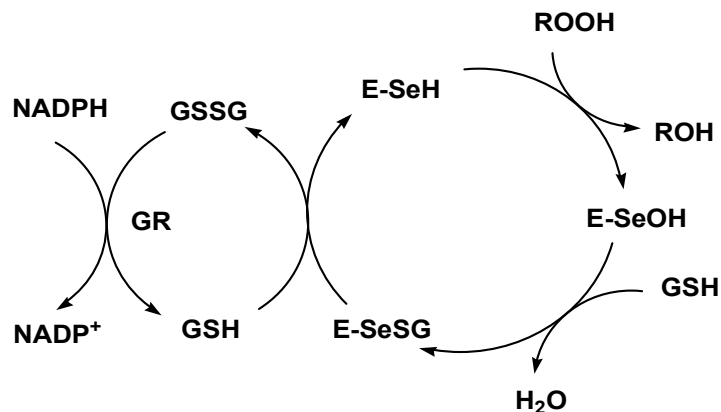
**GPx 3** a homotetramer is synthesized in the cells of proximal convoluted tubules of the kidney and secreted in the plasma. It is the only extracellular form of GPx known as plasma GPx (pGPx). Together with SelenoP, GPx 3 accounts for 97 % of the plasma selenium. It is also present in the basement membrane of epithelial cells of intestine, bronchi and cortex tubule of kidney. Like other GPxs, GPx 3 prevents from hydroperoxide mediated inflammation.

**GPx 4** also known as phospholipid hydroperoxide GPx (pHGPx) is an intracellular enzyme and reduces phospholipid and cholesterol ester hydroperoxides. In contrast to other GPxs, it is a monomer having three different isoforms, cytosolic (cGPx4), mitochondrial (mGPx4) and sperm nuclear (snGPx4)<sup>125,130</sup>. It can use either GSH or thiol as a reductant depending on the availability and thus functions as GSH peroxidase or thiol peroxidase. GPx 4 is expressed in the neuronal cells in the brain and plays a pivotal role in brain development and function.

**GPx 6** a close homologue of GPx 3, is present in the olfactory epithelium. It is a selenoprotein in humans but contains cysteine residue in rats and mice. Its function is not fully known.

#### 1.8.4. Catalytic mechanism of selenium containing GPx

The selenol ( $E\text{-SeH}$ ) present in SeCys residue plays a crucial role in the catalytic activity of GPx. It reacts in the form of selenolate ion ( $E\text{-Se}^-$ ) with  $\text{H}_2\text{O}_2$  and gets converted to selenenic acid ( $E\text{-SeOH}$ ). By using GSH as a reductant,  $E\text{-SeOH}$  gets converted to selenenyl sulfide ( $E\text{-Se-SG}$ ). A second GSH molecule regenerates the original selenol form by reducing  $E\text{-Se-SG}$  through a thiol-disulfide exchange. In the process, GSH gets converted to GSSG which is reduced back to GSH in presence of glutathione reductase (GR) using NADPH as a reducing equivalent<sup>131</sup> The regenerated  $E\text{-SeH}$  form is now available for the next cycle of reaction (Scheme 1.5).



*Scheme 1.5 Catalytic cycle of glutathione peroxidase<sup>126</sup>*

#### 1.8.5. Selenium as radioprotectors

As discussed in section 1.7.2.1, sulfur compounds are reported in literature for radioprotective activity, while similar reports on selenium were very few. Selenium being more nucleophilic with higher free radical scavenging activity than sulfur was

expected to be a better candidate for evaluation as a radioprotector. Additionally, as discussed in previous section selenium has advantage of being a micronutrient and a constituent of antioxidant selenoenzymes like *GPx*, *TrxR* and *SelenoP*<sup>107,109,125</sup>. In this regard, inorganic selenium compounds like sodium selenite have been extensively studied for radioprotection in pre-clinical models. These studies in general have indicated the beneficial effect of sodium selenite administration (100 µg to 1 mg/kg b.wt) in improving the 30 days survival as well reducing the organ specific toxicities<sup>132</sup>. Based on these observations, sodium selenite has even been tested in clinics to reduce radiotherapy induced side effects like mucositis, xerostomia, lymphedema and diarrhoea. As of today, as many as 17 clinical trials have been conducted involving sodium selenite and radiotherapy. These trials have concluded that sodium selenite supplementation neither reduced the effectiveness of radiotherapy nor caused any toxicity at the administered doses and at same time improved the quality of life of cancer patients<sup>133-136</sup>. Unlike inorganic selenium, organoselenium compounds are still under pre-clinical stage of evaluation and needs further studies.

#### **1.8.5.1. Organoselenium compounds as radioprotectors**

As organic form of selenium is considered to be lesser toxic than inorganic form due to the faster clearance of the selenide intermediates formed during selenium metabolism, researchers are focussing on the design and development of non-toxic organic selenium drugs as pharmacological agents. In 1964, Shimazu and Tappel for the first time showed that SeM protected amino acid and proteins from radiation damage. In a cell free system, different amino acids were exposed to  $\gamma$ -radiation with dose ranging up to  $10^5$  Gy and the half destruction dose ( $D_{1/2}$ ) was calculated. SeM showed significantly higher  $D_{1/2}$  values compared to analogous sulfur amino acids<sup>137,138</sup>.

Based on these early observations, various natural and synthetic organic selenium compounds were evaluated for their radioprotective activity in cellular and mice model systems. In brief, administration of SeM (0.8 to 4 mg/kg b.wt) either before (-24 hr and - 1 hr) or shortly after (+ 15 minute) WBI (6 - 9 Gy) increased the 30 day survival of mice in the range of 60 to 90 % depending on dosage of administration and the absorbed radiation dose<sup>117,139</sup>. In another study, SeM rich diet was shown to decrease the incidence of leukemia and other malignancies in mice exposed to WBI of 1.4 Gy<sup>140</sup>. Although SeM showed promising results in animal models, it was not found to be effective in recently concluded clinical trial which was aimed to investigate the effect of SeM supplementation on reducing the radiotherapy induced mucositis in patients with head and neck cancer<sup>141</sup>.

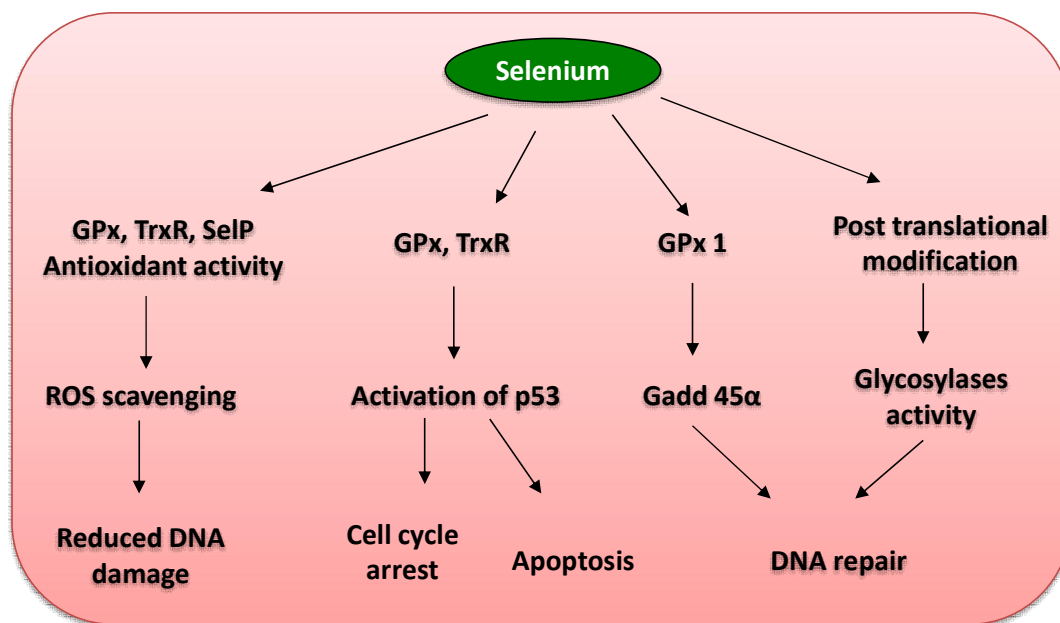
With regard to synthetic organoselenium compounds, linear and cyclic / aromatic compounds have been evaluated for radioprotection. Some of the linear organoselenium compounds evaluated for radioprotection include SeC derivatives like selenocysteamine, selenocystamine, selenourea, selenoxanthone and selenochromone<sup>142-144</sup>. Among these the most successful compound was selenourea although it showed considerable toxicity at the radioprotective dosage<sup>145</sup>. The cyclic compounds included 2-amino-selenazoles, 2-benzylidene-1,3,4-selenadiazolines and 2-arylidene-1,3-diselenols. All these compounds were the analogs of sulfhydryl compounds and were synthesized by replacing sulfur with selenium in the five membered ring structures. When examined for radioprotection, all these were found to be toxic. In recent years with increasing understanding that organoselenium compounds can mimic the activity of GPx enzyme, a few of such compounds have also been evaluated for radioprotection. For example, ebselen a synthetic cyclic organoselenium compound and a GPx mimic<sup>146</sup> showed inhibition of radiation induced cell killing and

oxidative damage in radiosensitive organs when administered at a dose of 10 mg/kg b.wt for 14 days prior to WBI of 8 Gy<sup>147</sup>. Our group has also been working on developing synthetic organoselenium compounds as radioprotectors and in this context, the radioprotective activity of diselenodipropionic acid (DSePA) was reported. This compound is a water-soluble derivative of SeC exhibiting GPx like activity<sup>148</sup>. When administered at a dose of 2 mg/kg b.wt in BALB/c for 5 days prior to WBI of 10 Gy, it showed 35 % improvement in 30 days survival of mice<sup>149</sup>. DSePA also prevented radiation induced hematopoietic and gastrointestinal syndrome in mice model system by reducing radiation induced oxidative damage and inflammatory response in the tissue<sup>149,150</sup>. The toxicological study in Chinese Hamster Ovary (CHO) cells showed DSePA to be anti-genotoxic against radiation exposure<sup>151</sup>. Further, DSePA was also reported for its ability to mitigate radiation induced lung toxicities in mice model<sup>152</sup>. Based on these results, currently DSePA is under pre-clinical examination as a lung radioprotector against thoracic irradiation through different modes of administration<sup>153</sup>.

#### **1.8.5.2. Mechanisms of action of selenium compounds**

Selenium exerts its radioprotective effect mainly by the induction of antioxidant enzymes like GPx, TrxR and SelenoP. They scavenge ROS and prevent initial DNA damage from occurring. For example, Baliga et al also showed that GPx 1 expression protected cells from ultraviolet induced cell death by DNA repair and preventing chromosomal damage<sup>154</sup>. In another study, the over expression of SelenoP in fibroblasts is shown to suppress the radiation-induced ROS accumulation<sup>155</sup>. Selenium supplementation is also shown to exert its benefit by enhancing DNA repair response. Selenoproteins like GPx and TrxR have been reported to play roles in redox regulation of DNA damage response proteins like p53, 8-oxoguanine DNA glycosylase, Gadd45  $\alpha$

and others. For example, radiation induced oxidation generates a modified nitrogenous base 8-OHdG in polynucleotide chain, which is repaired with the help of 8-oxoguanine DNA glycosylase (OGG1). OGG1 contains redox sensitive cysteine residue which is important for its activity<sup>156-158</sup>. The induction of selenoproteins can enhance the repair of oxidative DNA lesions by maintaining cysteine residue of OGG1 in reduced state. Similar kind of regulation has been reported in case of p53 and BRCA1. In addition to these, selenium may affect the activity of glycosylase also by regulating the post-translational modifications (acetylation or phosphorylation)<sup>158</sup>. Thus, multiple mechanisms contribute to the radioprotective action of selenium and are represented in scheme 1.6.



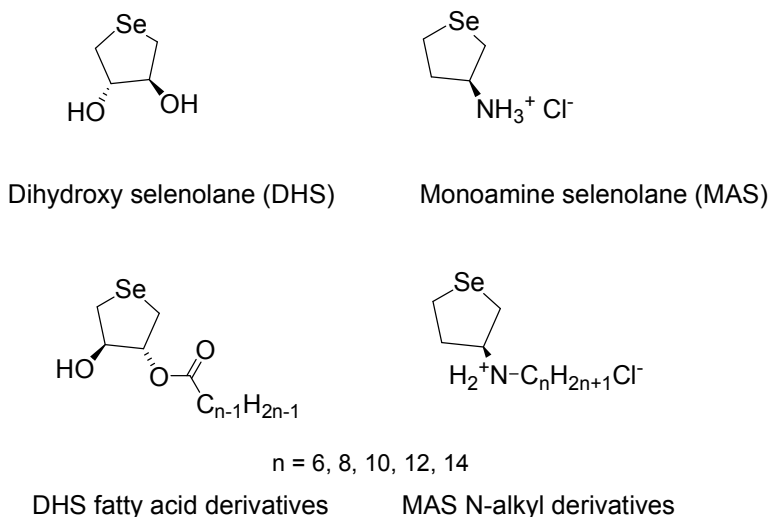
*Scheme 1.6 Role of selenium in DNA repair<sup>158</sup>*

### 1.8.6. Dihydroxyselenolane (DHS)

The present thesis deals with the *in vivo* and *in vitro* evaluation of a water soluble cyclic selenolane, DHS for the radioprotective activity. It contains two axial hydroxyl groups on a five membered ring structure. It was synthesised with an aim of

exploring as a redox modulator of cellular proteins containing a disulfide moiety<sup>159</sup>. The results showed that DHS was better than sulfur compounds like GSH, dithiothreitol (DTT) in maintaining proteins in reduced state. Further studies showed that DHS acted as a GPx mimic wherein it reduced H<sub>2</sub>O<sub>2</sub> in the presence of NADPH and GSH to water<sup>159,160</sup>. In liposomal system, DHS was found to reduce lipid hydroperoxides (LOOH) generated by a free radical inducer 2,2'-azobis (2-amidinopropane) dihydrochloride (AAPH)<sup>161</sup>. Later the fatty acid derivatives of DHS were synthesized with an aim to increase their affinity as well as antioxidant activity towards biomembrane<sup>162</sup>. Indeed, studies in cell free systems indicated increase in antioxidant activity of the derivatives with increasing alkyl chain length<sup>162</sup>. In subsequent studies, DHS was shown to accelerate healing of indomethacin-induced stomach ulceration in mice model by inhibiting inflammatory responses. The therapeutic response of DHS was better than omeprazole (a commercially available non-steroidal anti-ulcer drug) in preventing stomach ulcers at a dose of 2.5 mg/kg b.wt<sup>163,164</sup>. Mechanistically DHS was found to modulate arginine metabolism, reduce oxidative damage parameters like lipid peroxidation and protein carbonylation and to increase total antioxidant status (TAS) in mice<sup>163,164</sup>. Recently DHS was also reported to protect CHO cells from peroxynitrite induced toxicity. This was attributed to high yield and stability of selenoxide which can regenerate the parent compound DHS using thiols as reductant<sup>165</sup>. The conjugate of DHS and gold nanoparticle showed higher free radical scavenging compared to DHS alone in cell free system<sup>166</sup>. All these studies together prompted us to investigate whether DHS being GPx active, free radical scavenger, redox modulator and anti-inflammatory compound can exhibit radioprotective activity. Additionally, the effect of structural modulation and alkyl chain length on the antioxidant and radioprotective activities of DHS was studied. For comparison, a few studies were undertaken with

MAS and alkyl derivatives. However no detailed radioprotection studies were undertaken for MAS derivatives because they were relatively unstable unlike DHS and its derivatives. The chemical structure of DHS, MAS and their derivatives used in the present study are presented in scheme 1.7.



*Scheme 1.7 Chemical structures of DHS, MAS and their fatty acid / alkyl derivatives*

### 1.9. Rationale and objectives of the thesis

There is a significant interest in the recent past on development of functionalized organoselenium compounds to mimic GPx-like enzyme. GPx being an antioxidant enzyme, such compounds can have a potential to be developed as radioprotectors, to be used to minimize radiation induced oxidative stress and thereby minimize the side effects of radiation. Research work in this regard has started very recently and most of the initial work was undertaken with inorganic selenium compounds. Later on, it was understood that selenium in organic form has much better acceptability, in terms of toxicity than the inorganic form. With advancement of new synthetic methods, researchers have been designing several complex organoselenium compounds to fine tune the antioxidant activity, however bioavailability of such

compounds has become a problem. Later on, it was proposed that simple water soluble selenium compounds have faster clearance in the body and therefore can be employed as therapeutic antioxidants. With this aim, in the present thesis, investigations on *in vivo* radioprotection by DHS, a water soluble cyclic selenium compound was undertaken in detail. Further to modulate its activity, studies have been undertaken with DHS-C<sub>6</sub>, a fatty acid derivative of DHS (having 6 carbon chain). This modification has not only provided the optimum lipophilicity required to improve the bioavailability, but also increased the antioxidant activity of DHS. Further, attempts were made to understand the mechanism responsible for the observed radioprotection with these compounds. All these studies are expected to be useful in the design of new selenium compounds with improved efficacy as radioprotectors. The thesis has three objectives:

1. To study the radioprotective effects of DHS against WBI in mice model system.
2. To investigate the effect of alkyl chain length on the cellular uptake and antioxidant activity of DHS and MAS.
3. To compare the radioprotective activity of DHS and DHS-C<sub>6</sub> in cells and to understand their mechanism of action.

## **Chapter 2**

### **Materials and Methods**

This chapter describes different techniques used in the research study. It also provides details of the materials and the experimental conditions employed for different biochemical and molecular assays.

## 2.1. Chemicals

The test compounds DHS, MAS and their fatty acid / alkyl derivatives were synthesized, purified and characterised in the laboratory of Prof. Michio Iwaoka, Tokai University, Japan. Details of the synthesis and characterisation of these compounds have been reported previously<sup>159,161,162,167</sup>. In brief, DHS was synthesized as a product of the reaction between racemic mixtures of 1, 3-butadiene diepoxide and sodium hydrogen selenide (NaHSe). The fatty acid derivatives of DHS and MAS were synthesized by esterification with acid chloride of varying chain lengths<sup>159,162,167</sup>. All synthesized compounds were characterized by NMR, mass and IR spectroscopy. Selenomethionine (SeM), sodium chloride (NaCl), potassium dihydrogen phosphate (KH<sub>2</sub>PO<sub>4</sub>), dipotassium hydrogen phosphate (K<sub>2</sub>HPO<sub>4</sub>), potassium chloride (KCl), butylated hydroxy toluene (BHT), trichloroacetic acid (TCA), thiobarbituric acid (TBA), 2,2'-dinitrophenyl hydrazine (DNPH), guanidine hydrochloride, 2,2'-azobis (2-amidinopropane) dihydrochloride (AAPH), 1,6-diphenyl-1,3,5-hexatriene (DPH), dimethyl sulfoxide (DMSO), formaldehyde, triton X-100, phenylmethylsulphonyl fluoride (PMSF), low melting point agarose (LMPA), high melting point agarose (HMPA), ethidium bromide (EtBr), cytochalasin B, 2,7 dichlorodihydro fluorescein-diacetate (DCFDA), acridine orange, glutathione (GSH), glutathione disulfide (GSSG),  $\beta$ -nicotinamide adenine dinucleotide 2'-phosphate reduced tetrasodium salt hydrate (NADPH), glutathione reductase (GR), cumene hydroperoxide (CuOOH), (4,5-dimethylthiazol-2-yl)-2,5-diphenyltetrazolium bromide (MTT), tris base, propidium iodide (PI), mercaptosuccinic acid (MS), bovine serum albumin (BSA), sodium citrate, diethyl pyrocarbonate (DEPC), cell lytic<sup>®</sup> M reagent, 1X protease inhibitor cocktail, trizol for RNA isolation, tween-20, thioredoxin reductase (TrxR) assay kit,

metaphosphoric acid ( $\text{HPO}_3$ ), phthalaldehyde (OPT), N-ethylmaleimide (NEM), sodium hydroxide (NaOH) and amplification grade DNase were purchased from Sigma Chemical Company (St. Louis, MO, USA). 5, 5', 6, 6'-tetrachloro-1,1',3,3'-tetraethylbenzimidazo-carbocyanine iodide (JC-1) was obtained from Molecular Probes, USA. LightCycler<sup>®</sup>480 SYBR Green I Master Mix (2X) and lactate dehydrogenase (LDH) assay kit were obtained from Roche, Switzerland through local agents. Dulbecco Modified Eagle Medium (DMEM), Roswell Park Memorial Institute Medium-1640 (RPMI-1640), fetal calf serum (FCS), penicillin and streptomycin, trypsin-EDTA (0.5%) and crystal violet were purchased from Himedia, India. The Bradford protein assay kit was purchased from Bangalore Genei, India. cDNA synthesis kit, SYBR Green-II dye and ProLong<sup>®</sup> Gold antifade mountant with DAPI were obtained from Thermo Scientific, USA. Annexin V labeling assay kit and cytokine ELISA kits were purchased from Abcam, (Cambridge, USA). Anti phosphohistone H2AX (ser-139) human monoclonal IgG and Alexa Fluor 488 rabbit antihuman IgG were purchased from Upstate, USA and Invitrogen, USA respectively. 7-hydroxy staurosporine (UCN-01), 7-nitro-1H-indole-2-carboxylic acid {4-[1-(guanidinohydrazono)-ethyl]-phenyl}-amide (PV1091), 2-(Morpholin-4-yl)-benzo[h]chomen-4-one (NU7026) were purchased from Calbiochem (Switzerland). The gene specific primers for RT-PCR were custom synthesized from local agents. All other chemicals of highest purity were purchased from reputed local manufacturers.

## **2.2. Instruments**

The cells were cultured in Sanyo CO<sub>2</sub> incubator (MCO-17 AIC, Japan). The absorbance and fluorescence of samples were recorded on multimode plate reader (Synergy H1, BioTek, USA) and Jasco FR-6300 spectrofluorometer respectively. The

bright field, phase contrast and fluorescence images were captured using Olympus fluorescence microscope (model no - BX 53, Japan) attached to ProgRes® digital camera. The  $\gamma$ -H2AX images were captured using automated slide scanning Metacyte software module of the Metafer 4 scanning system (Meta Systems, Altlusheim, Germany). Real Time-Polymerase Chain reaction (RT-PCR) was carried out in Rotor-Gene Q machine (QIAGEN, Germany). The bands in DNA ladder assay were visualized and photographed under UV light using Geldoc (Syngene, UK). The cells labeled with PI or Annexin V were acquired on Partec PASIII flow cytometer (Germany) and analyzed for the distribution of cells in different phases of cell cycle (pre-G, G1, S, G2/M) using FlowJO software. The selenium uptake in cells was estimated using graphite furnace atomic absorption spectrometry 3000 (906AA with PAL, GBC Scientific Equipment, Australia). The other instruments used in the experimental work were stereomicroscope, tissue ruptor, hemocytometer and autoanalyzer.

### **2.3. Animal maintenance**

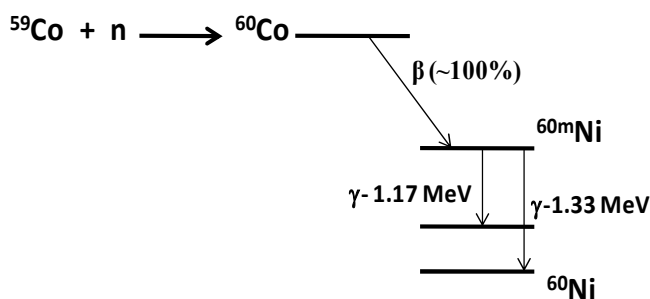
For *in vivo* experiments, seven to eight weeks old male BALB/c mice weighing approximately 20 – 25 g and maintained under standard environment (temperature, pressure and humidity) of the animal house facility of Bhabha Atomic Research Centre, Mumbai were used. The temperature of the room was  $20 \pm 2$  °C with 65 – 70 % humidity and 12 h/12 h light/dark cycle. The animals were fed with normal mouse chow and water *ad libitum* and kept in polypropylene cage containing sterile paddy husk as bedding. The experiments were conducted following the ethical guidelines of the Animal Ethics Committee of BARC with prior approval.

## 2.4. Maintenance of cell lines

Chinese Hamster Ovary (CHO) cells were obtained from Radiation Physics and Advisory Division, BARC, India. The cells were cultured in RPMI-1640 medium supplemented with 10 % FCS and antibiotics (100 U/ml penicillin and 100 µg/ml streptomycin) at 37 °C in a humidified atmosphere with 5 % CO<sub>2</sub>. The cells were sub-cultured at regular intervals and experiments were performed upon attaining 70 % to 80 % confluence.

## 2.5. Radiation source and irradiation

All irradiation experiments were performed using blood irradiator - 2000 and Bhabhatron (Department of Atomic Energy, India) which contains cobalt-60 (<sup>60</sup>Co) as the radiation source. <sup>60</sup>Co undergoes nuclear disintegration to form stable <sup>60</sup>Ni by emitting two γ-rays of energy 1.17 MeV and 1.33 MeV. <sup>60</sup>Co is generated in nuclear reactor by irradiating <sup>59</sup>Co with neutron and has a half life of 5.27 years.



*Scheme 2.1 Decay of <sup>60</sup>Co*

The absorbed dose rate of the source was estimated using Fricke dosimeter which is based on the radiation induced oxidation of the ferrous ion (Fe<sup>2+</sup>) to ferric ion (Fe<sup>3+</sup>) at low pH in the presence of the oxygen. The Fricke solution contains 1 mM ferrous ammonium sulfate and 1 mM NaCl in 0.4 M H<sub>2</sub>SO<sub>4</sub>. The primary radicals

generated due to radiolysis of water cause oxidation of  $Fe^{2+}$  ion to  $Fe^{3+}$  ion. The reactions involved are as follows:



The G-value of  $Fe^{3+}$  ions is estimated using the below given equation:

$$G(Fe^{3+}) = 3g(H\cdot) + g(\cdot OH) + 2g(H_2O_2) \quad (2.6)$$

Where, g is radiation chemical yield of primary radical species and G is the radiation chemical yield of the secondary species generated due to reaction between primary radicals and solute molecules. The G value of  $Fe^{3+}$  estimated using the above equation (2.6) corresponds to 15.5 (number per 100 eV) for  $^{60}Co$   $\gamma$  rays. The amount of  $Fe^{3+}$  formed is estimated by taking absorbance at 304 nm. The absorbed dose is calculated using the following formula:

$$Dose = \frac{9.684 \times 10^6 \times \Delta A}{\epsilon \rho G} Gy \quad (2.7)$$

where,  $\Delta A$  is the change in absorbance of the Fricke dosimeter solution before and after irradiation,  $e$  is the extinction coefficient ( $2201 \text{ M}^{-1}\text{cm}^{-1}$ ) of  $\text{Fe}^{3+}$  at the 304 nm,  $\rho$  is the density of dosimeter solution ( $1.024 \text{ g cm}^{-3}$ ) and  $l$  is the path length in cm.

For irradiation, the mice were placed in a ventilated perspex box and exposed to whole body irradiation (WBI) using Bhabhatron at a dose rate of 1 Gy/min and a source to sample distance of 60 cm. After irradiation, mice were housed under normal laboratory conditions until sacrificed at desired time points. For irradiation of cells, they were supplemented with fresh serum free medium and then exposed to varying doses of  $\gamma$ -radiation using  $^{60}\text{Co}$  blood irradiator at a dose rate of 1 Gy/min. Following this, cells were supplemented with 10 % FCS and cultured at 37 °C in 5 %  $\text{CO}_2$  atmosphere for desired time point prior to assay.

## **2.6. Methods for evaluating *in vivo* parameters**

### **2.6.1. Bronchoalveolar lavage fluid (BALF) collection and analysis**

Prior to sacrifice, mice were paralysed with an overdose of chloroform, a tracheotomy was performed and a cannula was inserted and tied. The lungs were infused with 1 ml PBS, and then the infusate was aspirated back, collected into a sterile eppendorf tube and centrifuged at  $400 \times g$  for 5 minutes at 4 °C. Cell free supernatant or BALF was used for protein concentration determination using a protein assay kit (Bangalore Genie, India) and stored at -70 °C until cytokine assessment. The cell pellet was resuspended in 0.25 ml PBS, total cell numbers were counted using a hemocytometer, and cytopspins were prepared ( $5 \times 10^4$  cells / slide). The cytopspins were stained with hematoxylin and eosin and viewed under Olympus microscope to identify

different cell types based on morphological characteristics. The differential cell counts were reported as the percentage of 500 cells counted from one cytospin per mouse<sup>152</sup>.

### **2.6.2. Estimation of cytokines like IL-6 and TNF- $\alpha$ in serum**

Following BALF collection, blood was collected in the centrifuge vials by intracardiac puncture, incubated at 4 °C overnight and centrifuged at 1,000 x g for 5 minutes to furnish serum as supernatant. The serum was stored at -70 °C until analyzed for cytokines using ELISA kits according to manufacturer's instruction.

### **2.6.3. Splenocytes preparation, spleen index and cellularity**

Spleen index and cellularity are considered as important parameters to monitor damage to the hematopoietic system. After sacrificing the mice, spleen was aseptically isolated, blotted free of blood and weighed to calculate spleen index (spleen weight / body weight). Following this, single cell suspension was prepared by teasing the spleen on a sterile nylon mesh placed in the dish. Red blood cells (RBCs) in the cell suspension were lysed by hypotonic shock using sterile water (5 ml, 10 sec) followed by the addition of 2X PBS (5 ml). The ghost RBCs were allowed to settle down after centrifugation at 1000 rpm for 15 - 30 seconds. The supernatant rich in lymphocytes were transferred to a fresh tube and checked for viability by trypan blue dye exclusion. This preparation was referred to as splenocytes and used for various molecular assays.

### **2.6.4. Endogenous spleen colony formation assay**

Endogenous spleen colony formation assay is used to study the proliferative ability of hematopoietic stem cells (HSCs) present in the bone marrow. When there is a loss of lymphocytes in hematopoietic organ like spleen, the residual HSCs migrate to

the damaged site, proliferate and form colonies<sup>168</sup>. In general, such macroscopic colonies can be seen in the spleen after 10 - 12 days of WBI. Therefore, mice were sacrificed on 11<sup>th</sup> day post irradiation and spleen was collected. The spleen was fixed in 10 % neutral buffered formalin. After 8 - 10 days of fixation, colonies became visible on the surface of the spleen, which were counted with naked eye<sup>169</sup>.

#### **2.6.5. Hematocount**

The counts of leukocytes, RBCs, platelets and hemoglobin in the whole blood are defined as the hematocount of an individual. To estimate the hematocount, about 50 µl of peripheral blood was collected from mice tail in heparinised tubes and analysed by an autoanalyzer.

#### **2.6.6. Histopathological study**

After sacrificing mice at desired time point, portions of tissues (lung, liver, jejunum) were washed and perfused with ice cold PBS. The tissues were fixed in 10 % formalin, dehydrated by passing through a graded series of alcohol and embedded into paraffin blocks. Tissue sections of 5 µm thickness were cut stained with hematoxylin and eosin and imaged using fluorescence microscope.

### **2.7. Methods of cytotoxicity studies in cells**

#### **2.7.1. MTT assay**

This is a colorimetric assay widely used for the estimation of the viability of the cell. The principle of this assay is based on the reduction of MTT by the mitochondrial reductases of viable cell to a blue colored insoluble formazan crystal, which is solubilized with SDS and measured spectrophotometrically at 570 nm<sup>170</sup>. In brief, cells

(1.0, 0.5 and 0.2×10<sup>4</sup>) following treatment with test compounds and or irradiation were incubated for 24, 48 and 72 h respectively in culture medium in quadruplicates. Following this, MTT solution (0.5 mg/ml in PBS) was added to cells and incubated at 37 °C for 4 h. The formazan metabolites formed from the reduction of MTT by the living cells were solubilized using 10 % SDS in 0.01 N HCl and detected by measuring the absorbance at 570 nm. The percentage (%) cytotoxicity of the compound was calculated with respect to control.

### 2.7.2. Clonogenic assay

Clonogenic assay or colony formation assay is an *in vitro* cell survival assay based on the ability of a single cell to grow into a colony. The colony consists of at least 25 - 50 cells. Clonogenic assay is the method of choice to determine cell reproductive death after treatment with ionizing radiation. In brief, cells were seeded in 30 mm culture dish and left overnight for attachment at 37 °C and 5 % CO<sub>2</sub>. Following this, cells were treated with test compounds and / or exposed to varying doses of radiation. After 7 days, the colonies were fixed in 100 % methanol, stained with 0.5 % crystal violet for 10 - 15 minutes and the excess stain was removed by slowly rinsing the dish with tap water. The colonies were dried and counted manually using a stereomicroscope<sup>171</sup>. The plating efficiency and the survival fraction (SF) were determined using equation 2.8 and 2.9 respectively.

$$\text{Plating Efficiency (P.E)} = [\text{No. of colonies} / \text{No. of cells plated}] \times 100 \quad (2.8)$$

$$\text{Survival fraction (SF)} = [\text{No. of colonies} / (\text{No. of cells plated} \times (\text{P.E} / 100))] \quad (2.9)$$

### **2.7.3. Estimation of apoptosis by DNA ladder assay**

During apoptosis, endonucleases cause breakdown of nuclear DNA into small fragments which can be visualized on agarose gel electrophoresis as a ladder<sup>172,173</sup>. In brief, cells at desired time points were suspended in 25  $\mu$ l of lysis buffer (50 mM Tris HCl, pH 8.0, 10 mM EDTA, 0.5 % SDS, 0.5 mg/ml proteinase K) and incubated at 55 °C for 1 h followed by addition of 5  $\mu$ l of RNase (1 mg/ml) and further incubation at 65 °C for 1 h. After the lysis, the crude DNA sample (10  $\mu$ l) was mixed with 3  $\mu$ l gel loading buffer and electrophoresed on 1.8 % agarose gel in TAE buffer (pH 8.0) containing EtBr. The bands were visualized and photographed using geldoc.

### **2.7.4. Estimation of apoptosis and cell cycle distribution by PI staining**

The principle of this assay is that cells stained with PI are analyzed for PI fluorescence after excitation at 580 nm using flow cytometer. The fluorescence intensity of PI from the cells represents the DNA content because PI binds to DNA in a stoichiometric manner. Live cells due to the presence of the intact DNA (n or 2n DNA content depending on the cell cycle stages such as G1, S, and G2) give higher PI fluorescence than the dead cells, which are known to have fragmented DNA (< n DNA content). Thus, cellular population representing pre-G1 peak was considered as dead cells. For the assay, cells at desired time points were stained with a solution containing 50  $\mu$ g/ml PI, 0.1 % sodium citrate and 0.1 % Triton X-100 and kept overnight at 4 °C in dark<sup>174</sup>. The labeled cells were acquired in flow cytometer and analyzed for the distribution of cells in different phases of cell cycle (pre G1, G1, S, G2/M) using FlowJO software.

### **2.7.5. Characterization of cell death by Annexin V-PI staining**

During apoptosis, phosphatidylserine (PS) present in the internal part of the cell membrane gets translocated to the external portion of the membrane. Annexin-V binds to the PS and represents cells undergoing apoptosis. For quantifying the cell death types, cells ( $1 \times 10^5$  cells/ml) following treatments with test compounds and / or irradiation were labeled using Annexin V-PI assay kit as per the manufacturer's instructions. The labeled cells were acquired on flow cytometer and analysed using FlowJo software into four groups: healthy, early apoptotic, late apoptotic and necrotic cells. The following staining criterion was adopted for characterization: cells that did not stain for either Annexin V or PI as healthy, which stained only with Annexin V as apoptotic, both PI and Annexin V as necrotic and only PI as dead cells with ruptured plasma membrane.

### **2.7.6. Estimation of mitochondrial membrane potential (MMP)**

MMP is an important parameter of the mitochondrial function. JC-1 is a mitochondrial specific fluorescent dye. In healthy cells, JC-1 concentrates and forms aggregates into mitochondria emitting red fluorescence (610 nm) upon excitation at 565 nm. During apoptosis, mitochondrion loses its integrity and due to this, JC-1 staining results in to its uniform distribution throughout the cells as monomer. The monomeric form of JC-1 emits green fluorescence (535 nm) upon excitation at 485 nm<sup>175</sup>. Thus, the ratio of green (535 nm) and red (610 nm) fluorescence intensity is used as an indicator of loss of MMP and cell death. For the assay, cells at desired time points were labeled with JC-1 (10 µg/ml, final concentration) for 20 minutes at 37 °C in the dark and the fluorescence emission was recorded at 535 nm and 610 nm after excitation at 485 nm

and 565 nm respectively using the multimode plate reader. The images showing green emission and red emission were captured using fluorescence microscope.

#### **2.7.7. Estimation of LDH release from cells**

LDH is an intracellular enzyme which catalyzes the conversion of lactate to pyruvic acid. During necrosis, plasma membrane gets damaged resulting in to the release of LDH in the extracellular medium<sup>176</sup>. The percentage (%) release of LDH from the cells in to culture medium was measured using LDH detection kit according to manufacturer's instruction. The kit contains tetrazolium salt (INT) and a catalyst diaphorase / NAD<sup>+</sup> mixture. LDH will catalyse the reduction of NAD<sup>+</sup> to NADH/H<sup>+</sup>. In the next step, diaphorase will transfer H<sup>+</sup> from NADH/H<sup>+</sup> to INT which is converted to a red colored formazon and is measured at 500 nm. For reference, cells were treated with distilled water and the absorbance at 500 nm was used as 100 % LDH release.

#### **2.7.8. Measurement of membrane fluidity**

Membrane fluidity is an important parameter which depends on the lipophilicity of the cell membranes. Cell membrane fluidity was measured by estimating fluorescence anisotropy value of a lipophilic fluorophore DPH<sup>177,178</sup>. The decrease in anisotropy is indicative of the loss of membrane integrity<sup>179</sup>. For the assay, cells ( $5 \times 10^6$ ) grown in culture flask were labeled with DPH at a final concentration of 1  $\mu$ M at 37 °C for 30 minutes. Following this, test compounds were added to the cells at a concentration of 25  $\mu$ M and cultured for 2 and 4 h in humidified incubator at 37 °C with 5 % CO<sub>2</sub>. Upon incubation, cells were harvested by scraping, washed twice with 1X PBS and resuspended in to 1 ml of 1X PBS. Steady-state fluorescence anisotropy measurements were performed on a fluorimeter. Excitation and emission wavelengths

were set at 365 nm and 430 nm respectively<sup>180</sup>. Fluorescence anisotropy (r) was calculated using equation (2.10)

$$r = \frac{I_{VV} - GI_{VH}}{I_{VV} + 2GI_{VH}} \quad (2.10)$$

Where  $I_{VV}$  and  $I_{VH}$  are the fluorescence intensities determined at vertical and horizontal orientations of the emission polarizer respectively when the excitation polarizer is set in the vertical position. The G factor, which compensates for differences in detection efficiency for vertically and horizontally polarized light was calculated from the fluorescence intensity ratio of vertical and horizontal emissions when the excitation polarizer is set in the horizontal position ( $I_{HV} / I_{HH}$ ).

## **2.8. Methods of biochemical assays in cell lysate and tissue homogenate**

### **2.8.1. Preparation of tissue homogenate and cell lysate**

The tissues collected from *in vivo* experiments were weighed and homogenized (10 % weight / volume) in 10 mM tris buffer (pH 7.4), containing 0.5 % Triton X-100, 5 mM BHT and 100  $\mu$ M PMSF using a tissue ruptor. Similarly, cells ( $5 \times 10^6$ ) harvested at desired time points were lysed using cellytic M® containing protease inhibitor cocktail. The resulting tissue or cell extract were centrifuged at 13,000 rpm for 10 minutes to yield supernatant termed as tissue homogenate or cell lysate and stored at -20 °C until used for biochemical assays.

### **2.8.2. Estimation of protein content**

The protein in the tissue homogenate or cell lysate was estimated using Bradford assay<sup>181</sup>. It is a colorimetric assay based on the non covalent binding of the coomassie brilliant blue dye with the carboxyl and amino group of the amino acids

present in the protein. After binding with the protein, the color of the dye is changed to blue color which can be measured by recording absorbance at 595 nm. Amount of protein in the unknown sample was estimated by plotting a standard curve using known concentration of protein (BSA) under identical condition. A minimum of 100 µg of protein was used for all the biochemical assays.

### 2.8.3. Estimation of GPx activity

GPx activity was determined by NADPH assay coupled with GSH-GSSG. Briefly, cell lysate / tissue homogenate was mixed with an assay buffer containing 50 mM of Tris-HCl (pH 7.5), 1 mM EDTA, 250 µM NADPH, 2.1 mM GSH and 0.5 Units GR. The reaction was initiated with the addition of 300 µM of CuOOH in a total reaction volume of 1ml. GPx will catalyze the reduction of hydroperoxide to corresponding alcohol using GSH as a reducing equivalent. During this process GSH is oxidized to GSSG which is recycled back to GSH using NADPH. It is an indirect method which monitors the decrease in the absorbance of NADPH at 340 nm. The change in the absorbance was recorded till 5 minutes. The GPx activity was calculated and expressed as Units/mg of protein. One unit is defined as the enzyme that catalyses the formation of 1 µmol of NADP<sup>+</sup> from NADPH per minute.

$$GPx \text{ activity (Units/ml)} = \frac{(\Delta Abs_{340(sample)})}{6.22 \times \text{Volume of sample (ml)}} \quad (2.11)$$

Where, ΔA is the change in absorbance of NADPH at 340 nm.

### 2.8.4. Estimation of ROS

Intracellular ROS levels were estimated using a cell permeable oxidation sensitive probe DCFDA. This probe is deacetylated by cellular esterases to a non-

fluorescent compound, which is oxidized by ROS into fluorescent molecule 2',7'-dichlorofluorescein (DCF). The fluorescence intensity of DCF is the indicative of intracellular ROS level<sup>182</sup>. For the assay, cells were labeled with 10  $\mu$ M of DCFDA at 37 °C for 20 minutes. The fluorescence intensity at 530 nm was recorded after excitation at 488 nm on a multimode plate reader. The mean fluorescence intensity of three measurements was presented as ROS level. The representative images showing DCF fluorescence were captured using fluorescence microscope.

#### **2.8.5. Estimation of GSH and GSSG**

GSH and GSSG were estimated in tissue homogenate or cell lysate using OPT as a detection probe. The principle of this assay is that OPT binds to GSH and GSSG at different pH of 8 and 12 respectively. OPT covalently binds to SH group of GSH to form a fluorescent conjugate (GS-OPT) which can be measured by recording fluorescence at 420 nm after excitation at 350 nm<sup>183</sup>. For the assay, protein in the cell lysate or tissue homogenate was precipitated using 25 % HPO<sub>3</sub> and centrifuged at 13000 rpm for 15 minutes to yield supernatant containing GSH and GSSG. For GSH estimation, the supernatant was incubated with OPT for 15 minutes at pH 8 and emission was recorded at 420 nm after excitation at 350 nm on a multimode plate reader. For GSSG estimation, similar method was used except that the supernatant was first incubated with NEM for 30 minutes to block GSH and then incubated with OPT in the presence of 0.1 M NaOH. The ratio of the fluorescence of OPT at pH 8 and pH 12 is presented as the ratio of GSH and GSSG.

### **2.8.6. Estimation of lipid peroxidation**

Thiobarbituric acid reactive substances (TBARS) method was used to estimate lipid peroxidation in tissue homogenate or cell lysate. During lipid peroxidation membrane lipids break down into number of products such as hydroperoxides, alkadienal, MDA, 4-HNE etc<sup>13</sup>. The principle of TBARS method is that MDA reacts with two molecules of TBA at 90 °C to form a pink colored MDA-TBA adduct which can be quantitatively measured by recording absorbance at 532 nm. As TBA reacts with other lipid peroxidation products also, the products formed are collectively termed as TBA reactive substance (TBARS)<sup>184</sup>.

For the assay, 300 µl of tissue homogenate or cell lysate containing minimum of 100 - 200 µg of protein was mixed with TBA reagent (0.375 % TBA, 0.25 M HCl, 15 % TCA and 6 mM EDTA), heated in water bath at 90 °C for 30 minutes and cooled at room temperature. The samples were then centrifuged at 13000 rpm for 10 minutes and TBARS was estimated in the supernatant by measuring the absorbance at 532 nm. Amount of TBARS in the sample was estimated by plotting a standard curve using known amount of 1, 1, 3, 3' tetra-ethoxy propane and expressed as nmols of TBARS per mg of protein.

### **2.8.7. Estimation of protein carbonylation**

The protein carbonyl content in tissue homogenate or cell lysate was measured by DNPH assay. The principle of the assay is that DNPH reacts with carbonyls forming the Schiff base to produce a hydrazone<sup>185</sup>. The amount of hydrazone can be measured spectrophotometrically at 370 nm. For the assay, a minimum of 100 µg of protein was precipitated using ice-chilled 10 % TCA for 20 minutes at 4 °C. It was followed by

centrifugation at 12000 rpm for 10 minutes. To the pellet, 100  $\mu$ l of 0.2 % DNPH in 2 N HCl was added and incubated at 37 °C for 2 h. Protein was reprecipitated using 10 % TCA. Excess DNPH was removed by washing 3 times with 50 % ethyl acetate in ethanol. Finally, pellet was dissolved in 100  $\mu$ l of 6M guanidine hydrochloride and the absorbance was recorded at 370 nm. The amount of protein carbonyls was determined by using an extinction coefficient of  $2.1 \times 10^4 \text{ M}^{-1} \text{ cm}^{-1}$  at 370 nm and expressed as nanomoles of protein carbonyls/mg of protein.

## **2.9. Methods for genotoxicity assessment in cells**

### **2.9.1. Estimation of DNA damage by alkaline single cell gel electrophoresis**

The alkaline single cell gel electrophoresis or comet assay is a technique used to know the extent of DNA damage caused by an agent. For this assay, 50  $\mu$ l of whole blood or cell suspension carrying 15000 cells was mixed with 0.8 % LMPA and layered on a slide pre-coated with 1 % HMPA. Immediately, cover slip was placed on the slide and kept at 4 °C for 5 - 10 minutes, After the solidification of LMPA, cover slip was removed and the slides were kept in a lysis solution containing 2.5 M NaCl, 100 mM EDTA, 10 mM Tris-HCl (pH 10), 1 % DMSO and 1 % Triton X-100 overnight at 4 °C. The next day, slides were removed carefully from the lysis solution, rinsed with alkaline solution containing 300 mM NaOH, 1 mM EDTA and 0.2 % DMSO, pH >13.0 and placed for 20 minutes on horizontal electrophoresis in a tank filled with freshly prepared alkaline solution for equilibration. The electrophoresis was carried out at 22 V, 299 mA in the alkaline solution for 30 minutes. After the completion of electrophoresis, the slides were kept in a neutralization buffer (0.4 M Tris-HCl buffer, pH 7.5 to remove any alkali present) and kept at 4 °C. The slides were stained with 50  $\mu$ l of SYBR Green-

II and at least fifty images were grabbed per slide using fluorescence microscope<sup>186</sup>. The images were analysed using CASP software version 1.2.0 ([www.casplab.com](http://www.casplab.com)) to calculate DNA damage parameters such as percent % tail DNA (% TDNA) and olive tail moment (OTM).

### **2.9.2. Micronuclei assay**

Micronuclei are small chromosomal bodies formed after exposure to radiation. They can be seen in dividing cells due to their inability to incorporate in the daughter cells. For the assay, cells treated with test compounds and / or exposed to radiation were incubated with cytochalasin-B (4 µg/ml in culture medium) to block cytokinesis and to induce micronuclei formation. Following this, cells were treated with hypotonic solution (0.9 % ammonium oxalate) and fixed in a methanol: acetic acid (5:1) solution<sup>187,188</sup>. Finally, cells were stained with acridine orange (10 mg/ml) and a total of 500 binucleate cells were counted using fluorescence microscope and analyzed for the presence of micronuclei per treatment condition.

### **2.9.3. $\gamma$ -H2AX assay**

Genotoxic stress induces formation of DSBs in DNA. An early event after generation of DSBs is the phosphorylation at  $\gamma$  - carbon of serine present at 139 position of H2AX protein. The phosphorylated protein termed as  $\gamma$ -H2AX, acts as a signal for the recruitment of the repair proteins at the site of the damage. Briefly, cells at desired time points were fixed using 2 % paraformaldehyde, permeabilized with 0.5 % Triton X-100, blocked with 5 % BSA for 1 h and stained with anti-p (ser139)- $\gamma$ H2AX (1:300 dilution for 1 h). Afterwards, cells were incubated with Alexa Fluor 488 rabbit antimouse IgG (1:300 dilutions for 1 h) and mounted on the slides with antifade

containing DAPI. The images were acquired using Metafer 4 scanning system<sup>189,190</sup>. At least 50 cells were counted for the presence of  $\gamma$ -H2AX foci per treatment group to calculate the average number of foci per cell.

## **2.10. Gene expression analysis in cells and tissues by RT-PCR**

RT-PCR is a method of choice to quantify messenger RNA (mRNA) in cells. Unlike traditional PCR, it monitors the amplified DNA in real time and not at the end. For the detection of amplified product, SYBR Green I dye (DNA binding dye) is used. An increase in DNA product with each cycle of PCR leads to an increase in fluorescence intensity thus allowing DNA concentrations to be quantified on line.

Isolation of RNA is the first and the most critical step for the RT-PCR. Total RNA was isolated from tissue or cells using Trizol reagent as per the manufacturer's instructions and dissolved in 20  $\mu$ l of DEPC treated water. The RNA content in the sample was quantified taking absorbance at 260 nm. About 2  $\mu$ g of total RNA was used to make cDNA by using reverse transcriptase cDNA synthesis kit and kept at -70°C until use. The RT-PCR was carried out in a 10  $\mu$ l reaction mixture containing 5  $\mu$ l of 2X SYBR green PCR master mix, 1  $\mu$ l of forward and reverse primer (10 picomoles each) and 4  $\mu$ l of diluted (10 times) cDNA using the Rotor Gene Q machine. The amplification steps were: step 1- denaturation at 95 °C for 5 minutes; step 2 - denaturation at 95 °C for 15 sec; step 3 - annealing at 58 °C for 15 sec; step 4 - extension at 72 °C for 20 sec; step 5 - melt curve analysis. Steps 2 – 4 were repeated for 40 cycles. The threshold cycle (the cycle at which the amplification enters into exponential phase) values ( $C_t$  value) obtained from above runs were used for calculating the expression levels using double delta ( $\Delta\Delta CT$ ) method<sup>191</sup>. The expression of genes was normalized against a house keeping gene  $\beta$ -actin and plotted as relative

change in the expression with respect to control. The list of primers used for the RT-PCR in the present thesis is given in table 2.1.

*Table 2.1: List of primers*

<b>Name of gene</b>	<b>Primer sequence</b>	<b>Gene Bank Accession No.</b>
<i>β actin</i>	5'- GGCTGTATTCCCCTCCATCG -3'	NM_007393
	5'- CCAGTTGGTAACAATGCCATGT -3'	
<i>Icam-1</i>	5'- GTGATGCTCAGGTATCCATCCA -3'	NM_010493
	5'- CACAGTTCTCAAAGCACAGCG -3'	
<i>Ccl-2</i>	5'- TAAAAACCTGGATCGGAACCAAA -3'	NM_011333
	5'- GCATTAGCTTCAGATTTACGGGT -3'	
<i>Csf-3</i>	5'- ATGGCTCAACTTTCTGCCAG -3'	NM_009971
	5'- CTGACAGTGACCAGGGGAAC -3'	
<i>iNos-2</i>	5'- GTTCTCAGCCCAACAATACAAGA -3'	NM_010927
	5'- GTGGACGGGTCGATGTCAC -3'	
<i>SelenoP-1</i>	5'- AGCTCTGCTTGTTACAAAGCC -3'	NM_001042613
	5'- CAGGTCTTCCAATCTGGATGC -3'	
<i>GPx 1</i>	5'- AGTCCACCGTGTATGCCTTCT -3'	NM_008160
	5'- GAGACGCGACATTCTCAATGA -3'	
<i>GPx 2</i>	5'- GCCTCAAGTATGTCCGACCTG -3'	NM_030677
	5'- GGAGAACGGGTCATCATAAGGG -3'	
<i>GPx 4</i>	5'- TGTGCATCCCGCGATGATT -3'	NM_008162
	5'- CCCTGTACTIONTATCCAGGCAGA -3'	

## **Chapter 3**

### **Radioprotective effect of DHS against whole body irradiation in mice**

In this chapter, the *in vivo* radioprotective effect of DHS in mice against whole body irradiation was evaluated in terms of 30 day survival, biochemical and histological changes in radiosensitive organs like spleen, intestine and lungs. The results for DHS were compared with a dietary organoselenium compound SeM.

### 3.1. Introduction

As discussed in chapter 1, organoselenium compounds both in linear and cyclic forms have been evaluated for antioxidant activity. Among the linear compounds, it was observed that diselenides are better than monoselenides in exhibiting antioxidant activity. Compared to linear compounds, cyclic compounds are advantageous with respect to overall stability. In our laboratory, it has been shown that compared to linear compounds, the cyclic isomer shows higher GPx activity<sup>165,192</sup>. Such GPx active antioxidants can be explored as radioprotectors. Agreeing this hypothesis, ebselen a cyclic organoselenium compound and stable GPx mimic has been reported for potential radioprotective activity in cells and *in vivo* model systems<sup>147</sup>. Recently our group has reported the synthesis of DHS, a water-soluble cyclic selenium compound structurally closer to a known sulfur compound<sup>159</sup>. Subsequently this compound was reported for wide range of biological activities like free radical scavenging, mimicking the function of GPx, catalyzing the oxidative folding of denatured proteins and anti-inflammatory action<sup>160,162–165,167</sup>. Encouraged by these results, it was hypothesized that DHS might also protect against radiation injuries which is linked with oxidative stress. Therefore, in the present study, DHS has been evaluated for radioprotection using mice model system. The radioprotective effect of DHS was monitored in terms of improvement in 30 day post irradiation survival and the biochemical, histological and inflammatory changes in radiosensitive organs like spleen, intestine and lungs after whole body irradiation (WBI). We also studied the effect of DHS administration on the radiation induced DNA damage in peripheral leukocytes and on the tissue specific expression of GPx and pro-inflammatory genes like *Icam-1*, *Ccl-2* and *iNOS-2*. Further, radioprotective effect of DHS was compared with selenomethionine (SeM) which is not

only a major dietary source of selenium to humans but has also been evaluated for radioprotection. Additionally, DHS and SeM being cyclic and linear selenium compounds respectively, such studies are useful to understand the importance of structure in their radioprotective activities.

### **3.2. Materials and Methods**

The solutions of DHS and SeM were prepared in sterile phosphate buffered saline (PBS) immediately before the experiment. The dosage of DHS was selected based on previous studies<sup>147</sup>. The mice were randomized and segregated in to four groups: sham control, drug control, radiation control and drug plus radiation treatment groups. The irradiated groups received PBS (radiation control) or the drug (DHS or SeM) through intraperitoneal (ip) mode of administration and subjected to WBI at an absorbed dose of 8 Gy to monitor survival and other mechanistic studies. The sham and drug control mice were not irradiated and received treatment either with PBS or drug (DHS or SeM) similar to the respective irradiated groups until sacrificed at the desired time point (30 day post irradiation). After irradiation, the mice were monitored daily for 30 days by recording body weight (b. wt) on regular interval and mortality (if any). Kaplan-Meier survival curves were drawn using Graph Pad Prism® (version 3.2). For mechanistic study, the irradiated mice were euthanized by cervical dislocation at an identical/common time point of 10 day post irradiation. Prior to sacrifice, tracheotomy was performed on the mice to collect BALF. Following this, mice were sacrificed by cardiac puncture and blood and tissues like spleen, lungs, liver, and jejunum were collected. The tissues were immediately washed and per-fused with ice cold PBS to remove trapped blood. A small portion of tissue was fixed in 10 % formalin for histopathological study, another in Trizol for RNA isolation and the remaining

homogenized (10 % weight / volume) for biochemical studies. In order to study the survival or 30 day post irradiation parameters, ten mice per group and for early data point (10 day post irradiation), five mice per group were analysed. In order to determine the protective effect of DHS and / or SeM against radiation induced genotoxicity (DNA damage), mice were randomized, grouped (n = 5) as described above, administered with PBS or drugs (DHS or SeM) and subjected to WBI at 5 Gy. The blood samples were taken from the tail vein at 15 and 30 minutes post irradiation and processed for the alkaline single cell gel electrophoresis or comet assay. The results are presented as mean  $\pm$  SEM (n = 3 - 5). Statistical significance ( $p < 0.05$ ) of the difference between the means of treatment groups was assessed by one-way ANOVA. A two-tailed student's t-test was used for the comparisons between the means of two groups and p values  $< 0.05$  were considered as statistically significant. Kaplan-Meier survival curves were analyzed for statistical significance ( $p < 0.05$ ) using Mantel-Cox log-rank test of Graph Pad Prism<sup>®</sup> (version 3.02).

### **3.3. Results**

#### **3.3.1. Dosage optimization of DHS to improve the 30 day post irradiation survival**

In order to find the effective dose of DHS, two experiments were performed. In the first experiment, DHS was administered in a dose range of 2 mg, 25 mg and 50 mg/kg b.wt into mice, 30 minutes prior to radiation exposure (8 Gy) and following this the survival of animals was monitored for 30 days. The exposure to radiation caused sickness, loss of appetite, lethargy, ruffling of hair, weight loss and diarrhea in mice. The median survival of radiation control group was found to be 10 day with complete mortality by

12<sup>th</sup> day. The pre-administration of DHS did not show any protection from radiation induced mortality as shown in figure 3.1 A.

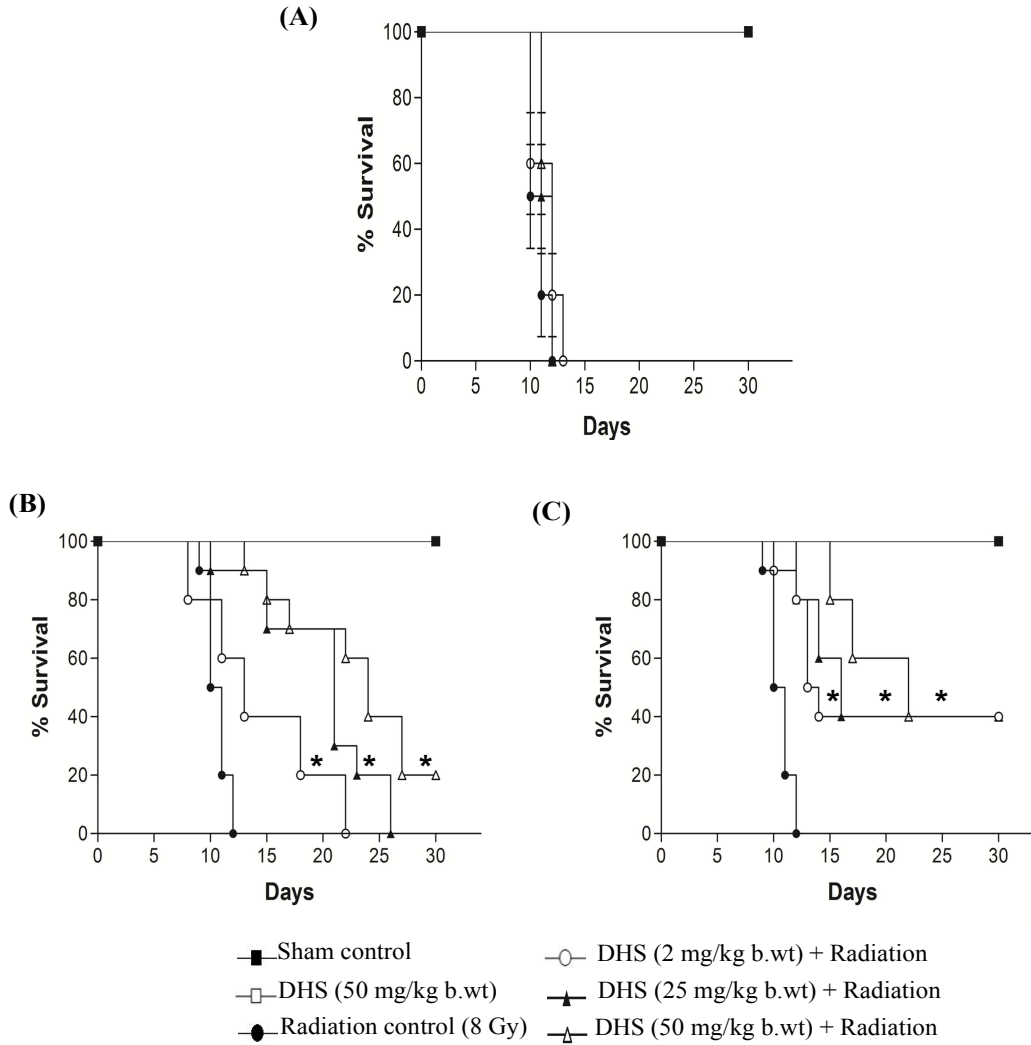


Figure 3.1 Kalpan-Meier survival curve representing the effect of DHS (2 - 50 mg/kg b.wt) administration (ip) on 30 day survival of mice exposed to WBI of 8 Gy. (A) Single ip administration of DHS at 30 minutes prior to radiation exposure. (B) DHS was administered for five consecutive days and 30 minutes after the last dose, mice were irradiated (C) DHS was administered for five consecutive days prior to irradiation and continued during the post irradiation period for three times per week till 30 days. \* $p < 0.05$  as compared to the radiation control.

In the second experiment, DHS was administered at similar dosages but for five consecutive days prior to radiation exposure. Interestingly under this treatment schedule, DHS showed significant protection against radiation induced mortality compared with single administration. For example, DHS at a dosage of 2, 25 and 50 mg/kg b.wt increased the median survival time to 13, 21 and 24 days respectively. However, in terms of 30 day survival only the highest tested dosage of 50 mg/kg b.wt was effective by 20 % (Fig. 3.1 B). This suggested that DHS may work better if administered as a supplement. Accordingly, in another experiment, DHS was administered not only for five consecutive days prior to radiation exposure but also during the post irradiation period for three days in a week till the end of experiment (30 day post irradiation) and the survival of animals was monitored. Our results indicated that under this treatment regime, DHS showed improvement by 40 % in 30 day survival even at the lowest tested dose of 2 mg/kg b.wt. Increasing the dose to 50 mg/kg b.wt did not increase protection (Fig. 3.1 C). The DHS control group did not show mortality or any other visible toxicity symptoms throughout the experiment. Based on these results, in all of our further studies, DHS was administered at a dosage of 2 mg/kg b.wt in the combined treatment regime of pre (5 days) and post (3 days in a week) administration until sacrificed at desired time point.

### **3.3.2. Effect of DHS and SeM on the 30 day post irradiation survival**

The radioprotective effect of DHS was compared with SeM at an identical dose (2 mg/kg b.wt) and treatment schedule. The survival curves comparing the effect of DHS and SeM on 30 day survival following WBI of 8 Gy are shown in figure 3.2 A. It can be seen from the figure that SeM significantly improved the 30 day survival of irradiated mice by 30 % which is comparable to that of DHS (40 %). The improvement

in 30 day survival by both DHS and SeM was also supported by their abilities to favorably increase the relative body weights as compared to radiation control group (Fig. 3.2 B). Like DHS, SeM control group did not show mortality or any other visible toxicity symptoms till 30 day. (Fig. 3.2 A & 3.2 B).

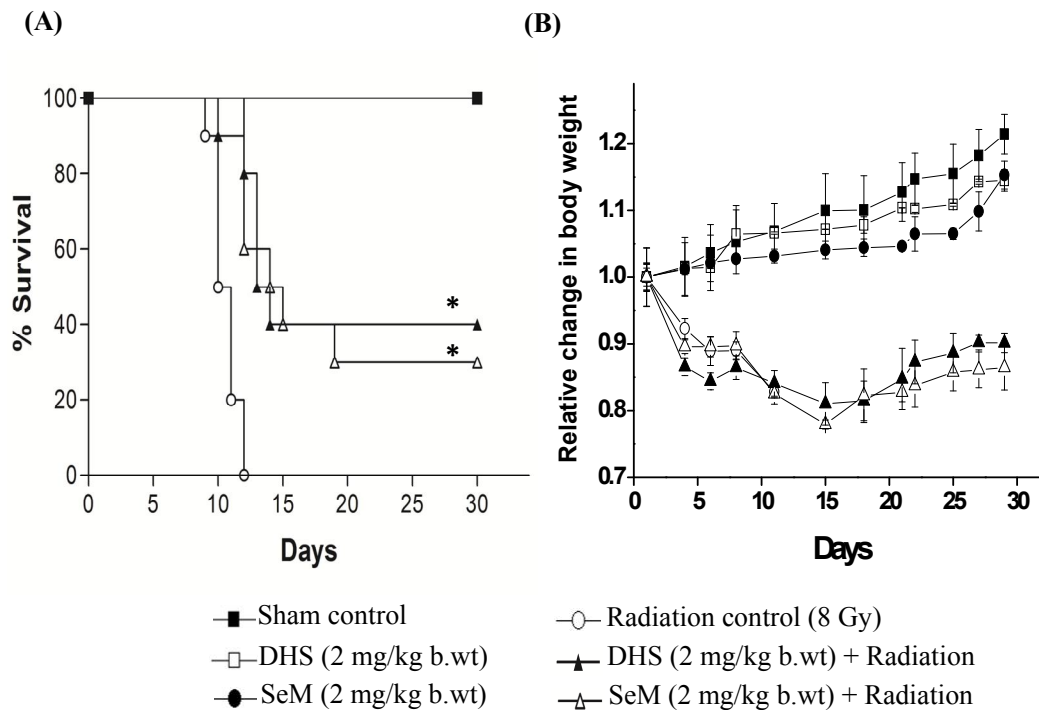


Figure 3.2 (A) Comparative effect of DHS (2 mg/kg b.wt) and SeM (2 mg/kg b.wt) administration (ip) on the 30 day survival of mice exposed to WBI at an absorbed dose of 8 Gy. Both drugs were administered for five consecutive days prior to irradiation and continued during the post irradiation period for three times a week till the end of experiment. \* $p < 0.05$  as compared to the radiation control. (B) Relative change in body weight for different treatment groups plotted as a function of time in days.

### 3.3.3. Effect of DHS and SeM on the radiation induced genotoxicity

Genomic DNA is the most critical target of radiation exposure. Therefore, the effects of DHS and SeM administration on radiation induced genotoxicity was monitored in peripheral lymphocytes by comet assay as a function of time (15 and 60 minutes). The DNA damage parameters such as % TDNA and OTM and the

representative fluorescence images indicating the extent of DNA damage under different treatment conditions are shown in figure 3.3 A and 3.3. B.

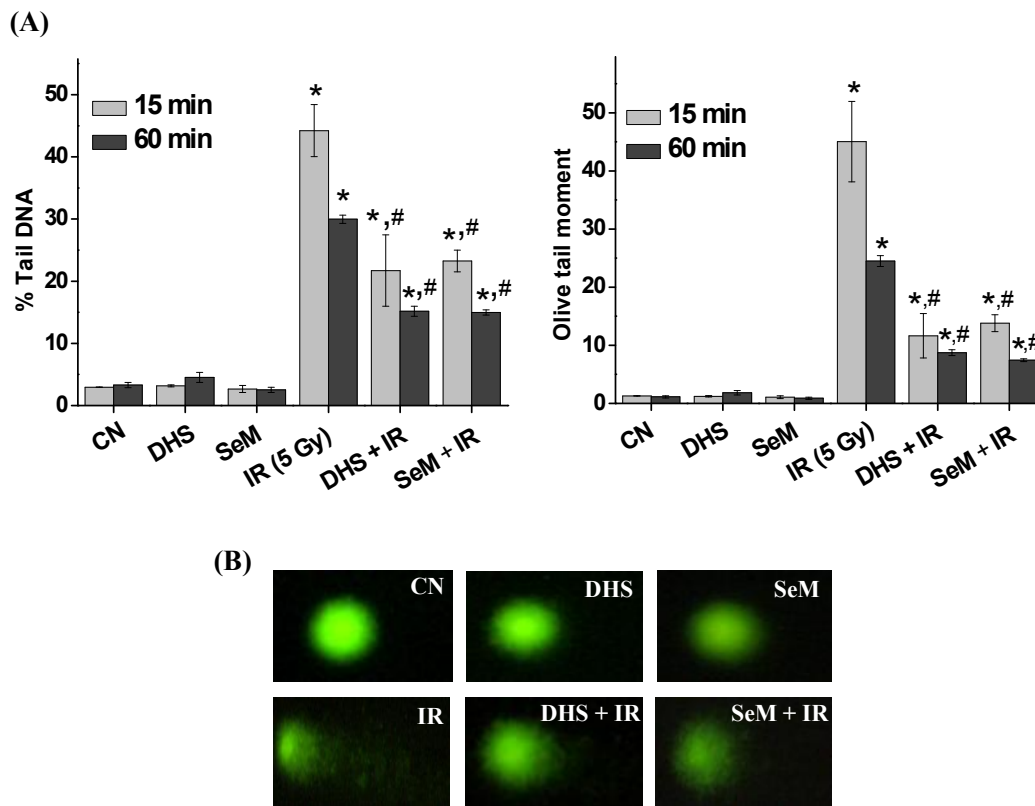


Figure 3.3 Effect of DHS (2 mg/kg b.wt) and SeM (2 mg/kg b.wt) administration (ip) on the radiation (5 Gy) induced DNA strand breaks in peripheral lymphocytes as assayed by comet assay. DHS and SeM were given for five consecutive days prior to irradiation and peripheral blood was drawn at 15 and 60 minutes post irradiation from the tail vein of mice. The blood containing peripheral lymphocytes were subjected to single cell gel electrophoresis. (A) Bar graphs shows % TDNA and OTM in various treatment groups. The results are presented as mean  $\pm$  SEM ( $n = 5$ ). \* $p < 0.05$  as compared to the sham control group. # $p < 0.05$  as compared to the radiation control group. (B) Representative fluorescent images shows nuclei stained with SYBR Green-II dye 15 minutes post irradiation under different treatment groups following electrophoresis. CN – Sham control, IR – Irradiation

Exposure to sub-lethal dose of  $\gamma$ -radiation (5 Gy) led to significant increase in % TDNA and OTM. As time progressed to 60 minutes, the extent of radiation induced DNA damage reduced considerably in the radiation control group. This is expected due to the activation of various inherent DNA repair pathways. Treatment with DHS and SeM showed significant reduction in the extent of radiation induced DNA damage at each time point compared to the radiation control group. However, the levels of residual DNA damage in DHS and SeM treated groups at the end of 60 minutes after radiation exposure was significantly higher than that of the control levels. The efficacy of both DHS and SeM was comparable. The drug control groups (DHS and SeM) did not show any induction of DNA damage at the evaluated dosage of 2 mg/kg b.wt.

#### **3.3.4. Effect of DHS and SeM on the radiation induced hematopoietic toxicity**

The ability of DHS and SeM to protect hematopoietic system from radiation exposure was evaluated by monitoring the spleen parameters and the hematocount in peripheral circulation. The changes in spleen parameters such as index and cellularity under the radiation and drug treated conditions are shown in figure 3.4 A and 3.4 B. Irradiation led to decrease in spleen index ( $0.0017 \pm .0003$ ) as compared to sham control ( $0.0043 \pm 0.0002$ ) at 10 day suggesting acute hematopoietic damage / syndrome. Treatment with either DHS or SeM did not show any significant improvement in the spleen index at 10 day while improving it to 0.0059 and 0.0053 respectively in the mice surviving till 30 day post irradiation as compared to radiation control.

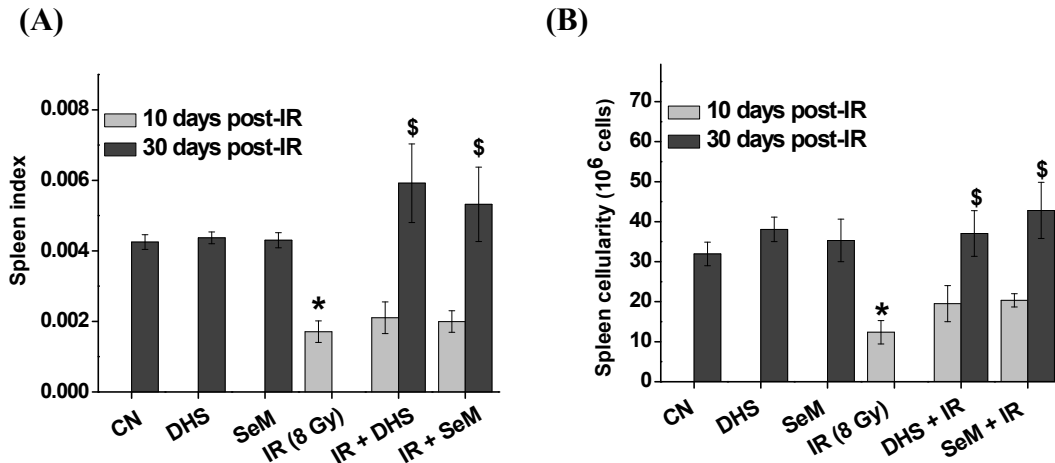


Figure 3.4 Bar graph shows effect of DHS (2 mg/kg b.wt) and SeM (2 mg/kg b.wt) supplementation (ip) on (A) spleen index (spleen weight/body weight) and (B) spleen cellularity against WBI of 8 Gy. The results are presented as mean  $\pm$  SEM ( $n = 3 - 5$ ). \* $p < 0.05$  as compared to the sham control group,  $^{\$}p < 0.05$  as compared to respective drug (DHS or SeM) plus radiation treated group evaluated at 10 day post irradiation. CN – Sham control, IR – Irradiation.

The spleen cellularity in mice under different treatment conditions were examined by counting number of viable cells using hemocytometer. The results showed similar trend as observed in case of spleen index. Irradiation led to a decrease in spleen cellularity ( $12.4 \pm 2.9 \times 10^6$ ) as compared to sham control ( $31.9 \pm 2.9 \times 10^6$ ) whereas pretreatment with DHS and SeM showed improvement in spleen cellularity ( $37.04 \pm 5.70 \times 10^6$  and  $42.8 \pm 7.00 \times 10^6$  respectively) on 30 day post irradiation.

The renewal of hematopoietic system also depends on the proliferation of the clonogenic stem cells in the spleen. Therefore, effect of DHS and SeM on the proliferation of clonogenic stem cells was investigated by monitoring the spleen colony forming unit (CFU) and the mRNA expression of colony stimulating factor -3 (*Csf-3*). The results are shown in figures 3.5 (A - C).

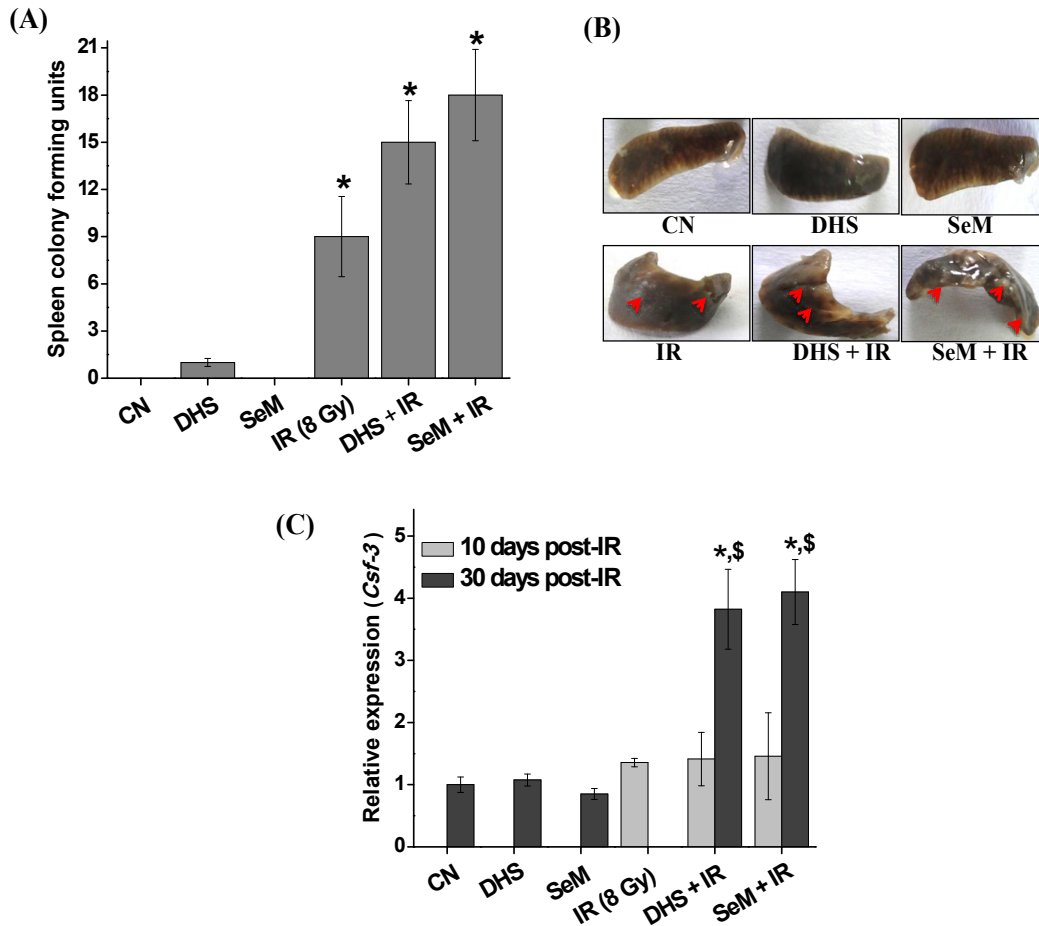


Figure 3.5 (A) Bar graph shows effect of DHS (2 mg/kg b.wt) and SeM (2 mg/kg b.wt) supplementation (ip) on spleen colonies against WBI of 8 Gy. (B) Images of spleen colonies under different treatment conditions. The spleen colony forming assay was performed only at 10 day post irradiation. (C) mRNA expression of *Csf-3* as monitored by RT-PCR. The expression of above gene in different treatment groups was normalized against the sham control group and the relative expression changes have been plotted. The results are presented as mean  $\pm$  SEM ( $n = 3 - 5$ ). \* $p < 0.05$  as compared to the sham control group,  $^{\$}p < 0.05$  as compared to respective drug (DHS or SeM) plus radiation treated group evaluated at 10 day post irradiation. CN – Sham control, IR – Irradiation.

It can be seen that irradiation induced the proliferation of clonogenic stem cells which was evidenced by the increase in the number of CFU in radiation control group compared to the sham control group at 10 day post irradiation. Treatment with DHS or SeM in irradiated mice did not alter this parameter significantly as compared to the radiation control. In agreement with the above results, DHS or SeM treated groups did not show any significant change in the expression of *Csf-3* at 10 day, however increased its expression significantly at 30 day post irradiation by 2.5 and 2.9-folds respectively (Fig. 3.5 C).

In addition to spleen parameters, the count of various cell types in peripheral circulation (hematocount) is important to know the status of the hematopoietic system. The effect of radiation and treatments of DHS and SeM on hematocount is presented in table 3.1. As expected, irradiation led to significant decrease in counts of neutrophils, lymphocytes, platelets and total white blood cells (WBC) at 10 day post irradiation as compared to the sham control group. Treatment with DHS or SeM in irradiated mice did not show any improvement in hematocount at 10 day post irradiation as compared to the radiation control. However, these parameters improved close to sham control levels at 30 day post irradiation in the surviving mice treated with DHS or SeM. The compounds DHS and SeM did not show any significant difference between the two in affecting the radiation induced hematopoietic changes. DHS and SeM control groups showed spleen parameters like spleen index, spleen cellularity, CFU and the expression of *Csf-3* and hematocount in peripheral circulation similar to that of sham control.

Table 3.1 Hematocount under different treatment conditions.

Treatment groups	Total WBC (10 <sup>3</sup> /μl)	Neutrophils (10 <sup>3</sup> /μl)	Lymphocytes (10 <sup>3</sup> /μl)	Platelets (10 <sup>3</sup> /μl)	Hemoglobin (% gm)
Sham control	4.35 ± 6.50	0.83 ± 0.02	3.33 ± 0.56	447 ± 0 58	14.45 ± 0.55
DHS control	3.55 ± 0.65	0.71 ± 0.04	2.59 ± 0.51	375 ± 0 35	13.55 ± 0.55
SeM control	3.25 ± 0.35	0.69 ± 0.15	2.32 ± 0.55	295 ± 0 60	14.5 ± 1.50
IR (8 Gy)	0.30 ± 0.02*	0.03 ± 0.01*	0.22 ± 0.02*	48 ± 0.21*	9.4 ± 1.35*
DHS + IR (10 day)	0.31 ± 0.08	0.07 ± 0.04	0.23 ± 0.04	85 ± 0.46	8.25 ± 0.92
DHS + IR (30 day)	2.60 ± 0.90 <sup>§</sup>	1.11 ± 0.42 <sup>§</sup>	1.28 ± 0.39 <sup>§</sup>	305 ± 0.55 <sup>§</sup>	14.2 ± 2.00
SeM + IR (10 day)	0.42 ± 0.11 <sup>#</sup>	0.10 ± 0.06	0.28 ± 0.05	99 ± 0.37	8.97 ± 0.79
SeM + IR (30 day)	3.05 ± 1.15 <sup>§</sup>	1.13 ± 0.33 <sup>§</sup>	1.80 ± 0.75 <sup>§</sup>	289 ± 0.19 <sup>§</sup>	14.15 ± 0.85 <sup>§</sup>

The results are presented as mean ± SEM (3 - 5 mice). \*  $p < 0.05$  as compared to the control group, <sup>#</sup> $p < 0.05$  as compared to the radiation control group, <sup>§</sup> $p < 0.05$  as compared to respective drug (DHS or SeM) plus radiation treated group evaluated at 10 day post irradiation.

### 3.3.5. Effect of DHS and SeM on the radiation induced intestinal toxicity and inflammatory responses

The small intestine is also an important radiosensitive organ. WBI of 8 Gy is known to cause damage to the gastrointestinal system resulting in GI syndrome. It is characterized by denudation of villi, decrease in number of crypt cells and infiltration of inflammatory cells. The protective effect of DHS and SeM on the radiation induced intestinal toxicity was evaluated through histological examination, monitoring the level of lipid peroxidation and mRNA expression of pro-inflammatory genes (*Icam-1*, *Ccl-2*, *iNOS-2*). The microvilli height in micrometer and hematoxylin and eosin stained slides of intestinal tissue section are shown in figures 3.6 and 3.7 respectively.

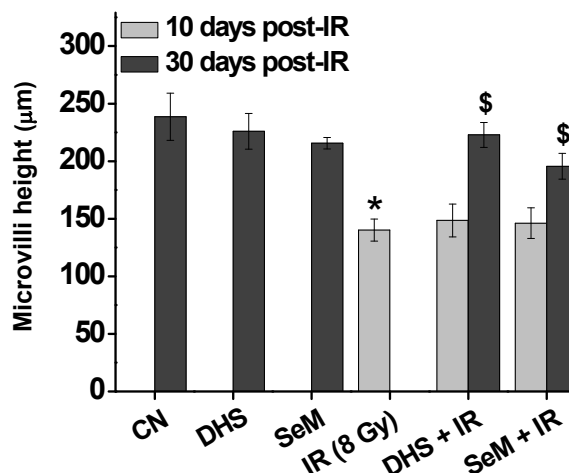


Figure 3.6 Bar graph shows the effect of DHS (2 mg/kg b.wt) and SeM (2 mg/kg b.wt) supplementation (ip) on microvilli height against WBI of 8 Gy. The results are presented as mean  $\pm$  SEM (n = 3 - 5). \* $p$ <0.05 as compared to the sham control group,  $^{\$}$  $p$ <0.05 as compared to respective drug (DHS or SeM) plus radiation treated group evaluated at 10 day post irradiation. CN – Sham control, IR – Irradiation.

It can be seen from figure 3.7 that DHS and SeM control groups did not show any adverse effect with respect to the intestinal structure. WBI of 8 Gy led to acute intestinal toxicity characterized by shortening and destruction of the villi structure. Irradiated mice treated with DHS or SeM did not show any significant protection in microvilli height as compared to radiation control at a common time point of 10 day. However, the mice surviving till 30 day post irradiation from this group showed maintenance in villi height.

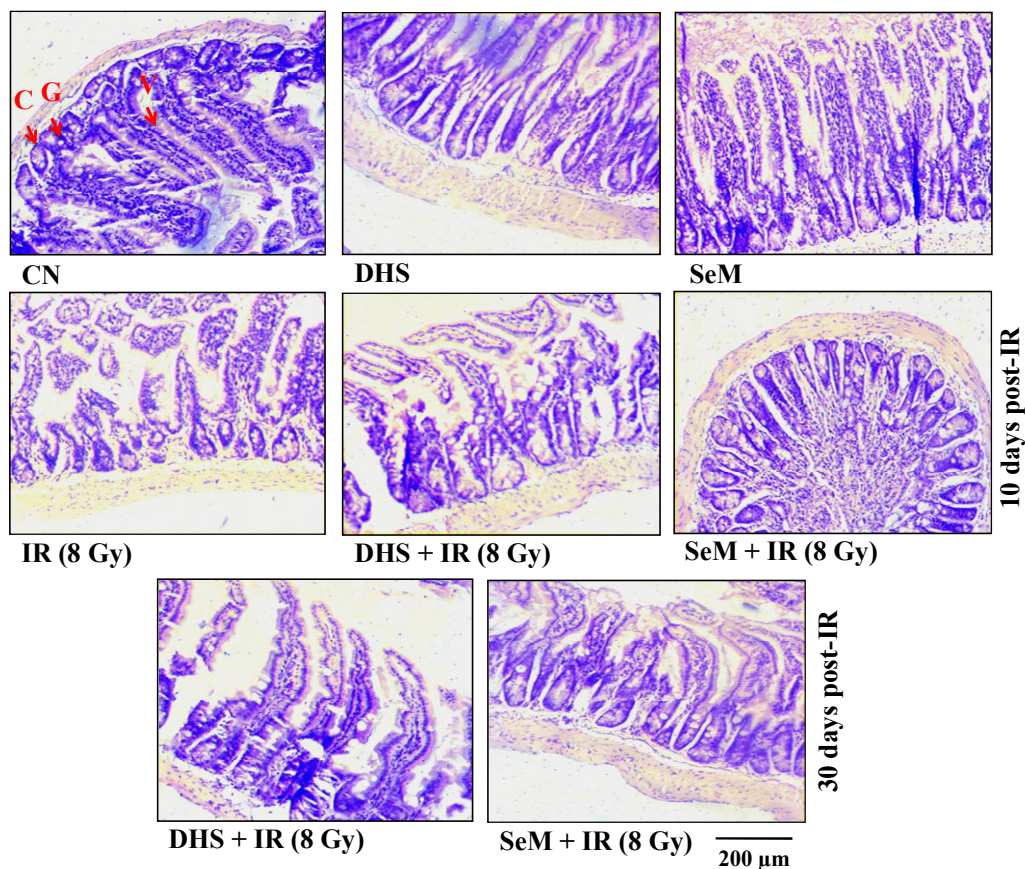


Figure 3.7 Effect of DHS (2 mg/kg b.wt) and SeM (2 mg/kg b.wt) supplementation (ip) on the radiation (8 Gy) induced intestinal toxicity. Images of representative tissue section of jejunum excised from the mice of the various groups and stained with hematoxylin and eosin. Magnification – 10 X. CN – Sham control, IR – Irradiation, C - Cryptic cell, G – Goblet cell, V – Villi.

The level of lipid peroxidation and the expression of pro - inflammatory genes in intestine as an indicator of oxidative damage are shown in figure 3.8. It indicates that the content of lipid peroxides increased by 4-fold at 10 day post irradiation as compared to the control groups. Irradiated mice treated with DHS and SeM showed significant reduction in the levels of lipid peroxidation by 3.1 and 3.7-folds respectively at 10 day and 1.9 and 2.8-folds respectively at 30 post irradiation.

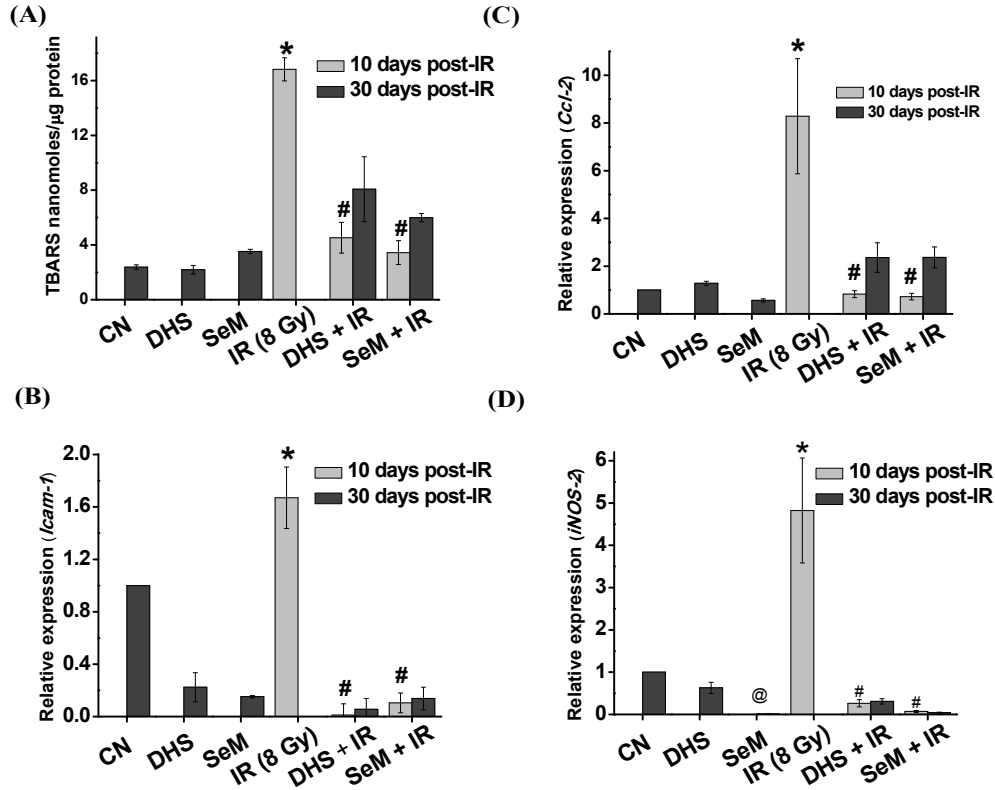


Figure 3.8 Effect of DHS (2 mg/kg b.wt) and SeM (2 mg/kg b.wt) supplementation (ip) on the radiation (8 Gy) induced intestinal inflammatory responses. (A) Level of lipid peroxidation in the jejunum excised from the mice of various groups. (B), (C) and (D) mRNA expressions of *Icam-1*, *Ccl-2* and *iNOS-2* respectively as monitored by RT-PCR. The expression of above genes in different treatment groups was normalized against the sham control group and the relative expression changes have been plotted. Actin expression was used as internal control. The results are presented as mean  $\pm$  SEM ( $n = 3 - 5$ ). \* $p < 0.05$  as compared to the sham control group, # $p < 0.05$  as compared to the radiation control group, @ $p < 0.05$  as compared to DHS treated group evaluated. CN – Sham control, IR – Irradiation.

The similar trend was observed in case of the expression of pro-inflammatory genes. WBI of 8 Gy led to an increase in the expression of these genes compared to control groups. Treatment with DHS or SeM showed significant reduction in the expression of pro-inflammatory genes at 10 day post irradiation. However, the mice surviving till 30 day post irradiation from this group showed unaltered expression of

pro-inflammatory genes (*Icam-1*, *Ccl-2* and *iNOS-2*) as compared to those evaluated at 10 day post irradiation (Fig. 3.8 B – D). Both DHS and SeM were comparable in protecting the intestine from radiation induced toxicities. DHS and SeM control groups did not show any adverse effect with respect to pro-inflammatory gene expressions except that the expression of *iNos-2* was significantly lower in SeM treated mice.

### 3.3.6. Effect of DHS and SeM on the radiation induced oxidative damage and inflammatory responses in the lung

The effect of DHS and SeM on the radiation induced inflammatory responses in the lung was evaluated by histologically assessing the infiltration of inflammatory cells in lung tissue and BAL. The inflammatory scores based on the semi quantitative examination and the representative lung tissue sections from different groups stained with hematoxylin and eosin are shown in figures 3.9 and 3.10 respectively.

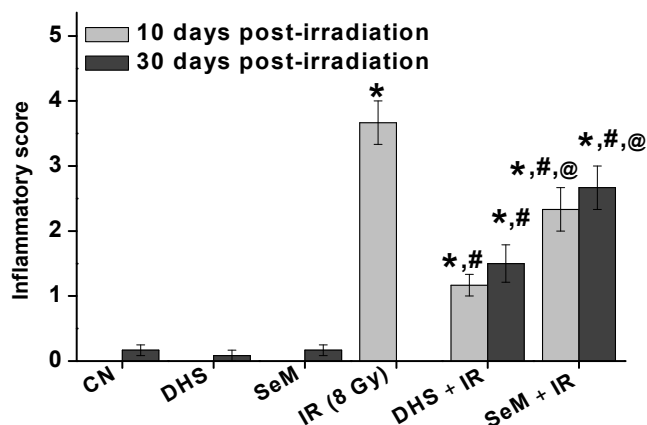


Figure 3.9 Effect of DHS (2 mg/kg b.wt) and SeM (2 mg/kg b.wt) supplementation (ip) on the radiation (8 Gy) induced lung inflammatory responses. Bar graph shows the inflammatory scores under different treatment conditions. The results are presented as mean  $\pm$  SEM (3 - 5 mice). \*  $p < 0.05$  as compared to the control group. #  $p < 0.05$  as compared to the radiation control group, @  $p < 0.05$  as compared to DHS plus radiation treated group evaluated at 10 / 30 day post irradiation. CN – Sham Control, IR - Irradiation

The scoring was given on a scale of 0 – 6; 0 being clear lung and 6 being maximally inflamed lung (characterized by excessive thickening of the alveolar walls with cellular infiltrate and exudates present in the alveolar space of the entire lung section). Further, the presence of different types of cells in the BAL is presented in table 3.2.

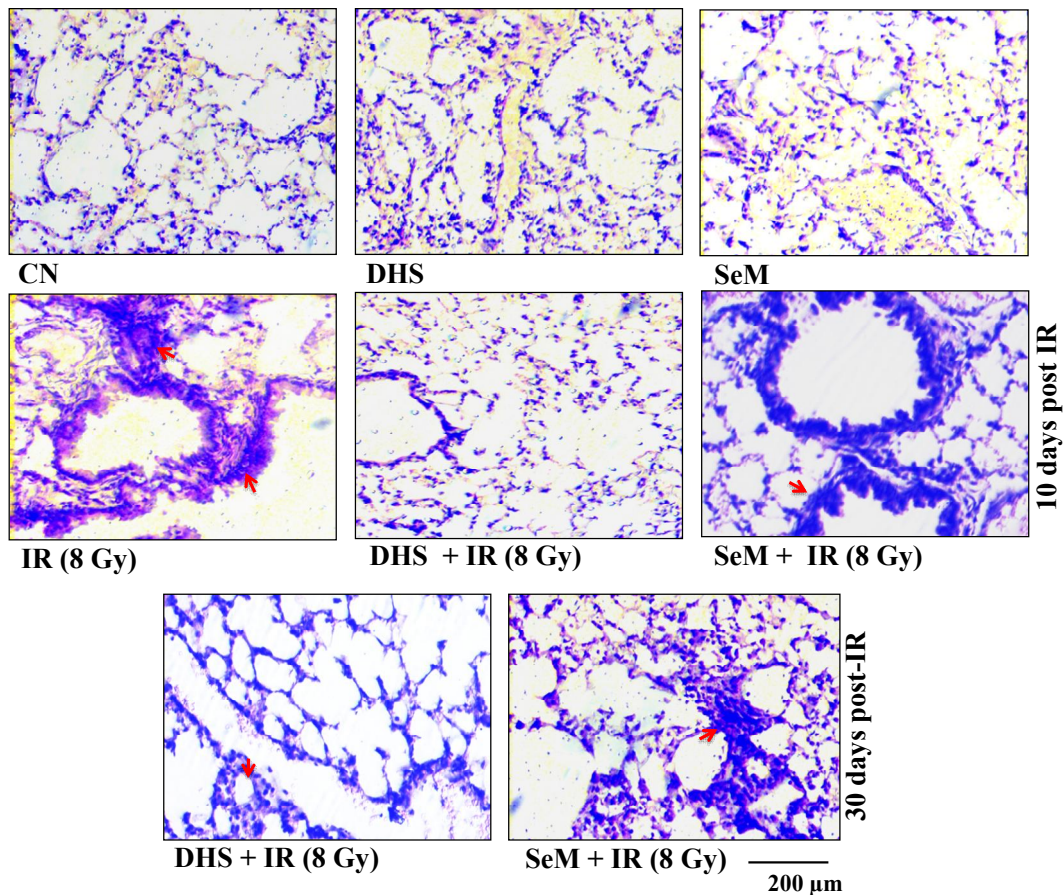


Figure 3.10 Representative tissue section of right lung stained with hematoxylin and eosin shows the effect of DHS (2 mg/kg b.wt) and SeM (2 mg/kg b.wt) supplementation (ip) on the radiation (8 Gy) induced lung damage. Magnification – 10 X. CN – Sham Control, IR - Irradiation

Table 3.2 Count of immune cell types in BALF cell under different treatment conditions

Treatment groups	Total BAL cellularity (10 <sup>3</sup> / ml)	BAL macrophages (% of total cells)	BAL lymphocytes (% of total cells)	BAL ciliary epithelial (% of total cells)	BAL neutrophils (% of total cells)
Sham control	74.72 ± 14.44	89.00 ± 0.60	6.80 ± 2.0	4.20 ± 1.40	-
DHS control	63.50 ± 6.50	85.00 ± 2.30	9.60 ± 1.20	5.40 ± 0.81	-
SeM control	66.35 ± 20.12	88.36 ± 1.50	7.46 ± 1.89	4.18 ± 01.20	-
IR (8 Gy)	149 ± 14.97*	86.99 ± 3.91	10.20 ± 3.17	3.20 ± 1.07	0.38 ± 0.11
DHS + IR (10 day)	68.75 ± 21.25 <sup>#</sup>	84.90 ± 1.70	11.3 ± 1.70	3.00 ± 0.20	0.8 0 ± 0.20
DHS + IR (30 day)	167.50 ± 26.16 <sup>\$</sup>	80.37 ± 3.74	14.98 ± 2.67	4.40 ± 2.83	0.20 ± 0.05
SeM + IR (10 day)	108.75 ± 13.65	80.9 ± 3.60	12.33 ± 2.10	6.27 ± 1.30	0.50 ± 0.20
SeM + IR (30 day)	202.77 ± 80.53 <sup>\$</sup>	77.53 ± 1.87	15.27 ± 3.20	7.00 ± 1.62	0.20 ± 0.10

The results are presented as mean ± SEM (3 - 5 mice). \*  $p < 0.05$  as compared to the control group. <sup>#</sup> $p < 0.05$  as compared to the radiation control group, <sup>\$</sup> $p < 0.05$  as compared to respective drug (DHS or SeM) plus radiation treated group evaluated at 10 day post irradiation.

The results indicated that WBI led to acute inflammatory response in the lung as evidenced by the presence of inflammatory cell infiltrates in lung parenchyma and BAL and the thickening of alveolar wall as compared to sham control group at 10 day post irradiation. It was also noted that WBI significantly increased the total BAL cellularity, did not alter the cell differentials (percentage of macrophages, neutrophils, lymphocytes and ciliary epithelial cells) compared to sham control group (Table 3.2). Treatment with DHS and SeM in irradiated mice showed significant protection from radiation induced inflammatory response as evidenced by the clear lung parenchyma and decrease in the BAL cellularity at the common time point of 10 day post irradiation. The irradiated mice treated with DHS was significantly better than SeM treated mice in reducing radiation induced inflammation.

We also analyzed the lung tissue for lipid peroxidation and BAL fluid for leaked proteins as indications of lung damage. The data are presented in figure 3.11 A

and 3.11 B. Irradiation led to an increase in the lipid peroxidation whereas pre-treatment with DHS showed reduction in the level of lipid peroxidation both at 10 and 30 day post irradiation by 70 % and 40 % respectively. SeM also resulted in decrease in the level of lipid peroxidation by 65 % and 42 % at 10 and 30 day post irradiation respectively. In agreement with the above results, significant reduction in radiation induced protein leakage in BAL was observed at 10 day post irradiation by 80 % and 75 % on treatment with DHS and SeM respectively.

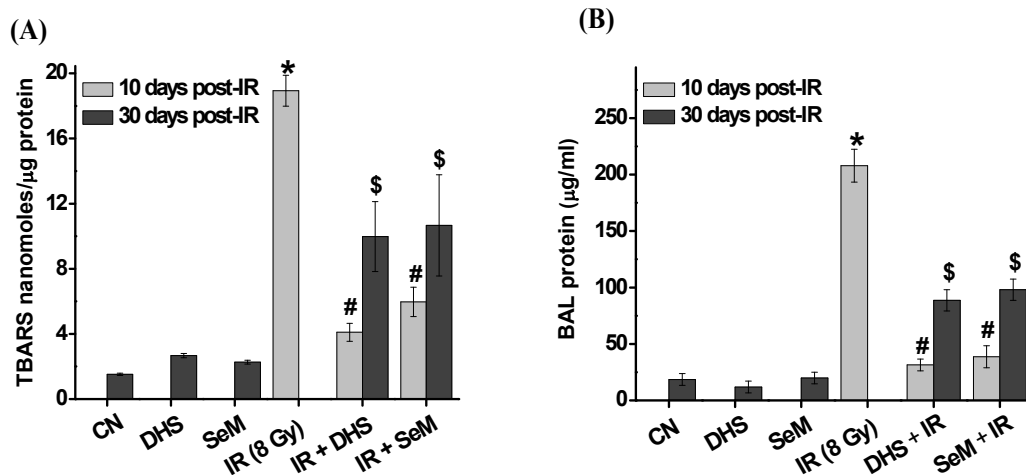


Figure 3.11 Effect of DHS (2 mg/kg b.wt) and SeM (2 mg/kg b.wt) supplementation (ip) on the radiation (8 Gy) induced changes in the level of (A) lipid peroxidation and (B) BAL protein in the lung. The results are presented as mean  $\pm$  SEM (n = 3-5). \* $p < 0.05$  as compared to the sham control group, # $p < 0.05$  as compared to the radiation control group, \$ $p < 0.05$  as compared to respective drug (DHS or SeM) plus radiation treated group evaluated at 10 day post irradiation. CN – Sham control, IR – Irradiation.

Further, radiation dose of 8 Gy caused an increase in the mRNA expression of pro-inflammatory genes like *Icam-1* ( $4.82 \pm 0.84$  folds) and *Ccl-2* ( $5.46 \pm 1.27$  folds) as shown in figures 3.12 A and 3.12 B.

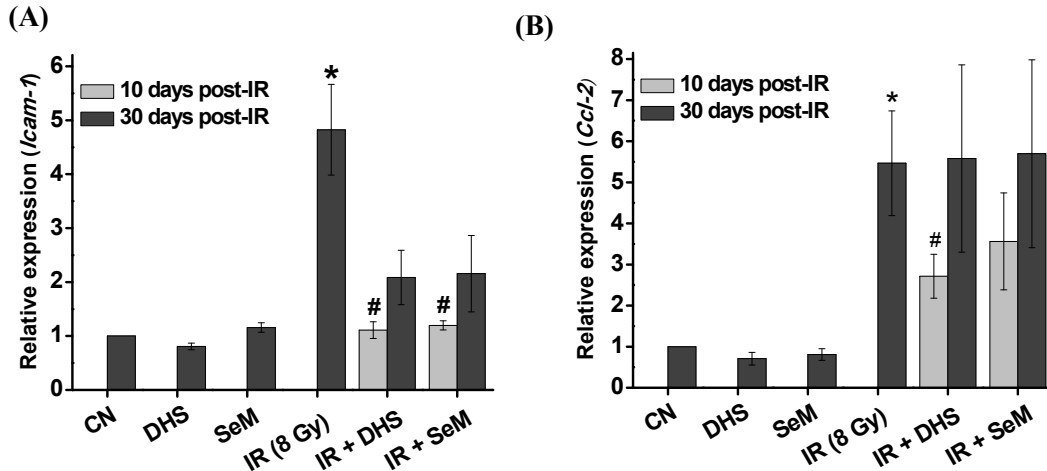


Figure 3.12 Bar graph shows effect of DHS (2 mg/kg b.wt) and SeM (2 mg/kg b.wt) supplementation (ip) against WBI of 8 Gy on pro-inflammatory gene expression (A) *Icam-1* and (B) *Ccl-2* in the lung. The expression of above genes in different treatment groups was normalized against the sham control group and the relative expression changes have been plotted. Actin expression was used as internal control. The results are presented as mean  $\pm$  SEM ( $n = 3-5$ ). \* $p < 0.05$  as compared to the sham control group, # $p < 0.05$  as compared to the radiation control group. CN – Sham control, IR – Irradiation.

Treatment with DHS and SeM in irradiated mice caused reduction in the expression of above genes as compared to the radiation control group. The expression of *Icam-1* at 10 day post irradiation in case of DHS and SeM treated mice were ( $1.10 \pm 0.15$ -folds) and ( $1.19 \pm 0.08$ -folds) respectively whereas the expression was ( $2.71 \pm 0.53$ -folds) and ( $3.56 \pm 1.17$ -folds) respectively in case of *Ccl-2*. Notably, mice from this group showed marginal elevation in lung inflammatory response marked by the influx of inflammatory cells in to lung and BAL, lung damage parameters (like lipid peroxidation and BAL protein content) and the expression of pro-inflammatory genes (*Icam-1* and *Ccl-2*) at 30 day post irradiation as compared to those evaluated at 10 day post irradiation. (Figs. 3.9 - 3.12, Table 3.2)

All the above results suggested the role of both DHS and SeM in suppressing inflammatory response in the lung. DHS and SeM did not differ significantly in affecting the radiation induced inflammatory response in the lung. The respective control groups did not show any adverse effect with respect to the lung toxicity parameters like histological changes, BAL cellularity, lipid peroxidation, BAL protein content and gene expression. (Figs. 3.9 - 3.12, Table 3.2)

### **3.3.7. Effect of DHS and SeM on the radiation induced systemic inflammation**

The effect of DHS and SeM on the radiation induced systemic inflammation was examined by monitoring the circulatory levels of pro-inflammatory cytokines like TNF- $\alpha$  and IL-6 in the serum at 10 day post radiation. The results presented in figure 3.13 indicate that WBI led to significant increase in the levels of TNF- $\alpha$  and IL-6 in circulation. Treatment with DHS or SeM in irradiated mice showed reduction in the levels of TNF- $\alpha$  by 35 % and 50 % respectively as compared to radiation control. Similarly, the decrease in IL-6 level in irradiated mice treated with DHS and SeM was 45 % and 42 % respectively as compared to radiation control. The mice which survived from these groups till 30 day post irradiation showed marginal increase in the levels of above cytokines as compared to those evaluated at 10 day. The drug and sham control groups showed comparable levels of TNF- $\alpha$  and IL-6 in serum.

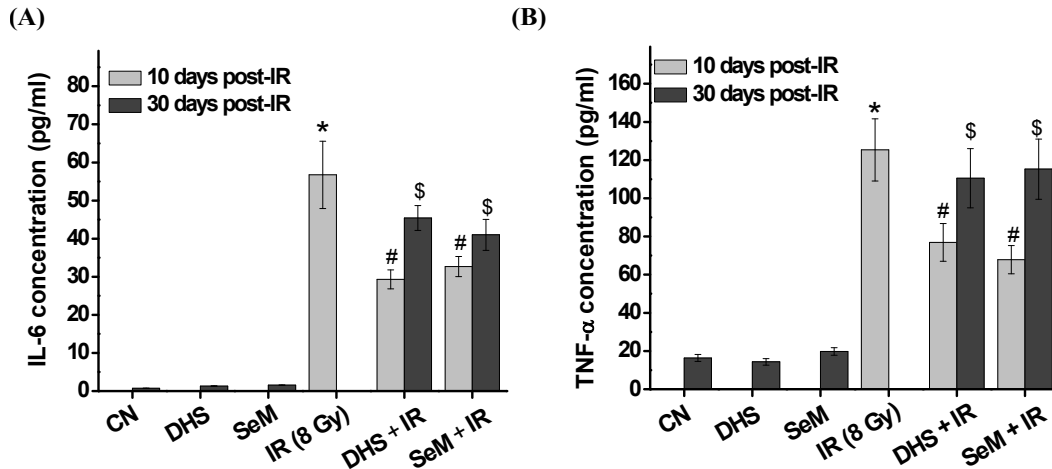


Figure 3.13 Bar graph shows effect of DHS (2 mg/kg b.wt) and SeM (2 mg/kg b.wt) supplementation (ip) on the radiation (8 Gy) induced systemic inflammation. Levels of (A) IL-6 & (B) TNF- $\alpha$  monitored in the serum using ELISA kit. The results are presented as mean  $\pm$  SEM (n = 3 - 5). \* $p < 0.05$  as compared to the sham control group, # $p < 0.05$  as compared to the radiation control group, \$ $p < 0.05$  as compared to respective drug (DHS or SeM) plus radiation treated group evaluated at 10 day post irradiation. CN – Sham control, IR – Irradiation

### 3.3.8. Effect of DHS and SeM on hepatic architecture

Further to determine hepatotoxicity if any, associated with DHS or SeM liver was evaluated histologically. The representative liver tissue sections stained with hematoxylin and eosin and the number of binucleate cells is shown in figures 3.14 and 3.15 respectively. It can be seen that WBI of 8 Gy led to an increase in the number of binucleate cells which are the major cell types in the regenerating liver. The number of binucleate cells was comparable between DHS / SeM treated and radiation control mice. Between DHS and SeM, the former induced significantly higher number of binucleate cells both under irradiated and unirradiated conditions at all the time points. However, neither of these treatments altered hepatic architecture as compared to the sham control at all time points.

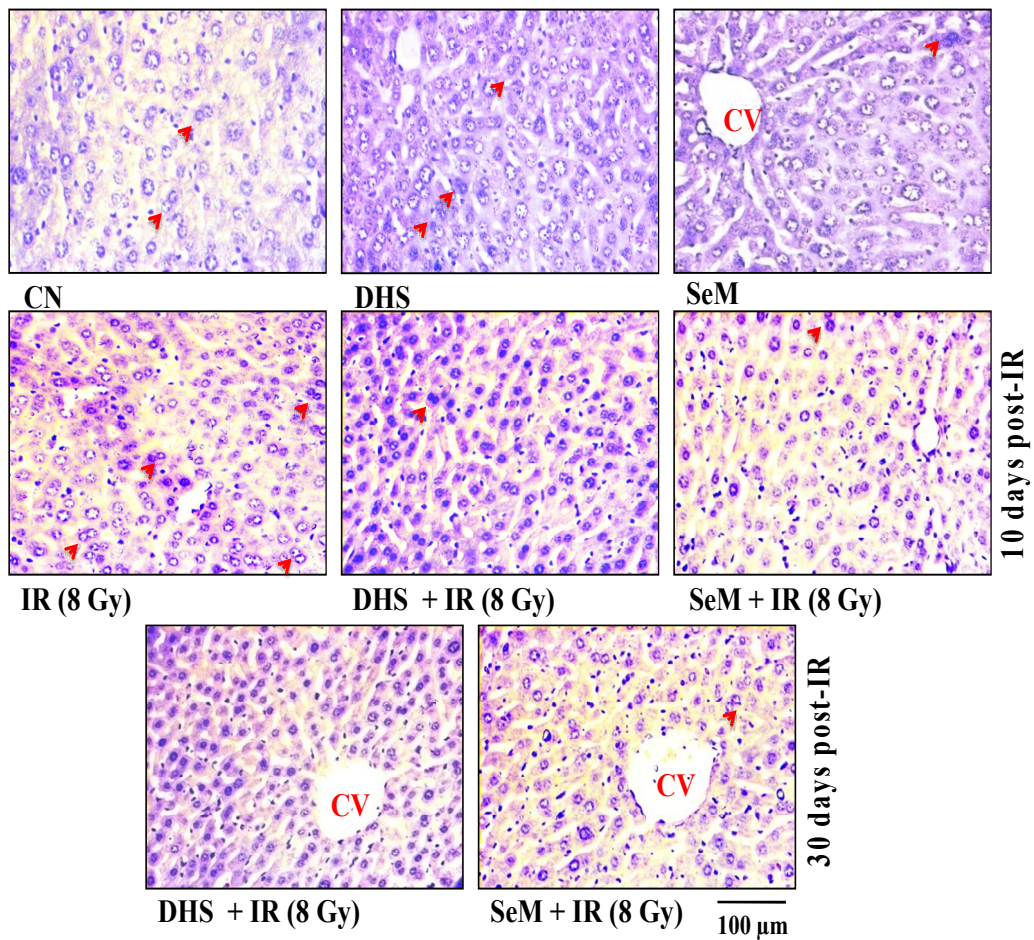


Figure 3.14 Representative tissue section stained with hematoxylin and eosin shows the effect of DHS (2 mg/kg b.wt) and SeM (2 mg/kg b.wt) supplementation (ip) on the radiation (8 Gy) induced changes in hepatic architecture. Magnification – 20 X. CV- Central vein. Arrow indicates binucleate cells. CN – Sham control, IR – Irradiation.

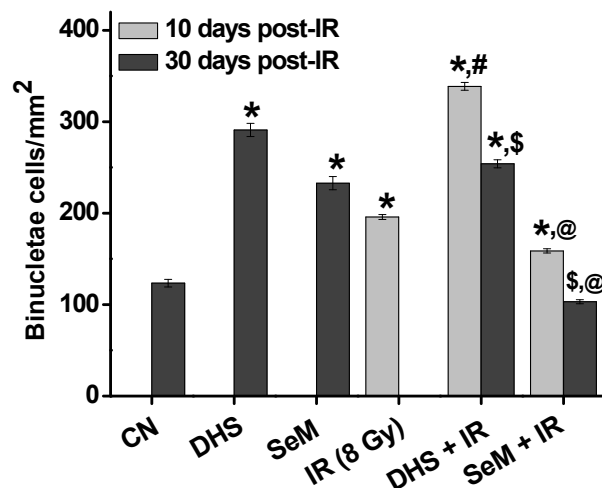


Figure 3.15 Bar graph shows the effect of DHS (2 mg/kg b.wt) and SeM (2 mg/kg b.wt) supplementation (ip) on the counts of binucleate cells in liver tissue section. \* $p < 0.05$  as compared to the sham control group, \$ $p < 0.05$  as compared to respective drug (DHS or SeM) plus radiation treated group evaluated at 10 day post irradiation, @ $p < 0.05$  as compared to DHS plus radiation treated group evaluated at 10 / 30 day post irradiation. CN – Sham control, IR – Irradiation

### 3.3.9. Effect of DHS and SeM on *SelenoP-1* expression in the liver

The antioxidant effect of DHS and SeM in response to radiation exposure was evaluated in terms of the mRNA expression of *SelenoP-1* in liver. The result shown in figure 3.16 clearly indicated that WBI of 8 Gy led to significant induction of *SelenoP-1* in liver (2.3-folds) at 10 day post irradiation as compared to the sham control. DHS and SeM control groups also showed significant induction in *SelenoP-1* level by 2.2 and 1.4-folds respectively as compared to the sham control. In irradiated mice their treatment showed higher level of *SelenoP-1* in liver than the radiation control group at 10 and 30 day. DHS was better than SeM in inducing *SelenoP-1* both under irradiated and un-irradiated conditions.

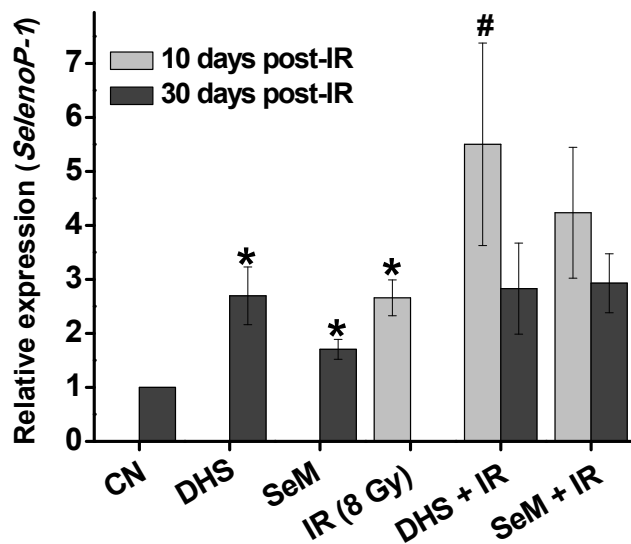


Figure 3.16 Effect of DHS (2 mg/kg b.wt) and SeM (2 mg/kg b.wt) supplementation (ip) on mRNA expression of SelenoP-1 in hepatic tissue against WBI of 8 Gy under different treatment conditions. The expression of gene in different treatment groups was normalized against the sham control group and the relative expression changes have been plotted. Actin expression was used as internal control. The results are presented as mean  $\pm$  SEM ( $n = 3 - 5$ ). \* $p < 0.05$  as compared to the sham control group, # $p < 0.05$  as compared to the radiation control group. CN – Sham control, IR – Irradiation

### 3.3.10. Effect of DHS and SeM on total GPx activity

As selenium compounds are known to exhibit their action by modulating the level of another important selenoenzyme GPx, herein we evaluated the total GPx activity in lungs, liver and spleen under different treatment conditions. The effect of DHS and SeM supplementation on GPx activity is shown in figure 3.17. It can be seen that irradiation led to significant increase in total GPx activity in spleen and lungs by ~ 2-folds whereas it did not cause any significant change in the intestine. DHS and SeM control groups also showed induction in GPx activity in all the three organs and their levels were comparable in the range of 1.5 to 2-folds (Fig. 3.17). In irradiated mice, pre-treatment with DHS or SeM caused either the augmentation or comparable effect in

GPx activity in intestine and spleen both at 10 and 30 day post irradiation. The induction of GPx in DHS treated irradiated mice was significantly more in lungs as compared to SeM both at 10 and 30 day post irradiation.

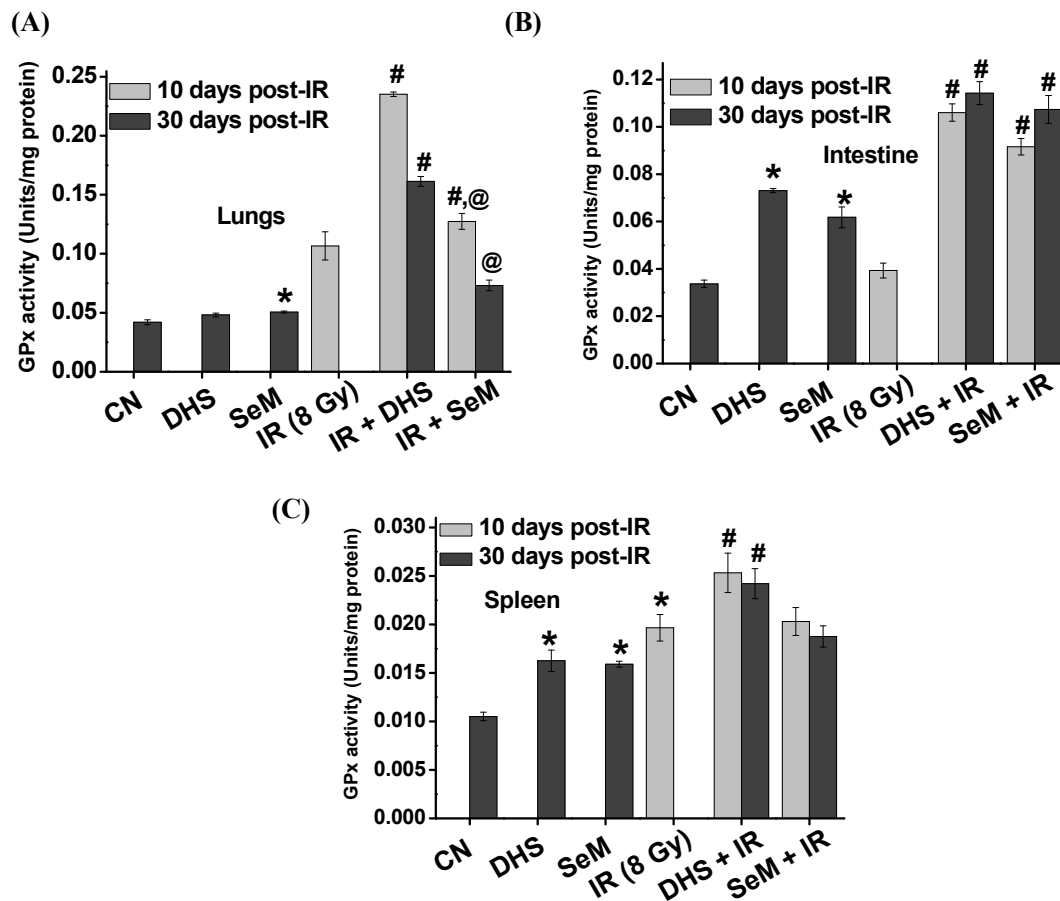


Figure 3.17 Effect of DHS (2 mg/kg b.wt) and SeM (2 mg/kg b.wt) supplementation (ip) on the radiation (8 Gy) induced changes in total GPx activity in (A) lung, (B) intestine and (C) spleen. The results are presented as mean  $\pm$  SEM (n = 3-5). \* $p < 0.05$  as compared to the sham control group, # $p < 0.05$  as compared to the radiation control group, @ $p < 0.05$  as compared to DHS plus radiation treated group evaluated at 10 / 30 day post irradiation CN – Sham control, IR – Irradiation.

### 3.3.11. Effect of DHS and SeM on the tissue specific expressions of GPx isoforms

Since GPx activity in cells is contributed by the expression of GPx isoforms, our next aim was to evaluate the mRNA expression of three major intracellular

isoforms such as *GPx 1*, *GPx 2* and *GPx 4* in lung, intestine and spleen. The expression of GPx isoforms under different treatment conditions are presented in figure 3.18. As shown, irradiation led to induction of all the three *GPx* isoforms in spleen, *GPx 2* and *GPx 4* in the intestine and *GPx 1* in the lung at 10 day post irradiation. DHS or SeM control groups also showed induction of all the three *GPx* isoforms, however differed in their tissue specific expressions. For example, DHS control group showed increase in the expression of *GPx 1* and *GPx 4* in spleen by ~2 and ~8-folds respectively. Similar treatment increased the expressions of *GPx 1* and *GPx 4* in intestine by ~4 and ~6-folds respectively. With regard to *GPx 2*, DHS administration increased its level only in intestine by ~ 2 folds. On the other hand, SeM control group increased the expression of *GPx 1* in the intestine by 4-folds and that of *GPx 2* in spleen and intestine by ~7 and ~4-folds respectively. SeM did not alter the level of *GPx 4* in any of the three tissues investigated (Fig. 3.18). In line with these results, treatments with DHS and SeM in irradiated mice although differed in their response, significantly augmented the radiation induced expression of *GPx* isoforms in different tissues at 10 and 30 day post irradiation. Interestingly, DHS significantly increased the radiation induced expression of *GPx 1* in all three organs and those of *GPx 2* and *GPx 4* in intestine and spleen respectively. Whereas, SeM treatment increased the radiation induced expression of *GPx 1* in intestine, of *GPx 2* in spleen and intestine and did not affect the expression of *GPx 4* (Fig. 3.18). These results confirmed the abilities of DHS and SeM to modulate the expression of *GPx 1*, *GPx 2* and *GPx 4* in radiosensitive organs of spleen, intestine and lung leading to an increase in total GPx activity which might favor protection from radiation induced oxidative damage and subsequent inflammatory response.

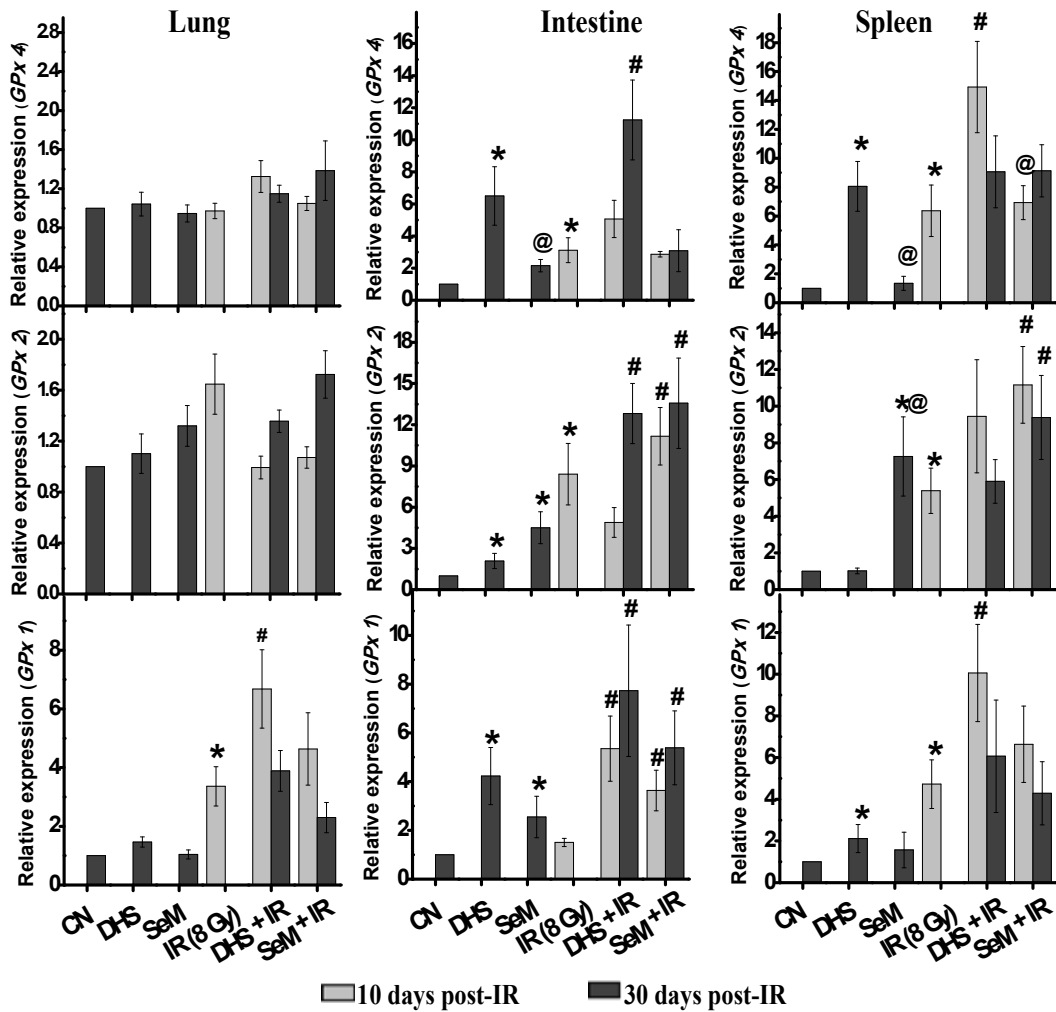


Figure 3.18 Effect of DHS (2 mg/kg b.wt) and SeM (2 mg/kg b.wt) supplementation (ip) on the mRNA expression of GPx 1, GPx 2 and GPx 4 in lung, intestine and spleen against WBI of 8 Gy. The expression of gene in different treatment groups was normalized against the sham control group and the relative expression changes have been plotted. Actin expression was used as internal control. The results are presented as mean  $\pm$  SEM (n = 3 - 5). \* $p$  < 0.05 as compared to the sham control group, # $p$  < 0.05 as compared to the radiation control group, @ $p$  < 0.05 as compared to DHS / DHS plus radiation treated group. CN – Sham control, IR – Irradiation.

### 3.4. Discussion

Exposure of animals to lethal dose of radiation (>6 Gy) is known to induce hematopoietic and gastrointestinal syndromes accompanied with systemic as well as organ specific inflammatory responses leading to multi-organ failure and ultimately the mortality<sup>193-197</sup>. For an ideal radioprotector to be used under radiation emergencies, the most important property that it should possess is the ability to provide survival advantage against the lethal absorbed doses of WBI<sup>198</sup>. Accordingly, we have examined DHS for *in vivo* radioprotection by monitoring its ability to improve the 30 day post irradiation survival and to prevent organ specific toxicities in mice model system exposed to WBI (5 - 8 Gy).

DHS administration for five consecutive days before WBI in mice significantly prevented DNA damage but did not provide significant improvement in 30 day survival. However, when DHS was administered as a supplement i.e. for 5 consecutive days prior to radiation exposure and continued for three times per week till the end of the experiment improved the 30 day survival of mice by 40 % at the lowest dose of 2 mg/kg b.wt. These results suggested that the availability of DHS during the post irradiation period (when organ toxicity is induced) is important. In subsequent studies, we focused on examining the effect of DHS supplementation (pre and post-irradiation) on organ-specific toxicity and inflammatory responses.

Hematopoietic stem cells and bone marrow cells are highly sensitive to radiation exposure<sup>194,199-201</sup>. These stem cells undergo differentiation to form mature blood cells like lymphocytes and platelets. Due to the damaging effect of ionizing radiation on stem cells, there is an acute loss of hematopoietic cells in the circulation and spleen characterised as leucopenia<sup>202-204</sup>. The deficiency in the number of

lymphocytes weakens the immune system of the individual resulting in haemorrhage and increased chance of infection, which in case of no supportive care may lead to mortality within 1 - 3 days<sup>56,204</sup>. Protection from hematopoietic syndrome by an agent depends on its ability to protect hematopoietic cells from undergoing radiation induced cell death or apoptosis as well as to renew the hematopoietic system by inducing proliferation of surviving stem cells<sup>201,205</sup>. Spleen index and cellularity are important parameters to monitor damage to the hematopoietic system. WBI to 8 Gy led to hematopoietic toxicity which was evidenced as decrease in spleen index, cellularity and CFU<sup>204</sup>. Treatment with DHS, although did not show any protection from radiation-induced acute hematopoietic toxicity but showed restoration of the spleen index, cellularity and CFU at late time point (30 day). This was further confirmed by the delayed proliferation of clonogenic stem cells, as marked by the remarkable increase in hematocount in circulation and the expression of *Csf-3* in spleen of animals surviving to irradiation until 30 day.

Like the hematopoietic system, the small intestine is also a highly radiosensitive organ<sup>195,150</sup>. The lining of small intestine is occupied by highly absorptive epithelial cells or the enterocytes in the form of special structures called villi. At the base of villi, intestinal stem cells (ISC) are located, which are radiosensitive due to their hyper proliferative capability<sup>206-208</sup>. ISC provide a constant supply of differentiated cells like enterocytes and epithelial cells which move up to the surface of the villi to form a mucosal lining<sup>206</sup>. At the lethal dosage of irradiation, these epithelial cells undergo oxidative damages and cell death resulting in to disruption of villi and mounting of inflammatory responses<sup>206,207,209</sup>. The lung is another radiosensitive organ known to be the target of radiation induced oxidative damages and inflammatory responses<sup>197,152</sup>. Treatment with DHS showed delayed restoration of villi structure and significantly

prevented radiation induced acute infiltration of inflammatory cells in lungs and intestine. The inhibition of inflammatory responses in intestine and lung by DHS was associated with its ability to prevent lipid peroxidation, an initiator of inflammatory responses, and to reduce the expression of genes like *Icam-1*, *Ccl-2*, and *iNos-2* known to be involved in the recruitment of inflammatory cells to the damaged tissues<sup>210-212</sup>. Further irradiation is also known to increase the circulatory level of cytokines like IL-6 and TNF- $\alpha$ <sup>211</sup>. These cytokines may play role in radioprotection as well as inflammatory responses by stimulating the proliferation of lymphocytes. For example, IL-6 level induced immediately after radiation exposure is expected to prevent leucopenia, however its sustained elevation for a long period leads to inflammatory responses. In present study, the levels of IL-6 and TNF- $\alpha$  were measured at 10 and 30 day post irradiation to monitor the effect of DHS treatment on systemic inflammatory responses and the results showed significant decrease in the levels of above cytokines by DHS. Further, it also prevented systemic inflammation marked by the decrease in the concentration of pro-inflammatory cytokine like IL-6 and TNF- $\alpha$  in the serum. The anti-inflammatory actions of DHS are in line with the previous report wherein, it has been shown to reduce the indomethacin induced gastric ulcers in mice model system.<sup>163,164</sup> Notably the above histological and biochemical analysis revealed that there was a marginal increase in inflammatory responses in the intestine, lung and circulation of DHS treated mice examined from 10 to 30 day of radiation exposure. The delayed increase in spleen cellularity and hematocount in circulation of these mice could also occur because of the inflammatory responses within body. Together these results suggested the delaying of radiation induced inflammatory responses in DHS treated mice and this could be attributed to its anti-inflammatory activity as reported in previous studies.

Considering the fact that DHS was able to prevent the radiation induced oxidative damages and inflammatory responses in radiosensitive organs, we thought to monitor the modulation in the tissue specific expression of genes involved in the antioxidant actions of selenium compounds such as *GPx* and *SelenoP-1*<sup>113,124,147,213-215</sup>. There are eight different isoforms of GPx known till date, of which *GPx 1*, *GPx 2* and *GPx 4* have been reported for antioxidant and anti-inflammatory roles<sup>216-219</sup>. *GPx 1* is the major cytosolic isoform accounting for the GPx activity and catalyses the reduction of hydroperoxides<sup>217</sup>. The other isoform, *GPx 2* is also localized in the cytoplasm and performs the same function as that of *GPx 1* but is mainly expressed in the gastrointestinal system<sup>126</sup>. On the other hand, *GPx 4* localizes in the cytosol, possesses the substrate specificity towards phospholipid hydroperoxide and thus plays a role in preventing the lipid peroxidation<sup>126,217</sup>. Treatment with DHS led to tissue-specific induction of GPx isoforms and the overall GPx activity in lung, intestine and spleen. This suggested that one of the mechanisms responsible for the ability of DHS to inhibit the radiation induced lipid peroxidation and subsequent inflammatory responses in the intestine and lung might be due to the induction of *GPx* isoforms<sup>216,218-220</sup>. Further, it is also possible that above GPx isoforms may be playing a tissue-specific role in protection. Earlier Mansur et al has reported that supplementation of human lymphoblast cell line Sup-T1 with 30 nM sodium selenite increased GPx activity by 8-fold but did not confer any radioprotection<sup>221,222</sup>. This explains the inability of DHS to provide significant protection against radiation induced acute hematopoietic toxicity. We also examined the effect of DHS administration on another important antioxidant selenoprotein, SelenoP<sup>223</sup>. SelenoP is synthesized in the liver and secreted in the plasma. It plays a role in maintaining selenium homeostasis in the body and is also reported for antioxidant effects in tissue through ROS / RNS scavenging.<sup>123,124</sup> The ability of DHS

to reduce the systemic inflammation could be attributed to the increase in the expression of *SelenoP-1* in liver.

One of the notable aspects of present investigation is that the radioprotective effect of DHS is comparable to SeM, a standard organoselenium compound shown to exhibit chemopreventive as well as radioprotective effects as a supplement<sup>214,224</sup>. Our results indicated that DHS is as good as SeM or marginally better in improving the 30 day survival of mice post irradiation under identical dosage and treatment condition. Most of the biochemical and histological parameters evaluated to monitor the radioprotective effect of DHS and SeM in irradiated mice were comparable. The most common mechanism by which a linear organoselenium compound like SeM could induce the expression of GPx isoforms is through its incorporation in to selenium pool by metabolism<sup>117</sup>. However, DHS being a cyclic organoselenium compound is expected to be metabolically stable and therefore its ability to induce GPx could be primarily due to alteration in cell signaling pathways which require further investigations. The most successful sulfur based radioprotector, amifostine, is reported to enhance the 30 day survival of  $\gamma$ -irradiated mice with a DMF of 2.7. However, the dosage of amifostine needed to achieve this is 900 mg/kg b.wt and is associated with severe side effects like like nausea, vomiting and bone marrow suppression.<sup>7,75,81</sup>. Due to the differential reactivity of sulfur and selenium compounds, we have not compared the radioprotective efficacy of DHS with that of amifostine in the present study. However, such study will be useful in later stage after thorough evaluation of the toxicity and pharmacokinetics of DHS *in vivo*. Further, DHS is highly water soluble and may be poorly bio-available. Therefore, in subsequent chapters, lipophilic derivatives of DHS were evaluated for bio-availability, antioxidant activity and radioprotective effect. The summary of the above studies is given below.

### 3.5. Summary

1. DHS administration in mice at a non-toxic dose of 2 mg/kg b.wt for five consecutive days prior to WBI of 8 Gy and continued for three times a week during the post irradiation period improved 30 day survival by 40 %.
2. DHS reduced DNA damage in peripheral leukocytes of irradiated mice.
3. DHS showed delayed restoration of hematopoietic system in irradiated mice by elevating parameters like spleen index, cellularity and colony forming units.
4. DHS led to an increase in the expression of *GPx* isoforms (*GPx 1*, *GPx 2*, *GPx 4*) and overall GPx activity in radiosensitive organs like lung, spleen and intestine. It also increased the expression of *SelenoP-1* in liver.
5. DHS suppressed inflammatory responses and oxidative damages in lung and intestine of irradiated mice.
6. DHS reduced systemic inflammation in irradiated mice by lowering the level of IL-6 and TNF- $\alpha$  in the serum.
7. DHS may be explored as an organ specific radioprotector.

## **Chapter 4**

### **Effect of alkyl chain length on the cellular uptake and antioxidant activity of DHS and MAS**

Attaching a fatty acid / alkyl group as a lipophilic unit with a pharmacologically important hydrophilic moiety is an effective approach to increase its bioavailability. Accordingly, a series of lipophilic derivatives of DHS and a structurally related molecule, MAS, were synthesized by attaching fatty acids or alkyl groups of variable chain length (C<sub>6</sub> - C<sub>14</sub>). All these derivatives were evaluated for cytotoxicity, uptake and antioxidant activity in Chinese Hamster Ovary (CHO) cells and the results are discussed in this chapter.

#### 4.1. Introduction

Previous studies established that DHS exhibited a wide range of pharmacological activities including radioprotection<sup>160,163–165,167</sup>. One of the factors which can further enhance the biological activity of DHS is its improved cellular uptake. For a compound to be optimally bio-available, it should possess the right balance of hydrophilicity and lipophilicity. DHS being an extremely hydrophilic molecule ( $\log P = -0.48$ )<sup>162</sup> is expected to be cleared very fast from the body. This necessitates the need to develop a strategy to impart lipophilicity in its structure. Interestingly, a number of studies have indicated that conjugation of a drug molecule containing alcohol functional group with a fatty acid / alkyl group imparts required hydrophobicity to the drug for its entry in the cell. Additionally, Lambert et al proposed that such drug-fatty acid conjugate can take advantage of the metabolic enzymes (like esterase, lipases) involved in lipid metabolism to increase membrane affinity, uptake and bioactivity of the principle drug<sup>225–228</sup>. For example, Geurts et al showed that an ester derivative of glycine, N-(benzyloxycarbonyl) glycine benzylamide showed higher anticonvulsant activity compared to that of the parent compound through increased uptake<sup>228</sup>. In another study, Jacob et al showed that esterase present in the brain tissue cleaved fatty acid derivatives of  $\gamma$ -aminobutyric acid (GABA) releasing GABA in the tissue whereas free GABA was not able to cross the blood brain barrier due to poor hydrophobicity<sup>226</sup>. On similar lines, it was hypothesised that incorporating lipophilicity in the structure of DHS might allow it to localize in the membranes and thereby increase its cellular availability<sup>161,162,167</sup>. Indeed, employing cell free system, our group had previously shown that the conjugation of a fatty acid of increasing alkyl chain length (C<sub>6</sub> to C<sub>14</sub>) to parent molecule DHS not only increased its specificity towards the

liposomal membranes but also improved its ability to inhibit lipid peroxidation in a chain length dependant manner<sup>161,162</sup>. Therefore, such derivatives were projected as better antioxidants compared to the parent compound DHS<sup>161,162,167</sup>. In addition to DHS, monoamine selenolane (MAS) a structurally related organoselenium compound has also been reported for similar biological activities *in vitro*. In fact, MAS is reported to be a better redox modulator than DHS in maintaining proteins in reduced state<sup>167</sup>. Keeping these considerations in view, this chapter explores the possibilities of derivatization of DHS / MAS with alkyl chain of variable length as a strategy to improve hydrophobicity in such a way that it increases cell uptake. Further all these derivatives were evaluated for cytotoxicity and antioxidant effects in cells in order to identify the most effective compound that can be further evaluated for radioprotection. The chemical structures of DHS, MAS and their fatty acid / alkyl derivatives used in the present study are given in Scheme 1.7.

#### **4.2. Materials and Methods**

The stock solutions of DHS and MAS were prepared in culture medium and the solution of alkyl derivatives of DHS and MAS were prepared in DMSO and then added to the culture medium to obtain the desired concentrations. The concentration of DMSO was kept constant within permissible limits of toxicity (0.25 %). The cells treated with selenium compounds were incubated in a humidified atmosphere with 5 % CO<sub>2</sub> at 37 °C for the desired time points prior to assay. The cytotoxicity was estimated by MTT assay, JC-1 staining, LDH release and Annexin V-PI staining. The interaction of the selenium compounds with cellular membrane and the subsequent changes in integrity and fluidity of membrane was estimated by following changes in the fluorescence intensity of DPH. The uptake / loading of DHS, MAS and their fatty acid /

alkyl derivatives into cells was estimated in terms of selenium level using graphite furnace atomic absorption spectrometry. The effect of selenium compounds on the mRNA expression of GPx was monitored by RT-PCR. The GPx activity was measured by NADPH assay coupled with GSH-GSSG. The level of lipid peroxidation and protein carbonylation were assessed by TBARS and DNPH assays respectively. All the experiments were carried out in triplicate and repeated at least two times. Data are presented as mean  $\pm$  SEM, n = 3 from an independent experiment. The data were analyzed by one-way ANOVA using Origin (version 6.1) software to confirm the variability of the data. The P values < 0.05 were considered as statistically significant.

### **4.3. Results**

#### **4.3.1. Effect of DHS, MAS and their fatty acid / alkyl derivatives on cytotoxicity in CHO cells**

The cytotoxic effects of DHS, MAS and their fatty acid / alkyl derivatives (C<sub>6</sub>–<sub>14</sub>) in CHO cells were evaluated using MTT assay at 24, 48 and 72 h in a concentration range of 1 - 50  $\mu$ M. The derivatives with carbon chain length lower than C<sub>6</sub> were not stable and therefore not included in the study. The results indicated that the parent compounds (DHS, MAS) in the concentration range of 1 - 50  $\mu$ M did not exhibit any significant cytotoxicity even after 72 h of their addition into the cells. The shorter chain (C<sub>6</sub>) derivatives of DHS and MAS did not show cytotoxicity up to the treatment concentration of 30  $\mu$ M. Further increase in treatment concentration up to 50  $\mu$ M showed a concentration and time dependency with marginal increase (~8 - 15 %) in the cytotoxicity. Longer chain (>C<sub>8</sub>) derivatives of DHS and MAS exhibited significantly higher cytotoxicity compared to the parent compound or C<sub>6</sub> derivatives at all treatment

concentrations and time point as shown in figure 4.1. At an identical treatment concentration of 25  $\mu\text{M}$ , the cytotoxicity effects of DHS derivatives followed the order  $C_6 < C_8 < C_{10} \sim C_{12} > C_{14}$  with 7 %, 44 %, 58 %, 56 % and 37 % toxicity respectively at 72 h. Whereas MAS derivatives followed the order of  $C_6 < C_8 < C_{10} \sim C_{12} \sim C_{14}$  with 9 %, 70 %, 78 %, 80 % and 81 % toxicity respectively at 72 h. Between DHS and MAS derivatives, the former showed significantly lesser cytotoxicity than the latter at each chain length and treatment concentration, evaluated up to 48 h time point.

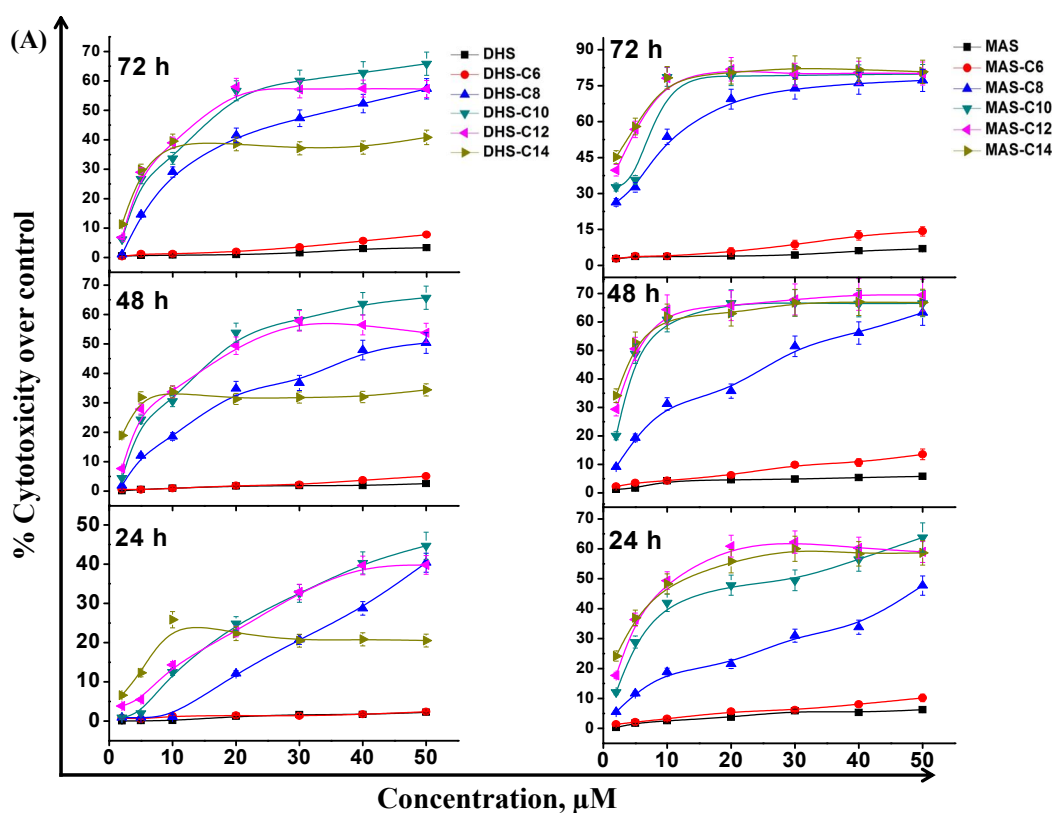


Figure 4.1 Cytotoxic effect of DHS, MAS and their derivatives ( $C_{6-14}$ ) in the concentration range of (1 - 50  $\mu\text{M}$ ) by MTT assay at different time points (24, 48 and 72 h) after their addition to CHO cells. Cytotoxicity is expressed as percentage of the control cells (DMSO, 0.25 %). Results are presented as mean  $\pm$  SEM,  $n = 3$ .

In order to understand, whether the cytotoxic effect was due to the selenium or the alkyl chain, a control experiment was performed in which cells were treated with

linear fatty acids of variable carbon chain length (C<sub>6</sub> to C<sub>14</sub>) without any selenide moiety for 72 h in the concentration range from 1 - 50 μM. The results showed that these fatty acids did not induce any significant (~ 4 %) toxicity in CHO cells as shown in figure 4.2.

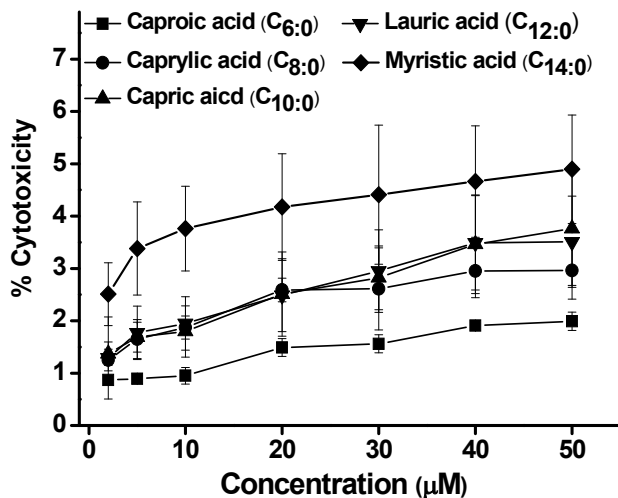


Figure 4.2 Cytotoxic effect of free fatty acids (C<sub>6:0</sub> to C<sub>12:0</sub>) in CHO cells. Cells were treated with increasing concentration of fatty acids for 72 h and the cytotoxicity was determined by MTT assay. Cytotoxicity is expressed as percentage of the control cells (DMSO, 0.25%). Results are presented as mean ± SEM, n = 3.

#### 4.3.2. Effect of DHS, MAS and their fatty acid / alkyl derivatives on LDH release in CHO cells

LDH is metabolic enzymes present in the cytosol which catalyses the conversion of lactate to pyruvic acid. During membrane disruption, LDH is released in the extracellular space. As, LDH is a stable enzyme and does not lose its activity during cell death process, the presence of LDH in the culture medium is used as a marker for membrane toxicity and cell death<sup>176,229</sup>. Since the lipophilic compounds may cause membrane disruption, treatment of cells with DHS, MAS and their derivatives was expected to cause the release of LDH. However before performing such assay, it was

important to know the suitability of LDH assay to be used, as organochalcogens are known to inhibit LDH by themselves<sup>230</sup>. In order to address this, the effect of the treatment with DHS or MAS on the activity of LDH freshly isolated from the cells, was evaluated. The results as shown in figure 4.3 indicated that neither DHS nor MAS affected the activity of LDH.

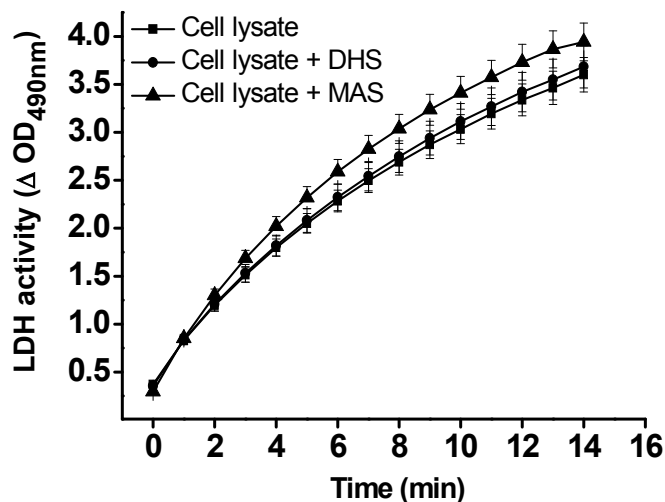


Figure 4.3 Effect of DHS and MAS treatment on LDH activity in cell lysate. The control sample represents untreated cell lysate subjected to LDH determination. Results are presented as mean  $\pm$  SEM,  $n = 3$ .

Based on this, the effect of DHS, MAS and their fatty acid / alkyl derivatives treatment at 25  $\mu$ M on plasma membrane integrity was evaluated by monitoring the leakage of LDH from cells to the culture medium in a time dependent manner (2 – 24 h). It can be seen from the figure 4.4 A and 4.4 B that the parent compound DHS and MAS did not induce much leakage of LDH from the cells (~1.5 %). Treatment with derivatives (C<sub>6-14</sub>) of DHS and MAS led to the time dependent increase in the leakage of LDH from the cells compared to the respective parent compound and this effect was significant for derivatives with chain lengths longer than C<sub>6</sub> suggesting their ability to cause plasma membrane disruption. DHS derivatives showed a non-linear response

with regard to the effect of chain length on LDH leakage at each time point. For example, LDH leakage increased with increasing chain lengths from C<sub>6</sub> to C<sub>10</sub>, saturated at C<sub>12</sub> and then decreased at C<sub>14</sub>. In comparison, MAS derivatives exhibited a chain length dependent increase in LDH release until C<sub>12</sub> and the saturation effect at C<sub>14</sub> at each time point. Among the DHS and MAS derivatives, the former was less effective in causing LDH leakage than the latter at each chain length. The percentage release of LDH with respect to control in C<sub>14</sub> derivatives of DHS and MAS were 18 % and 65 % respectively at a common time point of 6 h.

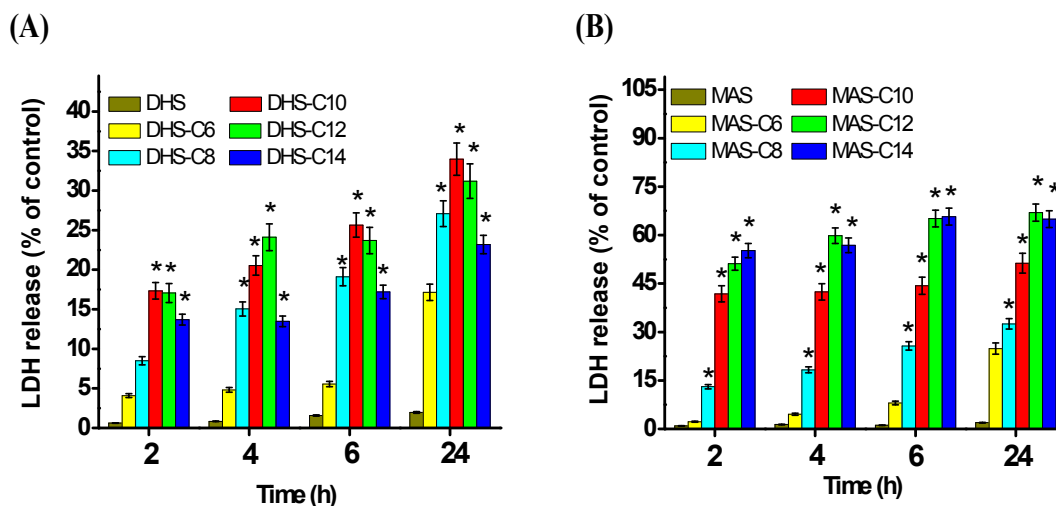
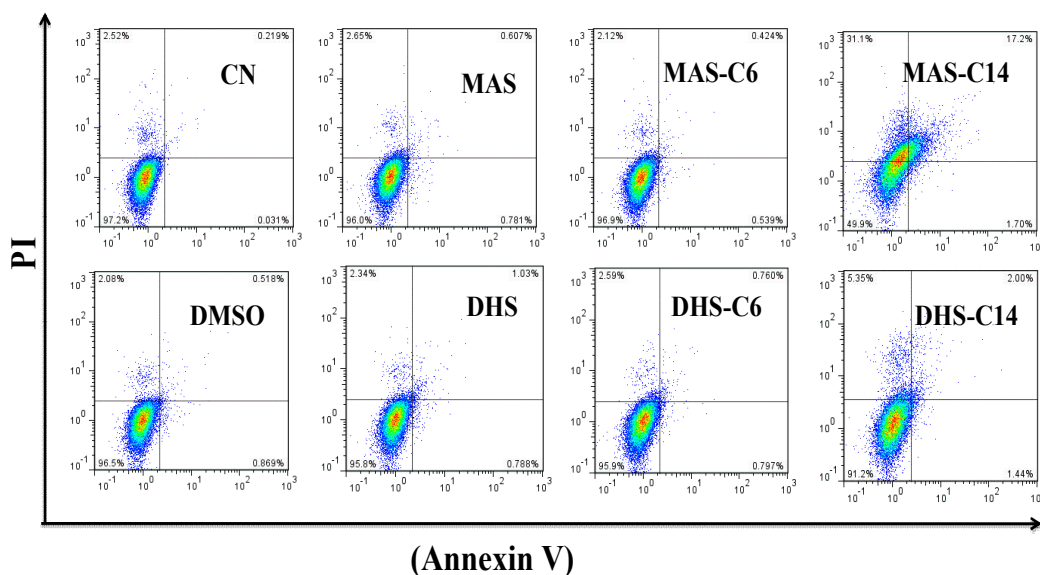


Figure 4.4 Effect of treatments (25  $\mu$ M) with (A) DHS and its derivatives and (B) MAS and its derivatives on LDH release compared to control at 2, 4, 6 and 24 h after their addition to cells. Results are presented as mean  $\pm$  SEM, n = 3. \* $p$ <0.05 as compared to DHS / MAS treated groups.

#### 4.3.3. Characterization of cell death by DHS, MAS and their fatty acid / alkyl derivatives in CHO cells

A compound can induce cell death through different mechanisms like apoptosis, necrosis and mitotic catastrophe as discussed in section 1.5 of chapter 1<sup>231</sup>. In general, synthetic organoselenium compounds have been shown to induce cell death by

apoptosis<sup>232</sup>. In contrast, lipophilic compounds are known to cause membrane disruption leading to necrotic death. As the alkyl derivatives of DHS and MAS are amphiphilic selenides, it was important to understand the mechanism of cell death induced by these compounds. In order to address this, only the shortest (C<sub>6</sub>) and longest (C<sub>14</sub>) chain derivatives of DHS and MAS were examined for cell death mechanism because of their contrasting behavior and toxicities. In brief, CHO cells treated with C<sub>6</sub> and C<sub>14</sub> derivatives of DHS and MAS for 16 h at an identical concentration of 25  $\mu$ M were subjected to Annexin V–PI staining. The representative dot plots and bar graphs are shown in figures 4.5 and 4.6 respectively.



*Figure 4.5 Characterization of cell death induced by the C<sub>6</sub> and C<sub>14</sub> derivatives of DHS and MAS by Annexin V-PI staining at 16 h after their addition to CHO cells. Representative dot plots acquired from flow cytometry shows distribution of cells under different treatment conditions. CN – Control.*

The results indicated that the parent compound DHS, MAS and their C<sub>6</sub> derivatives neither induced apoptosis nor necrosis confirming the non-toxic nature of these compounds. The number of healthy cells (Annexin V<sup>-ve</sup> PI<sup>-ve</sup>) in the groups treated with parent compounds (DHS and MAS) and their C<sub>6</sub> derivatives were

approximately ~ 94 %. However, the C<sub>14</sub> derivatives of DHS and MAS showed a significant decrease in the counts of healthy cells to 88 % and 55 % respectively. The decrease in the number of healthy cells in MAS-C<sub>14</sub> treated group was seen as a subsequent increase in the number of necrotic cells (combined counts of Annexin V<sup>+</sup>PI<sup>+</sup> and Annexin V<sup>-</sup>PI<sup>+</sup> cells) to ~ 45 % compared to its C<sub>6</sub> derivative (~2 %). Therefore, the major mode of cell death was confirmed to be necrosis.

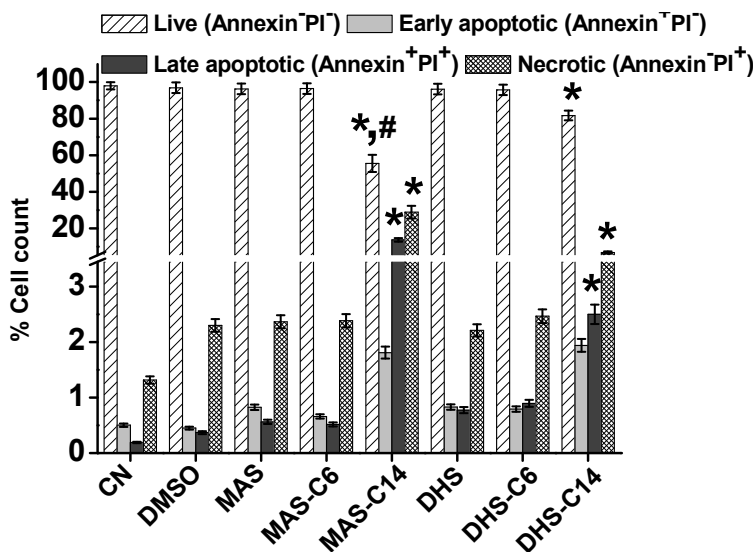


Figure 4.6 Bar graph shows percentage (%) live, apoptotic and necrotic cells after treatment with C<sub>6</sub> and C<sub>14</sub> derivatives of DHS and MAS for 16 h in CHO cells by Annexin V-PI staining. Results are presented as mean ± SEM, n = 3. \*p<0.05 as compared to the DHS control group, #p<0.05 as compared to the DHS-C<sub>14</sub> treated cells. CN – Control.

#### 4.3.4. Effect of DHS, MAS and their fatty acid / alkyl derivatives on MMP in CHO cells

Since necrosis is also marked by acute mitochondrial depolarization, we monitored the integrity of mitochondria using a fluorescent probe JC-1. It is known to accumulate in the mitochondria of healthy cells and forms J aggregates which upon

excitation at 565 nm emit red fluorescence. However, in dying cells mitochondria lose integrity and due to this JC-1 remains as monomer in the cytoplasm and emits green fluorescence. Therefore the ratio of red and green fluorescence is used as indicative of mitochondrial depolarization. The bar graph showing the ratio of red to green fluorescence and the fluorescent images of CHO cells stained with JC-1 are shown in figures 4.7 and 4.8 respectively.

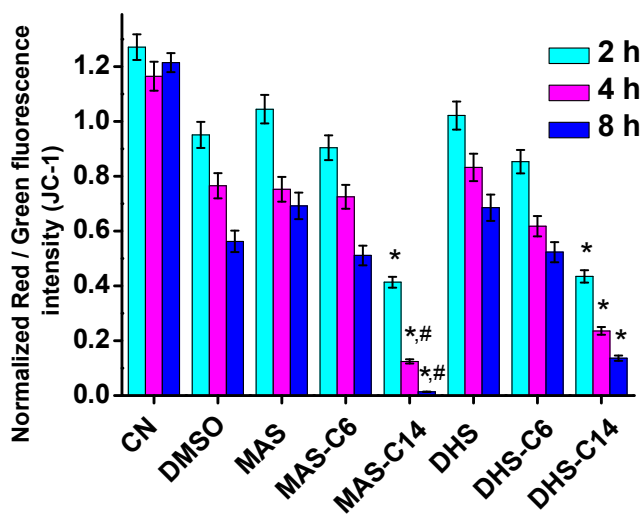


Figure 4.7 Bar graph shows the ratio of red ( $\lambda_{em} = 610 \text{ nm}$ ) and green ( $\lambda_{em} = 535 \text{ nm}$ ) fluorescence intensity of JC-1 staining at 2, 4 and 8 h after treatment with  $25 \mu\text{M}$  of  $\text{C}_6$  and  $\text{C}_{14}$  derivatives of DHS and MAS. Results are presented as mean  $\pm$  SEM,  $n = 3$ . \* $p < 0.05$  as compared to the DMSO control group, # $p < 0.05$  as compared to the DHS- $\text{C}_{14}$  treated cells. CN – Control.

The results indicated that control cells did not show much change in the ratio of red and green fluorescence as a function of time from 2 – 8 h, suggesting their mitochondria to be intact. Treatment of cells with  $\text{C}_{14}$  derivatives of DHS and MAS led to a much faster decrease in the ratio of red and green fluorescence as a function of time compared to  $\text{C}_6$  derivatives or the parent compounds (DHS and MAS) and vehicle control (DMSO) indicating acute mitochondrial depolarization by  $\text{C}_{14}$  derivatives

leading to necrosis. The ratio of the red and green fluorescence emission of JC-1 for control, DHS-C<sub>14</sub> and MAS-C<sub>14</sub> treated cells at 8 h were 1.214, 0.136 and 0.013 respectively (Fig. 4.7.)

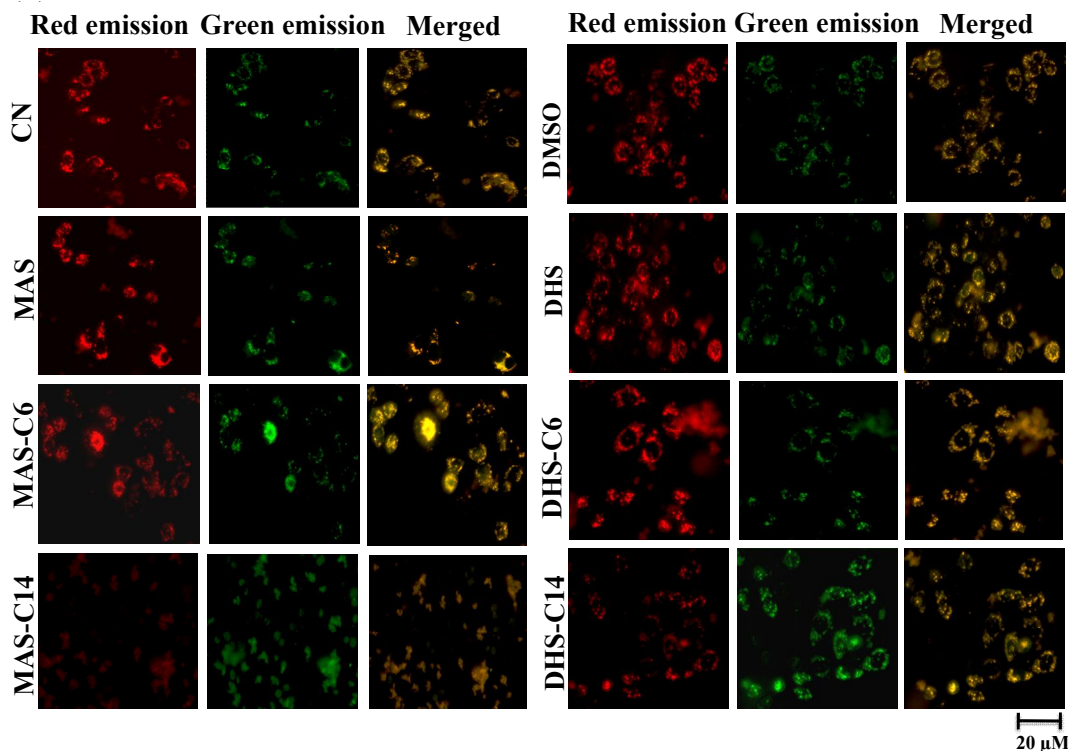


Figure 4.8 Representative photographs of red ( $\lambda_{em} = 610 \text{ nm}$ ) and green ( $\lambda_{em} = 535 \text{ nm}$ ) fluorescence emission of JC-1 staining at 8 h after treatment with 25  $\mu\text{M}$  of C<sub>6</sub> and C<sub>14</sub> derivatives of DHS and MAS. CN – Control.

#### 4.3.5. Effect of DHS, MAS and their fatty acid / alkyl derivatives on plasma membrane fluidity in CHO cells

Since plasma membrane disruption is marked by the changes in its fluidity, the effect of DHS, MAS and their derivatives on membrane fluidity was evaluated as an anisotropy value of a fluorophore DPH which is known to be localized in the plasma membrane<sup>178,180</sup>. For this, cells were labelled with DPH, treated with derivatives (C<sub>6</sub> and C<sub>14</sub>) of DHS and MAS for 4 h and the fluorescence polarization or anisotropy (r) of

DPH was monitored after exciting using a polarized light at 365 nm and recording polarized emission at 430 nm. The change in anisotropy value of DPH with time is shown in figure 4.9. Our results indicated that the control cells exhibited maximum anisotropy value of 0.17. Treatment with parent compounds (DHS and MAS) at 25  $\mu$ M did not affect the anisotropy value of DPH even after 4 h of their addition to cell suggesting that these compounds did not cause change in the fluidity of the plasma membrane. Treatments with C<sub>6</sub> and C<sub>14</sub> derivatives of DHS and MAS at identical concentration showed time dependent decrease in anisotropy of DPH and this effect was more prominent at longer chain length (C<sub>14</sub>). The anisotropy value of DPH in cells treated with DHS-C<sub>14</sub> and MAS-C<sub>14</sub> for 4 h was 0.13 and 0.09 respectively (Fig. 4.9). These results thus confirmed that the long chain (C<sub>14</sub>) derivatives of DHS and MAS caused membrane disruption resulting in to increase in membrane fluidity.

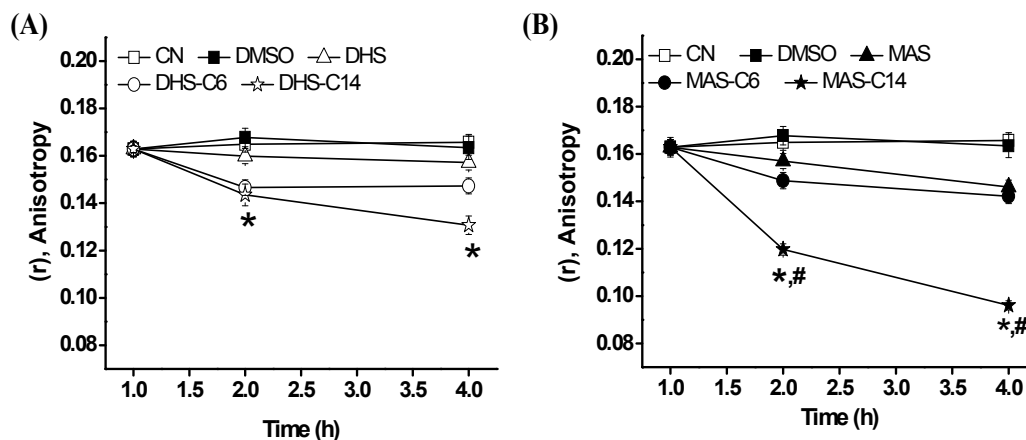


Figure 4.9 (A & B) Effect of treatment (25  $\mu$ M) with C<sub>6</sub> and C<sub>14</sub> derivatives of DHS and MAS respectively on plasma membrane fluidity measured as the change in the anisotropy value of a membrane bound flurophore, DPH at 2 and 4 h after their addition to CHO cells,  $\lambda_{ex} = 365$  nm,  $\lambda_{em} = 430$  nm. Results are presented as mean  $\pm$  SEM, n = 3. \* $p < 0.05$  as compared to the DMSO control group, # $p < 0.05$  as compared to the DHS-C<sub>14</sub> treated cells.

#### **4.3.6. Effect of alkyl chain length on the uptake of DHS and MAS derivatives in CHO cells**

From the above studies, it is anticipated that the conjugation of alkyl chain of variable length ( $C_{6-14}$ ) with DHS and MAS might be affecting its lipophilicity and thereby influencing their ability to incorporate within membranes and / or cells. For this, cells were treated with 25  $\mu$ M of compounds and selenium level after 1 h of treatment was estimated. The bar graph representing the percent loading / uptake under different treatment conditions is shown in figure 4.10. From the figure, it is clear that the basal selenium level in control cells and those treated with parent compounds such as DHS and MAS was not within detectable limits ( $<10$  ng). Treatment with the derivatives of DHS and MAS led to a significant increase in the percent of selenium incorporated into the cells compared to that of the amount present in the control cells. The MAS derivatives showed significantly higher loading compared to the DHS derivatives at each chain length (Fig. 4.10). The effect of lipophilic chain length on the cellular uptake of DHS and MAS derivatives was not observed to be correlated. For example, the percent incorporation increased with increasing chain length up to  $C_{12}$  and a further increase in chain length to  $C_{14}$  led to a decrease in loading (Fig. 4.10). The uptake studies performed at an early time point (1 h) may be indicative of the incorporation of derivatives mainly into the plasma membrane of cells. In order to determine the cellular uptake, cells were treated with DHS, MAS and their  $C_6$  derivatives at a concentration of 25  $\mu$ M for a longer time point i.e., 16 h and following this cell lysate was subjected to selenium estimation. The higher derivatives ( $>C_6$ ) were not used for the study as they were toxic. The results revealed that the uptake of DHS and MAS by cells were in nanograms only, which corresponded to about  $0.15 \pm 0.01$  % and  $0.23 \pm 0.01$  %

respectively of the amount added to cells. In contrast, the C<sub>6</sub> derivatives improved the uptake of DHS and MAS by 2.3 and 2.5-folds respectively. The above studies thus suggested that between DHS and MAS derivatives the latter exhibited greater affinity for cellular membranes and for each of these two series of compounds, such affinity increased up to a length of C<sub>12</sub>.

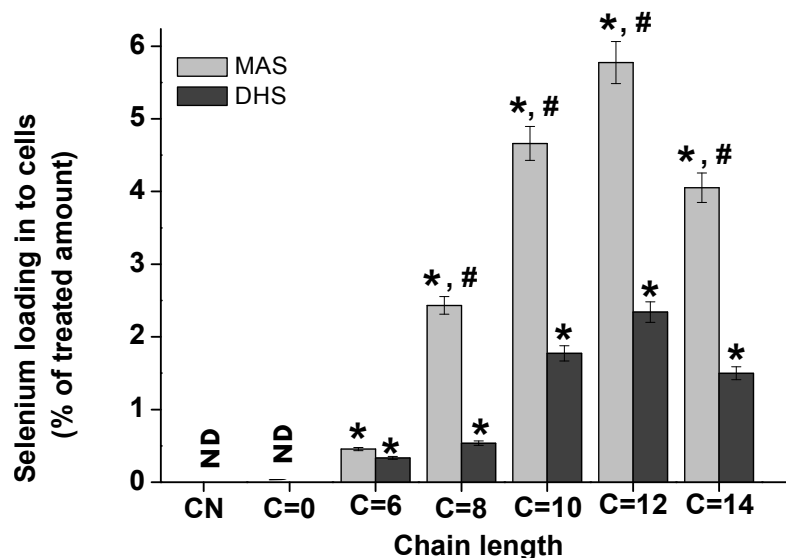


Figure 4.10 Effect of alkyl chain length (C<sub>6-14</sub>) on the uptake of DHS and MAS derivatives into membranes / cells following their addition to CHO cells at 25  $\mu$ M for an hour. Results are presented as mean  $\pm$  SEM, n = 3. \* $p$ <0.05 as compared to the DMSO control group, # $p$ <0.05 as compared to the DHS derivatives at each chain length. CN – Control cells, ND - Not detectable.

In order to revalidate the above conclusion, the binding / interaction of the longest C<sub>14</sub> derivatives of DHS and MAS to the plasma membrane of CHO cells was studied employing DPH as a probe. The fluorescence of DPH is highly sensitive to the changes in polarity of the membrane microenvironment<sup>177,178,180</sup>. Earlier it has been shown by Carfagna et al that time resolved changes in the fluorescence intensity of DPH can be used as a method to understand the binding of a hydrophobic drug to the plasma membrane of cells<sup>233</sup>. Such a binding is expected to increase the hydrophobic

environment around the DPH molecules resulting in the increase in its fluorescence intensity. However, membrane disruption by the derivatives can cause a decrease in DPH fluorescence. In the present study, addition of DHS-C<sub>14</sub> to the cells at 25 μM did not cause much change in the fluorescence intensity of DPH during the initial 30 minutes of interaction but decreased at later time. (Fig. 4.11)

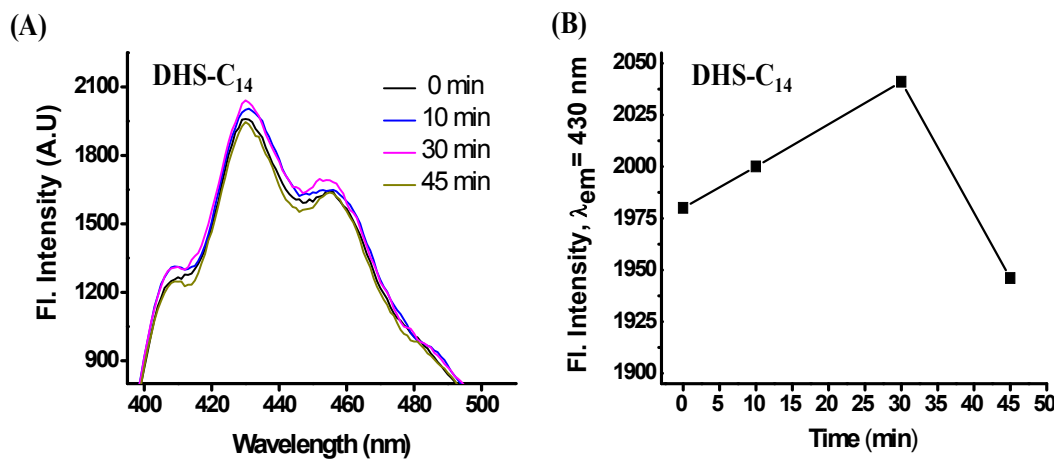


Figure 4.11 (A) Overlapped fluorescence spectra of CHO cells stained with a membrane bound fluorophore, DPH recorded soon after the addition of DHS-C<sub>14</sub> to the cell suspension in a time course manner (0 – 45 min). The excitation was performed at 365 nm. (B) Graph shows the interaction / binding of DHS-C<sub>14</sub> with the plasma membrane monitored in terms of the changes in the fluorescence intensity (λ<sub>em</sub> = 430 nm) of DPH.

Whereas treatment with MAS-C<sub>14</sub> at identical concentration led to a sharp increase in DPH fluorescence in 10 minutes and then decreased in a time dependent manner as shown in figure 4.12. Therefore, our results confirmed that DHS-C<sub>14</sub> caused lesser disruption of cell membrane compared to MAS-C<sub>14</sub>.

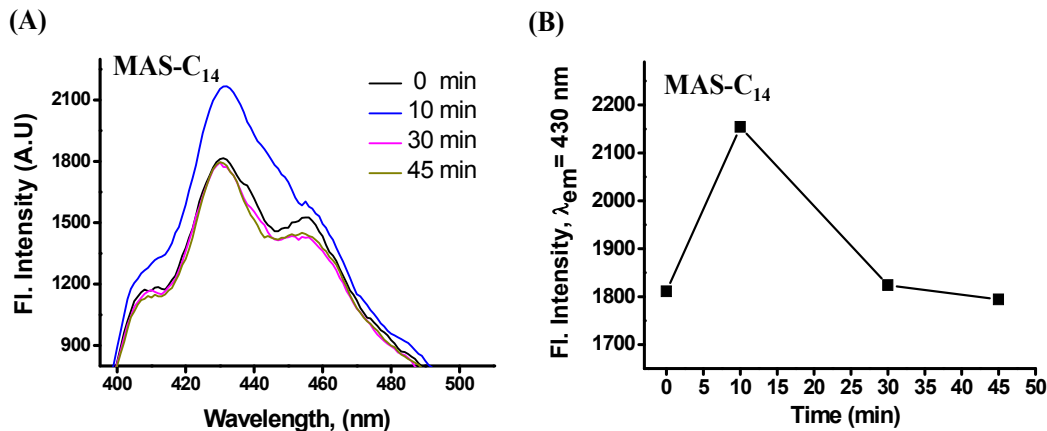


Figure 4.12 (A) Overlapped fluorescence spectra of CHO cells stained with a membrane bound fluorophore, DPH recorded soon after the addition of MAS-C<sub>14</sub> to the cell suspension in a time course manner (0 – 45 min). The excitation was performed at 365 nm. (B) Graph shows the interaction / binding of MAS-C<sub>14</sub> with the plasma membrane monitored in terms of the changes in the fluorescence intensity ( $\lambda_{em} = 430$  nm) of DPH.

#### 4.3.7. Effect of alkyl chain length on the self-aggregation properties of DHS and MAS derivatives

To further validate the above observation, the self aggregation behaviour of these compounds was studied. DHS and MAS derivatives being amphipathic in nature are expected to form aggregates or micelle structures which may explain their cytotoxic behaviour. Accordingly, the self-aggregation behaviour of the derivatives (C<sub>6</sub> - C<sub>14</sub>) of DHS and MAS were monitored by measuring the fluorescence of DPH in the presence of their increasing concentrations (2 - 50  $\mu$ M) in aqueous solution. DPH shows weak fluorescence ( $\lambda_{em} = 430$  nm) in aqueous solution, however once it goes in to micellar structure or the aggregates, its fluorescence increases significantly<sup>180</sup>. The fluorescence spectra and fluorescence enhancement after addition of selenium compound in CHO cells is shown in figures 4.13 and 4.14.

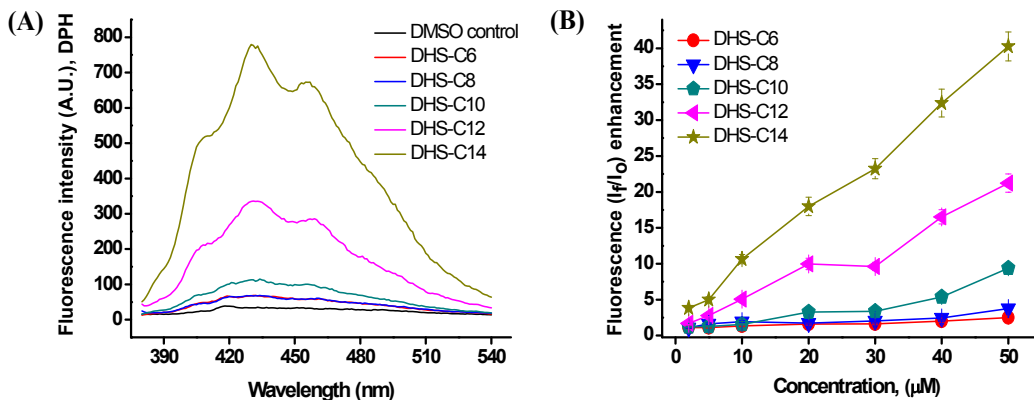


Figure 4.13 Aggregation studies of fatty acid derivatives of DHS ( $C_{6-14}$ ) using fluorescence enhancement of a lipophilic fluorophore DPH. (A) Representative fluorescence spectra of DPH in  $50 \mu\text{M}$  aqueous solution of DHS ( $C_{6-14}$ ) containing 0.25 % DMSO. (B) Line graph shows enhancement in the fluorescence intensity of DPH by DHS ( $C_{6-14}$ ) at their increasing concentrations of 2 to  $50 \mu\text{M}$ .  $I_f$  – Fluorescence intensity in presence of selenium compounds.  $I_o$  - Fluorescence intensity in absence of selenium compounds.  $\lambda_{ex} = 365 \text{ nm}$ ,  $\lambda_{em} = 430 \text{ nm}$ . Results are presented as mean  $\pm$  SEM,  $n = 3$ .

The addition of selenium compounds did not cause any shift in the peak position of the fluorescence spectra of DPH, however affected the fluorescence intensity. For example, the fluorescence intensity of DPH did not change much as a function of concentration for DHS and MAS derivatives up to a chain length of  $C_8$  and  $C_{10}$  respectively. However,  $C_{10-14}$  derivatives of DHS and  $C_{12-14}$  derivatives of MAS exhibited concentration and chain length dependent increase in the fluorescence intensity of DPH suggesting formation of aggregates by the long chain derivatives at higher concentration. When the derivatives of DHS and MAS of identical chain length and concentration were compared, the former showed significantly higher enhancement in the fluorescence emission of DPH compared to the latter. For example, at a concentration of  $25 \mu\text{M}$ , the longest chain derivatives; DHS- $C_{14}$  and MAS- $C_{14}$  showed

enhancement in the fluorescence intensity of DPH by  $\sim 20$  and  $\sim 8$  folds respectively (Figs. 4.13 and 4.14). This confirmed that longer chain ( $\geq C_{10}$ ) derivatives of DHS exhibited higher tendency of forming aggregates compared to MAS derivatives of identical chain length.

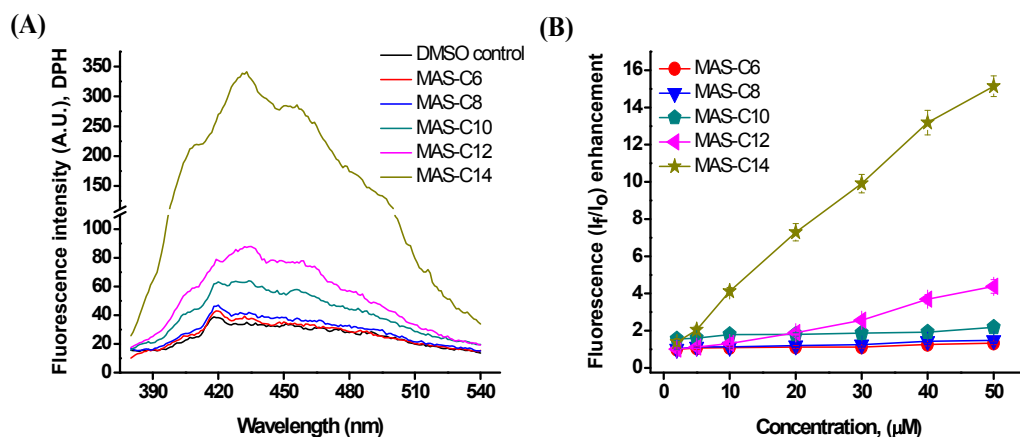


Figure 4.14 Aggregation studies of alkyl derivatives of MAS ( $C_{6-14}$ ) using fluorescence enhancement of a lipophilic fluorophore DPH. (A) Representative fluorescence spectra of DPH in  $50 \mu\text{M}$  aqueous solution of MAS ( $C_{6-14}$ ) containing 0.25 % DMSO. (B) Line graph shows enhancement in the fluorescence intensity of DPH by MAS ( $C_{6-14}$ ) in the increasing concentration (2 - 50  $\mu\text{M}$ ).  $I_f$  – Fluorescence intensity in presence of selenium compounds.  $I_o$  - Fluorescence intensity in absence of selenium compounds.  $\lambda_{ex} = 365 \text{ nm}$ ,  $\lambda_{em} = 430 \text{ nm}$ . Results are presented as mean  $\pm$  SEM,  $n = 3$ .

#### 4.3.8. Effect of DHS, MAS and their $C_6$ derivatives on the antioxidant activity in CHO cells

The non-toxic  $C_6$  derivatives of DHS and MAS screened from above studies were evaluated for their ability to modulate the expression of antioxidant selenoenzyme GPx and to protect from the AAPH (a free radical generator) induced oxidative damages in CHO cells. The results were compared with those of the parent compounds (DHS and MAS). For this, CHO cells were pre-treated with DHS, MAS and their  $C_6$

derivatives for 16 h. The GPx activity and relative expression of GPx isoform are shown in figure 4.15. The results indicated that treatment with DHS and MAS led to a significant increase in GPx activity. The compound MAS was more effective than DHS in inducing GPx activity. The value of GPx activity from the DHS and MAS treated cells was 0.049 and 0.059 Units/mg of protein respectively (Fig. 4.15 A). Supporting these observations, DHS and MAS treatment also showed significantly higher induction in the expressions of GPx isoforms (*GPx 1* and *GPx 4*) at the mRNA level. The relative expression of *GPx 1* and *GPx 4* in DHS treated cells were  $1.30 \pm 0.08$  and  $3.60 \pm 0.21$  respectively, whereas in MAS treated cells were  $1.72 \pm 0.11$  and  $2.45 \pm 0.14$ -folds respectively. The C<sub>6</sub> derivatives of DHS and MAS showed marginally higher induction in the expressions of GPx at mRNA and activity levels compared to the parent compounds DHS and MAS (Fig. 4.15). Further to examine antioxidant effect, CHO cells pre-treated with DHS, MAS and their C<sub>6</sub> derivatives for 16 h were subjected to AAPH exposure for 6 h and the levels of oxidative damage markers like lipid peroxidation and protein carbonylation was monitored and the results are shown in figure 4.16. The results indicated that AAPH treatment led to an increase in the level of malondialdehyde to  $831 \pm 141$  nmoles / mg of protein as compared to the control level of  $186 \pm 29$  nmoles / mg of protein. Treatment with DHS and MAS caused significant reduction in the level of malondialdehyde to  $457 \pm 122$  and  $427 \pm 81$  nmoles / mg protein respectively in cells indicating their ability to protect from AAPH induced lipid peroxidation

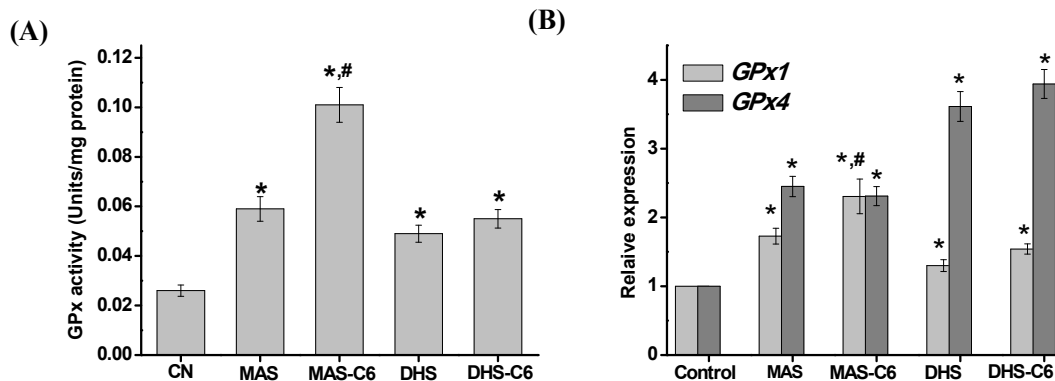


Figure 4.15 Effect of pre-treatment (25  $\mu$ M for 16 h) with DHS, MAS and their C<sub>6</sub> derivatives on (A) GPx activity and (B) expression of genes such as GPx 1 and GPx 4. The expression of above genes in different treatment groups was normalized against control group and the relative expression changes have been plotted. Actin expression was used as internal control. Results are presented as mean  $\pm$  SEM, n=3. \* $p$ <0.05 as compared to the control group, # $p$ <0.05 as compared to respective parent compound DHS and / or MAS. CN – Control.

Similarly, pre-treatment with DHS and MAS caused reduction in the level of protein carbonyls. The level of protein carbonyls in control cells and AAPH treated cells were  $1.09 \pm 0.04$  and  $2.01 \pm 0.15$  nmoles / mg whereas pre-treatment with DHS and MAS resulted in a decrease in the level of protein carbonyls to  $1.44 \pm 0.10$  and  $1.27 \pm 0.08$  nmoles / mg respectively. The C<sub>6</sub> derivatives of DHS and MAS showed better protection of cells from AAPH induced lipid peroxidation and protein carbonylation compared to the parent compound DHS and MAS (Fig. 4.16). For example, the level of malondialdehyde in DHS-C<sub>6</sub> and MAS-C<sub>6</sub> treated cells exposed to AAPH were  $304 \pm 65$  and  $167 \pm 48$  nmoles / mg respectively and those of protein carbonyls were  $1.31 \pm 0.04$  and  $1.13 \pm 0.08$  nmoles / mg respectively. Taken together, these results suggested that C<sub>6</sub> derivatives are better than the parent compounds in exhibiting antioxidant effects in cells.

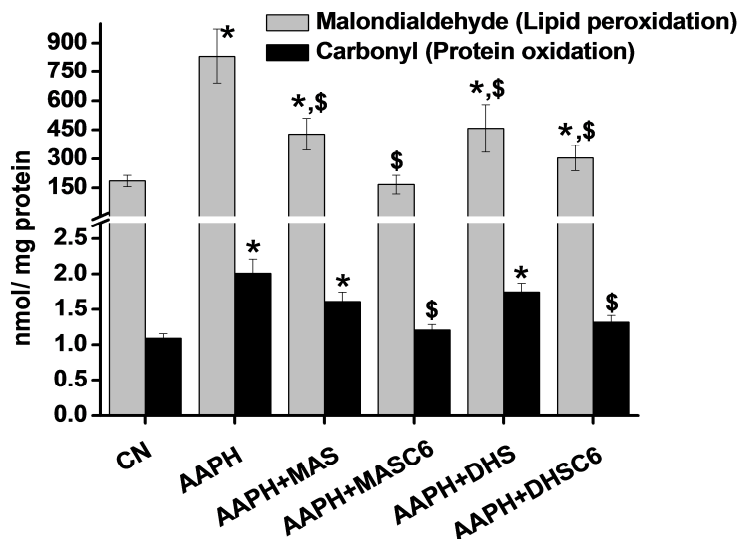


Figure 4.16 Effect of pre-treatment (25  $\mu\text{M}$  for 16h) with DHS, MAS and their  $\text{C}_6$  derivatives against AAPH (30 mM) induced lipid peroxidation and protein carbonylation estimated at 6 h post exposure by TBARS and DNPH assays respectively. Results are presented as mean  $\pm$  SE,  $n = 3$ . \* $p < 0.05$  as compared to the control group, # $p < 0.05$  as compared to respective parent compound DHS and / or MAS, \$ $p < 0.05$  as compared to AAPH alone group. CN – Control.

#### 4.4. Discussion

The present study was performed to evaluate the potential of attaching a fatty acid / alkyl group as a lipophilic unit with the redox active hydrophilic selenide moiety such as DHS and MAS as a strategy to increase their cellular interactions. Since the lipophilicity of a compound is often associated with biological functions as well as the toxicity<sup>234–237</sup>, the first parameter that was necessary to be evaluated prior to biological application of the derivatives of DHS and MAS is their toxicity to the cells. In order to address this, we used CHO cells representing the normal cell type. Our results indicated that neither the parent compounds (DHS and MAS) nor the free fatty acids ( $\text{C}_6$  to  $\text{C}_{14}$ ) in the concentration range of 1 – 50  $\mu\text{M}$  were toxic to CHO cells. However, the long chain derivatives ( $\geq \text{C}_8$ ) of DHS and MAS in a similar concentration range were

significantly toxic to the cells. Interestingly, the fatty acid derivatives of similar cyclic compounds containing oxygen in place of selenium in the ring structure (furan fatty acids) have been reported to be antioxidants and non-toxic to cells<sup>238,239</sup>. This prompted us to believe that the amphiphilic character resulting from the combination of a hydrophilic head as selenide and lipophilic tail as a fatty acid / alkyl group makes the derivatives membrane active, which finally dictates the cytotoxicity<sup>235,240-243</sup>. In general, amphipathic compounds through their insertion in to plasma membrane establish hydrophobic interactions with the membrane lipids to form microcluster or aggregates<sup>239,241,243</sup>. Such aggregates can cause local disturbance in the dynamics and packing order of lipids and proteins in the membrane, resulting in disintegration or pore formation followed by leakage of intracellular constituents, acute depolarization of mitochondria (the power house of cell) and necrosis<sup>242-246</sup>. Supporting this hypothesis, the derivatives of DHS and MAS were observed to cause an increase in the fluidity of plasma membrane, leakage of intracellular proteins like LDH and membrane disintegration (PI<sup>+ve</sup> cells). These findings are in agreement with the previous studies wherein similar mechanism of membrane disintegration and subsequent cytotoxicity has been proposed for surface active amphipathic drugs like N-alkylated iminosugars and antimicrobial peptides such as magainin and cecropins<sup>235,242,243,247</sup>. For example, Mellor et al showed that alkylation of an iminosugar deoxynojirimycin (DNJ) although increased its bioactivity and uptake in cells<sup>248</sup>, caused cytotoxicity in a chain length dependant manner<sup>247</sup>. Subsequent experiments by the same group revealed that the major mechanism of cell death induced by alkylated DNJ was through interaction of their alkyl chain with the membrane leading to fragmentation, pore formation and the leakage of intracellular components<sup>247,248</sup>. Similarly, Westerhoff and Bechinger showed that magainins and cercopins induced their anti microbial activities by disturbing the

lipid bilayer integrity and electrochemical gradient across the membrane of bacterial cells<sup>243,249</sup>. Further, MAS derivatives exhibited significantly higher toxicity than DHS derivatives at each chain length. It is well known that the plasma membranes of the mammalian cells are negatively charged<sup>250</sup>. Since the derivatives of MAS and DHS are cationic and neutral in nature respectively, the electrostatic affinity of the former for the plasma membranes is expected to be higher compared to the latter and this may account for their differential toxicity. This is in concurrence with previous reports wherein cationic surface-active drugs have been shown to be more toxic than the neutral ones<sup>243,251</sup>.

Further, the effect of chain length ( $C_{6-14}$ ) on the cytotoxicity of the derivatives of DHS and MAS was found to be non-linear, where the maximum toxicity was seen at  $C_{10}$  and decreased beyond. These results can be correlated with an earlier report wherein Kikuzaki et al showed that lipophilization of the phenolic compounds with aliphatic group of varying chain lengths improved the bioavailability of the compound with increase in the alkyl chain length<sup>227,252</sup>. In this study, the increase in the activity was found to be non-linear. For example, with the increase in alkyl chain, the activity increased up to a certain chain length beyond which there was a drastic decrease in the activity and this phenomenon was called as the *cut-off* effect<sup>227,253</sup>. The mechanism proposed by the authors to describe this effect was that the higher alkyl chain length caused self-aggregation (micelle formation) of the molecule making it bulkier and difficult to cross the cell membrane barrier. Anticipating similar mechanism, our results indicated that the long chain ( $\geq C_{10}$ ) derivatives of DHS and MAS formed aggregates as a function of concentration and this effect was prominent in the case of the DHS derivatives<sup>227,253</sup>. Such differences can be justified by the explanation that the aggregation of MAS derivatives being cationic in nature would be less favourable due

to repulsive forces. Since DHS derivatives showed higher aggregation behaviour, it can be understood that due to this supramolecular formation there would be lesser availability of free molecules to interact with the cell membrane causing lesser cytotoxicity. This was indeed supported by the uptake study wherein DHS and MAS derivatives showed increased incorporation in the cells with the increase in chain length up to C<sub>10</sub> and C<sub>12</sub> respectively and decreased beyond. Further, in all our studies the C<sub>14</sub> derivatives of DHS and MAS exhibited most notable differences in terms of cellular effects (such as cytotoxicity, membrane disruption, incorporation).

Among the derivatives of DHS and MAS, the shortest chain length derivatives DHS-C<sub>6</sub> and MAS-C<sub>6</sub> showed extremely low toxicity, making them suitable prototypes for new drug design. At this stage, it was felt necessary to evaluate the antioxidant effect of the parent compounds DHS, MAS and their C<sub>6</sub> derivatives in normal CHO cells. The antioxidant effect of compounds was examined in terms of their abilities to induce the expression of GPx and to inhibit the oxidative stress against a known stressor AAPH. The results indicated that, the parent compounds DHS and MAS significantly induced the expressions of GPx isoforms (*GPx 1* and *GPx 4*) and also provided protection against AAPH induced lipid peroxidation and protein carbonylation. Interestingly, the C<sub>6</sub> derivatives of DHS and MAS were even better than the parent compounds in imparting the above activities confirming the role of hydrophobic-lipophilic balance (HLB) in improving the antioxidant activity. It is also worth mentioning here that DHS-C<sub>6</sub> was less active than MAS-C<sub>6</sub> in inducing GPx and in protecting from AAPH mediated oxidative stress. However, DHS-C<sub>6</sub> being a chemically more stable compound than MAS-C<sub>6</sub> would be an ideal candidate for future exploration as radioprotector. Accordingly, in the next chapter we have performed radioprotection studies of DHS-C<sub>6</sub> and compared with parent compound DHS.

#### 4.5. Summary

1. The fatty acid / alkyl group of variable chain length (C<sub>6-14</sub>) of DHS and MAS not only improved their ability to incorporate within cells but also modulated their cytotoxicity.
2. The major mechanism of cell death for long chain derivatives ( $\geq C_8$ ) was found to be necrosis and plasma membrane disruption.
3. C<sub>6</sub> derivatives of DHS and MAS exhibited better antioxidant activity compared to parent compounds by protecting cells from AAPH induced oxidative stress.
4. C<sub>6</sub> derivatives of DHS and MAS appeared to possess the right hydrophilic – lipophilic balance (HLB) allowing them to pass through plasma membrane without causing any disintegration and thus suggested the importance of HLB in design of lipophilic antioxidants.

## **Chapter 5**

### **Comparative radioprotective activity of DHS and DHS-C<sub>6</sub> in cells and their mechanism of action**

In this chapter, the radioprotective effect of DHS and DHS-C<sub>6</sub> in Chinese Hamster Ovary (CHO) cells have been investigated by monitoring clonogenic survival against the increasing radiation absorbed doses (1 - 12 Gy). Further experiments were also performed to understand the mechanism of action of these compounds by monitoring GPx level, DNA repair kinetics, cell cycle analysis and oxidative stress.

## 5.1 Introduction

In chapter 3, it has been shown that DHS administration in mice provided survival advantage against the lethal dose of  $\gamma$ -radiation suggesting its radioprotective activity. Subsequently it was reported that C<sub>6</sub> derivative of DHS had the right HLB value that allowed for an increased uptake of DHS in CHO cells (Chapter 4). Therefore it has been proposed to examine how the increased cellular uptake can influence the radioprotective activity of DHS. Further observations in chapter 4, also indicated that both DHS and DHS-C<sub>6</sub> could induce GPx level in cells by  $\sim 2.5$ -fold. Interestingly there are several reports in the literature suggesting the involvement of GPx in protecting cells from radiation induced DNA damage as well as from various other sources of oxidative stress<sup>154,254,255</sup>. For example, Baliga et al showed that GPx 1 overexpression prevented MCF 7 cells from radiation induced DNA damage as assessed by micronuclei assay<sup>154</sup>. In this study, the DNA repair activity of GPx was found to be dependent on BRCA1 gene which activates the p53 dependant DNA repair pathway<sup>158</sup>. In another study, Morais et al showed that over expression of GPx 1 increased viability of MCF 7 cells following genotoxic stress by elevating the levels of phosphorylated CHK 1 and CHK 2<sup>254</sup>. This raised a question whether GPx plays any role in DHS mediated-radioprotection. The present study is therefore aimed to evaluate whether DHS-C<sub>6</sub>, a lipophilic derivative could be a better agent than DHS to achieve radioprotection. Subsequently, the role of GPx induced by DHS or DHS-C<sub>6</sub> on DNA repair kinetics, cell cycle progression and the radioprotective activity was investigated using a pharmacological inhibitor, mercaptosuccinic acid. The chemical structures of DHS and DHS-C<sub>6</sub> used in the present study are given in Scheme 1.7.

## 5.2. Materials and Methods

The stock solution of DHS was prepared in culture medium and DHS-C<sub>6</sub> was first dissolved in DMSO and then added to the culture medium to obtain the desired concentrations. The concentration of DMSO was kept constant within permissible limits of toxicity (0.25 %). In brief, CHO cells were treated with DHS or DHS-C<sub>6</sub> for 16 h, washed with 1X PBS and exposed to increasing absorbed doses (1 - 12 Gy) of  $\gamma$ -radiation using <sup>60</sup>Co Blood Irradiator 2000 (BRIT, India) at a dose rate of 1 Gy/min. Clonogenic assay was used to determine the survival fraction under different treatment conditions. For this assay about 250 cells were seeded for control groups whereas for irradiated groups the cell numbers were varied depending on the absorbed dose (250 cells - 1 Gy, 300 cells - 2 Gy, 400 cells - 3 Gy, 500 cells - 4 Gy, 750 cells - 5 Gy, 1000 cells - 6 Gy, 1500 cells - 7 Gy, 2000 cells - 8 Gy, 3000 cells - 9 Gy, 4000 cells - 10 Gy, 5000 cells - 11 Gy, 6000 cells - 12 Gy). The effect of DHS or DHS-C<sub>6</sub> treatment on cell cycle progression was studied by PI assay. The anti-genotoxic effect of DHS or DHS-C<sub>6</sub> was evaluated by micronuclei,  $\gamma$ -H2AX and comet assays. In order to block the target molecules like GPx and DNA-PK, cells pre-treated with DHS / DHS-C<sub>6</sub> were exposed to inhibitors like MS (10 mM) and NU7026 (10  $\mu$ M) respectively for 2 h and then irradiated. Similarly, to block CHK 1 and CHK 2, cells were incubated with inhibitors such as UCN-01 (25 nM) and PV-1091 (400 nM) respectively for 16 h along with DHS / DHS-C<sub>6</sub> and then irradiated. The concentrations and the incubation times of inhibitors used in the study were taken as per the reported data<sup>256,257</sup>. All the experiments were carried out in triplicate and repeated at least two times. Data are presented as mean  $\pm$  SEM, n = 3 from an independent experiment. The data were

analyzed by one-way ANOVA using Origin (version 6.1) software to confirm the variability of data. The P values < 0.05 were considered as statistically significant.

### 5.3. Results

#### 5.3.1. Effect of DHS pre-treatment on toxicity in CHO cells by clonogenic assay

In order to evaluate the safe dose range of DHS for radioprotection study, a toxicity study was performed wherein cells were treated with DHS in a concentration range of 0.1 - 100  $\mu$ M for 16 h and the survival fraction was estimated using clonogenic assay. The concentration effect of DHS on the survival fraction of CHO cells is presented and the representative images are shown in figure 5.1.

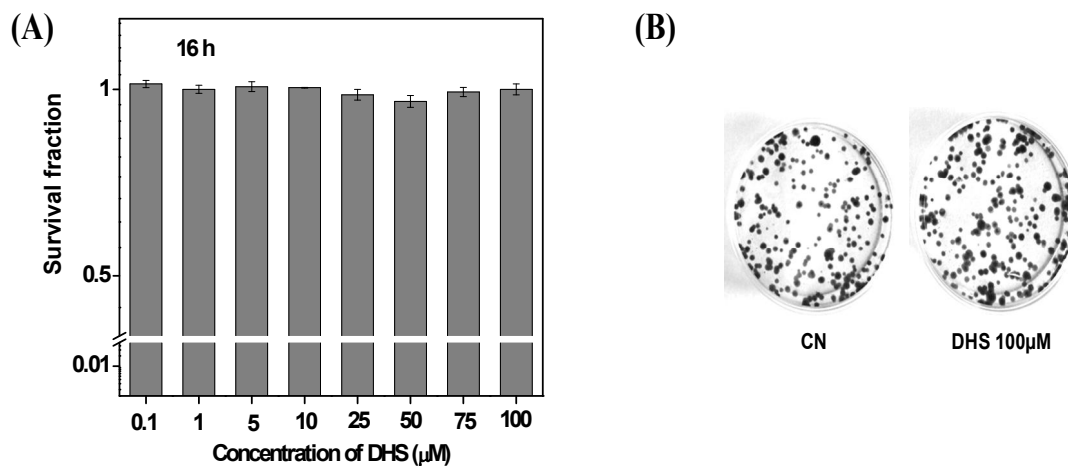


Figure 5.1 (A) Bar graph shows the cytotoxic effect of DHS in CHO cells by clonogenic assay. (B) Representative images show colonies of CHO cells. Cells were pre-treated with DHS in a concentration ranging from 0.1 - 100  $\mu$ M for 16 h, washed with 1X PBS, supplemented with fresh culture medium and cultured for 7 days to form colonies. Results are presented as mean  $\pm$  SEM, n = 3.

It can be clearly seen that DHS pre-treatment up to a concentration of 100  $\mu\text{M}$  did not cause any decrease in survival fraction of CHO cells. Thus DHS concentrations up to 100  $\mu\text{M}$  appeared to be safe for exploring radioprotective activity. This result is also in line with our previous study (Chapter 4) by MTT assay showing that DHS treatment for 72 h in the concentration range of 1 - 50  $\mu\text{M}$  did not cause any toxicity in CHO cells.

### **5.3.2. Effect of DHS pre-treatment on the radiation induced cell death in CHO cells**

Since DHS treatment for 16 h did not show any toxicity in CHO cells by clonogenic assay, similar concentration range was employed to evaluate the effect of DHS pre-treatment on the radiation-induced cell death. For this, CHO cells were pre-treated with DHS in a concentration range of 0.1  $\mu\text{M}$  to 100  $\mu\text{M}$  for 16 h, subjected to  $\gamma$ -irradiation at 4 Gy and cell viability was determined by clonogenic assay (Fig 5.2). The results obtained by clonogenic assay showed a significant decrease in the survival fraction of irradiated cells ( $0.3 \pm 0.1$ ) compared to the control cells ( $1.00 \pm 0.01$ ). DHS pre-treatment up to a concentration of 1  $\mu\text{M}$  did not show any improvement in the survival fraction as compared to radiation control. As the concentration of DHS is increased, there is an increase in the survival fraction with maximum protection of 24 % at 25  $\mu\text{M}$ . Further increase in the concentration up to 100  $\mu\text{M}$  led to saturation effect (Fig. 5.2).

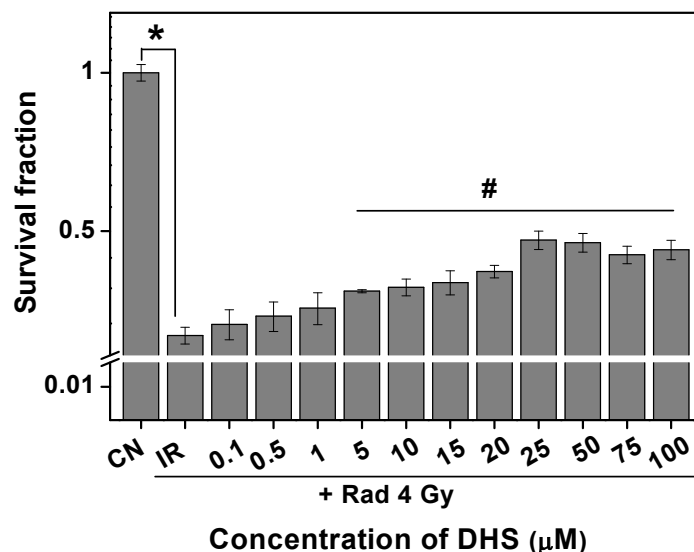


Figure 5.2 Bar graph shows the effect of the varying concentration (0.1 - 100  $\mu\text{M}$ ) of DHS pre-treatment for 16 h on the survival fraction in CHO cells against  $\gamma$ -irradiation (4 Gy) as estimated by clonogenic assay. Results are presented as mean  $\pm$  SEM,  $n = 3$ . \*  $p < 0.05$  as compared to control group, #  $p < 0.05$  as compared to radiation control group. CN - Control, IR - Radiation.

### 5.3.3. Comparative effect of DHS and DHS-C<sub>6</sub> pre-treatment on the radiation induced cell death in CHO cells

Based on the above results, a pre-treatment concentration of 25  $\mu\text{M}$  was chosen to compare the radioprotective effect of DHS with DHS-C<sub>6</sub>. Since DMSO was used as carrier, the vehicle control was also included in the study. The survival fractions recorded under different treatment conditions are represented in figure 5.3. The results revealed that at an identical concentration of 25  $\mu\text{M}$ , DHS-C<sub>6</sub> pre-treatment for 16 h significantly increased the survival fraction of irradiated (4 Gy) cells by 75 % as compared to 50 % by the parent compound DHS. DMSO (0.25 %) treatment did not affect the survival fraction of control and the irradiated cells. DHS and DHS-C<sub>6</sub> control groups showed survival fractions comparable to that of control cells.

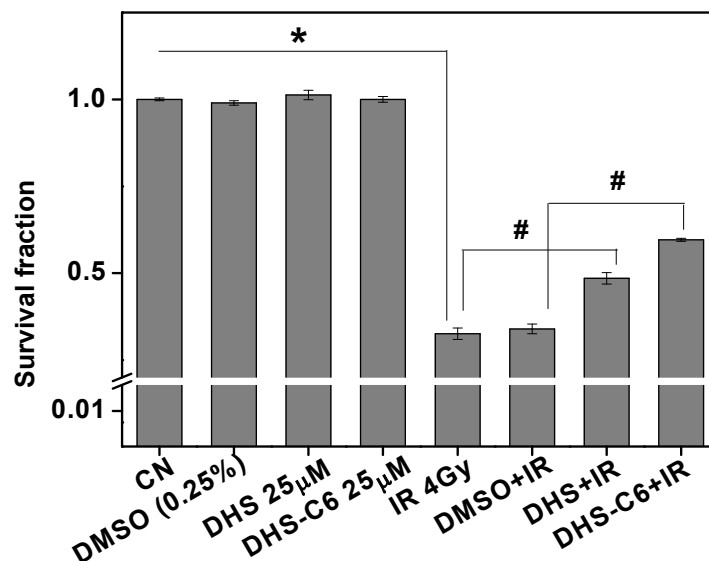


Figure 5.3 Bar graph shows the effect of DHS and DHS-C<sub>6</sub> pre-treatment (25 µM for 16 h) on survival fraction against radiation exposure of 4 Gy. Results are presented as mean ± SEM, n = 3. \*p < 0.05 as compared to control group, #p < 0.05 as compared to respective radiation control groups. CN - Control, IR – Radiation.

Encouraged by above results, we investigated the radiation dose response of DHS and DHS-C<sub>6</sub> by evaluating SF at different absorbed doses (1 - 12 Gy) of radiation exposure through clonogenic assay. The survival curves were plotted by fitting the data of survival fraction (log scale) against the radiation absorbed dose (D) (linear scale) with the quadratic dose response equation ( $SF = \alpha D + \beta D^2$ ). Survival curve and the representative images of colonies under different treatment conditions are presented in figures 5.4 A and 5.4 B respectively. It can be seen that irradiation led to dose dependent decrease in survival fraction. Pre-treatment with DHS or DHS-C<sub>6</sub> improved the survival fraction at all irradiation doses studied. From the survival curves, D<sub>0</sub> (the dose which decreased survival fraction from 0.1 to 0.037) values under drug pre-treatment and untreated conditions were estimated.

From this, DMF was calculated using equation 5.1.

$$DMF = \frac{D_{0(DHS / DHS-C_6 + Radiation)}}{D_{0(Radiation)}} \quad \text{Eq. 5.1}$$

Using  $D_0$  values, DMF for DHS and DHS- $C_6$  was determined to be 1.14 and 1.24 respectively.

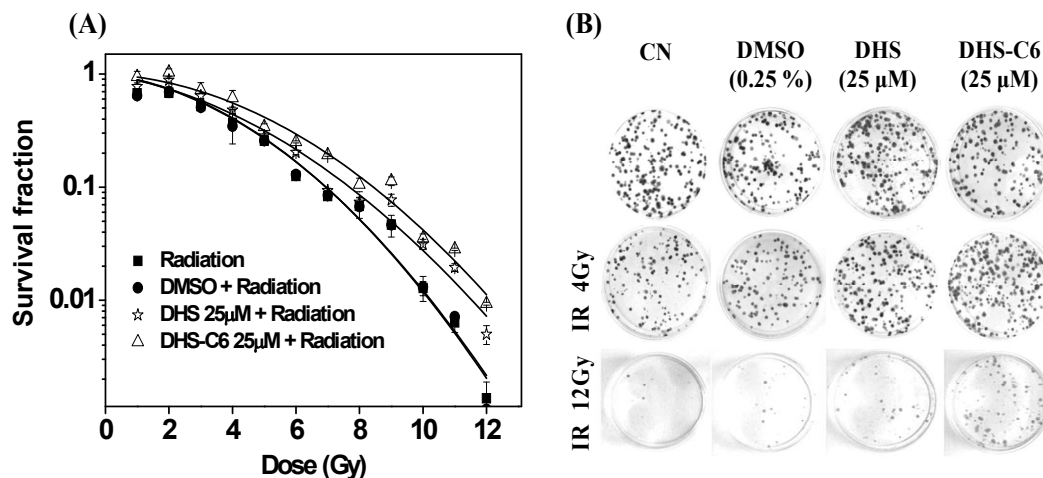


Figure 5.4 (A) Semi log plot shows radiation dose (1 - 12 Gy) response curve of DHS and DHS- $C_6$  pre-treatment (25 μM for 16 h) in CHO cells by clonogenic assay. (B) Representative images shows colonies of CHO cells under different treatment conditions. Results are presented as mean  $\pm$  SEM,  $n = 3$ . CN – Control, IR – Radiation.

### 5.3.4. Effect of DHS and DHS- $C_6$ treatment on GPx level in CHO cells

As described in chapter 3, the radioprotective effect of DHS in BALB/c mice was associated with its ability to induce GPx levels in a tissue specific manner. Similarly, in chapter 4, DHS and DHS- $C_6$  treatment showed an increase in GPx activity and protection from AAPH induced oxidative damage in CHO cells. These results prompted us to speculate the role of GPx in the radioprotective effect of DHS or DHS- $C_6$ . In order to address this issue, an inhibitor study was performed employing mercaptosuccinic acid (MS), a pharmacological inhibitor of GPx<sup>258,256</sup>. In this

experiment firstly, we established the extent of GPx inhibition by incubating CHO cells pre-treated with DHS and DHS-C<sub>6</sub> (25 μM for 16 h) with MS for 2 h and then monitoring the level of GPx activity. The results of this treatment condition on GPx activity is shown in figure 5.5.

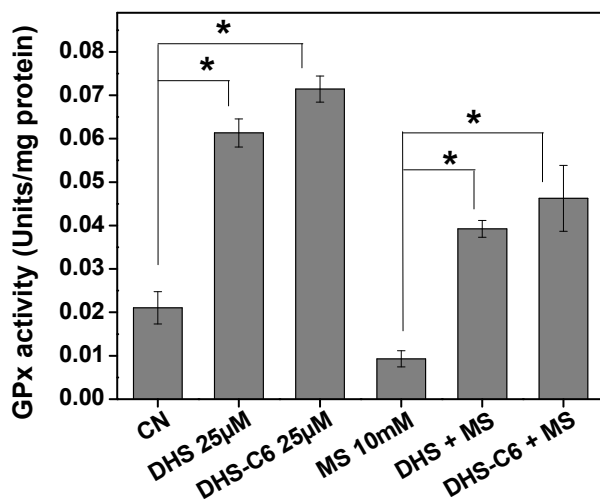


Figure 5.5 Effect of pre-treatment with DHS, DHS-C<sub>6</sub> (25 μM for 16 h) on GPx activity and its modulation by MS (10 mM for 2 h) in CHO cells. Results are presented as mean ± SEM, n = 3. \**p* < 0.05 as compared to respective control group. CN – Control, MS - Mercaptosuccinic acid.

It can be seen that treatment with DHS and DHS-C<sub>6</sub> increased GPx activity level in cells to 0.061 ± 0.003 Units/mg protein and 0.071 ± 0.003 Units/mg protein respectively as compared to control level of 0.021 ± 0.003 Units/mg protein. Incubation with MS decreased the GPx activity in cells by ~ 55 % as compared to control. Further, MS treatment significantly inhibited the DHS and DHS-C<sub>6</sub> mediated increase in GPx activity by 32 % and 33 % respectively. Based on these results, CHO cells pre-treated with DHS or DHS-C<sub>6</sub> (25 μM for 16 h) were incubated with MS, exposed to γ radiation dose of 4 Gy and 11 Gy and monitored for cell survival by clonogenic assay.

Further, to know the effect of GPx inhibition on the radioprotective activity of DHS and DHS-C<sub>6</sub>, cells were subjected to similar treatment conditions as discussed

above, exposed to  $\gamma$ -radiation of 4 Gy and 11 Gy and evaluated for cell survival by clonogenic assay. The survival fractions and the representative images of colonies are presented in figures 5.6 (A - C).

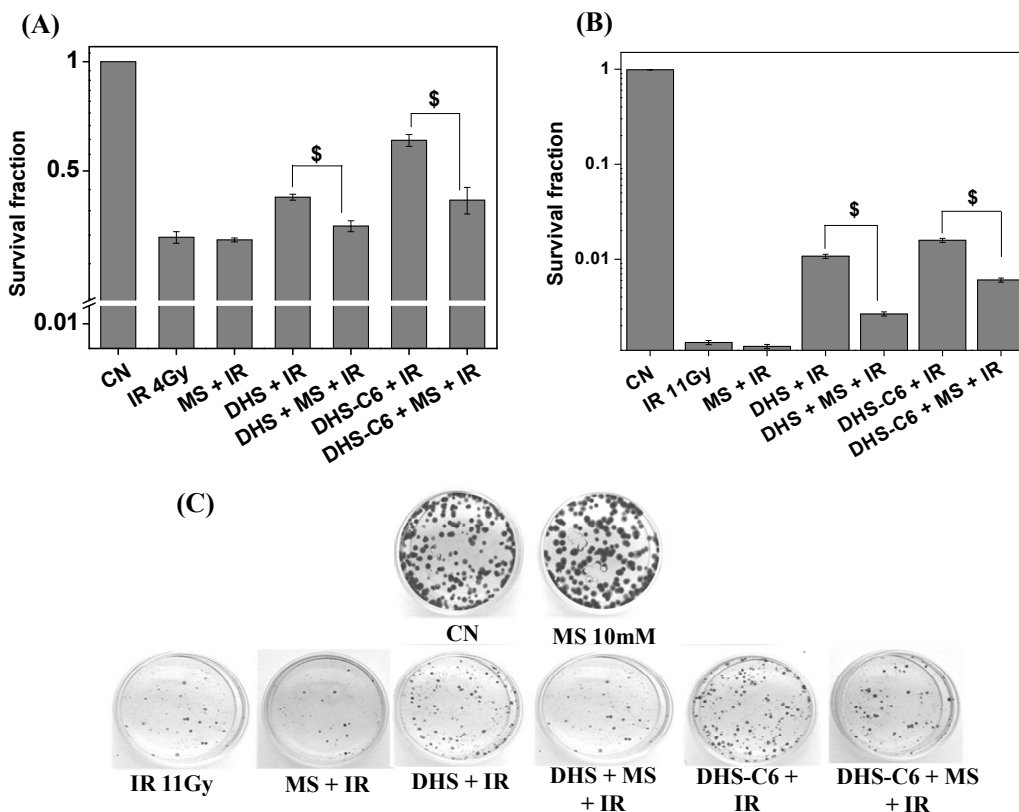


Figure 5.6 (A & B) Effect of MS (10 mM) on radioprotective activity of DHS and DHS-C<sub>6</sub> (25  $\mu$ M for 16 h) against radiation dose of 4 Gy and 11 Gy respectively in terms of survival fraction estimated by clonogenic assay in CHO cells. (C) Representative images shows colonies of CHO cells under different treatment conditions at 11 Gy. Results are presented as mean  $\pm$  SEM,  $n = 3$ .  $^{\$}p < 0.05$  as compared to DHS or DHS-C<sub>6</sub> plus radiation treated groups. CN - Control, IR – Radiation, MS - Mercaptosuccinic acid.

It can be seen that irradiation led to a decrease in the survival fraction as compared to control. The inhibitor (MS) treatment did not show any significant change in the survival fraction both under irradiated and un-irradiated conditions. As expected pre-treatments with both DHS and DHS-C<sub>6</sub> showed increase in the survival fraction

compared to the radiation control. The addition of MS abrogated the radioprotective ability of DHS and DHS-C<sub>6</sub> by 20 % and 40 % respectively at 4 Gy and by 70 % and 60 % respectively at 11 Gy (Fig. 5.6 (A - C)). This confirmed the involvement of GPx in the radioprotection offered by DHS and DHS-C<sub>6</sub>.

### **5.3.5. Effect of DHS and DHS-C<sub>6</sub> pre-treatment on the radiation induced G2/M arrest in CHO cells**

Further to understand the cause of radiation-induced cell death in CHO cells, we performed cell cycle analysis through PI assay in a time dependant manner starting from 48 h to 96 h. The distribution of cells in to different phases of cell cycle and their modulation by various treatment conditions is presented in figure 5.7. The results indicated that exposure of cells to radiation dose of 4 Gy led to time dependant increase in G2/M arrest from 25 % at 48 h to 36 % at 96 h. (Fig. 5.7 A, 5.7 B). Pre-treatment (25 µM for 16 h) with DHS and DHS-C<sub>6</sub> showed significant inhibition of G2/M arrest in irradiated cells as compared to radiation control cells. For example, the percentage of cells in G2/M phase of DHS and DHS-C<sub>6</sub> plus radiation treated groups was 23 % and 21 % respectively. Incubation with MS (GPx inhibitor) showed partial restoration of G2/M arrest in cells pre-treated with DHS or DHS-C<sub>6</sub> and exposed to radiation (Fig. 5.7 C and 5.7 D). The inhibitor (MS), DMSO and drug (DHS or DHS-C<sub>6</sub>) control groups showed cell cycle phases similar to those of control cells both under irradiated and un-irradiated conditions.

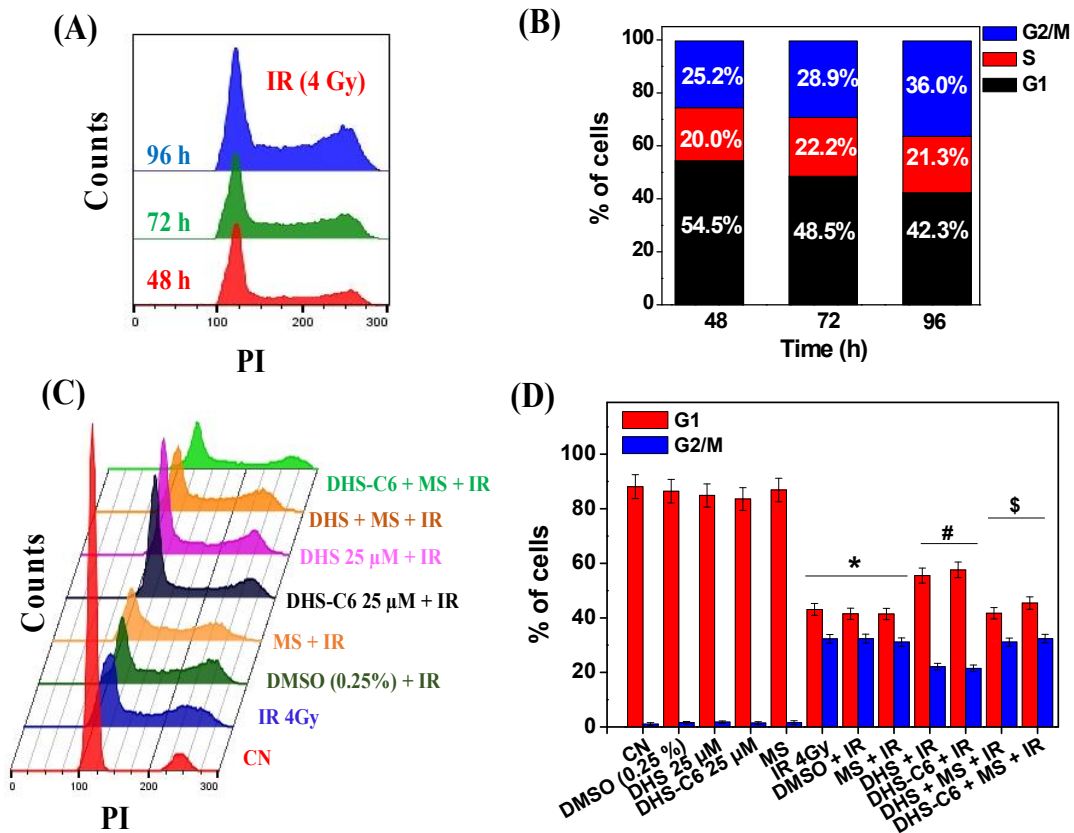


Figure 5.7 (A & B) Representative figure and bar graph respectively shows distribution of cells in different phases of cell cycle (G1, S, and G2/M) at 48 h, 72 h and 96 h following radiation exposure of 4 Gy by PI staining in CHO cells. (C & D) Representative figure and bar graph respectively shows distribution of cells in different phases of cell cycle (G1, S and G2/M) at 96 h post irradiation (4 Gy) under different treatment conditions. Results are presented as mean  $\pm$  SEM,  $n = 3$ . \* $p < 0.05$  as compared to respective control groups. # $p < 0.05$  compared to radiation control groups,  $^{\$}p < 0.05$  as compared to DHS / DHS-C<sub>6</sub> plus radiation treated groups. CN - Control, IR – Radiation, MS - Mercaptosuccinic acid.

### 5.3.6. Effect of DHS and DHS-C<sub>6</sub> pre-treatment on the radiation induced DNA damage in CHO cells

Since radiation-induced G2/M arrest and the cell death are the consequences of DNA damage, it was hypothesized that DHS or DHS-C<sub>6</sub> mediated increase in survival fraction against radiation exposure might be due to their abilities to inhibit DNA damage in a GPx dependant manner. Therefore, the ability of DHS and DHS-C<sub>6</sub> to protect cells from radiation-induced DSBs was evaluated through  $\gamma$ -H2AX assay at 30 minutes post-irradiation. The cells pre-treated with DHS and DHS-C<sub>6</sub> (25  $\mu$ M for 16 h) were exposed to radiation dose of 2 Gy and processed for  $\gamma$ -H2AX assay. The radiation dose of 2 Gy was used as high radiation dose will cause generation of a large number of  $\gamma$ -H2AX foci which cannot be easily counted. The results as presented in figures 5.8 A and 5.8 B indicated that number of  $\gamma$ -H2AX foci in various treatment controls such as DMSO, DHS, DHS-C<sub>6</sub>, and MS were comparable to that of control cells ( $\sim 5.0 \pm 0.7$  foci per cell). Exposure to radiation (2 Gy) led to 10 - fold increase in the number of  $\gamma$ -H2AX foci in the nucleus of the cells ( $55.0 \pm 1.8$  foci/cell). The pre -treatment with DMSO did not affect the number of  $\gamma$ -H2AX foci in irradiated cells whereas MS pre-treatment marginally increased the number of  $\gamma$ -H2AX foci to  $64.0 \pm 3.4$  foci per cell. Further, pre-treatment with DHS and DHS-C<sub>6</sub> significantly reduced the number of  $\gamma$ -H2AX foci in the irradiated cells to ( $34.0 \pm 1.6$  foci per cell) and ( $24.0 \pm 1.2$  foci per cell) respectively suggesting the effect of above compounds in preventing the radiation-induced DSBs. The compound DHS-C<sub>6</sub> was better than DHS in reducing the radiation-induced DSBs (Fig. 5.8 A and 5.8 B). Interestingly the presence of MS abrogated the abilities of DHS or DHS-C<sub>6</sub> to protect from DSBs by 20 % and 50 % respectively.

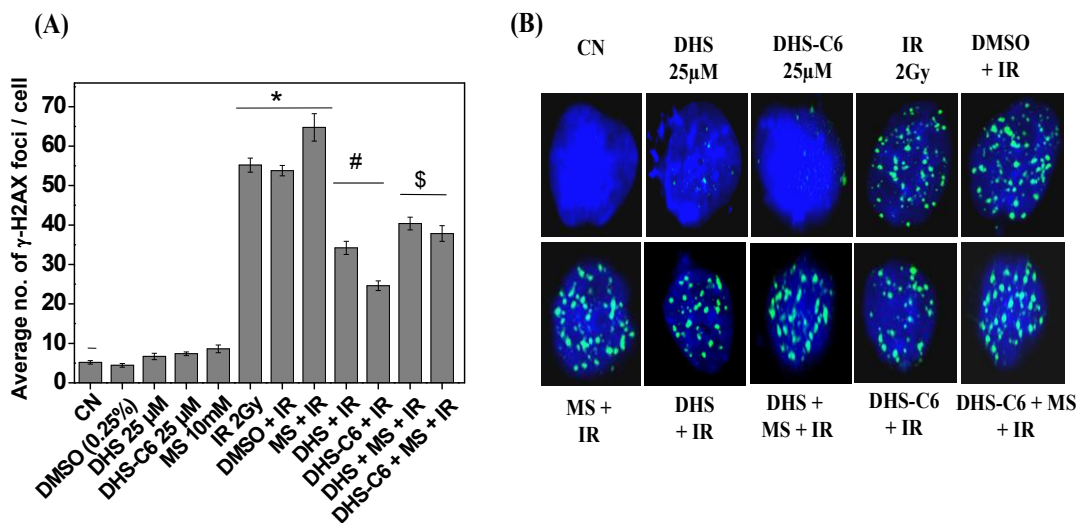


Figure 5.8 Effect of DHS and DHS-C<sub>6</sub> pre-treatment (25  $\mu$ M for 16 h) on  $\gamma$ -H2AX foci after radiation (2 Gy) exposure in CHO cells. (A) Bar graph shows the number of radiation (2 Gy) induced  $\gamma$ -H2AX foci at 30 minutes post irradiation. (B) Representative fluorescent images under different treatment conditions in CHO cells. Magnification – 63 X. Results are presented as mean  $\pm$  SEM, n = 3. \**p* < 0.05 as compared to respective control groups, #*p* < 0.05 as compared to radiation control groups, \$*p* < 0.05 as compared to DHS or DHS-C<sub>6</sub> plus radiation treated groups. CN - Control, IR - Radiation, MS - Mercaptosuccinic acid.

DSBs, if remain un-repaired leads to chromosomal fragmentation, which can be seen as micronuclei in dividing cells. Any compound which protects cells from radiation-induced DNA damage should also reduce the number of micronuclei formed post-radiation exposure. Accordingly, DHS and DHS-C<sub>6</sub> were investigated for their abilities to prevent radiation (4 Gy) induced micronuclei formation. The micronuclei frequency under different treatment conditions is shown in figure 5.9. According to the figure, cells treated with DMSO, DHS, DHS-C<sub>6</sub> and MS showed basal level of micronuclei (7.0  $\pm$  1.0 per 500 binucleate cells). Irradiation at a dose of 4 Gy led to an increase in the micronuclei frequency by ~ 11 folds. The effect of DMSO and MS in irradiated cells was comparable to that of radiation control. Pre-treatment with DHS

and DHS-C<sub>6</sub> significantly reduced the number of micronuclei in irradiated cells by 40 % and 56 % respectively. Interestingly, the addition of a GPx inhibitor, MS in cells pre-treated with DHS and DHS-C<sub>6</sub>, significantly abrogated their ability in terms of protection from micronuclei formation.

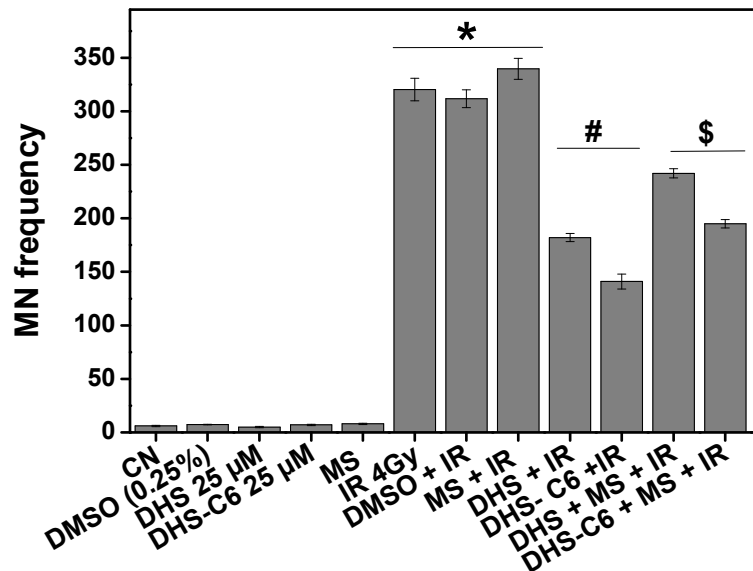


Figure 5.9 Effect of DHS and DHS-C<sub>6</sub> pre-treatment (25 μM for 16 h) on radiation (4 Gy) induced micronuclei frequency in CHO cells. Bar graph shows counts of radiation (4 Gy) induced micronuclei under different treatment conditions. Results are presented as mean ± SEM, n = 3. \**p* < 0.05 as compared to respective control groups. #*p* < 0.05 as compared to radiation control groups, \$*p* < 0.05 as compared to DHS or DHS-C<sub>6</sub> plus radiation treated groups. CN - Control, IR - Radiation, MS - Mercaptosuccinic acid.

### 5.3.7. Effect of DHS and DHS-C<sub>6</sub> pre-treatment on DNA repair kinetics in CHO cells following radiation exposure

In continuation to the above study, we investigated the effect of pre-treatment with DHS and DHS-C<sub>6</sub> on DNA repair kinetics after radiation exposure (4 Gy) by monitoring the levels of DNA damage as a function of post irradiation time ranging

from 0 to 60 minutes through comet assay. The comet parameters such as % TDNA and OTM and their representative fluorescent images are shown in figure 5.10 and 5.11.

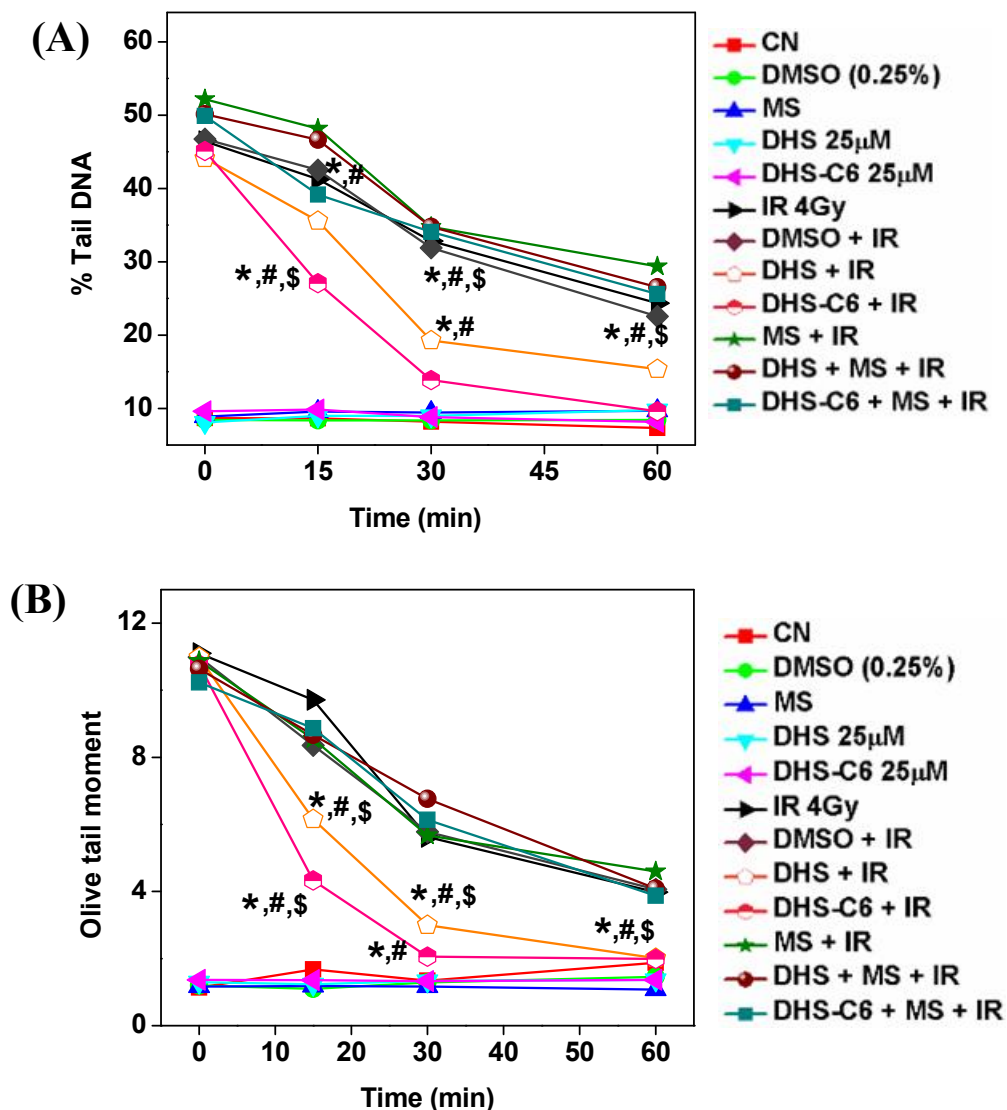
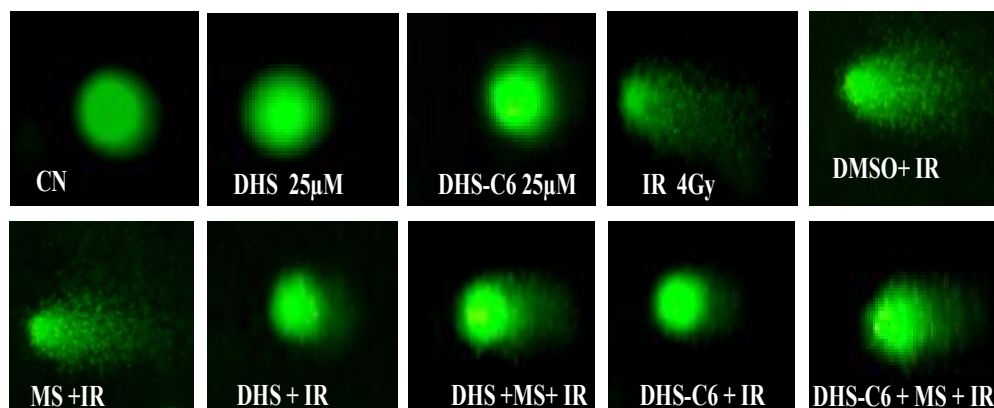


Figure 5.10 (A & B) Effect of DHS and DHS-C<sub>6</sub> pre-treatment (25 µM for 16 h) on DNA repair kinetics in CHO cells after radiation (4 Gy) exposure and its modulation by mercaptosuccinic acid (10 mM) in terms of % TDNA and OTM respectively. DNA repair was monitored by comet assay as a function of post irradiation time (0 - 60 minutes). Results are presented as mean ± SEM, n = 3. \*p < 0.05 as compared to respective control groups. #p < 0.05 as compared to radiation control groups, \$p < 0.05 as compared to DHS / DHS-C<sub>6</sub> plus radiation treated groups. CN - Control, IR - Radiation, MS - Mercaptosuccinic acid.

It can be seen from the figure that the control groups treated with DHS, DMSO, DHS-C<sub>6</sub> and MS did not show any increase in comet parameters as a function time. The irradiation dose of 4 Gy led to increase in % TDNA and OTM by 4.1 and 4.2-fold respectively as compared to control at a common time point of 30 minutes. These parameters decreased with time suggesting the normal DNA repair process of cells but did not reach to the control level. It can be seen from the figure that the control groups treated with DHS, DMSO, DHS-C<sub>6</sub> and MS did not show any increase in comet parameters as a function time. The irradiation dose of 4 Gy led to increase in % TDNA and OTM by 4.1 and 4.2-fold respectively as compared to control at a common time point of 30 minutes. These parameters decreased with time suggesting the normal DNA repair process of cells but did not reach to the control level. The % TDNA and OTM in DMSO treated and irradiated cell is comparable to that of radiation control. The MS treated and irradiated cells showed marginally higher level of % TDNA and OTM compared to irradiated cells. Interestingly, pre-treatment with DHS and DHS-C<sub>6</sub> led to faster repair of DNA compared to radiation control. At 30 minutes, there was a decrease in % TDNA and OTM by 1.7 and 1.8-fold respectively in DHS and by 1.8 and 2.8-folds respectively in DHS-C<sub>6</sub> pre-treated group compared to respective radiation control groups. DHS-C<sub>6</sub> appeared to be better than DHS in augmenting the DNA repair after radiation exposure. Blocking or inhibiting GPx through MS reversed the effects of DHS and DHS-C<sub>6</sub> with respect to DNA repair and showed level of % TDNA and OTM almost same to that of the radiation control. (Figs. 5.10 and 5.11). This suggested the role of DHS or DHS-C<sub>6</sub> in DNA repair through GPx induction.



*Figure 5.11 Representative fluorescent images of cells stained with SYBR-Green-II at 30 minutes post irradiation under different treatment conditions by comet assay. CN - Control, IR – Radiation, MS - Mercaptosuccinic acid.*

### **5.3.8. Effect of DHS and DHS-C<sub>6</sub> pre-treatment on DNA repair and cell cycle checkpoint pathways in CHO cells following radiation exposure**

Since above results indicated a GPx-mediated role of DHS or DHS-C<sub>6</sub> in affecting the cell cycle arrest (G2/M) and DNA repair, experiments were performed to validate the crosstalk between GPx induction by DHS or DHS-C<sub>6</sub> and the signalling mediators of repair pathways as well as cell cycle points by using combinatorial inhibition approach. The signalling proteins chosen for this study were DNA-PK of non homologous end joining (NHEJ) pathway and CHK 1 and CHK 2 of cell cycle arrest pathways. In first experiment, CHO cells pre-treated with DHS or DHS-C<sub>6</sub> were incubated with inhibitors NU-7026 (of DNA-PK) / UCN-01 (of CHK 1) / PV1019 (of CHK 2) and MS (of GPx) both separately and in combination, irradiated (4 Gy and 11 Gy) and analysed for cell viability by clonogenic assay.

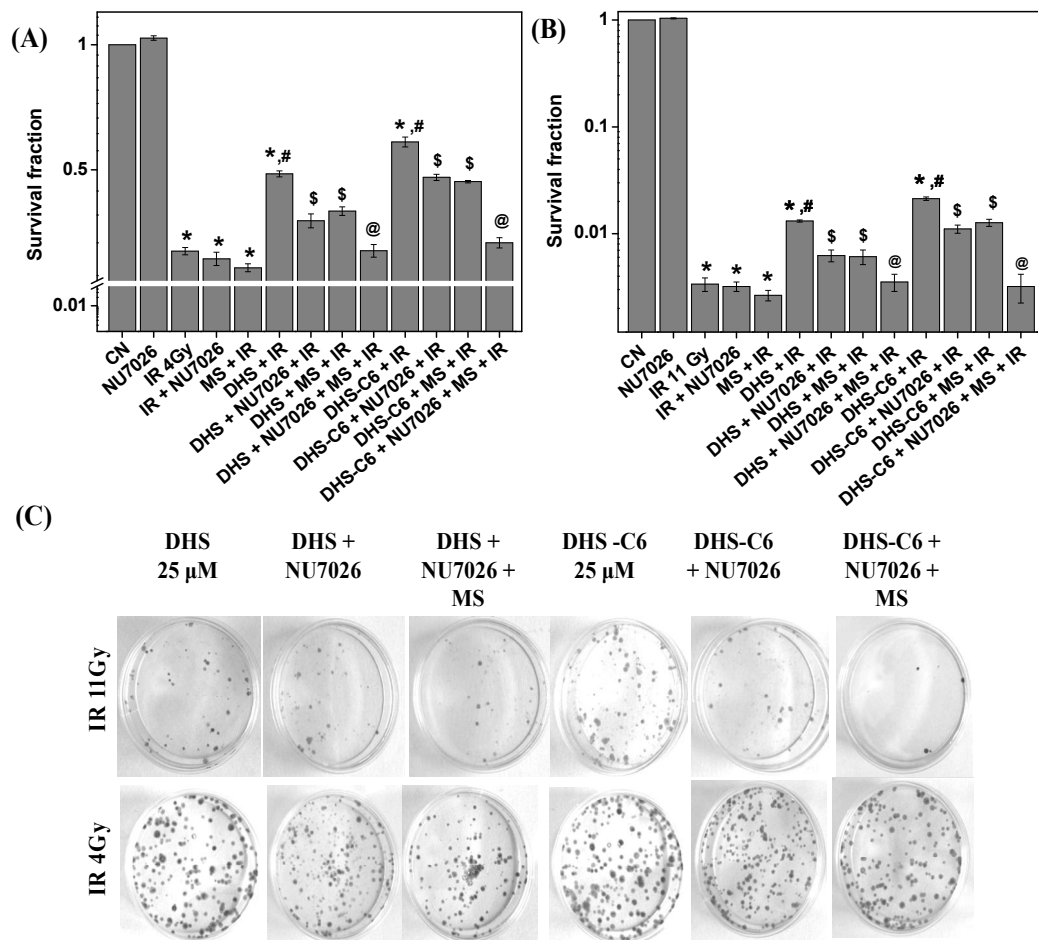


Figure 5.12 (A & B) Effect of NU-7026 (10  $\mu$ M) and MS (10 mM) on the radioprotective activity of DHS and DHS-C<sub>6</sub> pre-treatment at 25  $\mu$ M for 16 h in CHO cells against radiation dose of 4 Gy and 11 Gy respectively by clonogenic assay. (C) Representative images show colonies of CHO cells under different treatment combinations. \* $p < 0.05$  compared to control groups. Results are presented as mean  $\pm$  SEM,  $n = 3$ . # $p < 0.05$  compared to radiation control groups, \$ $p < 0.05$  compared to DHS or DHS-C<sub>6</sub> plus radiation treated groups, @ $p < 0.05$  compared to DHS plus inhibitor plus radiation treated group. CN - Control, IR - Radiation, MS - Mercaptosuccinic acid.

The survival fractions and the representative images of colonies under the combinatorial inhibitions of GPx (MS) with DNA-PK (NU-7026), CHK 1 (UCN-01), CHK 2 (PV1019) are presented in figures 5.12, 5.13 and 5.14 respectively. According

to figures, the controls groups of the inhibitors of DNA-PK (NU-7026), CHK 1 (UCN-01), CHK 2 (PV1019) and GPx (MS) did not show much change in the survival fraction under un-irradiated condition compared to control group. Exposure of radiation led to a dose (4 Gy and 11 Gy) dependant decrease in survival fraction. The inhibitors of DNA-PK, CHK 1 and GPx showed a marginal decrease in the survival fraction compared to radiation control. As expected pre-treatment with DHS or DHS-C<sub>6</sub> showed significant increase in survival fraction compared to radiation control groups. The presence of inhibitor of DNA-PK (NU-7026) in cells pre-treated with DHS and DHS-C<sub>6</sub> caused abrogation in their abilities to increase survival fraction by 22 % and 17 % respectively at 4 Gy and by 52 % and 48 % respectively at 11 Gy. Similarly, the inhibitor of GPx (MS) showed abrogation of DHS and DHS-C<sub>6</sub> mediated increase in survival fraction by 19 % and 30% respectively at 4 Gy and by 53 % and 40% respectively at 11 Gy. However, the presence of above two inhibitors together showed the higher abrogation of DHS and DHS-C<sub>6</sub> mediated increase in survival fraction by 30 % and 41% respectively at 4 Gy and by 72 % and 75 % respectively at 11 Gy.

With regard to checkpoint proteins, inhibition of CHK 1 (UCN-01) individually led to abrogation of DHS and DHS-C<sub>6</sub> mediated increase in survival fraction by 23 % and 25% respectively at 4 Gy and by 48 % and 46% respectively at 11 Gy. The inhibitor of CHK 2 (PV1019) per se did not affect the radioprotective effect of DHS and DHS-C<sub>6</sub>. Further combinatorial inhibitions of GPx (MS) and CHK 2 (PV1019) showed the same level of abrogation as that observed with only GPx inhibitor. In contrast, inhibitors of CHK 1 (UCN-01) and GPx (MS) together showed higher abrogation of 35 % and 42% respectively at 4 Gy and of 68 % and 78% respectively at 11 Gy.

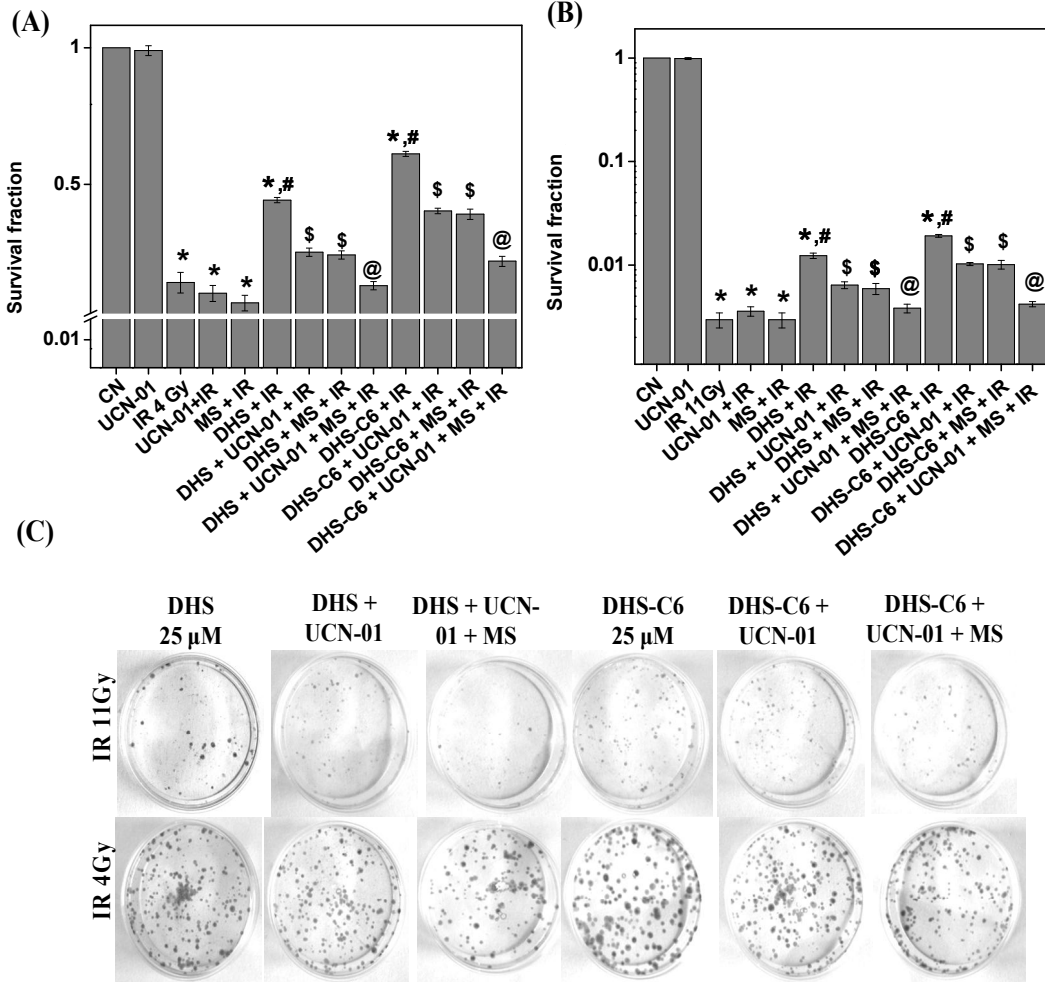


Figure 5.13 (A & B) Effect of UCN-01 (25 nM) and MS (10 mM) on the radioprotective activity of DHS and DHS-C<sub>6</sub> pre-treatment at 25 μM for 16 h in CHO cells against radiation dose of 4 Gy and 11 Gy respectively by clonogenic assay. (C) Representative images show colonies of CHO cells under different treatment combinations. \**p* < 0.05 compared to control groups. Results are presented as mean ± SEM, *n* = 3. #*p* < 0.05 compared to radiation control groups, \$*p* < 0.05 compared to DHS or DHS-C<sub>6</sub> plus radiation treated groups, @*p* < 0.05 compared to DHS plus inhibitor plus radiation treated group. CN - Control, IR - Radiation, MS - Mercaptosuccinic acid.

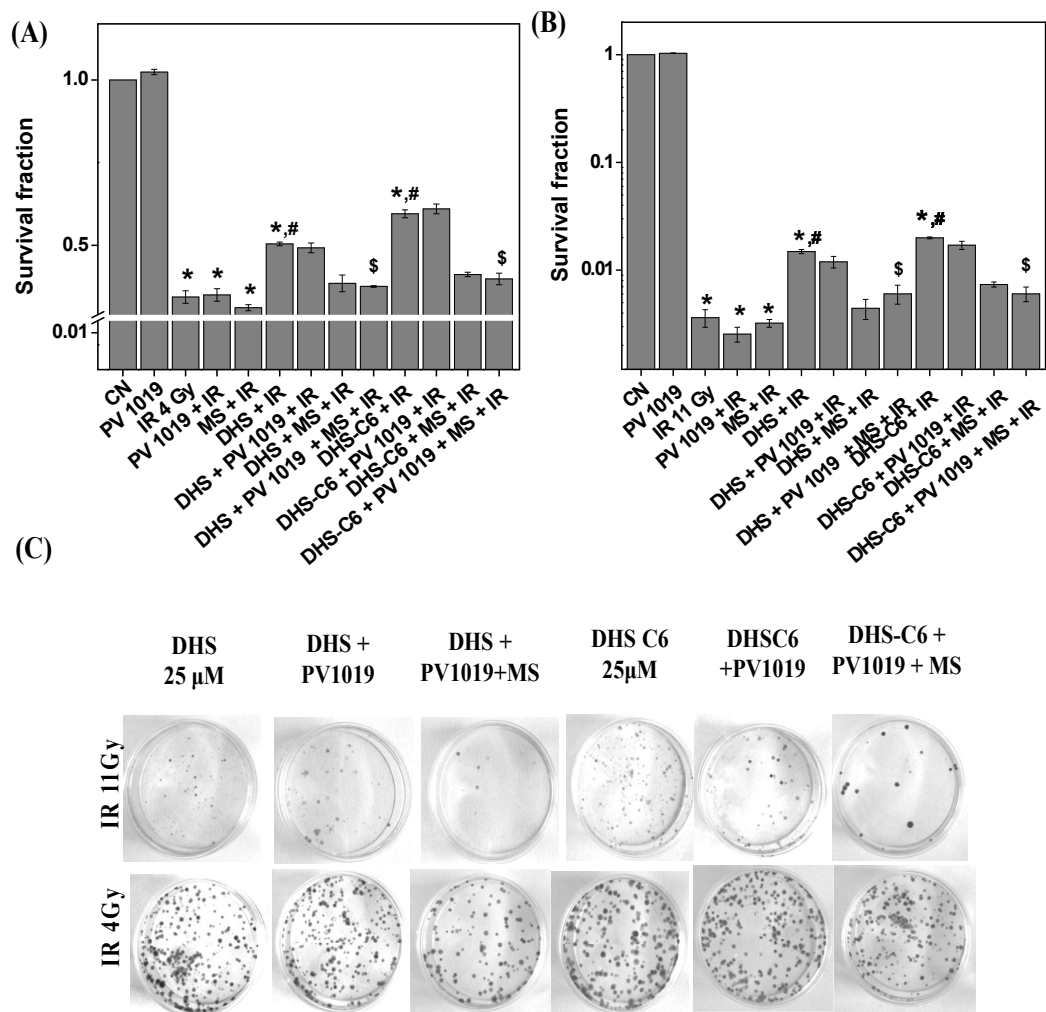


Figure 5.14 (A & B) Effect of PV-1019 (400 nM) and MS (10 mM) on the radioprotective activity of DHS and DHS-C<sub>6</sub> pre-treatment at 25 μM for 16 h in CHO cells against radiation dose of 4 Gy and 11 Gy respectively by clonogenic assay. (C) Representative images show colonies of CHO cells under different treatment combinations. \**p* < 0.05 compared to control groups. Results are presented as mean ± SEM, *n* = 3. #*p* < 0.05 compared to radiation control groups, \$*p* < 0.05 compared to DHS or DHS-C<sub>6</sub> plus radiation treated groups, @*p* < 0.05 compared to DHS plus inhibitor plus radiation treated group. CN - Control, IR - Radiation, MS - Mercaptosuccinic acid.

Above results together suggested that the abrogations by the inhibitors of CHK1 (UCN-01) or DNA-PK (NU-7026) on the radioprotective effect of DHS or DHS-C<sub>6</sub>

was increased in combination with the inhibitor of GPx, however the extent was less than additive when above proteins were inhibited individually. Thus it appears that GPx level induced by DHS or DHS-C<sub>6</sub> contributes to radioprotection through DNA-PK and CHK 1 mediated cell cycle arrest and DNA repair.

### **5.3.9. Effect of DHS and DHS-C<sub>6</sub> pre-treatment on the radiation induced oxidative stress in CHO cells**

Having understood the effect of DHS or DHS-C<sub>6</sub> on the radiation induced DNA damage and cell cycle arrest, it was thought that these two compounds previously reported for antioxidant activity might also modulate the intracellular redox state in favour of radioprotection. In order to address this, CHO cells pre-treated with DHS or DHS-C<sub>6</sub> were exposed to radiation and following this the level of ROS and ratio of GSH and GSSG were monitored at 30 minutes and 6 h respectively. GSH is a non-enzymatic antioxidant enzyme present in the cells which scavenges ROS and gets converted to GSSG. Thus, the ratio of GSH to GSSG is used as a marker of the oxidative stress in the cells. The mean fluorescence intensity of DCF and representative images indicating ROS level and the ratio of GSH and GSSG are presented in figure 5.15.

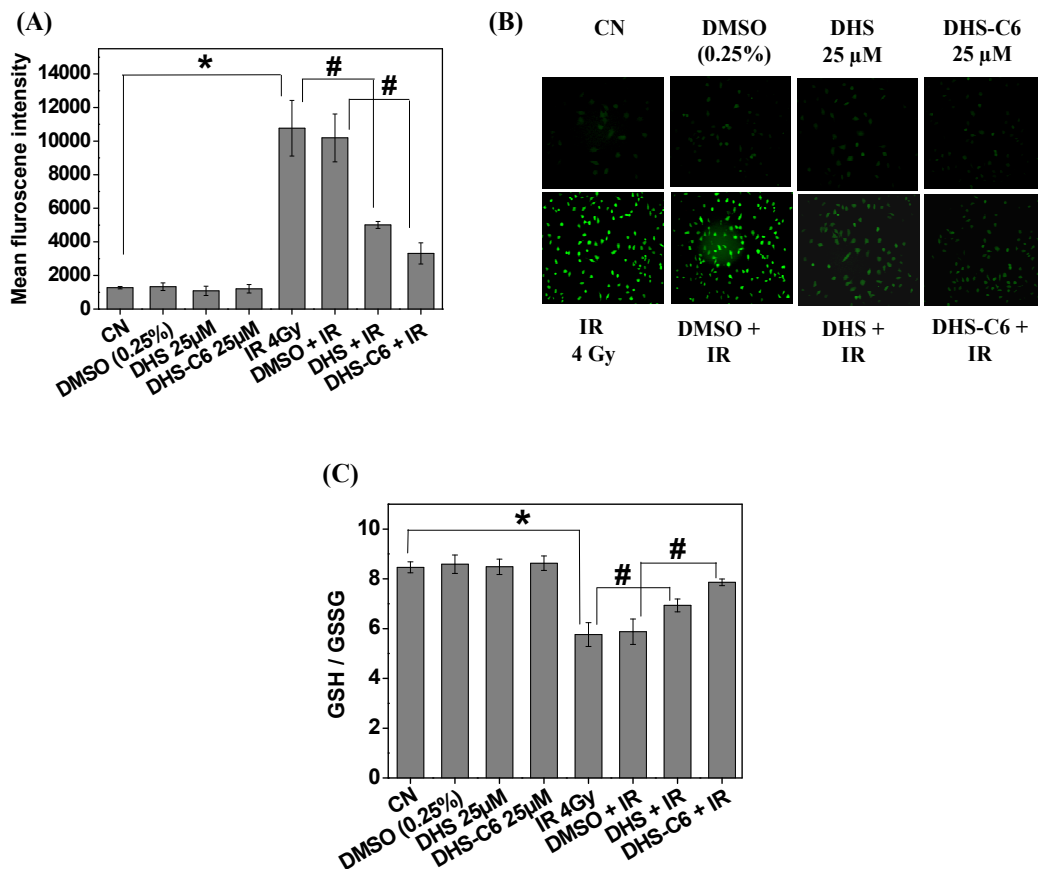


Figure 5.15 (A) Effect of DHS or DHS-C<sub>6</sub> pre-treatment (25  $\mu$ M for 16 h) on intracellular ROS production at 30 minutes post irradiation (4 Gy) in CHO cells. (B) Representative images of DCFDA stained cells under different treatment conditions at 30 minutes post irradiation (4 Gy). (C) Effect of DHS and DHS-C<sub>6</sub> pre-treatment (25  $\mu$ M for 16 h) on GSH/GSSG ratio at 6 h post  $\gamma$ -irradiation (4 Gy). Results are presented as mean  $\pm$  SEM, n = 3. \*  $p$  < 0.05 as compared to control groups, #  $p$  < 0.05 as compared to respective radiation control groups. CN – Control, IR - Radiation.

The results indicated that DHS and DHS-C<sub>6</sub> treatment themselves did not change ROS levels in cells as compared to control. Exposure to radiation at a dose of 4 Gy led to a significant increase in the ROS level by ~10 fold. Pre-treatment with DHS and DHS-C<sub>6</sub> resulted in reduction of ROS by 5 and 7-fold respectively as compared to radiation control. The similar effect was observed in case of GSH/GSSG ratio. The radiation exposure of 4 Gy in CHO cells decreased GSH/GSSG by 32 % whereas DHS

and DHS-C<sub>6</sub> pre-treatment increased GSH / GSSG ratio by 21 % and 35 % respectively suggesting partial restoration of GSH level in cells 5.12 (A – C). In all above observations, DHS-C<sub>6</sub> was found to be better than DHS in preventing radiation-induced oxidative stress.

### 5.3.10. Effect of DHS and DHS-C<sub>6</sub> pre-treatment on *SelenoP-1* expression in CHO cells

In continuation to above studies DHS and DHS-C<sub>6</sub> were also evaluated for their effects on the expression of *Sel-P1*. Like GPx, it is an important selenoprotein reported for antioxidant activity in literature<sup>123,124</sup>. The expression of *SelenoP-1* was monitored at mRNA transcript level by RT-PCR and the results are presented in figure 5.16.

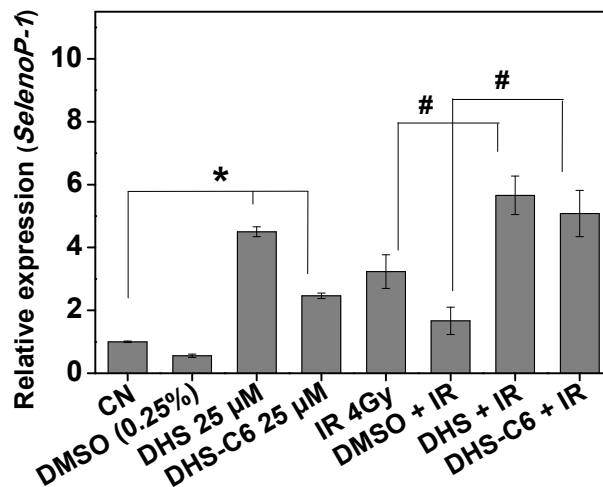


Figure 5.16 Effect of DHS and DHS-C<sub>6</sub> pre-treatment (25 µM for 16 h) on mRNA expressions of *SelenoP-1* in CHO cells at 6 h post irradiation (4 Gy) as estimated by RT-PCR. The expression of above genes in different treatment groups was normalized against control group and the relative expression changes have been plotted. Actin expression was used as internal control. Results are presented as mean ± SEM, n = 3. \*p < 0.05 compared to control groups, #p < 0.05 compared to radiation control groups. CN - Control, IR - Radiation.

It can be seen that DHS and DHS-C<sub>6</sub> treatment themselves led to an increase in the expression of *SelenoP-1* by 4 and 3-fold respectively compared to their respective controls. Exposure to radiation at a dose of 4 Gy also induced the expression of *SelenoP-1* but that was less than that of DHS and DHS-C<sub>6</sub> treatment. Further, pre-treatment with DHS and DHS-C<sub>6</sub> in irradiated cells augmented this level by 2.1-fold and 3-fold respectively.

#### **5.3.11. Effect of DHS and DHS-C<sub>6</sub> pre-treatment on the radiation induced apoptosis in splenic lymphocytes and CHO cells**

Above results from CHO cells prompted us to evaluate the radioprotective effect of DHS and DHS-C<sub>6</sub> in other cell type like lymphocytes which are known to be the most radiosensitive and undergo apoptosis after radiation exposure<sup>173,259</sup>. For this, spleen lymphocytes were freshly isolated from BALB/C mice under aseptic condition, treated with 25 μM of DHS or DHS-C<sub>6</sub> for 16 h, exposed to γ-radiation at 4 Gy and then evaluated for apoptotic parameters at 48 h. The histogram and bar graphs presented in figures 5.17 A and 5.17 B show the distribution of cells in different phases of cell cycle by PI assay. According to the results, irradiation (4 Gy) led to a significant increase in pre-G1 population ( $85.5 \pm 1.3$  %) as compared to control cells ( $28.1 \pm 0.2$  %) indicative of apoptosis and pre-treatment with DHS or DHS-C<sub>6</sub> did not reduce the percentage of cells in pre-G1 phase. This clearly suggested that DHS or DHS-C<sub>6</sub> did not protect lymphocytes from the radiation-induced apoptosis. The results of other apoptotic markers such as DNA ladder and mitochondrial membrane potential (using JC-1) are presented in figures 5.18 A and 5.18 B and indicated similar results.

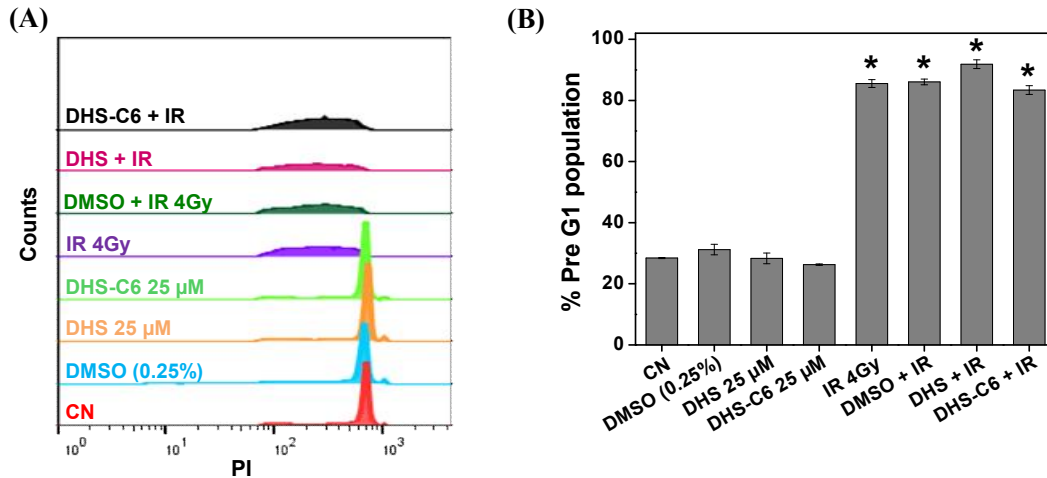


Figure 5.17 Effect of DHS and DHS-C<sub>6</sub> pre-treatment (25  $\mu$ M for 16 h) on the radiation (4 Gy) induced apoptosis in lymphocytes. (A) Representative figure showing pre-G1 population at 48 h post irradiation by PI staining. (B) Bar graph shows percentage (%) of cells in pre-G1 phase under different treatment conditions at 48 h post irradiation by PI staining. Results are presented as mean  $\pm$  SEM, n = 3. \*p < 0.05 compared to control groups. CN - Control, IR – Radiation.

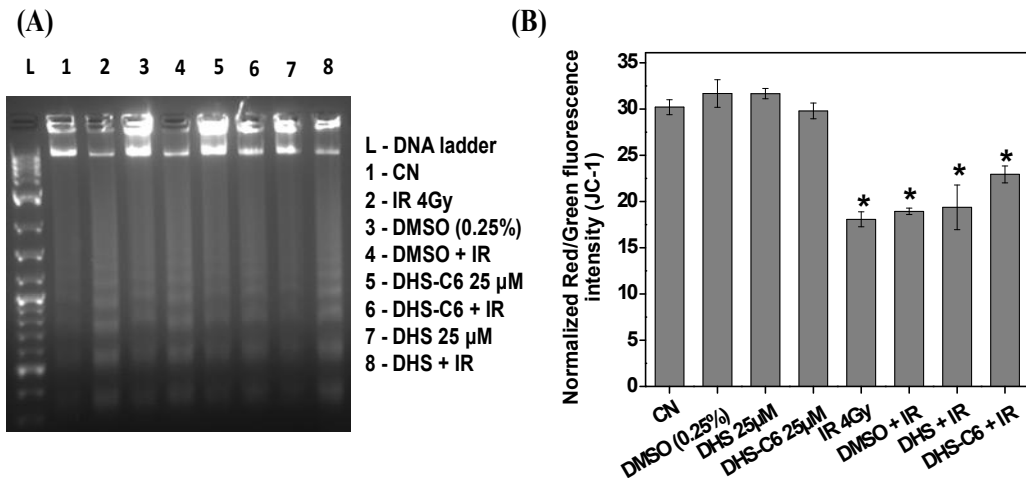


Figure 5.18 Effect of DHS and DHS-C<sub>6</sub> pre-treatment (25  $\mu$ M for 16 h) on the radiation (4 Gy) induced apoptosis in lymphocytes. (A) DNA ladder assay at 24 h post irradiation (4 Gy) under different treatment conditions. (B) Effect on MMP estimated as ratio of red ( $\lambda_{em} = 610$  nm) and green ( $\lambda_{em} = 535$  nm) fluorescence intensity of JC-1 staining at 18 h post irradiation under different treatment conditions. Results are presented as mean  $\pm$  SEM, n = 3. \*p < 0.05 compared to control groups. CN - Control, IR – Radiation.

Further to know whether DHS and DHS-C<sub>6</sub> protect CHO cells from apoptosis, CHO cells pre-treated with DHS or DHS-C<sub>6</sub> (25 μM for 16 h) were subjected to irradiation at very high acute dose of 15 Gy<sup>260</sup> for induction of apoptotic death pathway and examined for pre-G1 population by PI assay. The results as presented in figures 5.19 clearly indicated that 15 Gy led to significant increase in pre-G1 population. However, pre-treatment with DHS and DHS-C<sub>6</sub> did not reduce the apoptotic population. Taken together, these results suggested that DHS and DHS-C<sub>6</sub> treatment did not protect cells from radiation-induced early apoptosis irrespective of the cell type.

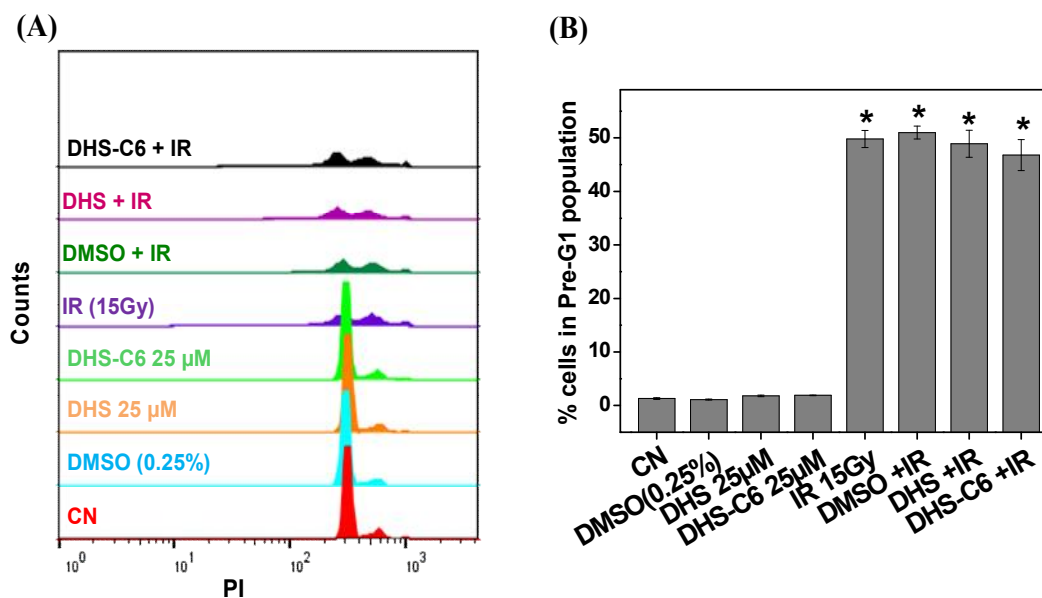


Figure 5.19 Effect of DHS and DHS-C<sub>6</sub> pre-treatment (25 μM for 16 h) on the radiation (15 Gy) induced apoptosis in CHO cells. (A) Representative figure shows pre-G1 population at 48 h post irradiation by PI staining. (B) Bar graph showing percentage (%) of cells in pre-G1 phase under different treatment conditions at 48 h post irradiation by PI staining. Results are presented as mean ± SEM, n = 3. CN - Control, IR - Radiation.

#### 5.4. Discussion

In this chapter, DHS (a water soluble organoselenium compound) which has been shown to improve 30 day survival of mice and prevent radiation induced organ toxicity as discussed in chapter 3 is studied in cellular model system to investigate its mechanism of action. Additionally, we also investigated whether DHS-C<sub>6</sub>, a pro-drug previously reported to increase the cellular uptake of DHS could be a better agent than DHS to achieve radioprotection. For the study, CHO cell of epithelial origin was employed as they have been widely used in radiation related research work and are well characterised with respect to radiation response<sup>7</sup>. For example, CHO cells exposed to radiation accumulate DNA damage leading to G2/M arrest and delayed mitotic death<sup>7,261</sup>. Therefore, radioprotective effect of DHS and DHS-C<sub>6</sub> in CHO cells was evaluated by monitoring cell survival, DNA damage and cell cycle progression. Analysis of these parameters revealed that treatment with DHS or DHS-C<sub>6</sub> at 25 µM for 16 h prior to radiation exposure augmented DNA repair leading to inhibition of G2/M arrest and mitotic death. The pro-drug DHS-C<sub>6</sub> showed better efficacy than DHS with a DMF value of 1.24.

Previously we had observed that *in vivo* radioprotective activity of DHS was associated with its ability to cause tissue specific induction of GPx when monitored at activity and mRNA levels. Supporting this observation, here in the present study, we observed that DHS treatment induced GPx activity in CHO cells. However, DHS-C<sub>6</sub> showed only a marginal increase in GPx activity compared to DHS. It is well documented in literature suggesting that selenium is essential for GPx activity but afterwards it reaches saturation with the increasing availability of selenium and this could be the reason for the above observed effect<sup>262,263</sup>. Further selenium compounds in general are known to regulate the expression of selenoproteins including GPx by

modulating mRNA stability and activating transcription factors such as Nrf2 and p53<sup>264-267</sup>. Tan et al showed the presence of p53 binding site at the promoter region of GPx and selenium compounds are known to regulate the p53 activity by modulating redox active cysteine residues (275/277). In another study, Banning et al showed that gastrointestinal GPx is target of Nrf2.<sup>267</sup> The exact mechanism through which DHS or DHS-C<sub>6</sub> induces GPx activity is not clear to us at this stage and this will be addressed in future studies. Nevertheless above results prompted us to investigate the role of GPx in DHS or DHS-C<sub>6</sub>-mediated radioprotection. In order to address this issue, we employed MS known to inhibit GPx through non-covalent interactions and evaluated its effect on the radiation response of DHS or DHS-C<sub>6</sub> in CHO cells<sup>258</sup>. Importantly, treatment with MS blocked the DNA repair and radioprotective activity shown by DHS or DHS-C<sub>6</sub>. Thus, it is confirmed that GPx indeed played a role in radioprotective effect of DHS or DHS-C<sub>6</sub> through modulating DNA repair. Further to get more insight in to this mechanism, the involvement of the signalling proteins of DNA repair pathways were investigated. In general, mammalian cells assess for any DNA damage induced by radiation exposure through checkpoints (such as G1/S and G2/M) regulated by CHK 1 and CHK 2 and activate DNA repair mechanisms through DNA protein kinase (DNA-PK)<sup>37,268-270</sup>. Therefore to establish the crosstalk if any of the above signalling proteins with the GPx level induced by DHS or DHS-C<sub>6</sub>, we employed combinatorial inhibition approach. If there was cross talk between the GPx and CHK 1/CHK 2/DNA-PK, their combined inhibitions would not cause any additive effect with respect to affecting the cell survival against radiation exposure. Interestingly our results showed that inhibitions of CHK 1 and DNA-PK abrogated the radioprotective ability of DHS or DHS-C<sub>6</sub> separately but did not result in additive effect in combination with inhibitor of GPx. Taken together, it is confirmed that GPx level induced by DHS and DHS-C<sub>6</sub>

influenced DNA repair by involving CHK 1 and DNA-PK. These results are consistent with growing evidences in literature suggesting the role of GPx in DNA repair and maintaining the genome stability<sup>158,254,271</sup>

In the past, various other research groups have also evaluated GPx for reducing the radiation-induced cell killing employing cellular models. The results are mostly incongruent with some studies suggesting that GPx is an important factor in cellular radio sensitivity<sup>272,221</sup>, while others indicating that cells treated with sodium selenite or genetically engineered to over express cytosolic GPx prior to radiation exposure did not show any improvement in the survival<sup>222,273</sup>. In the present investigation, DHS-C<sub>6</sub> treatment although showed similar elevation in GPx level, resulted in higher radioprotection compared to DHS. This suggested that GPx may not be the only factor contributing to the radioprotective effect of DHS and DHS-C<sub>6</sub>. Justifying this assumption, DHS or DHS-C<sub>6</sub> treatment showed lowering of oxidative stress in irradiated CHO cells and DHS-C<sub>6</sub> was more effective than DHS in this respect. Previously, Beena et al showed that DHS scavenges ROS<sup>274</sup> and therefore DHS-C<sub>6</sub> through increasing the cellular uptake may contribute to higher ROS scavenging<sup>160,162</sup>. Further both DHS and DHS-C<sub>6</sub> were also observed to up-regulate other antioxidant selenoprotein like *SelenoP-1* which can be linked to antioxidant effects. Thus, the abilities of DHS and DHS-C<sub>6</sub> to augment DNA repair and reduce the oxidative stress appeared to be contributing towards radioprotective activity.

Having understood the radioprotective action of DHS and DHS-C<sub>6</sub> in CHO cells, it was important to evaluate the effect of these compounds in radiosensitive cells like lymphocytes<sup>259</sup>. Notably treatment with DHS or DHS-C<sub>6</sub> did not protect lymphocytes from radiation exposure. Lymphocytes undergo transient G1 arrest and apoptosis after radiation exposure suggesting the inability of above compounds in

preventing the radiation-induced early apoptosis. Collectively, the present study gains significance in view of the fact that late-responding normal tissue involved in the radiotherapy side effects undergo delayed mitotic death following radiation exposure. DHS-C<sub>6</sub> a lipophilic conjugate of DHS showing potent protection against radiation-induced mitotic death can be a model compound for *in vivo* evaluation as selenium based radioprotector.

### **5.5. Summary**

1. DHS and DHS-C<sub>6</sub> protected CHO cells of epithelial origin from radiation induced mitotic death.
2. DMF of DHS and DHS-C<sub>6</sub> for preventing the radiation induced mitotic death in CHO cells was estimated to be 1.14 and 1.24 respectively at 25 μM.
3. Pre-treatment with DHS and DHS-C<sub>6</sub> reduced oxidative stress in irradiated CHO cells as seen by reduction in ROS level with a concurrent increase in GSH/GSSG ratio.
4. DHS and DHS-C<sub>6</sub> pre-treatment augmented DNA repair and prevented G2/M arrest in irradiated CHO cells through cross talk between GPx and CHK 1 or DNA-PK.
5. DHS-C<sub>6</sub> is better than DHS as a radioprotector which has been attributed to the higher uptake of DHS due to its increased lipophilicity.

## **Chapter 6**

### **Summary and future scope**

This chapter gives summary of the results described in different chapters of the thesis along with the future scope.

Exposure of living cells to ionizing radiation results in the production of highly reactive free radical and molecular species like  $\bullet\text{OH}$ ,  $\text{O}_2^{\bullet-}$ , and  $\text{H}_2\text{O}_2$  termed as ROS. ROS cause damage to bio-molecules like DNA, lipids and proteins which are essential for the functioning of the cells<sup>14,21</sup>. The cellular internal defense system plays an important role in preventing ROS induced damage. For example, endogenous antioxidants like thiols, SOD, GPx and catalase are capable of donating an electron to the ROS thus terminating a free radical initiated chain reaction<sup>24,25</sup>. Cells also have an internal DNA repair pathway to minimize damage to DNA in order to prevent transfer of genomic alterations to the daughter cells<sup>31,36,37</sup>. If the generation of ROS exceeds the capacity of the cells defense machinery to neutralize, it results in a pathological condition termed as oxidative stress which may lead to cell death<sup>39</sup>. Exposure to radiation is also known to induce oxidative stress through ROS generation. Such exposure is a matter of concern during radiotherapy, which is a common modality to treat malignant tumors<sup>6</sup>. The major limiting factor in the use of radiation is that apart from killing tumor cells it also kills the nearby healthy cells which results in the deterioration of the health condition of an individual. This needs for the development of an agent which can prevent cells from harmful effects of radiation.

Traditionally used sulfur compounds for radioprotection, suffer from dose limiting toxicity, warranting search for new class of radioprotectors. In this context, selenium compounds are gaining importance in the present days for the development as radioprotectors due to their similarity with sulfur compounds. Moreover, selenium is an essential micronutrient and a constituent of redox regulating selenoenzymes like GPx<sup>110,217</sup>, which catalyses the reduction of  $\text{H}_2\text{O}_2$  or organic hydroperoxides to water or alcohols<sup>126,264</sup>. In the past two decades, there is a lot of interest among researchers to

develop selenium compounds mimicking GPx like activity to be explored as antioxidants / radioprotectors. For example, ebselen, an organoselenium compound and a GPx mimic has been reported in the literature to inhibit radiation induced killing and oxidative damage in the cells<sup>146,147</sup>. Similarly, diselenodipropionic acid, a water soluble selenium compound with GPx activity showed potent radioprotection in mice model<sup>149,152</sup>. In contrast, there are some reports in the literature which showed that there is no effect of GPx overexpression in protecting cells from radiation induced cell damage<sup>222,273</sup>. Therefore, the motivation behind the present thesis is to find a correlation between the GPx activity and the radioprotective activity of selected organoselenium compounds. As a part of this work, an attempt was also made to know the effect of structural modification on the radioprotective activity of the selenium compounds. The compounds studied in the present thesis are dihydroxyselenolane (DHS) and monoamine selenolane (MAS) which are, water soluble cyclic selenium compounds<sup>159,167</sup>. The results of the thesis are divided into three parts and presented in chapter 3, chapter 4 and chapter 5. In chapter 3, radioprotective effect of DHS is studied in detail in mice model system. In chapter 4, role of lipophilicity and structural modification in the uptake and the antioxidant effect of selenium compounds are studied in cellular model system. In chapter 5, role of GPx level on cell cycle progression, DNA repair kinetics, redox state and overall radioprotective efficacy of DHS and its fatty acid derivative is studied. Highlights of these chapters are discussed briefly.

In chapter 3, it was observed that DHS supplementation at a non-toxic dose of 2 mg/kg b.wt for five consecutive days prior to WBI of 8 Gy and continued for three times a week during the post irradiation period improved the 30 day survival of BALB/c mice by 40 %. The improvement was related with the ability of DHS to

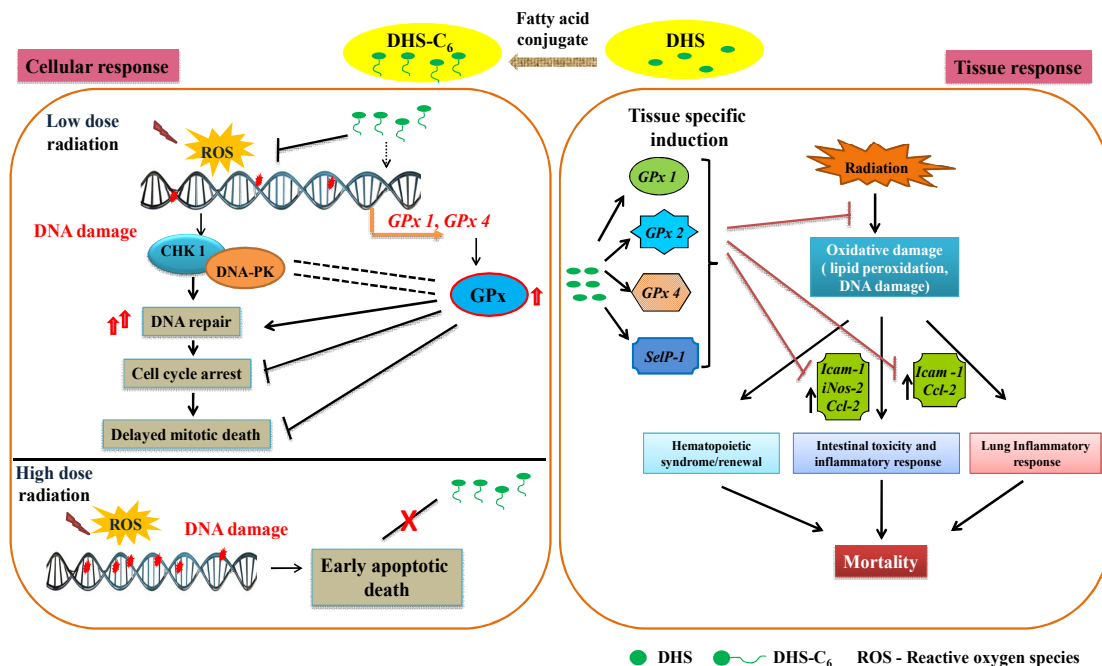
prevent the mice from radiation induced oxidative damage in radiosensitive organs. Subsequent studies indicated that DHS supplementation led to delayed recovery of the radiation induced hematopoietic toxicity by restoring spleen parameters like index, cellularity, spleen colonies and expression of *Csf-3*. DHS also protected mice from radiation induced inflammation by decreasing the level of pro-inflammatory cytokines like IL-6 and TNF- $\alpha$  in the serum and the expression of the inflammatory genes like *Icam-1*, *Ccl-2* and *iNos-2* in lungs and intestine. Moreover, DHS supplementation caused an increase in the expression of a selenoenzyme *SelenoP-1* and induction in overall GPx activity in a tissue specific manner. This chapter confirms *in vivo* radioprotective effect of DHS and it also indicates that GPx activation has some role in radioprotection.

The aim of chapter 4 is to investigate the effect of alkylation and lipophilicity of DHS on its uptake and antioxidant activity in CHO cells. For the study, DHS, and its fatty acid derivatives (C<sub>6</sub>-C<sub>14</sub>) were used. Toxicity evaluation studies indicated that the derivatives greater than C<sub>8</sub> improved the ability of DHS to incorporate in the cells but at the same time exhibited toxicity which is directly related with the length of the alkyl chain. Further studies revealed that the major mechanism of cytotoxicity was plasma membrane disintegration leading to necrosis. When these studies were compared with MAS, an amino substituted analogue of DHS and its alkyl derivatives with varying chain length, the results substantiated the observations from DHS. Overall, it was confirmed that C<sub>6</sub> derivatives of DHS and MAS possess the right balance of hydrophilicity and lipophilicity allowing the parent molecule to cross the cell membrane exhibiting higher antioxidant activity in cells.

Based on the results from chapters 3 and 4, chapter 5 is designed to address two specific problems. First to compare the cellular radioprotective effect of DHS and

DHS-C<sub>6</sub> and second to affirmatively conclude the role of GPx in the radioprotective activity. In CHO cells, DHS or DHS-C<sub>6</sub> pre-treatment prevented radiation induced delayed mitotic cell death along with increase in GPx activity. In contrast DHS or DHS-C<sub>6</sub> although increased the GPx level in lymphocytes (radiosensitive cells) did not protect them from the radiation induced apoptosis. Studies involving pharmacological inhibitors, established that the radioprotective effect of DHS or DHS-C<sub>6</sub> is due to their abilities to augment DNA repair and prevent G2/M cell cycle arrest in a GPx dependent pathway. Overall in all these studies, DHS-C<sub>6</sub> was better than DHS as a radioprotector and restoration of redox homeostasis in cells.

In conclusion, DHS and DHS-C<sub>6</sub> showed pleiotropy involving mechanisms like induction of selenoproteins (GPx, SelenoP-1), ROS scavenging, restoration of redox homeostasis and suppression of inflammatory cytokines to facilitate radioprotection. The overall mechanisms of radioprotection by DHS or DHS-C<sub>6</sub> are summarized in scheme 6.1.



Scheme.6.1. Proposed model for the radioprotective effect of DHS / DHS-C<sub>6</sub>

## Future scope

One of the major findings of the present thesis is that the lipophilic analogue, DHS-C<sub>6</sub> is more active than DHS in protecting the cellular model from radiation exposure. However in order to appreciate the potential of DHS-C<sub>6</sub> as a radioprotector, it is necessary to understand its toxicity, dosage, time and the mode of administration in detail employing *in vivo* model system. In addition, pharmacokinetics studies are needed to correlate the tissue availability / distribution of DHS-C<sub>6</sub> with its improved radioprotective effect over parent compound DHS. Further if DHS or DHS-C<sub>6</sub> has to be used against radiotherapy, it should not protect tumor cells. Therefore DHS or DHS-C<sub>6</sub> should be evaluated for their effects on radiation response of tumor cells. Further, it was shown that the *in vivo* radioprotective effect of DHS was associated with tissue specific increase in the expressions of the GPx isoforms (*GPx 1*, *GPx 2*, *GPx 4*). Considering this, it is required to investigate whether GPx plays any tissue specific role in radioprotection. It is also important to understand the mechanisms through which DHS or DHS-C<sub>6</sub> up-regulates GPx level in cells. Finally, all these studies needs be compared with sodium selenite and other selenium radioprotectors which will provide an insight for the design of synthetic organoselenium compounds as an antioxidant / radioprotector.

## REFERENCES

- 1 C. Von Sonntag, in: *Taylor and Francis, New York*, 1987, p. 515.
- 2 W. Roentgen, in: *Otto Glasser: Wilhelm Conrad Roentgen and the early history of the Roentgen rays*, C. Thomas, Springfield, Wuerzburg, 1934, p. 20.
- 3 H. Becquerel, *CR Acad Sci*, 1896, **122**, 420–421.
- 4 H. Becquerel, *CR Acad Sci Paris*, 1896, **122**, 201–503.
- 5 M. D. Blaufox, *Semin. Nucl. Med.*, 1996, **26**, 145–154.
- 6 H. D. Kogelnik, *Int. J. Radiat. Oncol. Biol. Phys.*, 1996, **35**, 219–26.
- 7 E. J. Hall, *Radiobiology for the Radiologist*, Lippincott Williams & Wilkins, 5th edn., 2006.
- 8 J. W. T. Spinks, R. J. Woods, *An introduction to radiation chemistry*, 3rd edn., 1976.
- 9 R. J. Walker, R. I. Cervený, *Medical Consequences of Nuclear Warfare*, Falls Church, VA: Office of the Surgeon General, U.S. Government Printing Office, 1989.
- 10 P. A. Riley, *Int. J. Radiat. Biol.*, 1994, **65**, 27–33.
- 11 G. V. Buxton, C. L. Greenstock, W. P. Helman, A. B. Ross, *J. Phys. Chem. Ref. Data*, 1988, **17**, 513–886.
- 12 M. C. R. Symons, J. M. C. Gutteridge, *Free Radicals and Iron: Chemistry, Biology and Medicine*, 1998.

- 13 A. Ayala, M. F. Munoz, S. Arguelles, *Oxid. Med. Cell. Longev.*, 2014, doi:10.1155/2014/360438.
- 14 R. Kohen, A. Nyska, *Toxicol. Pathol.*, 2002, **30**, 620–650.
- 15 E. Shacter, *Drug Metab. Rev.*, 2000, **32**, 307–326.
- 16 K. J. Davies, *J. Biol. Chem.*, 1987, **262**, 9895–9901.
- 17 R. L. Levine, E. R. Stadtman, *Exp. Gerontol.*, 2001, **36**, 1495–1502.
- 18 T. Grune, T. Reinheckel, K. J. Davies, *FASEB J.*, 1997, **11**, 526–34.
- 19 M. Dizdaroglu, P. Jaruga, M. Birincioglu, H. Rodriguez, *Free Radic. Biol. Med.*, 2002, **32**, 1102–1115.
- 20 T. P. Devasagayam, S. Steenken, M. S. Obendorf, W. A. Schulz, H. Sies, *Biochemistry*, 1991, **30**, 6283–6289.
- 21 K. B. Beckman, B. N. Ames, *J. Biol. Chem.*, 1997, **272**, 19633–19636.
- 22 J. Cadet, M. Berger, T. Douki, J. L. Ravanat, *Rev Physiol Biochem Pharmacol*, 1997, 1–87.
- 23 J. Tremp, *Radiat. Res.*, 1981, **85**, 554–566.
- 24 M. Valko, C. J. Rhodes, J. Moncol, M. Izakovic, M. Mazur, *Chem. Biol. Interact.*, 2006, **160**, 1–40.
- 25 M. Valko, D. Leibfritz, J. Moncol, M. T. D. Cronin, M. Mazur, J. Telser, *Int. J. Biochem. Cell Biol.*, 2007, **39**, 44–84.

- 26 D. O. Morgan, *Nature*, 1995, **374**, 131–134.
- 27 T. Hunt, K. Nasmyth, B. Novak, *Philosophical Trans. R. Soc. B*, 2011, **366**, 3494–3497.
- 28 J. M. Mitchison, *Cambridge Univ. Press*, doi:10.1113/expphysiol.1972.sp002169.
- 29 K. Collins, T. Jacks, N. P. Pavletich, in: *Proc. Natl. Acad. Sci.*, 1997, vol. 94, pp. 2776–2778.
- 30 K. J. Barnum, M. J. O'Connell, *Methods Mol. Biol.*, 2014, **1170**, 29–40.
- 31 R. T. Abraham, *Genes Dev.*, 2001, **15**, 2177–2196.
- 32 C. S. Sorensen, R. G. Syljuasen, J. Falck, T. Schroeder, L. Ronnstrand, K. K. Khanna, B. B. Zhou, J. Bartek, J. Lukas, *Cancer Cell*, 2003, **3**, 247–258.
- 33 L. Zannini, D. Delia, G. Buscemi, *J. Mol. Cell Biol.*, 2014, **6**, 442–457.
- 34 J. Bartek, J. Lukas, *Cancer Cell*, 2003, **3**, 421–429.
- 35 N. Bucher, C. D. Britten, *Br. J. Cancer*, 2008, **98**, 523–528.
- 36 T. Iyama, D. M. Wislon III, *DNA Repair*, 2013, **12**, 620–636.
- 37 A. J. Davis, D. J. Chen, *Transl. Cancer Res.*, 2013, **2**, 130–43.
- 38 X. Li, W. D. Heyer, *Cell Res.*, 2008, **18**, 99–113.
- 39 H. Sies, *Redox Biol.*, 2015, **4**, 180–183.
- 40 S. Elmore, *Toxicol. Pathol.*, 2007, **35**, 495–516.

- 41 P. Golstein, G. Kroemer, *Trends Biochem. Sci.*, 2007, **32**, 37–43.
- 42 D. Eriksson, T. Stigbrand, *Tumor Biol.*, 2010, **31**, 363–372.
- 43 L. Latella, J. Lukas, C. Simone, P. L. Puri, J. Bartek, *Mol. Cell. Biol.*, 2004, **24**, 6350–6361.
- 44 V. A. Tronov, Y. V. Vinogradova, M. Y. Loginova, V. A. Paplinskaya, M. A. Ostrovsky, *Tsitologiya*, 2012, **54**, 261–269.
- 45 J. D. Chapman, C. C. Stobbe, T. Gales, I. J. Das, D. L. Zellmer, S. Biade, Y. Matsumoto, *Radiat. Res.*, 1999, **151**, 433–41.
- 46 A. McNair, *J. Label. Compd. Radiopharm.*, 1981, **18**, 1398–1398.
- 47 M. Mi. Garau, A. L. Calduch, E. C. Lopez, *Reports Pract. Oncol. Radiother.*, 2011, **16**, 123–130.
- 48 E. J. Ainsworth, S. M. J. Afzal, D. A. Crouse, W. R. Hanson, R. J. M. Fry, *Adv. Sp. Res.*, 1989, **9**, 299–313.
- 49 D. W. van Bekkum, *Radiat Res*, 1991, **128**, S4-8.
- 50 T. Inoue, Y. Hirabayashi, H. Mitsui, H. Sasaki, E. P. Cronkite, J. E. Bullis Jr., V. P. Bond, K. Yoshida, *Exp Hematol*, 1995, **23**, 1296–1300.
- 51 A. E. Baranov, A. K. Guskova, N. M. Nadejina, VYu. Nugis, *Stem Cells*, 1995, **13 Suppl 1**, 69–77.
- 52 R. E. Goans, E. C. Holloway, M. E. Berger, R. C. Ricks, *Health Phys.*, 1997, **72**, 513–8.

- 53 J. F. Weiss, M. R. Landauer, J. B. Hogan, P. J. Gunter-Smith, K. A. Benson, R. Neta, W. R. Hanson, *Adv. Exp. Med. Biol.*, 1997, **400B**, 865–872.
- 54 T. J. MacVittie, J. F. Weiss, D. Browne, *Advances in the Treatment of Radiation Injuries.*, 1996.
- 55 J. F. Weiss, *Environ. Health Perspect.*, 1997, **105**, 1473–1478.
- 56 P. Grammaticos, E. Giannoula, G. P. Fountos, *Hell J Nucl Med*, 2013, **16**, 56–59.
- 57 W. G. Spector, D. A. Willoughby, *Bacteriol. Rev.*, 1963, **27**, 117–154.
- 58 T. Matsuse, S. Teramoto, H. Katayama, E. Sudo, H. Ekimoto, H. Mitsuhashi, Y. Uejima, Y. Fukuchi, Y. Ouchi, *Eur. Respir. J.*, 1999, **13**, 71–77.
- 59 R. Zamora, Y. Vodovotz, T. R. Billiar, *Mol. Med.*, 2000, **6**, 347–73.
- 60 K. Blirando, F. Milliat, I. Martelly, Jean-Christophe Sabourin, M. Benderitter, A. Francois, *Am. J. Pathol.*, 2011, **178**, 640–651.
- 61 C. W. Langberg, M. Hauer-Jensen, C. C. Sung, C. J. Kane, *Radiother. Oncol.*, 1994, **32**, 29–36.
- 62 D. Schaeue, E. L. Kachikwu, W. H. McBride, *Radiat Res*, 2012, **178**, 505–523.
- 63 A. Leask, D. J. Abraham, *The FASEB J.*, 2004, **18**, 816–827.
- 64 M. H. Branton, J. B. Kopp, *Microbes Infect.*, 1999, **1**, 1349–1365.
- 65 V. K. Singh, V. S. Yadav, *Exp. Mol. Pathol.*, 2005, **78**, 156–169.
- 66 J. R. Maisin, *Int. J. Radiat. Biol.*, 1998, **73**, 443–450.

- 67 J. F. Weiss, M. R. Landauer, *Toxicology*, 2003, **189**, 1–20.
- 68 T. M. Seed, *Health Phys.*, doi:10.1097/01.HP.0000175153.19745.25.
- 69 J. F. Weiss, M. R. Landauer, *Int. J. Radiat. Biol.*, 2009, **85**, 539–573.
- 70 J. F. Weiss, M. R. Landauer, *Ann. N. Y. Acad. Sci.*, 2000, **899**, 44–60.
- 71 D. Citrin, A. P. Cotrim, F. Hyodo, B. J. Baum, M. C. Krishna, J. B. Mitchell, *Oncologist*, 2010, **15**, 360–371.
- 72 F. Dumont, A. L. Roux, P. Bischoff, *Expert Opin. Ther. Pat.*, 2010, **20**, 73–101.
- 73 H. M. Patt, E. B. Tyree, R. L. Straube, D. E. Smith, *Science*, 1949, **110**, 213–214.
- 74 T. R. Sweeney, *Washington, DC U.S. Government Print. Off.*
- 75 C. N. Andreassen, C. Grau, J. C. Lindegaard, *Semin. Radiat. Oncol.*, 2003, **13**, 62–72.
- 76 D. Rades, F. Fehlaue, A. Bajrovic, B. Mahlmann, E. Richter, W. Alberti, *Radiother. Oncol.*, 2004, **70**, 261–264.
- 77 M. R. Landauer, V. Srinivasan, T. M. Seed, *J. Appl. Toxicol.*, 2003, **23**, 379–385.
- 78 N. Tacyildiz, D. Ozyoruk, G. Yavuz, E. Unal, H. Dincaslan, F. Dogu, K. Sahin, O. Kucuk, *Nutr. Cancer*, 2010, **62**, 1001–5.
- 79 P. W. Finch, J. S. Rubin, *Adv. Cancer Res.*, 2004, **91**, 69–136.
- 80 A. W. Beaven, T. C. Shea, *Drugs of today*, 2007, **43**, 461–473.
- 81 J. M. Yuhas, J. B. Storer, *Int. J. Radiat. Biol.*, 1969, **15**, 233–237.

- 82 M. L. Patchen, T. J. MacVittie, *Semin Oncol*, 1994, **21**, 26–32.
- 83 R. Neta, J. J. Oppenheim, *Blood*, 1988, **1**, 41–45.
- 84 T. J. MacVittie, A. M. Farese, F. Herodin, L. B. Grab, C. M. Baum, J. P. McKearn, *Blood*, 1996, **87**, 4129–4135.
- 85 A. M. Farese, F. Herodin, J. P. McKearn, C. Baum, E. Burton, T. J. MacVittie, *Blood*, 1996, **87**, 581–91.
- 86 S. M. Hahn, M. C. Krishna, A. M. Deluca, D. Coffin, J. B. Mitchell, *Free Radic. Biol. Med.*, 2000, **28**, 953–958.
- 87 S. N. Upadhyay, B. S. Dwarakanath, T. Ravindranath, T. L. Mathew, *Def. Sci. J.*, 2005, **55**, 403–425.
- 88 S. J. Hosseinimehr, *Drug Discov. Today*, 2007, **12**, 794–805.
- 89 J. J. Berzelius, *Afhandl. Fys. Kemi Mineral.*, 1818, **6**, 42.
- 90 J. Hogberg, J. Alexander, *Handb. Toxicol. Met.*, 2007, 783–807.
- 91 T. Madison, in: *Cong. 36<sup>th</sup> 1st Session Senate Ex. Doc*, Washington, D. C., 1860, p. 37–41.
- 92 A. L. Moxon, *South Dakota State Univ. Agric. Bull.*, 1937, **311**, 1–88.
- 93 H. G. Knight, *Sigma Xi Q.*, 1937, **25**, 1–9.
- 94 H. G. Knight, *Jour. Assoc. Off. Agr. Chem*, 1935, **18**, 103–8.
- 95 S. H. Knight, O. A. Beath, *Wyoming Agr. Exp. Sta. Bul.*, 1937, **221**, 1–64.

- 96 K. W. Franke, *J. Nutr.*, 1934, **8**, 597–608.
- 97 K. W. Franke, *J. Nutr.*, 1934, **8**, 609–612.
- 98 D. D. Magg, M. W. Glen, *Selenium Biomed. Conn. AVI, Westport*, 1967, 127–140.
- 99 C. W. Nogueira, J. B. T. Rocha, *Arch. Toxicol.*, 2011, **85**, 1313–1359.
- 100 K. Schwarz, C. M. Foltz, *J. Am. Chem. Soc.*, 1957, **15**, 255.
- 101 M. Navarro-Alarcon, M. C. Lopez-Martinez, *Sci. Total Environ.*, 2000, **249**, 347–371.
- 102 Epidemiologic Studies on the Etiologic Relationship of Selenium and Keshan Disease. *Chin. Med. J. (Engl)*. **1979**, *92*, 477–482.
- 103 G. Q. Yang, J. S. Chen, Z. M. Wen, K.Y. Ge, L. Z. Zhu, X. C. Chen, X. S. Chen, *Adv. Nutr. Res.*, 1984, **6**, 203–31.
- 104 J. E. Cone, R. M. Del Rio, J. N. Davis, T. C. Stadtman, *Proc. Natl. Acad. Sci.*, 1976, **73**, 2659–2663.
- 105 J. B. Jones, T. C. Stadman, *J. Biol. Chem.*, 1981, **256**, 656–663.
- 106 B. Akesson, T. Bellew, R. F. Burk, *Biochim. Biophys. Acta*, 1994, **1204**, 243–249.
- 107 J. R. Arthur, F. Nicol, G. J. Beckett, *Biochem. J.*, 1990, **272**, 537–540.
- 108 J. C. Davey, K. B. Becker, M. J. Schneider, D. L. St. Germain, V. A. Galton, *J Biol Chem*, 1995, **270**, 26786–26789.

- 109 T. Tamura, T. C. Stadtman, *Proc. Natl. Acad. Sci.*, 1996, **93**, 1006–1011.
- 110 J. T. Rotruck, A. L. Pope, H. E. Ganther, A. B. Swanson, D. G. Hafeman, W. G. Hoekstra, *Science*, 1973, **179**, 588–590.
- 111 P. D. Whanger, *Br. J. Nutr.*, 2004, **91**, 11–28.
- 112 P. D. Whanger, *J. Am. Coll. Nutr.*, 2002, **21**, 223–232.
- 113 H. Tapiero, D. M. Townsend, K. D. Tew, *Biomed. Pharmacother.*, 2003, **57**, 134–144.
- 114 A. A. Turanov, Xue-Ming Xu, B. A. Carlson, Min-Hyuk Yoo, V. N. Gladyshev, D. L. Hatfield, *Adv. Nutr.*, 2011, **2**, 122–128.
- 115 I. Chambers, J. Frampton, P. Goldfarb, N. Affara, W. McBain, P. R. Harrison, *EMBO J.*, 1986, **5**, 1221–7.
- 116 L. V. Papp, Lu J, A. Holmgren, K. K. Khanna, *Antioxid. Redox Signal.*, 2007, **9**, 775–806.
- 117 J. F. Weiss, V. Srinivasan, K. S. Kumar, M. R. Landauer, *Adv. Sp. Res.*, 1992, **12**, 223–231.
- 118 T. C. Stadtman, *Annu. Rev. Biochem.*, 1996, **65**, 83–100.
- 119 A. V. Lobanov, D. E. Fomenko, Y. Zhang, A. Sengupta, D. L. Hatfield, V. N. Gladyshev, *Genome Biol.*, 2007, **8**, R198.
- 120 A. Holmgren, J. Lu, *Free Radic. Biol. Med.*, 2014, **66**, 75–87.
- 121 A. Holmgren, J. Lu, *Biochem. Biophys. Res. Commun.*, 2010, **396**, 120–124.

- 122 J. Kohrle, *Rev. Endocr. Metab. Disord.*, 2000, **1**, 49–58.
- 123 V. Mostert, *Arch. Biochem. Biophys.*, 2000, **376**, 433–438.
- 124 R. F. Burk, K. E. Hill, *Biochim. Biophys. Acta*, 2009, **1790**, 1441–1447.
- 125 R. Brigelius-Flohé, *Free Radic. Biol. Med.*, 1999, **27**, 951–965.
- 126 L. Flohe, W. A. Günzler, H. H. Schock, *FEBS Lett.*, 1973, **32**, 132–134.
- 127 M. S. Baliga, V. Diwadkar-Navsariwala, T. Koh, R. Fayad, G. Fantuzzi, A. M. Diamond, *Mol. Nutr. Food Res.*, 2008, **52**, 1300–1304.
- 128 A. P. Kipp, M. F. Müller, E. M. Goken, S. Deubel, R. Brigelius-Flohe, *Biochim. Biophys. Acta - Gen. Subj.*, 2012, **1820**, 1588–1596.
- 129 R. S. Esworthy, Y. Lixin, P. H. Frankel, F.-F. Chu, *J. Nutr.*, 2005, **135**, 740–745.
- 130 R. Brigelius-Flohe, K-D. Aumann, H. Blocker, G. Gross, M. Kiess, K-D. Kloppel, M. Maiorino, A. Roveri, R. Schuckelt, F. Ursini, E. Wingender, L. Flohe, *J. Biol. Chem.*, 1994, **269**, 7342–8.
- 131 G. Mugesh, W-W. du Mont, *Chemistry*, 2001, **7**, 1365–1370.
- 132 F. Sieber, S. A. Muir, E. P. Cohen, P. E. North, B. L. Fish, A. A. Irving, M. Mäder, J. E. Moulder, *Radiat Res*, 2009, **171**, 368–373.
- 133 A. Pakdaman, *Biol. Trace Elem. Res.*, 1998, **62**, 1–6.
- 134 I. M. Puspitasari, R. Abdulah, C. Yamazaki, S. Kameo, T. Nakano, H. Koyama, *Radiat. Oncol.*, 2014, **9**, 125.

- 135 Z Jahangard-Rafsanjani, K. Gholami, M. Hadjibabaie, A. R. Shamshiri, K. Alimoghadam, A. Sarayani, M. Mojtahedzadeh, M. Ostadali-Dehaghi, A. Ghavamzadeh, *Bone Marrow Transplant.*, 2013, **48**, 832–836.
- 136 O. Micke, F. Bruns, R. Mücke, U. Schäfer, M. Glatzel, A. F. DeVries, K. Schönekaes, K. Kisters, J. Buntzel, *Int. J. Radiat. Oncol. Biol. Phys.*, 2003, **56**, 40–49.
- 137 F. Shimazu, A. L. Tappel, *Science*, 1964, **143**, 369–71.
- 138 F. Shimazu, A. L. Tappel, *Radiat. Res.*, 1964, **23**, 210–217.
- 139 J. F. Weiss, R. L. Hoover, K. S. Kumar, *Free Radic. Res. Commun.*, 1987, **3**, 33–38.
- 140 V. A. Knizhnikov, N. K. Shandala, M. Cand, V. A. Komleva, B. Cand, V. A. Knyazhev, M. Card, V. A. Tutelyan, *Nutr. Res.*, 1996, **16**, 505.
- 141 M. Mix, N. Ramnath, J. Gomez, C.de Groot, S. Rajan, W. Tan, Y. Rustum, M. B. Jameson, A. K. Singh, *World J. Clin. Oncol.*, 2015, **6**, 156.
- 142 C. Shih-Hsi, H. G. Mautner, *J. Org. Chem.*, 1962, **27**, 2899–2901.
- 143 W. H. H. Gunther, H. G. Mautner, *J. Am. Chem. Soc.*, 2001, **82**, 2762–2765.
- 144 D. L. Klayman, *J. Org. Chem.*, 1965, **30**, 2454-.
- 145 A. Breccia, R. Badiello, A. Trenta, M. Matti, *Radiat Res*, 1969, **38**, 483–492.
- 146 H. Sies, *Free Radic. Biol. Med.*, 1993, **14**, 313–323.
- 147 J. K. Tak, J. W. Park, *Free Radic. Biol. Med.*, 2009, **46**, 1177–1185.

- 148 A. Kunwar, B. Mishra, A. Barik, L. B. Kumbhare, R. Pandey, V. K. Jain, K. I. Priyadarsini, *Chem. Res. Toxicol.*, 2007, **20**, 1482–1487.
- 149 A. Kunwar, P. Bansal, S. Jayakumar, P. P. Bag, P. Paul, N. D. Reddy, L. B. Kumbhare, V. K. Jain, R. C. Chaubey, M. K. Unnikrishnan, K. I. Priyadarsini, *Free Radic. Biol. Med.*, 2010, **48**, 399–410.
- 150 A. Kunwar, P. P. Bag, S. Chattopadhyay, V. K. Jain, K. I. Priyadarsini, *Arch. Toxicol.*, 2011, **85**, 1395–1405.
- 151 R. K. Chaurasia, S. Balakrishnan, A. Kunwar, U. Yadav, N. Bhat, K. Anjaria, R. Nairy, B. K. Sapra, V. K. Jain, K. I. Priyadarsini, *Mutat. Res. - Genet. Toxicol. Environ. Mutagen.*, 2014, **774**, 8–16.
- 152 A. Kunwar, V. K. Jain, K. I. Priyadarsini, C. K. Haston, *Am. J. Respir. Cell Mol. Biol.*, 2013, **49**, 654–661.
- 153 V. Gota, J. S. Goda, K. Doshi, A. Patil, S. Sunderajan, K. Kumar, M. Varne, A. Kunwar, V. K. Jain, K. I. Priyadarsini, *Eur. J. Drug Metab. Pharmacokinet.*, 2015, **41**, 839–844.
- 154 M. S. Baliga, H. Wang, P. Zhuo, J. L. Schwartz, A. M. Diamond, *Biol. Trace Elem. Res.*, 2007, **115**, 227–241.
- 155 J. C. Eckers, A. L. Kalen, W. Xiao, E. H. Sarsour, P. C. Goswami, *Int. J. Radiat. Oncol. Biol. Phys.*, 2013, **87**, 619–625.
- 156 Y. R. Seo, C. Sweeney, *Oncogene*, 2002, **21**, 3663–3669.
- 157 J. Brozmanová, D. Mániková, V. Vlčková, M. Chovanec, *Arch. Toxicol.*, 2010,

**84**, 919-938.

- 158 S. Bera, V. De Rosa, W. Rachidi, A. M. Diamond, *Mutagenesis*, 2013, **28**, 127–134.
- 159 M. Iwaoka, T. Takahashi, S. Tomoda, *Heteroat. Chem.*, 2001, **12**, 293–299.
- 160 F. Kumakura, B. Mishra, K. I. Priyadarsini, M. Iwaoka, *European J. Org. Chem.*, 2010, 440–445.
- 161 M. Iwaoka, A. Katakura, J. Mishima, Y. Ishihara, A. Kunwar, K. I. Priyadarsini, *Molecules*, 2015, **20**, 12364–12375.
- 162 M. Iwaoka, N. Sano, Y-Y. Lin, A. Katakura, M. Noguchi, K. Takahashi, F. Kumakura, K. Arai, B. G. Singh BG, A. Kunwar, K. I. Priyadarsini, *ChemBioChem*, 2015, **16**, 1226–1234.
- 163 S. Chakraborty, S. K. Yadav, M. Subramanian, K. I. Priyadarsini, M. Iwaoka, S. Chattopadhyaya, *Free Radic. Res.*, 2012, **46**, 1378–1386.
- 164 S. Chakraborty, S. K. Yadav, M. Subramanian, M. Iwaoka, K. I. Priyadarsini, *Biochim. Biophys. Acta - Gen. Subj.*, 2014, **1840**, 3385–3392.
- 165 P. V. Kumar, B. G. Singh, A. Kunwar, M. Iwaoka, K. I. Priyadarsini, *Bull. Chem. Soc. Jpn.*, 2016, **89**, 490–497.
- 166 P. V. Kumar, B. G. Singh, N. Maiti, M. Iwaoka, K. Indira Priyadarsini, *J. Colloid Interface Sci.*, 2014, **436**, 179–185.
- 167 K. Arai, K. Moriai, A. Ogawa, M. Iwaoka, *Chem. - An Asian J.*, 2014, **9**, 3464–

3471.

- 168 T. Grande, J. A. Bueren, *Int. J. Radiat. Oncol. Biol. Phys.*, doi:10.1016/j.ijrobp.2005.09.036.
- 169 J. E. Till, E. A. McCulloch, *Radiat Res*, 1961, **14**, 213–222.
- 170 T. Mosmann, *J. Immunol. Methods*, 1983, **65**, 55–63.
- 171 Na P. Franken, H. M. Rodermond, J. Stap, J. Haveman, C. van Bree, *Nat. Protoc.*, 2006, **1**, 2315–9.
- 172 M. C. Yeung, *Biotechniques*, 2002, **33**, 734–736.
- 173 N. M. Khan, S. K. Sandur, R. Checker, D. Sharma, T. B. Poduval, K. B. Sainis, *Free Radic. Biol. Med.*, 2011, **51**, 115–128.
- 174 C. Riccardi, I. Nicoletti, *Nat Protoc.*, 2006, **1**, 1458-61.
- 175 A. Cossarizza, M. Baccarani-Contrì, G. Kalashnikova, C. Franceschi, *Biochem. Biophys. Res. Commun.*, 1993, **197**, 40–5.
- 176 F. K-M. Chan, K. Moriwaki, M. J. De Rosa, *Methods Mol Bio*, 2013, **979**, 65–70.
- 177 M. Shinitzky, Y. Barenholz, *BBA - Rev. Biomembr.*, 1978, **515**, 367-394.
- 178 L. A. Royce, P. Liu, M. J. Stebbins, B. C. Hanson, L. R. Jarboe, *Appl. Microb. Cell Physiol.*, 2013, **97**, 8317–8327.
- 179 B. Mely-Goubert, M. H. Freedman, *BBA - Biomembr.*, doi:10.1016/0005-2736(80)90536-2.

- 180 J. Plasek, P. Jarolim, *Gen Physiol Biophys*, 1987, **6**, 425–37.
- 181 M. M. Bradford, *Anal. Biochem.*, 1976, **72**, 248–254.
- 182 R. Cathcart, E. Schwiers, B. N. Ames, *Anal. Biochem.*, 1983, **134**, 111–116.
- 183 P. J. Hissin, R. Hilf, *Anal Biochem.*, 1976, **74**, 214–226.
- 184 N. Sreejayan, M. N. A. Rao, K. I. Priyadarsini, T. P. A. Devasagayam, *Int. J. Pharm. 151*, 1997, **151**, 127–130.
- 185 C. N. Oliver, B. W. Ahn, E. J. Moerman, S. Goldstein, E. R. Stadtman, *J. Biol. Chem.*, 1987, **262**, 5488–5491.
- 186 N.P. Singh, M. McCoy, R. R. Tice, E. Schneider, *Exp. Cell Res.*, 1988, **175**, 184–191.
- 187 M. Fenech, *Mutat. Res.*, 2000, **455**, 81–95.
- 188 M. Fenech, *Methods Mol. Biol.*, 2007, **2**, 1084–104.
- 189 C. E. Redon, A. J. Nakamura, O. Sordet, J. S. Dickey, K. Gouliaeva, B. Tabb, S. Lawrence, R. J. Kinders, W. M. Bonner, O. A. Sedelnikova, *Methods Mol. Biol.*, 2011, **682**, 249–270.
- 190 V. Vandersickel, J. Depuydt, B. Van Bockstaele, G. Perletti, J. Philippe, H. Thierens, A. Vral, *J. Radiat. Res.*, 2010, **51**, 633–641.
- 191 K. J. Livak, T. D. Schmittgen, *Methods*, 2001, **25**, 402–408.
- 192 P. V. Kumar, B. G. Singh, P. P. Phadnis, V. K. Jain, K. I. Priyadarsini, *Chem. - A Eur. J.*, 2016, **22**, 12189–12198.

- 193 I. V. Mavragani, D. A. Laskaratou, B. Frey, S. M. Candéias, U. S. Gaipl, K. Lumniczky, A. G. Georgakilas, *Toxicol. Res.*, doi:10.1039/C5TX00222B.
- 194 A. L. Carsten, in *Response of Different Species to Total Body Irradiation*, 1984, vol. 10, pp. 59–86.
- 195 K. E. Hume, S.P. Eftarh, R. Carr, E. A. McCullough, in *Radiation and the Gastrointestinal Tract*, 1995, pp. 113–128.
- 196 J. W. Denham, M. Hauer-Jensen, *Radiother. Oncol.*, 2002, **63**, 129–145.
- 197 L. B. Marks, X. Yu, Z. Vujaskovic, W. Small, R. Folz, M. S. Anscher, *Semin. Radiat. Oncol.*, 2003, **13**, 333–345.
- 198 G. C Jagetia, *J. Clin. Biochem. Nutr.*, 2007, **40**, 74–81.
- 199 N. Dainiak, *Exp. Hematol.*, 2002, **30**, 513–528.
- 200 J. P. Williams, S. L. Brown, G. E. Georges, M. Hauer-jensen, R. P. Hill, A. K. Huser, D. G. Kirsch, T. J. Macvittie, K. A. Mason, M. M. Medhora, J. E. Moulder, P. Okunieff, M. F. Otterson, E. Michael, J. B. Smathers, W. H. McBride, *Radiat Res*, 2010, **173**, 557–578.
- 201 S. Suryavanshi, D. Sharma, R. Checker, M. Thoh, V. Gota, S. K. Sandur, K. B. Sainis, *Free Radic. Biol. Med.*, , doi:10.1016/j.freeradbiomed.2015.04.007.
- 202 K. I. Leonova, J. Shneyder, M. P. Antoch, I. A. Toshkov, L. R. Novototskaya, P. G. Komarov, E. A. Komarova, A. V. Gudkov, *Cell Cycle*, 2010, **9**, 1434–1443.
- 203 H. Li, Y. Wang, S. K. Pazhanisamy, L. Shao, I. Batinic-Haberle, A. Meng, D.

- Zhou, *Free Radic. Biol. Med.*, 2011, **51**, 30–37.
- 204 Y. Wang, B. A. Schulte, A. C. Larue, M. Ogawa, D. Zhou, 2006, **107**, 358–366.
- 205 R. J. Hauke, S. R. Taarntolo, *Lab. Med.*, 2000, **31**, 613–615.
- 206 P. Kaur, C. S. Potten, *Cell Prolif.*, 1986, **19**, 601–610.
- 207 H. Cheng, C. P. Leblond, *Am. J. Anat.*, 1974, **141**, 537–561.
- 208 S. P. Bach, A. G. Renehan, C. S. Potten, *Carcinogenesis*, 2000, **21**, 469–476.
- 209 A. Polistena, L. B. Johnson, S. Ohiami-Masseron, L. Wittgren, S. Back, C. Thornberg, V. Gadaleanu, D. Adawi, B. Jeppsson, *BMC Surg*, 2008, **8**, 1.
- 210 M. Molla, M. Gironella, R. Miquel, V. Tovar, P. Engel, A. Biete, J. M. Pique, J. Panes, *Int. J. Radiat. Oncol. Biol. Phys.*, 2003, **57**, 264–273.
- 211 M. A. Brach, H. J. Grub, T. Kaishoy, Y. Asanog, T. Hiranon, F. Herrmann, *J. of Chem.*, 1993, **268**, 8466-8472.
- 212 S. L. Freeman, W. K. MacNaughton, *Am. J. Physiol. Gastrointest. Liver Physiol.*, 2000, **278**, G243–G250.
- 213 A. M. Diamond, J. L. Murray, P. Dale, R. Tritz, D. J. Grdina, *Radiation Oncology Investigations*, 1995, **3**, 383-386
- 214 J. F. Weiss, V. Srinivasan, K. S. Kumar, M. L. Patchen, M. R. Landauer, *Biol. Trace Elem. Res.*, 1992, **33**, 164–165.
- 215 D. Bhowmick, S. Srivastava, P. D’Silva, G. Muges, *Angew. Chemie - Int. Ed.*, 2015, **54**, 8449–8453.

- 216 A. M. Dittrich, H. A. Meyer, M. Krokowski, D. Quarcoo, B. Ahrens, S. M. Kube, M. Witzenrath, R. S. Esworthy, F. F. Chu, E. Hamelmann, *Eur. Respir. J.*, 2010, **35**, 1148–1154.
- 217 R. Brigelius-Flohe, M. Maiorino, *Cell. Funct. glutathione*, 2013, **1830**, 3289–3303.
- 218 P. Geraghty, A. A. Hardigan, A. M. Wallace, O. Mirochnitchenko, J. Thankachen, L. Arellanos, V. Thompson, J. M. D’Armiento, R. F. Foronjy, *Am. J. Respir. Cell Mol. Biol.*, 2013, **49**, 721–730.
- 219 C. Duong, H. J. Seow, S. Bozinovski, P. J. Crack, G. P. Anderson, R. Vlahos, *Am. J. Physiol. Cell. Mol. Physiol.*, 2010, **299**, L425–L433.
- 220 S. A. Mattmiller, B. A. Carlson, L. M. Sordillo, *J. Nutr. Sci.*, 2013, **2**, e28.
- 221 J. Sun, Y. Chen, M. Li, Z. Ge, *Free Radic Biol Med*, 1998, **24**, 586–593.
- 222 D. B. Mansur, Y. Kataoka, D. J. Grdina, A. M. Diamond, *Radiat. Res.*, 2001, **155**, 536–542.
- 223 R. F. Burk, K. E. Hill, A. K. Motley, *J. Nutr.*, 2003, **133**, 1517S–20S.
- 224 E. N. Bermingham, J. E. Hesketh, B. R. Sinclair, J. P. Koolaard, N. C. Roy, *Nutrients*, , doi:10.3390/nu6104002.
- 225 D. M. Lambert, *Eur. J. Pharm. Sci.*, 2000, **S2**, S15-27.
- 226 J. N. Jacob, V. E. Shashoua, A. Campbell, R. J. Baldessarini, *J. Med. Chem.*, 1985, **28**, 106-110.

- 227 M. Laguerre, C. Bayrasy, J. Lecomte, B. Chabi, E. A. Decker, C. Wrutniak-Cabello, G. Cabello, P. Villeneuve, *Biochimie*, 2013, **95**, 20-6.
- 228 M. Geurts, J. H. Poupaert, G. K. E. Scriba, D. M. Lambert, *J. Med. Chem.*, 1998, **41**, 24–30.
- 229 B. S. Cummings, L. P. Wills and R. G. Schnellmann, *Curr Protoc Phamacol*, 2004, **1**, 1–30.
- 230 T. H. Lugokenski, L. G. Müller, P. S. Taube, J. B. Rocha, M. E. Pereira, *Drug Chem. Toxicol.*, 2011, **34**, 66–76.
- 231 G. Majno, I. Joris, *Am. J. Pathol.*, 1995, **146**, 3–15.
- 232 C. Sanmartín, D. Plano, A. K. Sharma, J. A. Palop, *Int. J. Mol. Sci.*, 2012, **13**, 9649–9672.
- 233 M. A. Carfagna, B. B. Muhoberac, *Mol. Pharmacol.*, 1993, **44**, 129–141.
- 234 S. C. Mckarns, C. Hansch, W. S. Caldwell, W. T. Morgan, S. K. Moore, D. J. Doolittle, *Fundam. Appl. Toxicol. J. Fundam. Appl. Toxicol.*, 1997, **36**, 62–70.
- 235 H. R. Mellor, J. Nolan, L. Pickering, M. R. Wormald, F. M. Platt, R. A. Dwek, G. W. J. Fleet, T. D. Butters, *Biochem. J.*, 2002, **366**, 225–233.
- 236 S. Matsunaga, M. Jimbo, M. B. Gill, L. L. Lash-van Wyhe, M. Murata, K. Nonomura, G. T. Swanson, R. Sakai, *ChemBioChem*, doi:10.1002/cbic.201100329.
- 237 M. A. Gauthier, P. Simard, Z. Zhang, X. X. Zhu, *J. R. Soc. Interface*, 2007, **4**,

1145–1150.

- 238 A. Teixeira, R. C. Cox, M. R. Egmond, *Food Funct.*, 2013, **4**, 1209–15.
- 239 I. Lengler, T. Buhrke, E. Scharmach, A. Lampen, *Lipids*, 2012, **47**, 1085–1097.
- 240 M. Dymond, G. Attard, A. D. Postle, *J. R. Soc., Interface*, 2008, **5**, 1371–1386.
- 241 A. S. Inacio, K. A. Mesquita, M. Baptista, J. Ramalho-Santos, W. L. C. Vaz, O. V. Vieira, *PLoS One*, , doi:10.1371/journal.pone.0019850.
- 242 S. Schreier, V. P. Malheiros, E. De Paula, *Biochim. Biophys. Acta*, 2000, **1508**, 210–234.
- 243 B. Bechinger, K. Lohner, *Biochim. Biophys. Acta - Biomembr.*, 2006.
- 244 D. A. Brown, E. London, *J. Biol. Chem.*, 2000, **275**, 17221–17224.
- 245 T. M. De Lima, M. Fernanda. C. Boaventura, G. Giannocco, M. T. Nunes, R. Curi, *Clin. Sci.*, 2006, **111**, 307–317.
- 246 W.-X. Zong, C. B. Thompson, *Genes Dev.*, 2006, **20**, 1–15.
- 247 H. R. Mellor, F. M. Platt, R. A. Dwek, T. D. Butters, *Biochem. J.*, 2003, **374**, 307–14.
- 248 H. R. Mellor, D. C. A. Neville, D.J. Harvey, F. M. Platt, R. A. Dwek, T. D. Butters, *Biochem. J.*, 2004, **381**, 861–866.
- 249 H. V. Westerhoff, D. Juretic, R. W. Hendler, M. Zasloff, *Proc. Natl. Acad. Sci. U. S. A.*, 1989, **86**, 6597–6601.

- 250 E. J. Ambrose, D. M. Easty, P. C. T. Jones, *Br J Cancer*, 1958, **12**, 439–447.
- 251 C. E. Carpenter, J. R. Broadbent, *J Food Sci*, 2009, **74**, R12-15.
- 252 H. Kikuzaki, M. Hisamoto, K. Hirose, K. Akiyama, H. Taniguchi, *J. Agric. Food Chem.*, 2002, **50**, 2161–2168.
- 253 P. Balgavf, F. Devinsky, *Adv. Colloid Interface Sci.*, 1996, **66**, 23–63.
- 254 A. Jerome-Morais, S. Bera, W. Rachidi, P. H. Gann, A. M. Diamond, *Biochim. Biophys. Acta - Gen. Subj.*, 2013, **1830**, 3399–3406.
- 255 M. A. Nasr, M. J. Fedele, K. Esser, A. M. Diamond, *Free Radic. Biol. Med.*, 2004, **37**, 187–195.
- 256 S. Dunning, A. Rehman, M. H. Tiebosch, R. A. Hannivoort, F. W. Haijer, J. Woudenberg, F. A. J. van den Heuvel, M. Buist-Homan, K. N. Faber, H. Moshage, *Biochim. Biophys. Acta - Mol. Basis Dis.*, 2013, **1832**, 2027–2034.
- 257 E. C. Busby, D. F. Leistritz, R. T. Abraham, L. M. Karnitz, J. N. Sarkaria, *Cancer Res.*, 2000, **60**, 2108–2112.
- 258 J. Chaudiere, E. C. Wilhelmsen, A. L. Tappel, *J. Biol. Chem.*, 1984, **259**, 1043–1050.
- 259 O. A. Trowell, *J. Pathol. Bacteriol.*, 1952, **64**, 687–704.
- 260 A. K. Sharma, S. Bhattacharya, S. A. Khan, B. Khade, S. Gupta, *Mutat. Res.*, 2015, **773**, 83–91.
- 261 T. Hu, C. M. Miller, G. M. Ridder, M. J. Aardema, *Mutat. Res.*, 1999, **426**, 51–

62.

- 262 R. A. Sunde, in: *Selenium its Molecular Biology and Role in Human Health*, ed. D.L. Hatfield, M.J. Berry and V.N. Gladyshev, Springer, New York, 2006.
- 263 R. F. Burk, P. F. Surai, *Selenium in nutrition and health*, Nottingham University Press, Nottingham, 2006.
- 264 E. Lubos, J. Loscalzo, D. E. Handy, *Antioxid. Redox Signal.*, 2011, **15**, 1957–1997.
- 265 V. Tamasi, J. M. Jeffries, G. E. Arteel, K. C. Falkner, *Arch. Biochem. Biophys.*, 2004, **431**, 161–168.
- 266 M. Tan, S. Li, M. Swaroop, K. Guan, L.W. Oberley, Y. Sun, *J. Biol. Chem.*, 1999, **274**, 12061–12066.
- 267 A. Banning, S. Deubel, D. Kluth, Z. Zhou, R. Brigelius-Flohe, *Mol. Cell. Biol.*, 2005, **25**, 4914–4923.
- 268 G. Iliakis, Y. Wang, J. Guan, H. Wang, *Oncogene*, 2003, **22**, 5834–5847.
- 269 C. S. Sorensen, L. T. Hansen, J. Dziegielewski, R. G. Syljuasen, C. Lundin, J. Bartek, T. Helleday, *Nat. Cell Biol.*, 2005, **7**, 195–201.
- 270 T. N. T. Nguyen, R. S. Z. Saleem, M. J. Luderer, S. Hovde, R. W. Henry, J. J. Tepe, *ACS Chem. Biol.*, 2012, **7**, 172–184.
- 271 L. R. Ferguson, N. Karunasinghe, S. Zhu, A. H. Wang, *Mutat. Res. - Fundam. Mol. Mech. Mutagen.*, 2012, **733**, 100–110.

- 272 S. L. Marklund, N. G. Westman, G. Roos, J. Carlsson, *Radiat. Res.*, 1984, **100**, 115–123.
- 273 B. E. Sandstrom, J. Carlsson, S. L. Marklundf, 1989, **325**, 318–325.
- 274 B. G. Singh, E. Thomas, F. Kumakura, K. Dedachi, M. Iwaoka and K. I. Priyadarsini, *J. Phys. Chem. A*, 2010, **114**, 8271–8277.



# Mechanism of radioprotection by dihydroxy-1-selenolane (DHS): Effect of fatty acid conjugation and role of glutathione peroxidase (GPx)



Prachi Verma<sup>a, b</sup>, Amit Kunwar<sup>a, b, \*</sup>, Kenta Arai<sup>c</sup>, Michio Iwaoka<sup>c</sup>, K. Indira Priyadarsini<sup>b, d</sup>

<sup>a</sup> Radiation and Photochemistry Division, Bhabha Atomic Research Centre, Mumbai, 400085, India

<sup>b</sup> Homi Bhabha National Institute, Anushaktinagar, Mumbai, 400094, India

<sup>c</sup> Department of Chemistry, School of Science, Tokai University, Kanagawa 259-1292, Japan

<sup>d</sup> Chemistry Division, Bhabha Atomic Research Centre, Mumbai, 400085, India

## ARTICLE INFO

### Article history:

Received 23 June 2017

Accepted 25 October 2017

Available online 31 October 2017

### Keywords:

Organoselenium  
Radioprotection  
Glutathione peroxidase  
DNA repair  
Cell cycle arrest

## ABSTRACT

Dihydroxy-1-selenolane (DHS) previously reported to exhibit radioprotective activity was investigated to understand its mechanism of action in CHO cells of epithelial origin. DHS pre-treatment at 25  $\mu$ M for 16 h significantly protected CHO cells from radiation (4–11 Gy)-induced delayed mitotic cell death. Further to examine, how increased cellular uptake can influence this mechanism, studies have been performed with DHS-C<sub>6</sub>, a lipophilic conjugate of DHS. Accordingly CHO cells pre-treated with DHS-C<sub>6</sub>, showed increased survival against radiation exposure. Notably treatment with both DHS and DHS-C<sub>6</sub> significantly increased glutathione peroxidase (GPx) activity in cells by ~ 2.5 fold. Additionally, the compound DHS or DHS-C<sub>6</sub> led to faster repair of DNA in irradiated cells and subsequently inhibited the G2/M arrest. Anticipating the role of GPx in radioprotection, our investigations revealed that addition of mercaptosuccinic acid, a pharmacological inhibitor of GPx reversed all the above effects of DHS or DHS-C<sub>6</sub>. Further inhibitors of check point kinase 1 (CHK1) and DNA-protein kinase (DNA-PK) although abrogated the radioprotective effect of DHS or DHS-C<sub>6</sub> separately, did not show additive effect in combination with GPx inhibitor, suggesting their cross talk. In contrast to these results, both DHS and DHS-C<sub>6</sub> treatment did not protect spleen lymphocytes from the radiation-induced apoptosis. Thus results confirmed that both DHS and DHS-C<sub>6</sub> protected cells from radiation-induced mitotic death by augmenting DNA repair in a GPx dependant manner.

© 2017 Elsevier B.V. and Société Française de Biochimie et Biologie Moléculaire (SFBBM). All rights reserved.

## 1. Introduction

Radiation exposure depending on its type, energy and absorbed dose can induce serious health hazards ranging from mutation, radiation syndromes and cancer to even death [1–3]. The primary event during the interaction of radiation with a cell is radiolysis of cellular water leading to generation of reactive oxygen species (ROS) followed by damage to bio-molecules (such as DNA, protein and lipid) and cell death [4–6]. In spite of the extensive research, there is no ideal radioprotector available till today to protect normal

cells from such radiation toxicities [7,8]. This has led to the continued interest in developing radioprotectors from natural as well as synthetic origins [8].

Selenium is a micronutrient and the constituent of redox regulatory selenoproteins such as glutathione peroxidase (GPx), thio-redoxin reductase (TrxR) and selenoprotein P (SeP) among others, which play a very important role in maintaining cellular redox homeostasis [9–11]. Synthetic selenium compounds in different chemical forms have been explored for various pharmacological actions like antioxidant, immune-modulatory, chemo-preventive, anti-inflammatory and radioprotective activities [12–18]. For example, ebselen, an organoselenium and a GPx mimic, has been tested in clinic to prevent neurological and inflammatory disorders [19]. Another organoselenium compound 3, 3'-diselenodipropionic

\* Corresponding author. Radiation and Photochemistry Division, Bhabha Atomic Research Centre, Mumbai, 400085, India.

E-mail address: [kamit@barc.gov.in](mailto:kamit@barc.gov.in) (A. Kunwar).

acid (DSePA) is reported for potential radioprotective activity in cells and *in vivo* model system [17,18]. On similar lines, dihydroxy-1-selenolane (DHS) a water soluble cyclic monoselenide has been recently studied for different biological activities. It shows GPx like activity, inhibits lipid peroxidation and catalyses oxidative folding of denatured proteins in cell free systems [20–25]. Further DHS was also found to be nontoxic and induced GPx level in cells [26]. It is reported to accelerate the healing of indomethacin-induced stomach ulceration in mice by modulating arginine metabolism and anti-inflammatory pathways [27,28]. Encouraged by these results, DHS has been evaluated for radioprotection in mice model system. These studies revealed that intraperitoneal (i.p.) injection of DHS at a dosage of 2 mg/kg body weight for five consecutive days prior whole body irradiation (WBI) of 8 Gy and subsequently continued at the same dosage for three times per week during the post-irradiation period, improved the 30 day survival by 40% [29]. In irradiated mice, DHS treatment prevented oxidative damage (such as lipid peroxidation and DNA damage) and inflammatory response in radiosensitive organs like hematopoietic and gastrointestinal system. The radioprotective effect of DHS in mice was found to be associated with tissue specific induction in GPx level [29]. Subsequent studies using *in vitro* models reported that DHS-C<sub>6</sub>, a fatty acid conjugate of DHS showed higher cellular uptake (~by 2 folds) as well as increased antioxidant activity [23,24,26]. For example DHS-C<sub>6</sub> was better than DHS in preventing the AAPH-induced lipid peroxidation in liposome and CHO cells [23,24,26]. Based on all these reports, the present study was aimed to evaluate the detailed radioprotective effect of DHS-C<sub>6</sub> and DHS employing cellular models. Further we also examined the mechanism of action of these compounds by monitoring GPx level, DNA repair kinetics and cell cycle analysis. The chemical structures of the compounds studied are presented in Scheme 1.

## 2. Materials and methods

### 2.1. Chemicals

DL-trans-3,4-dihydroxy-1-selenolane (DHS) and its fatty acid derivative (DHS-C<sub>6</sub>) were synthesized, purified and characterized as reported previously [20,23]. Dimethyl sulfoxide (DMSO), glutathione (GSH), β-nicotinamide adenine dinucleotide 2'-phosphate reduced tetra sodium salt hydrate (NADPH), glutathione reductase, cumene hydroperoxide, cytochalasin B, diethyl pyrocarbonate (DEPC), 2',7'-dichlorofluorescein diacetate (DCFDA), cellytic<sup>®</sup> reagent, paraformaldehyde, o-phthalaldehyde (OPT), N-ethylmaleimide (NEM), meta-phosphoric acid, mercaptosuccinic acid, tri reagent, 2-(morpholin-4-yl)-benzo[h]chomen-4-one (NU7026), high and low melting point agarose, SYBR Green-II dye, protease inhibitor cocktail, and amplification grade DNase from Sigma Chemical Company (St. Louis, MO, USA) were purchased from local agents. The cDNA synthesis kit and ProLong<sup>®</sup> Gold antifade mountant with DAPI from Thermo Scientific (USA), 2X SYBR green polymerase chain reactions (PCR) mix from Roche Chemical Co

(Indianapolis, USA) and 5,5',6,6'-tetrachloro-1,1',3,3'-tetraethylbenzimidazolo-carbocyanineiodide (JC-1) from Molecular Probes (USA) were procured through local agents. Roswell Park Memorial Institute Medium-1640 (RPMI-1640), fetal bovine serum (FBS), penicillin and streptomycin were purchased from Himedia, India. Anti phospho-histone H2AX (ser-139) human monoclonal IgG were purchased from Upstate, USA. Alexa fluor 488 rabbit antihuman IgG, propidium iodide (PI) and trypsin-EDTA from Invitrogen (USA) were purchased through local agents. The inhibitors like 7-hydroxy staurosporine (UCN-01), 7-nitro-1H-indole-2-carboxylic acid {4-[1-(guanidinohydrazono)-ethyl]-phenyl}-amide (PV 1091) were purchased from Calbiochem (Switzerland). The Bradford protein assay kit was purchased from Bangalore Genei, India. The gene specific primers for RT-PCR were custom synthesized from local agents. All other chemicals with maximum available purity were purchased from reputed local manufacturers/suppliers.

### 2.2. Cell culture, drug treatment and irradiation

Chinese Hamster Ovary epithelial (CHO) cells were obtained from National Centre for Cell Sciences (NCCS), Pune, India. Splenic lymphocytes were freshly isolated from BALB/C mice under aseptic condition according to the method described earlier [30]. Cells were cultured in RPMI-1640 medium supplemented with 10% FBS, 100 Units/ml penicillin and 100 µg/ml streptomycin in a humidified atmosphere with 5% CO<sub>2</sub> at 37 °C. The stock solution of DHS was prepared in RPMI-1640 medium while that of DHS-C<sub>6</sub> was prepared in DMSO. The concentration of DMSO was fixed at 0.25% which is within the acceptable limit of toxicity. For radioprotection studies, cells were incubated with DHS or DHS-C<sub>6</sub> for 16 h as per previous reports [26], washed with phosphate buffered saline (1X PBS, pH 7.4), supplemented with serum free medium and irradiated using <sup>60</sup>Co Blood Irradiator 2000 (BRIT, India) at a dose rate of 1 Gy/min. Following this, 10% serum was added to the culture medium and cells were incubated in humidified atmosphere with 5% CO<sub>2</sub> at 37 °C for desired time points prior to any assay. In order to block the target molecules like GPx and DNA-protein kinase (DNA-PK), cells pre-treated with DHS or DHS-C<sub>6</sub> for 16 h were exposed to inhibitors like mercaptosuccinic acid and NU7026 respectively for 2 h and then irradiated. Similarly to block the check point kinase 1 (CHK1) and check point kinase 2 (CHK2), cells were incubated with inhibitors such as UCN-01 and PV-1091 respectively for 16 h along with DHS or DHS-C<sub>6</sub> and then irradiated. The concentrations and the incubation times of inhibitors used in the study were taken from previous reports [31–33].

### 2.3. Clonogenic assay

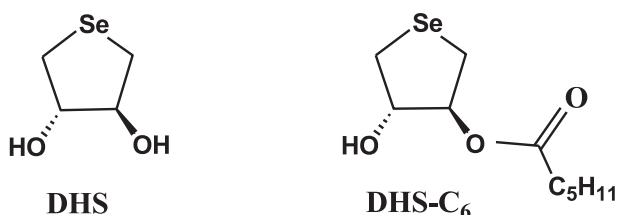
Following radiation and/or drug treatment, cells were cultured for 7 days for the development of macroscopic colonies and processed for clonogenic assay as reported previously without any modification [34]. The plating and survival fractions were determined using following equations:

$$\text{Plating Efficiency} = [\text{No. of colonies}/\text{No. of cells plated}] \times 100$$

$$\text{Survival fraction} = [\text{No. of colonies}/(\text{No. of cells plated} \times (\text{plating efficiency}/100))]$$

### 2.4. Dose modification factor (DMF)

Survival fractions of the control and drug pre-treated cells were



**Scheme 1.** Chemical structures of dihydroxy selenolane and C<sub>6</sub> derivative of dihydroxy selenolane.

determined through clonogenic assay at varying absorbed doses of  $\gamma$ -radiation ranging from 1 to 12 Gy. The survival curves were plotted by fitting the data of survival fraction (log scale) against the radiation absorbed dose (D) (linear scale) with the quadratic dose response equation ( $SF = \alpha D + \beta D^2$ ). From the survival curves,  $D_0$  (the dose which decreased survival fraction from 0.1 to 0.037) values under drug pre-treatment and untreated conditions were estimated. From this, DMF was calculated as  $(DMF = D_{0(DHS/DHS-C6+Radiation)}/D_{0(Radiation)})$ .

### 2.5. GPx activity and GSH assays

Following irradiation and/or drug treatment, cell lysate was prepared in cellytic-M<sup>®</sup> containing protease inhibitor cocktail as per manufacturer's instruction. The protein content of cell lysate was estimated using Bradford reagent and about 100  $\mu$ g of protein content was taken to measure GPx activity and GSH/GSSG ratio as per the methods reported previously [30,35].

### 2.6. DNA ladder assay

To assess apoptosis, DNA ladder assay was performed at 24 h after radiation exposure of cells. In brief, DNA was extracted from the cells ( $1 \times 10^6$ ) of various treatment groups and analysed on an agarose gel as described previously [36].

### 2.7. Mitochondrial membrane potential (MMP)

MMP as a marker of cell death was determined at 18 h after radiation exposure of cells using a mitochondrial-specific fluorescent probe JC-1 according to the method reported earlier [37].

### 2.8. Cell cycle analysis by PI staining

The cells cycle analysis was performed at 48, 72 and 96 h after radiation exposure of cells. In brief, cells were stained with a solution containing 50  $\mu$ g/ml PI, 0.1% sodium citrate and 0.1% Triton X-100 and kept overnight at 4 °C in dark. The labelled cells were acquired in Partec PASIII flow cytometer and analysed for the distribution of cells in different phases of cell cycle (G1, S, G2/M) using FlowJO software. The pre-G1 phase population represented the apoptotic cells [30].

### 2.9. Micronuclei assay

In brief, cells following irradiation were incubated with cytochalasin-B (4  $\mu$ g/ml in culture medium) for 18 h to block cytokinesis and processed for micronuclei detection using acridine orange according to previously reported method [38,39]. A total of 500 binucleated cells were analysed for the presence of micronuclei per treatment condition.

### 2.10. $\gamma$ -H2AX assay

The  $\gamma$ -H2AX foci analysis was carried out at 30 min post irradiation of cells using immunofluorescence method as reported previously [39]. The images were acquired using automated slide scanning Metacyte software module of the Metafer 4 scanning system (MetaSys-tems, Altlußheim, Germany). At least 50 cells were counted per treatment group to calculate the average number of foci per cell.

### 2.11. Alkaline single cell gel electrophoresis

Alkaline single cell gel electrophoresis or comet assay was

performed to study the DNA repair kinetics by following the extent of DNA damage as a function of time ranging from 0 to 60 min after radiation exposure of cells. In brief ~15000 cells in 50  $\mu$ l of cell culture medium were mixed with 0.8% low melting point agarose and layered on a slide pre-coated with 1% high melting point agarose and processed for comet assay as described previously [40]. The slides were stained with SYBR Green-II and at least fifty images were grabbed per slide using a Carl Zeiss Axio-plan fluorescence microscope (Germany). The images were analysed using CASP software version 1.2.0 ([www.Casplab.com](http://www.Casplab.com)) to calculate DNA damage parameters such as percent (%) DNA in tail, tail length (TL), tail moment (TM) and olive tail moment (OTM).

### 2.12. Quantitative real-time PCR

In brief, cells from different treatment groups were subjected to total RNA isolation using tri reagent according to the manufacturer's instruction. About 4  $\mu$ g of total RNA was reverse transcribed using cDNA synthesis kit (Thermo Scientific, USA) and real time PCR was carried out using the template (~90–100 ng of cDNA), SYBR green master mix (Roche Applied Science, Germany) and gene specific primers in a Rotor-Gene Q (QIAGEN, Germany) machine as described previously [26,29]. The relative expression was calculated from the threshold cycle (CT) values obtained from above runs using the method as described earlier [41]. The expressions of genes were normalized against a house keeping gene,  $\beta$  actin. The primers (forward and reverse) used for cDNA amplification are included in Table 1.

### 2.13. Assessment of ROS

The intracellular ROS level was determined at 30 min after radiation exposure of cells using a cell permeable and oxidation sensitive fluorescence probe, DCFDA. In brief, irradiated cells were labelled with 10  $\mu$ M of DCFDA at 37 °C for 30 min and the increase in fluorescence resulting from the oxidation of DCFDA to DCF was detected by monitoring the emission at 530 nm after excitation at 488 nm on a multimode plate reader (Synergy H1, Biotek, Germany) [42]. The representative images showing DCF fluorescence was captured using an Olympus fluorescence microscope (Model no. CKX41, Japan) equipped with ProgRes<sup>®</sup> camera.

### 2.14. Statistical analysis

All the experiments were carried out in triplicate and repeated at least two times. Data were presented as mean  $\pm$  SEM, n = 3 from an independent experiment. The data were analysed by one-way ANOVA using Origin (version 6.1) software to confirm the variability of the data. The P values < 0.05 were considered as statistically significant.

**Table 1**  
List of gene specific primers used in the study.

Name of gene	Primer sequence	Gen Bank Accession No.
$\beta$ -actin	5'-GGCTGTATTCCCCTCCATCG-3' 5'-CCAGTTGGTAACAATGCCATGT-3'	NM_007393
Rad 51	5'-AAGTTTTGGTCCACAGCTATTT-3' 5'-CGGTGCATAAGCAACAGCC-3'	NM_011234
Gadd 45 $\alpha$	5'-CCGAAAGGATGGACACGGTG-3' 5'-TTATCGGGGTCTACGTTGAGC-3'	NM_007836
SelP 1	5'-AGCTCTGCTTGTTACAAGCC-3' 5'-CAGGTCTTCCAATCTGGATGC-3'	NM_001042613

### 3. Results

#### 3.1. Effect of DHS or DHS-C<sub>6</sub> pre-treatment on the radiation-induced cell death in CHO cells

DHS treatment of CHO cells for 16 h up to a concentration of 100  $\mu\text{M}$  did not reduce the survival fraction as estimated by clonogenic assay (Fig. S1). Thus DHS concentrations up to 100  $\mu\text{M}$  appeared to be safe for exploring radioprotective activity. Accordingly, CHO cells were pre-treated with DHS in a concentration range of 0.1  $\mu\text{M}$ –100  $\mu\text{M}$  for 16 h and subjected to  $\gamma$ -irradiation at 4 Gy. The results of clonogenic assay showed a significant decrease in survival fraction of irradiated cells compared to control cells (Fig. 1A). DHS pre-treatment up to a concentration of 1  $\mu\text{M}$  did not show any improvement in the survival fraction as compared to radiation control (Fig. 1A). Increasing DHS concentration up to 25  $\mu\text{M}$  showed a concentration dependant improvement in survival fraction and further increase in concentration up to 100  $\mu\text{M}$  led to saturation effect (Fig. 1A). The percent protection offered by DHS at the most effective treatment concentration of 25  $\mu\text{M}$  was 24%. Based on these results, we also evaluated the radioprotective effect of DHS-C<sub>6</sub> (a lipophilic conjugate previously shown to increase the cellular uptake of DHS in CHO cells) [25]. Our results revealed that at an identical concentration of 25  $\mu\text{M}$ , DHS-C<sub>6</sub> pre-treatment offered significantly higher protection (40%) against the radiation (4 Gy)-induced cell death as compared to the parent compound DHS (Fig. S2). Encouraged by these results, we studied the radiation dose response of DHS and DHS-C<sub>6</sub> by evaluating survival fractions

at different absorbed doses (1–12 Gy) of radiation exposure through clonogenic assay. Survival curve and the representative images of colonies under different treatment conditions are shown in Fig. 1B and C respectively. Using  $D_0$  values, DMF for DHS and DHS-C<sub>6</sub> was determined to be 1.14 and 1.24 respectively.

#### 3.2. Effect of GPx inhibition on the radioprotective effect of DHS or DHS-C<sub>6</sub> in CHO cells

In line with previous reports [26,29], treatment (25  $\mu\text{M}$  for 16 h) with DHS or DHS-C<sub>6</sub> significantly elevated (~2.5 fold) GPx activity level in CHO cells (Fig. 2A). The cells treated with DHS-C<sub>6</sub> showed marginally higher GPx activity compared to those treated with DHS (Fig. 2A). Further to know whether GPx plays any role in radioprotective actions of DHS and DHS-C<sub>6</sub>, CHO cells pre-treated with these compounds were incubated with mercaptosuccinic acid (a pharmacological inhibitor of GPx), exposed to  $\gamma$ -radiation (4 Gy and 11 Gy) and evaluated for cell survival (by clonogenic assays). The results indicated that incubation with mercaptosuccinic acid significantly inhibited DHS or DHS-C<sub>6</sub> mediated increase in GPx activity (Fig. 2A). Further this treatment condition showed decrease in survival fraction compared to respective selenium compound (DHS or DHS-C<sub>6</sub>) plus radiation (4 Gy and 11 Gy) treated cells (Fig. 2B, C and Fig. S2). This suggested that inhibiting/blocking the GPx activity abrogated the radioprotective effect of DHS or DHS-C<sub>6</sub>. The inhibitor (mercaptosuccinic acid) treatment per se did not show any significant change in survival fraction both under irradiated and un-irradiated conditions (Fig. 2B, C and Fig. S2). Above

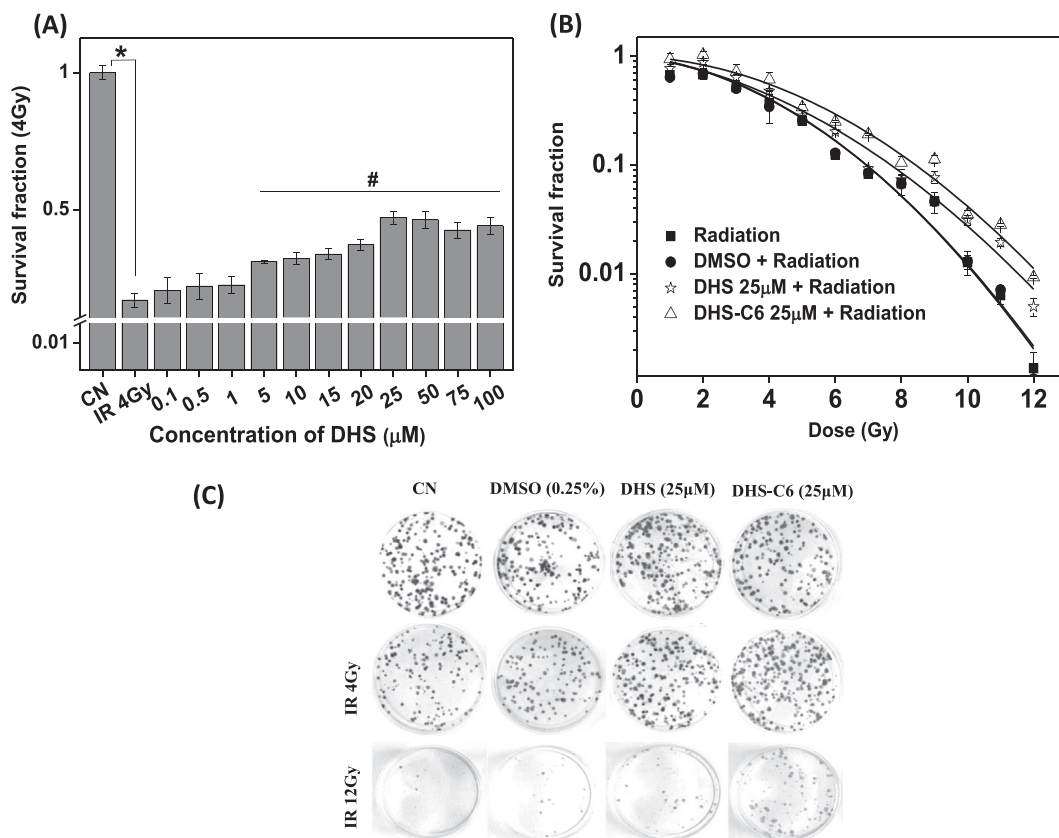


**Fig. 1.** (A) Bar graph showing the effect of the varying concentrations (0.1–100  $\mu\text{M}$ ) of DHS pre-treatment for 16 h on the survival fraction in CHO cells against  $\gamma$ -irradiation (4 Gy) as estimated by clonogenic assay. (B) Semi log plot showing radiation dose (1–12 Gy) response curve of DHS or DHS-C<sub>6</sub> pre-treatment (25  $\mu\text{M}$  for 16 h) in CHO cells by clonogenic assay. (C) Representative images showing colonies of CHO cells under different treatment conditions. The cell numbers were varied depending on the absorbed dose. (250–1 Gy, 300–2 Gy, 400–3 Gy, 500–4 Gy, 750–5 Gy, 1000–6 Gy, 1500–7 Gy, 2000–8 Gy, 3000–9 Gy, 4000–10 Gy, 5000–11 Gy, 6000–12 Gy). Results are presented as means  $\pm$  SEM,  $n = 3$ . \* $p < 0.05$  as compared to control group, # $p < 0.05$  as compared to radiation control group. CN – Control, IR – Radiation.

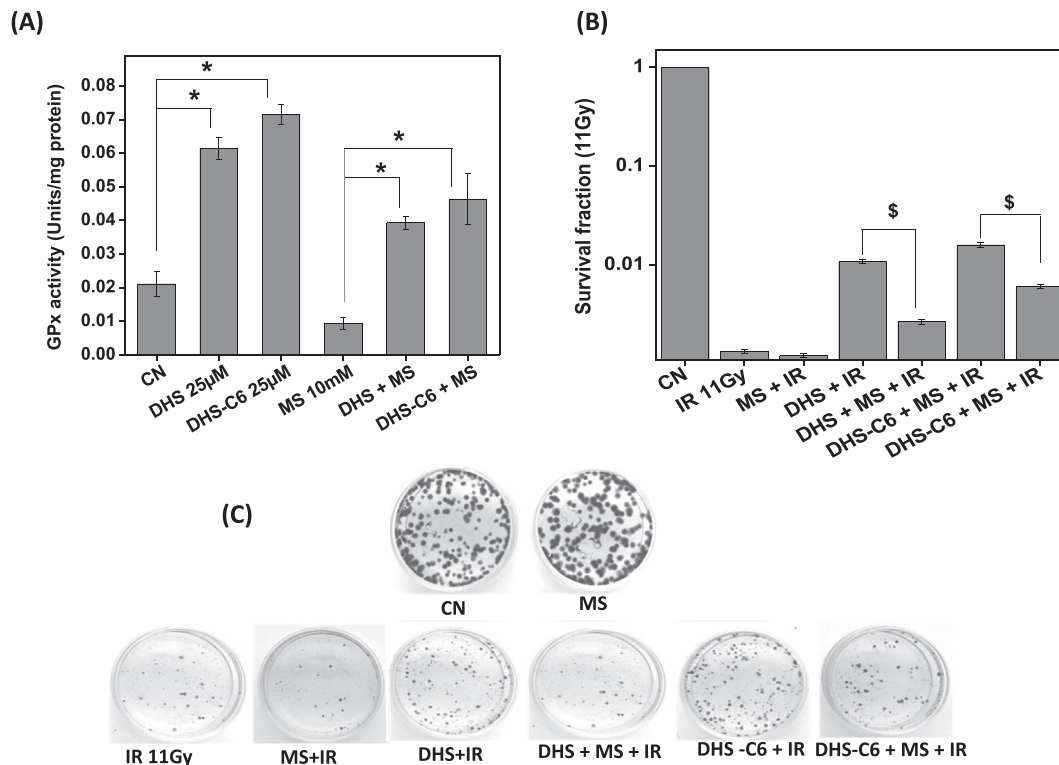


**Fig. 2.** (A) Effect of mercaptosuccinic acid (10 mM) on the GPx activity of DHS or DHS-C<sub>6</sub> pre-treatment (25 µM for 16 h) in CHO cells. One unit of GPx is the amount of enzyme that catalyses the oxidation of 1 µmol of NADPH to NADP<sup>+</sup> per minute. (B) Effect of mercaptosuccinic acid (10 mM) on the radioprotective activity of DHS or DHS-C<sub>6</sub> against radiation dose of 11 Gy in terms of survival fraction estimated by clonogenic assay in CHO cells. (C) Representative image showing colonies of CHO cells under different treatment combination. Results are presented as means ± SEM, n = 3. \*p < 0.05 as compared to respective control group/MS control group, §p < 0.05 as compared to DHS or DHS-C<sub>6</sub> plus radiation treated groups. CN - Control, IR - Radiation, MS - Mercaptosuccinic acid.

results together confirmed the involvement of GPx induced by DHS or DHS-C<sub>6</sub> in preventing the radiation-induced cell death in CHO cells.

### 3.3. Effect of DHS or DHS-C<sub>6</sub> treatment on radiation-induced G2/M arrest in CHO cells

Further to understand the cause of radiation-induced cell death in CHO cells, we performed cell cycle analysis through PI assay in a time dependant manner starting from 48 h to 96 h. The results indicated that exposure to radiation (4 Gy) led to G2/M arrest with increasing time of incubation (Fig. S3). This suggested the participation of G2/M arrest-mediated delayed mitotic cell death in irradiated CHO cells, which is in agreement with previous reports [43,44]. Pre-treatment (25 µM for 16 h) with DHS or DHS-C<sub>6</sub> showed significant inhibition of G2/M arrest in irradiated cells compared to control cells (Fig. 3A and B). DHS-C<sub>6</sub> was better than DHS in this respect. Incubation with mercaptosuccinic acid (GPx inhibitor) showed partial restoration of G2/M arrest in cells pre-treated with DHS or DHS-C<sub>6</sub> and exposed to radiation (Fig. 3A and B). The inhibitor and drug control groups showed cell cycle phases similar to those of control cells.

### 3.4. Effect of DHS or DHS-C<sub>6</sub> treatment on radiation-induced DNA damage in CHO cells

Radiation-induced G2/M arrest is a consequence of DNA damage. Therefore the ability of DHS or DHS-C<sub>6</sub> to protect cells from radiation-induced double strand breaks (DSBs) was evaluated through γ-H2AX assay at 30 min post-irradiation. The results as presented in Fig. 4A and B indicated that irradiation (2 Gy) led to 10

fold increase in the number of γ-H2AX foci in the nucleus of the cells. However pre-treatment (25 µM for 16 h) with DHS or DHS-C<sub>6</sub> significantly reduced the number of γ-H2AX foci in the irradiated cells suggesting their role in preventing the radiation-induced DSBs. The compound DHS-C<sub>6</sub> was better than DHS in reducing the radiation-induced DSBs (Fig. 4A and B). Further, DSBs if remain unrepaired leads to chromosomal fragmentation which can be seen as micronuclei in dividing cells. Any compound which protects cells from radiation-induced DNA damage will also reduce the number of micronuclei formed post-radiation exposure. Accordingly DHS or DHS-C<sub>6</sub> were investigated for their abilities to prevent the radiation (4 Gy) induced micronuclei formation. The results clearly indicated that pre-treatment (25 µM for 16 h) with DHS or DHS-C<sub>6</sub> significantly reduced the number of micronuclei in irradiated cells compared to the radiation control group (Fig. 4C). The percent reduction offered by DHS and DHS-C<sub>6</sub> with respect to radiation-induced micronuclei formation was 40% and 56% respectively. Interestingly, the addition of a GPx inhibitor, mercaptosuccinic acid in cells pre-treated with DHS or DHS-C<sub>6</sub> significantly abrogated their anti-genotoxic effect against radiation exposure (Fig. 4A-C). Groups treated with DHS or DHS-C<sub>6</sub> and inhibitor control showed basal level of γ-H2AX foci and micronuclei formation. Mercaptosuccinic acid treatment showed marginal increase in DNA damage in irradiated cells (Fig. 4A-C).

### 3.5. Effect of DHS or DHS-C<sub>6</sub> treatment on DNA repair kinetics in CHO cells following radiation exposure

In continuation to the above study, we investigated the effect of pre-treatment with DHS and DHS-C<sub>6</sub> on DNA repair kinetics after radiation exposure (4 Gy) by monitoring the levels of DNA damage

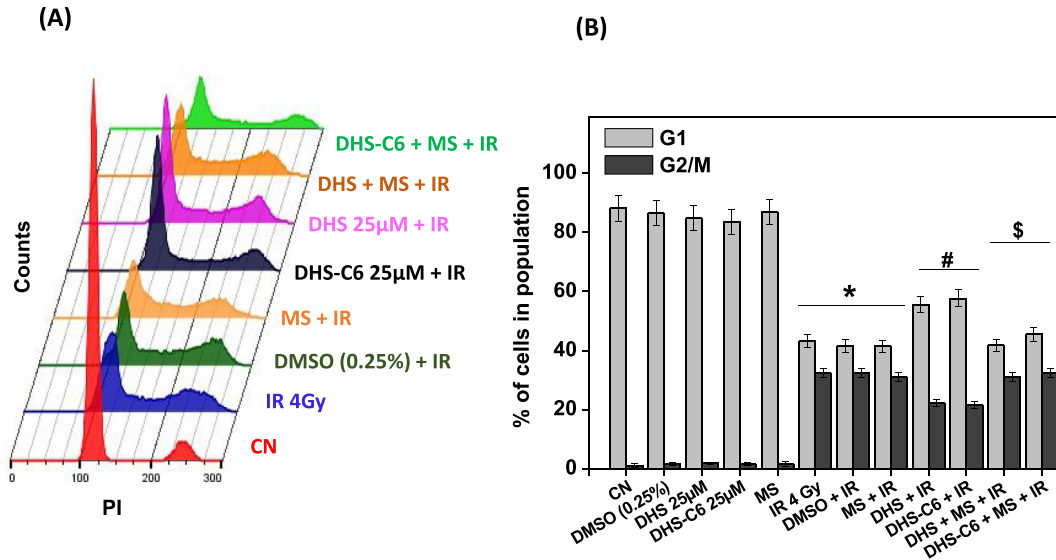


**Fig. 3.** Effect of pre-treatment with DHS or DHS-C<sub>6</sub> (25 µM for 16 h) on the cell cycle distribution in CHO cells as estimated by PI staining and its modulation by mercaptosuccinic acid (10 mM). (A) Representative figure showing distribution of cells in different phase of cell cycle (G1, S, and G2/M) at 96 h post irradiation (4 Gy) (B) Bar graph showing the percentage (%) of cells in G1 and G2/M phases of cell cycle. Results are presented as mean ± SEM, n = 3. \*p < 0.05 as compared to respective control groups. #p < 0.05 compared to radiation control groups, \$p < 0.05 as compared to DHS or DHS-C<sub>6</sub> plus radiation treated groups. CN - Control, IR – Radiation, MS - Mercaptosuccinic acid.

as a function of post irradiation time ranging from 0 to 60 min through alkaline single cell gel electrophoresis. As shown in Fig. 5, irradiation dose of 4 Gy led to a significant increase in the comet

parameters such as % tail DNA, TM, TL and OTM which decreased with time suggesting the normal DNA repair process of cells. Interestingly, pre-treatment (25 µM for 16 h) with DHS and DHS-C<sub>6</sub>

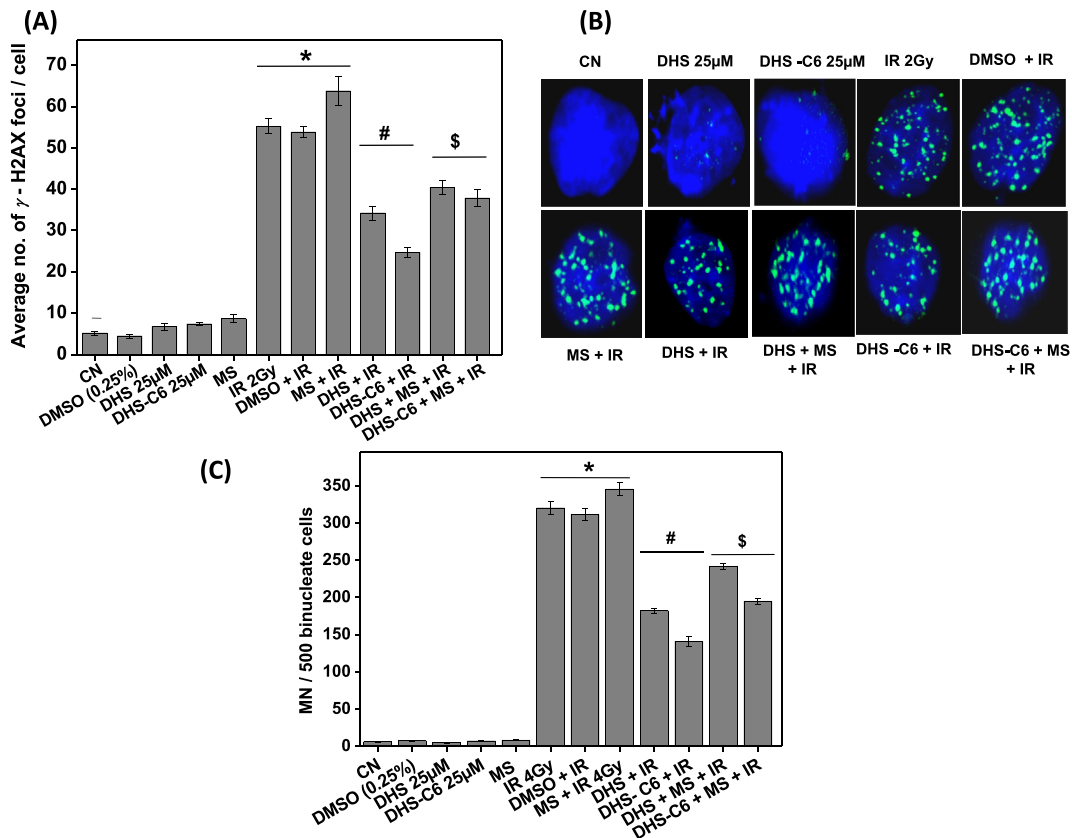


**Fig. 4.** Protective effect of DHS or DHS-C<sub>6</sub> pre-treatment (25 µM for 16 h) against radiation-induced DNA damage in CHO cells and its modulation by mercaptosuccinic acid (10 mM). (A) Bar graph showing the number of radiation (2 Gy)-induced γ-H2AX foci under different treatment conditions. (B) Representative fluorescent images showing γ-H2AX foci formed under different treatment conditions. The cells were labelled with primary anti-phospho-histone H2AX human monoclonal IgG antibody followed by secondary antibody labelled with FITC. Magnification – 63x. (C) Bar graph showing counts of radiation (4 Gy)-induced micronuclei under different treatment conditions. Results are presented as mean ± SEM, n = 3. \*p < 0.05 as compared to respective control groups, #p < 0.05 compared to radiation control groups, \$p < 0.05 as compared to DHS/DHS-C<sub>6</sub> plus radiation treated groups. CN - Control, IR - Radiation, MS - Mercaptosuccinic acid.

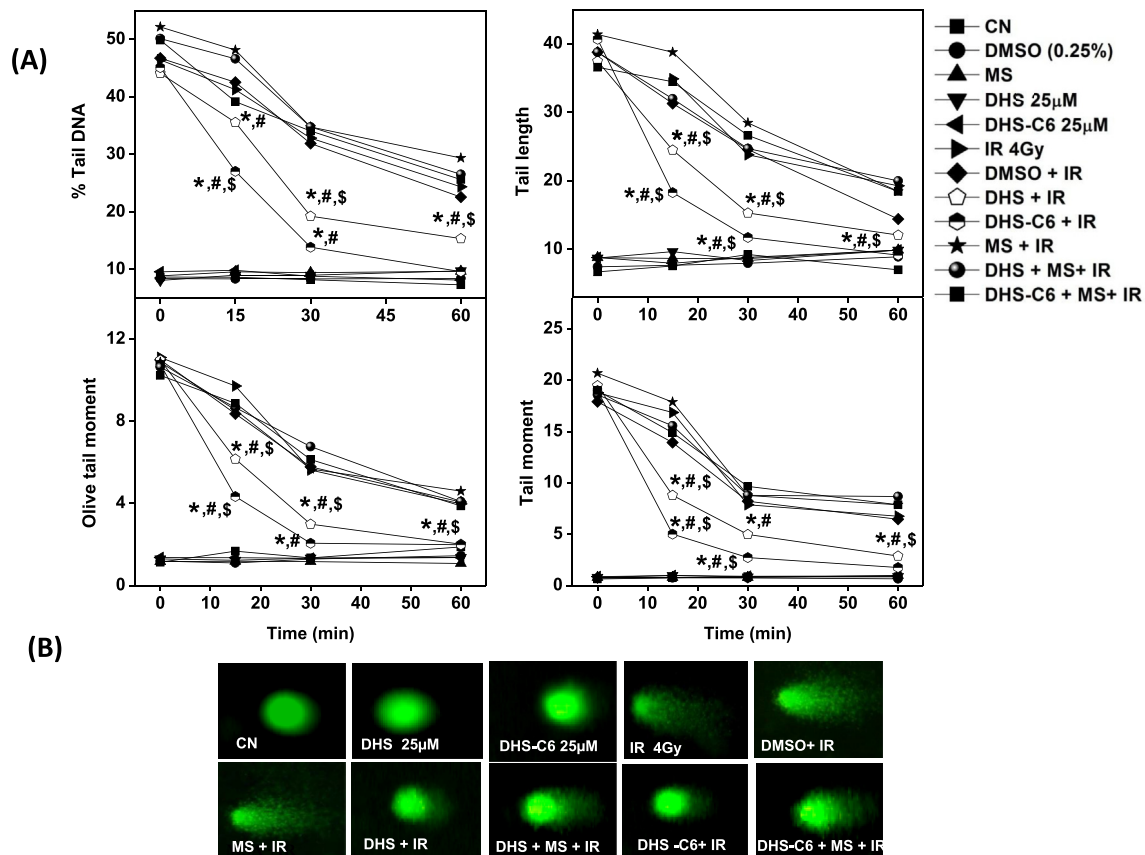


**Fig. 5.** (A) Effect of DHS or DHS-C<sub>6</sub> pre-treatment (25  $\mu$ M for 16 h) on DNA repair kinetics in CHO cells after radiation (4 Gy) exposure and its modulation by mercaptosuccinic acid (10 mM). DNA repair was monitored by comet assay as a function of post irradiation time (0–60 min) (B) Representative fluorescent images of cells stained with SYBR-Green-II at 30 min post-irradiation. Results are presented as mean  $\pm$  SEM, n = 3. \*p < 0.05 as compared to respective control groups. #p < 0.05 compared to radiation control groups, \$p < 0.05 as compared to DHS/DHS-C<sub>6</sub> plus radiation treated groups. CN - Control, IR - Radiation, MS - Mercaptosuccinic acid.

led to faster repair of DNA compared to radiation control. At 30 min, there was a decrease in all four comet parameters (% DNA tail, TM, TL and OTM) by 41%, 36%, 35% and 46% respectively in DHS and by 57%, 50%, 52% and 66% respectively in DHS-C<sub>6</sub> pre-treated group compared to radiation control. DHS-C<sub>6</sub> appeared to be better than DHS in augmenting the DNA repair after radiation exposure. Blocking or inhibiting GPx through mercaptosuccinic acid reversed the effects of DHS and DHS-C<sub>6</sub> with respect to DNA repair (Fig. 5). Groups treated with DHS or DHS-C<sub>6</sub> and inhibitor showed comet parameters comparable to sham control group.

Above results confirmed the role of DHS or DHS-C<sub>6</sub> in DNA repair through GPx induction which in turn may influence the cell viability after radiation exposure. In order to validate this, CHO cells pre-treated with DHS or DHS-C<sub>6</sub> were incubated with NU-7026 (an inhibitor of DNA-PK of non homologous end joining (NHEJ) pathway) and mercaptosuccinic acid both separately or in combination, irradiated (4 Gy and 11 Gy) and analysed for cell viability by clonogenic assay. It was evidenced that inhibitors of DNA-PK and GPx individually led to partial abrogation of DHS or DHS-C<sub>6</sub> mediated radioprotective effect (Fig. 6A, Figs. S4A and S5A). However combinatorial inhibitions of DNA-PK and GPx showed complete abrogation establishing that the radioprotective activity of DHS and DHS-C<sub>6</sub> was due to the GPx induction and DNA repair (Fig. 6A, Figs. S4A and S5A). Further to know whether DHS or DHS-C<sub>6</sub> plays any role in homologous recombination (HR) repair pathway, their effects on the mRNA expression of genes such as *Rad 51* and *GADD 45 $\alpha$*  were investigated by RT-PCR. The bar graph showing relative expression of above genes under different

treatment conditions is given in Fig. 6B. It can be seen that irradiation led to significant suppression of *Rad 51* and *GADD 45 $\alpha$*  compared to sham control group. The compound DHS significantly induced the expression of above genes both under irradiated as well as un-irradiated conditions compared to respective controls. As expected DHS-C<sub>6</sub> showed similar trend however the effects were more pronounced. Thus it suggests the possible role of DHS and DHS-C<sub>6</sub> in homologous recombination repair post radiation exposure.

### 3.6. Effect of inhibition of CHK1 and CHK2 on the radioprotective effect of DHS or DHS-C<sub>6</sub> in CHO cells

Based on the above results, experiments were performed to understand whether DHS and DHS-C<sub>6</sub> modulates checkpoint kinase (CHK1/2) involved in DNA repair to facilitate its radioprotective activity. For this CHO cells treated with DHS or DHS-C<sub>6</sub> were incubated with inhibitors UCN-01 (CHK1)/PV 1019 (CHK2) and mercaptosuccinic acid both separately or in combination, irradiated (4 Gy and 11 Gy) and analysed for cell viability by clonogenic assay. The results showed that the inhibition of CHK2 did not affect the radioprotective effect of DHS or DHS-C<sub>6</sub> (Fig. 7A, Figs. S4B and S5B). Further combinatorial inhibitions of GPx and CHK2 showed the same level of abrogation as that observed with only GPx inhibitor. Together these observations indicated that treatment with DHS or DHS-C<sub>6</sub> did not influence CHK2. In contrast, inhibitors of CHK1 and GPx together although showed abrogation of DHS or DHS-C<sub>6</sub>-mediated radioprotection, the response was not the additive of

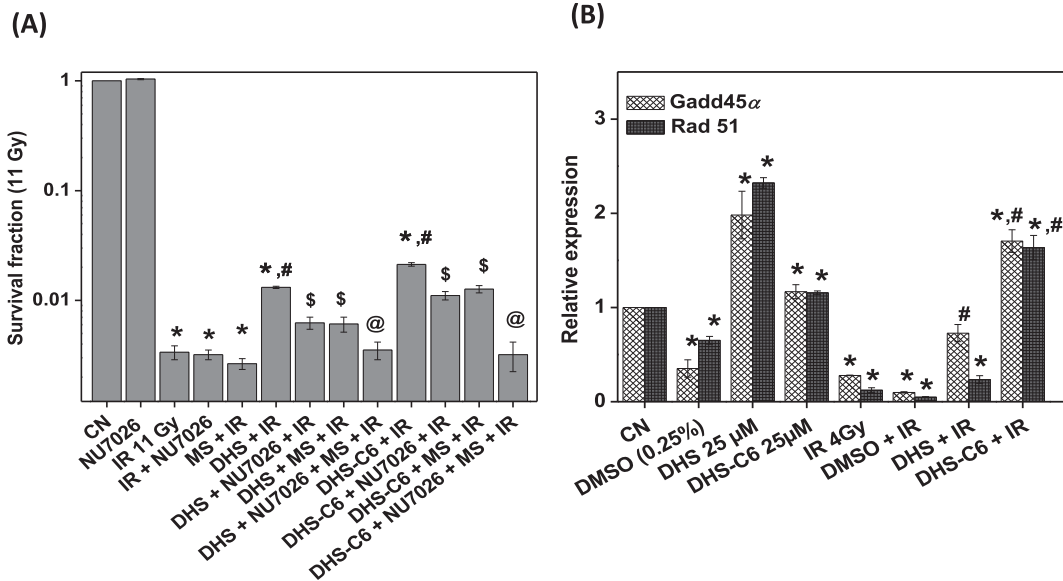


**Fig. 6.** (A) Effect of NU-7026 (10 μM), inhibitor of DNA-PK and mercaptosuccinic acid (10 mM) on the radioprotective activity of DHS or DHS-C<sub>6</sub> in CHO cells against radiation dose of 11 Gy by clonogenic assay. (B) Effect of DHS or DHS-C<sub>6</sub> pre-treatment (25 μM for 16 h) on the mRNA expressions of *GADD45α* and *Rad 51* in CHO cells at 72 h after exposure to γ-radiation (4 Gy) as estimated by real-time PCR. Plot represents the expression of above genes normalized with respective control groups. Expression of β-actin mRNA was used as internal control. Results are presented as mean ± SEM, n = 3. \*p < 0.05 compared to control groups, #p < 0.05 compared to radiation control groups, \$p < 0.05 compared to DHS or DHS-C<sub>6</sub> plus radiation treated groups, @p < 0.05 compared to DHS plus inhibitor plus radiation treated group. CN - Control, IR - Radiation, MS - Mercaptosuccinic acid.

individual inhibitor effect (Fig. 7B, Figs. S4C and S5C). Thus it appears that GPx level induced by DHS or DHS-C<sub>6</sub> contributes to radioprotection at least through CHK1-mediated cell cycle arrest and DNA repair.

### 3.7. Effect of DHS or DHS-C<sub>6</sub> treatment on radiation-induced oxidative stress in CHO cells

Radiation is known to induce oxidative stress in cells through ROS generation and subsequent depletion of GSH levels. Thus, we

evaluated the effect of DHS and DHS-C<sub>6</sub> on radiation-induced changes in ROS and GSH/GSSG levels at 30 min and 6 h post irradiation respectively as given in Fig. 8 (A-C). It can be seen that pre-treatment (25 μM for 16 h) with DHS and DHS-C<sub>6</sub> significantly reduced the ROS generation and increased the ratio of GSH and GSSG in irradiated cells compared to radiation control. On similar lines, DHS and DHS-C<sub>6</sub> treatment itself led to an increase in the expression of an antioxidant selenoprotein *Selp-1* (Fig. 8D). Exposure to radiation induced the expression of *Selp-1* and pre-treatment with DHS or DHS-C<sub>6</sub> augmented this level. In all above

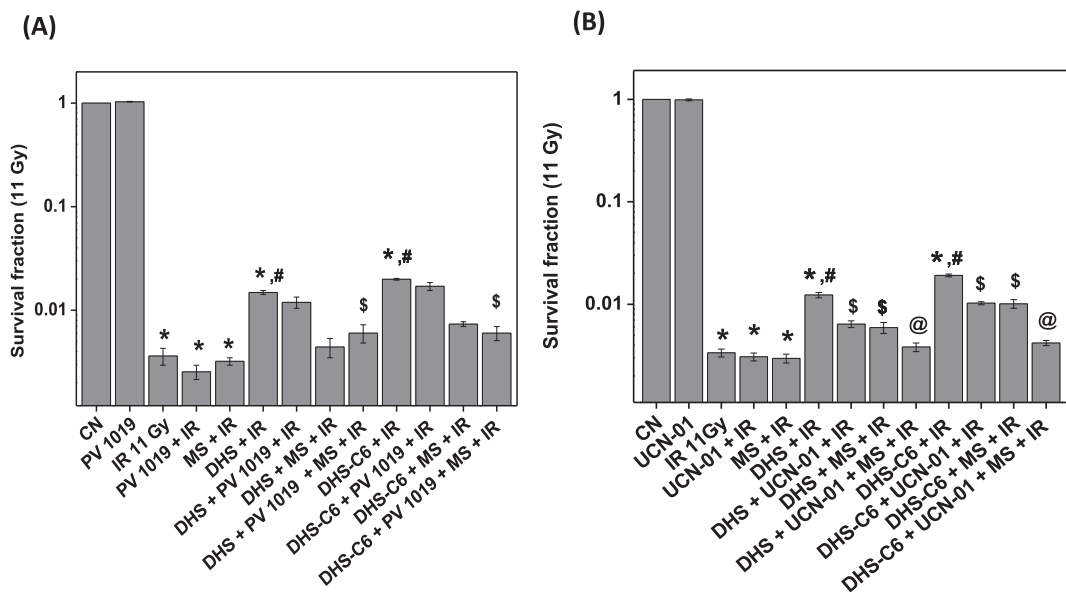


**Fig. 7.** (A) Effect of PV1091 (400 nM), inhibitor of CHK2 and mercaptosuccinic acid (10 mM) on the radioprotective activity of DHS or DHS-C<sub>6</sub> in CHO cells against radiation dose of 11 Gy by clonogenic assay. (B) Effect of UCN-01 (25 nM), inhibitor of CHK1 and mercaptosuccinic acid (10 mM) on the radioprotective activity of DHS or DHS-C<sub>6</sub> in CHO cells against radiation dose of 11 Gy by clonogenic assay. \*p < 0.05 compared to control groups, #p < 0.05 compared to radiation treated groups, \$p < 0.05 compared to DHS/DHS-C<sub>6</sub> plus radiation treated groups, @p < 0.05 compared to DHS plus inhibitor plus radiation treated group. CN - Control, IR - Radiation, MS-Mercaptosuccinic acid.

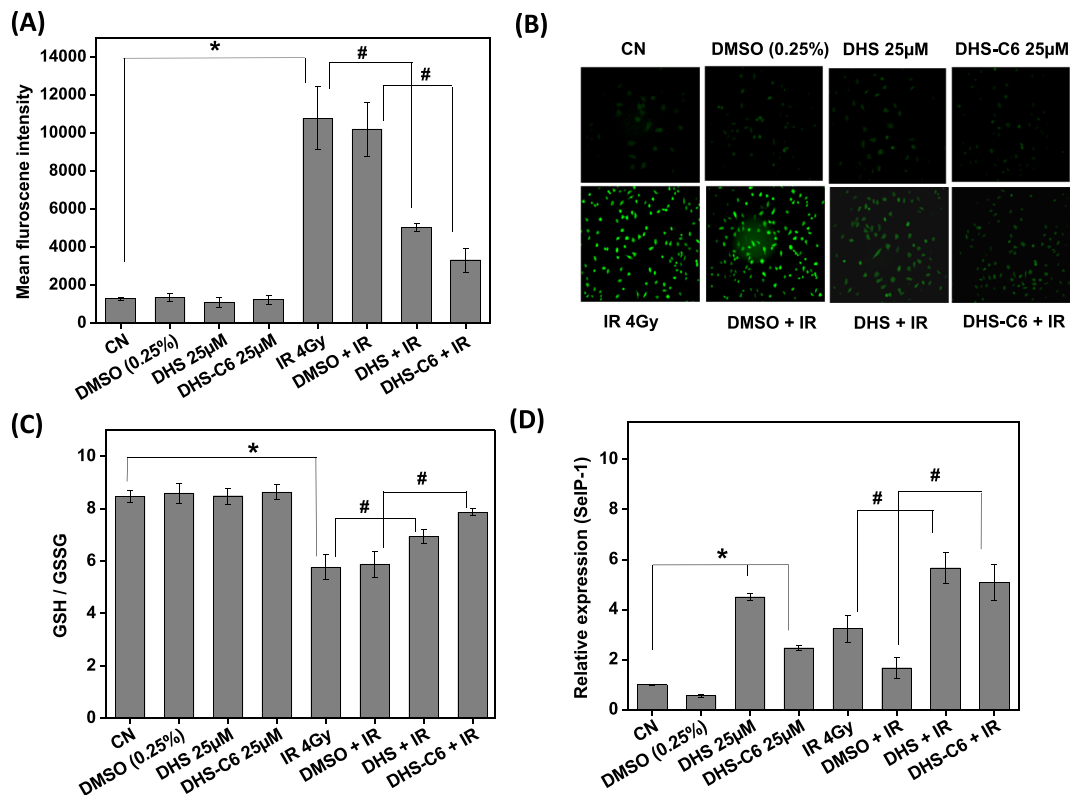


**Fig. 8.** (A) Effect of DHS or DHS-C<sub>6</sub> pre-treatment (25 µM for 16 h) on intracellular ROS production at 30 min post irradiation (4 Gy) in CHO cells estimated using an oxidation sensitive fluorophore DCFDA ( $\lambda_{\text{exc}} = 488 \text{ nm}$ ). (B) Representative images of DCFDA stained cells under different treatment conditions at 30 min post irradiation (4Gy). (C) Effect of DHS and DHS-C<sub>6</sub> pre-treatment on GSH/GSSG ratio at 6 h post  $\gamma$ -irradiation of 4 Gy (D) Effect of DHS and DHS-C<sub>6</sub> pre-treatment on mRNA expressions of *SelP-1* in CHO cells at 6 h after exposure to  $\gamma$ -radiation (4 Gy) as estimated by real-time PCR. Plot represents the expression of above gene normalized with respective control group. Expression of  $\beta$ -actin mRNA was used as internal control. Results are presented as mean  $\pm$  SEM, n = 3. \*p < 0.05 compared to control groups, #p < 0.05 compared to radiation control groups. CN - Control, IR - Radiation.

observations, DHS-C<sub>6</sub> was found to be better than DHS in preventing radiation-induced oxidative stress.

### 3.8. Effect of DHS or DHS-C<sub>6</sub> pre-treatment on radiation-induced apoptosis in splenic lymphocytes and CHO cells

Lymphocytes are the most radiosensitive cell types and are known to undergo apoptosis after radiation exposure [45]. Thus the effect of DHS or DHS-C<sub>6</sub> pre-treatment on preventing the radiation-induced apoptosis was evaluated in spleen lymphocytes using PI assay. The results as presented in Fig. 9A and B indicated that irradiation (4 Gy) led to significant increase in pre-G1 population indicative of apoptosis and pre-treatment (25 µM for 16 h) with DHS or DHS-C<sub>6</sub> did not protect lymphocytes from radiation-induced apoptosis. The evaluation of other apoptotic markers such as DNA ladder and mitochondrial membrane potential (using JC-1) showed similar result (Fig. 9C and D). Further we also studied the effect of DHS or DHS-C<sub>6</sub> treatment on the radiation-induced apoptosis in CHO cells. For this CHO cells pre-treated (25 µM for 16 h) with DHS or DHS-C<sub>6</sub> were subjected to irradiation at very high acute dose of 15 Gy and examined for pre-G1 population by PI assay. The results clearly indicated that irradiation at 15 Gy led to significant increase in pre-G1 population (Fig. S6). However, pre-treatment with DHS or DHS-C<sub>6</sub> did not reduce the apoptotic population (Fig. S6). Taken together, these results suggested that DHS or DHS-C<sub>6</sub> treatment did not protect from radiation-induced early apoptosis irrespective of the cell type.

## 4. Discussion

Having known that DHS, a water soluble organoselenium compound, exhibited potential *in vivo* radioprotection, the present study was focused to understand the mechanism of its action [29]. Additionally, we also investigated whether DHS-C<sub>6</sub>, a pro-drug previously reported to increase the cellular uptake of DHS could be a better agent to achieve radioprotection [26]. To address these issues, we employed CHO cells of epithelial origin. These cells have been widely used in radiation-related research work and are well characterized with respect to radiation response [44]. For example CHO cells under irradiated condition show tendency to accumulate DNA damage, which in turn leads to G2/M arrest and delayed mitotic death [43,44]. The results from our experiments indicated that pre-treatment with both DHS and DHS-C<sub>6</sub> protected CHO cells from radiation-induced mitotic death. The pro-drug DHS-C<sub>6</sub> showed better efficacy than DHS with a DMF value of 1.24. Since DNA is the most critical target of radiation exposure to cells [4–6], it was anticipated that radioprotective effect of DHS or DHS-C<sub>6</sub> might be related to its effect on DNA damage/repair and cell cycle arrest. Analysis of these parameters revealed that DHS or DHS-C<sub>6</sub> treatment prior to radiation exposure augmented DNA repair leading to inhibition of G2/M arrest and mitotic death.

Previously we had observed that *in vivo* radioprotective activity of DHS was associated with its ability to cause tissue specific induction of GPx at activity and mRNA levels [29]. Supporting this observation, here in present study DHS treatment induced GPx activity in CHO cells. Notably DHS-C<sub>6</sub> showed only a marginal increase in GPx activity compared to DHS. It is well documented in

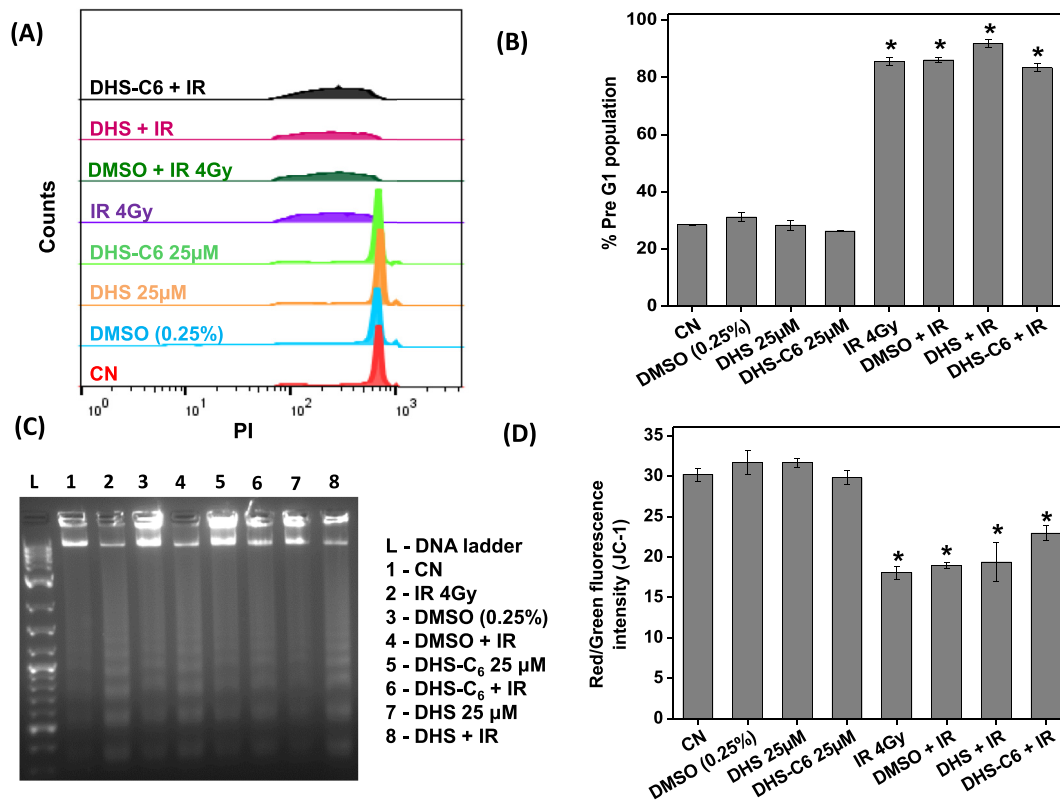


**Fig. 9.** Effect of DHS or DHS-C<sub>6</sub> pre-treatment (25  $\mu$ M for 16 h) on the radiation (4 Gy)-induced apoptosis in lymphocytes. (A) Representative figure showing distribution of lymphocytes in different phase of cell cycle (G1, S, and G2/M) under different treatment conditions at 48 h post  $\gamma$ -irradiation by PI staining. (B) Bar graph showing percentage (%) of cells in pre-G1 phase under different treatment conditions at 48 h post  $\gamma$ -irradiation in lymphocytes. (C) DNA ladder assay at 24 h post irradiation. (D) Bar graph showing the effect of DHS or DHS-C<sub>6</sub> on mitochondrial membrane potential at 18 h post irradiation as determined by JC-1 staining in lymphocytes. Results are presented as means  $\pm$  SEM, n = 3. \*p < 0.05 compared to control groups. CN - Control, IR - Radiation.

literature that GPx activity reaches saturation with the increasing availability of selenium and this could be the reason for the above observed effect [46,47]. Further, selenium compounds in general are known to regulate the expression levels of selenoproteins including GPx by modulating mRNA stability and activating transcription factors such as Nrf2 and p53 [48–50]. The exact mechanism through which DHS or DHS-C<sub>6</sub> induces GPx activity is not clear to us at this stage and this will be addressed in future studies. Nevertheless above results prompted us to ask a question whether GPx plays any role in DHS or DHS-C<sub>6</sub>-mediated radioprotection. In order to address this issue, we employed mercaptosuccinic acid which is known to inhibit GPx through non-covalent interactions and evaluated the radiation response of DHS or DHS-C<sub>6</sub> in CHO cells [51]. Importantly, treatment with mercaptosuccinic acid blocked the DNA repair and radioprotective activity shown by DHS or DHS-C<sub>6</sub>. Thus it is confirmed that GPx indeed played a role in radioprotective effect of DHS or DHS-C<sub>6</sub> through modulating DNA repair. Now GPx being a cytoplasmic enzyme is unlikely to play a role in preventing the DNA damage induced mainly by the hydroxyl radicals generated within the nucleus of a cell through ROS scavenging mechanism [52,53]. Therefore, it was obvious to presume that GPx level induced by DHS or DHS-C<sub>6</sub> might be influencing DNA repair machinery. Mammalian cells assess for any DNA damage induced by radiation exposure through the checkpoints (such as G1/S and G2/M) regulated by CHK1 and CHK2 and activate repair mechanisms like NHEJ and HR to facilitate DNA repair [54–57]. If GPx has to modulate DNA repair through these checkpoints or the repair pathways their combinatorial inhibition is expected not to show additive effect in reducing survival against radiation exposure. Our

results revealed that inhibitors of DNA-PK (NHEJ pathway) and CHK1 (HR pathway) when used in combination with GPx inhibitor caused complete abrogation of the radioprotective effect of DHS and DHS-C<sub>6</sub>. However, the effect of above combinatorial inhibition on survival fraction was less than additive, when these two proteins (DNA-PK/CHK1 and GPx) were inhibited individually. Additionally, treatment with DHS or DHS-C<sub>6</sub> induced the expression of genes like *Gadd 45 $\alpha$*  and *Rad 51* of HR pathway. Taken together, it appeared that GPx level induced by DHS and DHS-C<sub>6</sub> influenced DNA repair by involving both NHEJ and HR pathways. These results are consistent with growing evidences in literature suggesting the role of GPx in DNA repair and maintaining the genome stability [58–60].

In past, GPx has been evaluated for reducing the radiation-induced cell killing employing cellular models. The results are mostly incongruent: some suggesting that GPx is an important factor in cellular radio sensitivity [61,62] while others indicating that cells treated with sodium selenite or genetically engineered to overexpress cytosolic GPx prior to radiation exposure did not show any improvement in the survival [63,64]. In the present investigation, DHS and DHS-C<sub>6</sub> treatment although showed similar elevation in GPx level, resulted in varied extent of radioprotection in CHO cells. This suggested that GPx may not be the only factor contributing to the radioprotective effect of DHS and DHS-C<sub>6</sub>. Justifying this assumption, DHS or DHS-C<sub>6</sub> treatment showed lowering of oxidative stress in irradiated CHO cells and DHS-C<sub>6</sub> was more effective than DHS in this respect. Previously DHS was reported to scavenge ROS and therefore DHS-C<sub>6</sub> through increasing the cellular uptake may contribute to higher ROS scavenging [22,26]. Further

DHS and DHS-C<sub>6</sub> were also observed to up-regulate other antioxidant selenoproteins like Selp-1 and TrxR which can be linked to antioxidant effects [26,29]. Thus the abilities of DHS or DHS-C<sub>6</sub> to augment DNA repair and reduce the oxidative stress appeared to be contributing towards radioprotective activity.

Having understood the radioprotective action of DHS and DHS-C<sub>6</sub> in CHO cells, it was important to evaluate the effect of these compounds in radiosensitive cells like lymphocytes. Notably, treatment with DHS and DHS-C<sub>6</sub> did not protect lymphocytes from radiation exposure. Lymphocytes undergo transient G1 arrest and apoptosis after radiation exposure [36,45] suggesting the inability of above compounds in preventing the radiation-induced early apoptosis.

## 5. Conclusions

The present study gains significance in a view of the fact that late-responding normal tissue cells involved in the radiotherapy side effects undergo delayed mitotic death following radiation exposure. Therefore DHS-C<sub>6</sub> a lipophilic conjugate of DHS showing potent protection against radiation-induced mitotic death can be a model compound for *in vivo* evaluation as selenium based radioprotector to reduce radiation toxicities in late-responding normal cells during radiotherapy. The mechanistic investigation confirmed the role of GPx in DHS-C<sub>6</sub>-mediated radioprotection through taking part in DNA repair.

## Conflict of interest

None.

## Acknowledgments

The author, (P.V.) acknowledges Homi Bhabha National Institute for financial assistance in the form of Senior Research Fellowship. Authors are also grateful to Dr. B. S. Patro of Bio-organic Division and Miss. Usha Yadav, Radiological Physics and Advisory Division for their assistance during the course of experiments.

## Transparency document

Transparency document related to this article can be found online at <https://doi.org/10.1016/j.biochi.2017.10.021>.

## Appendix A. Supplementary data

Supplementary data related to this article can be found at <https://doi.org/10.1016/j.biochi.2017.10.021>.

## References

- [1] P. Grammaticos, E. Giannoula, G.P. Fountos, Acute radiation syndrome and chronic radiation syndrome, *Hell. J. Nucl. Med.* 16 (2013) 56–59.
- [2] K.E. Carr, S.P. Hume, R.R. Ertarh, E.A. Carr, S. McCollough, Radiation-induced changes to epithelial and non-epithelial tissue, in: *Radiation and the Gastrointestinal Tract*, Taylor and Francis, 1995, pp. 113–128.
- [3] A.L. Carsten, Acute Lethality: the Hematopoietic Syndrome in Different Species, in: *Response of Different Species to Total Body Irradiation*, Springer, 1984, pp. 59–86.
- [4] J.R. Hubenak, Q. Zhang, C.D. Branch, S.J. Kronowitz, Mechanisms of injury to normal tissue after radiotherapy: a review, *Plast. Reconstr. Surg.* 133 (2014) 49e–56e.
- [5] H.B. Stone, C.N. Coleman, M.S. Anscher, W.H. McBride, Effects of radiation on normal tissue: consequences and mechanisms, *Lancet Oncol.* 4 (2003) 529–536.
- [6] P.A. Riley, Free radicals in biology: oxidative stress and the effects of ionizing radiation, *Int. J. Radiat. Biol.* 65 (1994) 27–33.
- [7] C.N. Andreassen, C. Grau, J.C. Lindegaard, Chemical radioprotection: a critical review of amifostine as a cytoprotector in radiotherapy, *Semin. Radiat. Oncol.* 13 (2008) 62–72.
- [8] J.F. Weiss, M.R. Landauer, History and development of radiation-protective agents, *Int. J. Radiat. Biol.* 85 (2009) 539–573.
- [9] L.V. Papp, J. Lu, A. Holmgren, K.K. Khanna, From selenium to selenoproteins: synthesis, identity, and their role in human health, *Antioxid. Redox. Signal.* 9 (2007) 775–806.
- [10] P. Brenneisen, H. Steinbrenner, H. Sies, Selenium oxidative stress, and health aspects, *Mol. Asp. Med.* 26 (2005) 256–267.
- [11] M.P. Rayman, The importance of selenium to human health, *Lancet* 356 (2000) 233–241.
- [12] C.W. Nogueira, J.B. Rocha, Toxicology and pharmacology of selenium: emphasis on synthetic organoselenium compounds, *Arch. Toxicol.* 85 (2011) 1313–1359.
- [13] J. Brozmanova, D. Mánikova, V. Vlčková, M. Chovanec, Selenium: a double-edged sword for defense and offence in cancer, *Arch. Toxicol.* 84 (2010) 919–938.
- [14] H. Tapiero, D.M. Townsen, K.D. Tew, The antioxidant role of selenium and selenol-compounds, *Biomed. Pharmacother.* 57 (2003) 134–144.
- [15] T. Schewe, Molecular actions of ebselen—an anti-inflammatory antioxidant, *Gen. Pharmacol.* 26 (1995) 1153–1169.
- [16] J.K. Tak, J.W. Park, The use of ebselen for radioprotection in cultured cells and mice, *Free Radic. Biol. Med.* 46 (2009) 1177–1185.
- [17] A. Kunwar, P. Bansal, S.J. Kumar, P.P. Bag, P. Paul, N. Reddy, L.B. Kumbhare, V.K. Jain, R.C. Chaubey, M.K. Unnikrishnan, K.I. Priyadarsini, *In vivo* radioprotection studies of 3,3-diselenodipropionic acid, a selenocystine derivative, *Free Radic. Biol. Med.* 48 (2010) 399–410.
- [18] A. Kunwar, P.P. Bag, S. Chattopadhyay, V.K. Jain, K.I. Priyadarsini, Anti-apoptotic anti-inflammatory, and immunomodulatory activities of 3,3-diselenodipropionic acid in mice exposed to whole body -radiation, *Arch. Toxicol.* 85 (2011) 1395–1405.
- [19] T. Yamaguchi, K. Sano, K. Takakura, I. Saito, Y. Shinohara, T. Asano, H. Yasuhara, Ebselen in acute ischemic stroke: a placebo-controlled, double-blind clinical trial. Ebselen Study Group, *Stroke* 29 (1998) 12–17.
- [20] M. Iwaoka, T. Takahashi, S. Tomoda, Synthesis and structural characterization of water-soluble selenium reagents for the redox control of protein disulfide bonds, *Heteroat. Chem.* 12 (2001) 293–299.
- [21] F. Kumakura, B. Mishra, K.I. Priyadarsini, M. Iwaoka, A water-soluble cyclic selenide with enhanced glutathione peroxidase-like catalytic activities, *Eur. J. Org. Chem.* 44 (2010) 440–445.
- [22] B.G. Singh, E. Thomas, F. Kumakura, K. Dedachi, M. Iwaoka, K.I. Priyadarsini, One-electron redox processes in a cyclic selenide and a selenoxide: a pulse radiolysis study, *J. Phys. Chem. A* 114 (2010) 8271–8277.
- [23] M. Iwaoka, A. Katakura, J. Mishima, Y. Ishihara, A. Kunwar, K.I. Priyadarsini, Mimicking the lipid peroxidation inhibitory activity of phospholipid hydroperoxide glutathione peroxidase (GPx4) by using fatty acid conjugates of a water soluble selenolane, *Molecules* 20 (2015) 12364–12375.
- [24] M. Iwaoka, N. Sano, Y.Y. Lin, A. Katakura, M. Noguchi, K. Takahashi, F. Kumakura, K. Arai, B.G. Singh, A. Kunwar, K.I. Priyadarsini, Fatty acid conjugates of water-soluble (±)-trans-Selenolane-3,4-diol: effects of alkyl chain length on the antioxidant capacity, *ChemBioChem* 16 (2015) 1226–1234.
- [25] K. Arai, K. Moriai, A. Ogawa, M. Iwaoka, An amphiphilic selenide catalyst behaves like a hybrid mimic of protein disulfide isomerase and glutathione peroxidase, *Chem. Asian J.* 12 (2014) 3464–3471.
- [26] P. Verma, A. Kunwar, K. Arai, M. Iwaoka, K.I. Priyadarsini, Alkyl chain modulated cytotoxicity and antioxidant activity of bioinspired amphiphilic selenolanes, *Toxicol. Res.* 5 (2016) 434–445.
- [27] S. Chakraborty, S.K. Yadav, M. Subramanian, K.I. Priyadarsini, M. Iwaoka, S. Chattopadhyay, DL-trans-3, 4-dihydroxy-1-selenolane (DHS<sub>red</sub>) accelerates healing of indomethacin-induced stomach ulceration in mice, *Free Radic. Res.* 46 (2012) 1378–1386.
- [28] S. Chakraborty, S.K. Yadav, M. Subramanian, M. Iwaoka, S. Chattopadhyay, DL-trans-3,4-Dihydroxy-1-selenolane (DHS<sub>red</sub>) heals indomethacin-mediated gastric ulcer in mice by modulating arginine metabolism, *Biochim. Biophys. Acta* 1840 (2014) 3385–3392.
- [29] A. Kunwar, P. Verma, H.N. Bhilwade, M. Iwaoka, K.I. Priyadarsini, Dihydroxy-selenolane (DHS) supplementation improves survival following whole-body irradiation (WBI) by suppressing tissue-specific inflammatory responses, *Mutat. Res. Genet. Toxicol. Environ. Mutagen* 807 (2016) 33–46.
- [30] A. Kunwar, H. Narang, K.I. Priyadarsini, M. Krishna, R. Pandey, K.B. Sainis, Delayed activation of PKC $\delta$  and NF $\kappa$ B and higher radioprotection in splenic lymphocytes by copper(II)–curcumin (1:1) complex as compared to curcumin, *J. Cell. Biochem.* 102 (2007) 1214–1224.
- [31] S. Jayakumar, D. Pal, S.K. Sandur, Nrf2 facilitates repair of radiation induced DNA damage through homologous recombination repair pathway in a ROS independent manner in cancer cells, *Mutat. Res.* 779 (2015) 33–45.
- [32] E.C. Busby, D.F. Leistritz, R.T. Abraham, L.M. Karnitz, J.N. Sarkaria, The radiosensitizing agent 7-hydroxystaurosporine (UCN-01) inhibits the DNA damage checkpoint kinase Chk1, *Cancer Res.* 60 (2000) 2108–2112.
- [33] S. Dunning, A. Rehman, M.H. Tiebosch, R.A. Hannivoort, F.W. Haijer, J. Woudenberg, F.A. van den Heuvel, M. Buist-Homan, K.N. Faber, H. Moshage, Glutathione and antioxidant enzymes serve complementary roles in protecting activated hepatic stellate cells against hydrogen peroxide-induced cell death, *Biochim. Biophys. Acta* 1832 (2013) 2027–2034.
- [34] M. Raghuraman, P. Verma, A. Kunwar, P.P. Phadnis, V.K. Jain, K.I. Priyadarsini, Cellular evaluation of diselenonitricotinamide (DSNA) as a radioprotector

- against cell death and DNA damage, *Metalomics* 9 (2017) 715–725.
- [35] P.J. Hissin, R. Hilf, A fluorometric method for determination of oxidized and reduced glutathione in tissues, *Anal. Biochem.* 74 (1976) 214–226.
- [36] N.M. Khan, S.K. Sandur, R. Checker, D. Sharma, T.B. Poduval, K.B. Sainis, *Free Radic. Biol. Med.* 51 (2011) 115–128.
- [37] A. Cossarizza, M. Baccarancioni, G. Kalashnikova, C. Franceschi, A new method for the cytofluorometric analysis of mitochondrial membrane potential using the J-aggregate forming lipophilic cation 5,5',6,6'-Tetrachloro-1,1',3,3'-tetra ethyl benzimidazol carbocyanine Iodide (JC-1), *Biochem. Biophys. Res. Commun.* 197 (1993) 40–45.
- [38] M. Fenech, The in vitro micronucleus technique, *Mutat. Res.* 455 (2000) 81–95.
- [39] R.K. Chaurasia, S. Balakrishnan, A. Kunwar, U. Yadav, N. Bhat, K. Anjaria, R. Nairy, B.K. Sapra, V.K. Jain, K.I. Priyadarsini, *Mutat. Res. Genet. Toxicol. Environ. Mutagen* 774 (2014) 8–16.
- [40] T. Sandhya, K.M. Lathika, B.N. Pandey, H.N. Bhilwade, R.C. Chaubey, K.I. Priyadarsini, K.P. Mishra, Protection against radiation oxidative damage in mice by Triphala, *Mutat. Res.* 609 (2006) 17–25.
- [41] K.J. Livak, T.D. Schmittgen, Analysis of relative gene expression data using real-time quantitative PCR and the 2(-Delta Delta C(T)) Method, *Methods* 25 (2001) 402–408.
- [42] A. Kunwar, S. Jayakumar, A.K. Srivastava, K.I. Priyadarsini, Dimethoxycurcumin-induced cell death in human breast carcinoma MCF7 cells: evidence for pro-oxidant activity, mitochondrial dysfunction, and apoptosis, *Arch. Toxicol.* 86 (2012) 603–614.
- [43] T. Hu, M.M. Cathy, M.R. Gregg, J.A. Marilyn, Characterization of p53 in Chinese hamster cell lines CHO-K1, CHO-WBL, and CHL: implications for genotoxicity testing, *Mutat. Res.* 426 (1999) 51–62.
- [44] E.J. Hall, A.J. Giaccia, *Radiobiology for the Radiologist*, Wolters Kluwer Press, 2006, pp. 1–546.
- [45] O.A. Trowell, The sensitivity of lymphocytes to ionizing radiation, *J. Pathol.* 64 (1952) 687–704.
- [46] R.F. Burk, P.F. Surai, *Selenium in Nutrition and Health*, Nottingham University Press, Nottingham, 2006.
- [47] R.A. Sunde, in: D.L. Hatfield, M.J. Berry, V.N. Gladyshev (Eds.), *Selenium its Molecular Biology and Role in Human Health*, Springer, New York, 2006.
- [48] V. Tamasi, J.M. Jeffries, G.E. Arteel, K.C. Falkner, Ebselen augments its peroxidase activity by inducing nrf-2-dependent transcription, *Arch. Biochem. Biophys.* 431 (2004) 161–168.
- [49] M. Tan, S. Li, M. Swaroop, K. Guan, L.W. Oberley, Y. Sun, Transcriptional activation of the human glutathione peroxidase promoter by p53, *J. Biol. Chem.* 274 (1999) 12061–12066.
- [50] E. Lubos, J. Loscalzo, D.E. Handy, Glutathione Peroxidase-1 in Health and Disease: from molecular mechanisms to therapeutic opportunities, *Antioxid. Redox Signal.* 15 (2011) 1957–1997.
- [51] J. Chaudiere, E.C. Wilhelmsen, A.L. Tappel, Mechanism of selenium-glutathione peroxidase and its inhibition by mercaptocarboxylic acids and other mercaptans, *J. Biol. Chem.* 259 (1984) 1043–1050.
- [52] J. Vignard, G. Mirey, B. Salles, Ionizing-radiation induced DNA double-strand breaks: a direct and indirect lighting up, *Radiother. Oncol.* 108 (2013) 362–369.
- [53] J. Liebmann, J. Fisher, C. Lipschultz, R. Kuno, D.C. Kaufman, Enhanced glutathione peroxidase expression protects cells from hydroperoxides but not from radiation or doxorubicin, *Cancer Res.* 55 (1995) 4465–4470.
- [54] G. Iliakis, Y. Wang, J. Guan, H. Wang, DNA damage checkpoint control in cells exposed to ionizing radiation, *Oncogene* 22 (2003) 5834–5847.
- [55] C.S. Sorensen, L.T. Hansen, J. Dziegielewska, R.G. Syljuasen, C. Lundin, J. Bartek, T. Helleday, The cellcycle checkpoint kinase Chk1 is required for mammalian homologous recombination repair, *Nat. Cell Biol.* 7 (2005) 195–201.
- [56] T.N.T. Nguyen, R.S.Z. Saleem, M.J. Luderer, S. Hovde, R.W. Henry, J.J. Tepe, Radioprotection by hymenialdisine-derived checkpoint kinase 2 inhibitors, *ACS Chem. Biol.* 7 (2012) 172–184.
- [57] A.J. Davis, D.J. Chen, DNA double strand break repair via non-homologous end-joining, *Transl. Cancer Res.* 2 (2013) 130–143.
- [58] L.R. Ferguson, N. Karunasinghe, S. Zhu, A.H. Wang, Selenium and its' role in the maintenance of genomic stability, *Mutat. Res.* 733 (2012) 100–110.
- [59] J. Morais, S. Bera, W. Rachidi, P.H. Gann, A.M. Diamond, The effects of selenium and the GPx-1 selenoprotein on the phosphorylation of H2AX, *Biochim. Biophys. Acta* 1830 (2013) 3399–3406.
- [60] M.S.D. Baliga, H. Wang, P. Zhuo, J.L. Schwartz, A.M. Diamond, Selenium and GPx-1 overexpression protect mammalian cells against UV-induced DNA, *Biol. Trace Elem. Res.* 115 (2007) 227–242.
- [61] S.L. Marklund, N.G. Westman, G. Roos, J. Carlsson, Radiation resistance and the Cu Zn superoxide dismutase, Mn superoxide dismutase, catalase, and glutathione peroxidase activities of seven human cell lines, *Radiat. Res.* 100 (1984) 115–123.
- [62] J. Sun, Y. Chen, M. Li, Z. Ge, Role of antioxidant enzymes on ionizing radiation resistance, *Free Radic. Biol. Med.* 24 (1998) 586–593.
- [63] B.E. Sandström, J. Carlsson, S.L. Marklund, Selenite-induced variation in glutathione peroxidase activity of three mammalian cell lines: no effect on radiation-induced cell killing or DNA strand breakage, *Radiat. Res.* 117 (1989) 318–325.
- [64] D.B. Mansur, Y. Kataoka, D.J. Grdina, A.M. Diamond, Radiosensitivity of mammalian cell lines engineered to overexpress cytosolic glutathione peroxidase, *Rad. Res.* 155 (2001) 536–542.



Cite this: DOI: 10.1039/c5tx00331h

## Alkyl chain modulated cytotoxicity and antioxidant activity of bioinspired amphiphilic selenolanes†

Prachi Verma,<sup>a,b</sup> Amit Kunwar,<sup>\*a</sup> Kenta Arai,<sup>c</sup> Michio Iwaoka<sup>c</sup> and K. Indira Priyadarsini<sup>a,b</sup>

A series of amphiphilic conjugates of dihydroxy selenolane (DHS) and monoamine selenolane (MAS), which we had previously reported to inhibit lipid peroxidation and assist the oxidative protein folding reaction respectively in cell free systems, were evaluated for cytotoxicity, associated mechanisms and antioxidant effects in cells. Our results indicated that a fatty acid/alkyl group of variable chain lengths (C<sub>6–14</sub>) as a lipophilic moiety of the DHS/MAS conjugates not only improved their ability to incorporate within the plasma membrane of cells but also modulated their cytotoxicity. In the concentration range of 1–50 μM, C<sub>6</sub> conjugates were non-toxic whereas the long chain (≥C<sub>8</sub>) conjugates showed significant cytotoxicity. The induction of toxicity investigated by the changes in membrane leakage, fluidity, mitochondrial membrane potential and annexin-V–propidium iodide (PI) staining by using flow cytometry revealed plasma membrane disintegration and subsequent induction of necrosis as the major mechanism. Further, the conjugates of DHS and MAS also showed differential as well as nonlinear tendency in cytotoxicity with respect to chain lengths and this effect was attributed to their self-aggregation properties. Compared with the parent compounds, C<sub>6</sub> conjugates not only exhibited better antioxidant activity in terms of the induction of selenoproteins such as glutathione peroxidase 1 (GPx1), GPx4 and thioredoxin reductase 1 (TrxR1) but also protected cells from the AAPH induced oxidative stress. In conclusion, the present study suggests the importance of hydrophilic–lipophilic balance (HLB) in fine tuning the toxicity and activity of bioinspired amphiphilic antioxidants.

Received 8th September 2015,  
Accepted 18th November 2015

DOI: 10.1039/c5tx00331h

www.rsc.org/toxicology

## Introduction

Design, synthesis and development of intracellular enzyme mimics have been the major thrust area of research for biochemists over the years and the latest among these are the glutathione peroxidases (GPx 1, 4 and 7) and protein disulfide isomerase (PDI) models.<sup>1,2</sup> GPx is an important antioxidant enzyme, whose major function is to protect the cells from oxidative stress.<sup>3</sup> To date seven different isoforms of this enzyme have been reported of which GPx1–4 and GPx6 are selenoenzymes, whereas GPx5 and GPx7 are sulfur containing enzymes.<sup>3,4</sup> These isoforms also vary in their subcellular localization, tissue distribution, substrate specificity and apparent biological function.<sup>3,4</sup> Among these, GPx1 is the major cytosolic enzyme accounting for most of the cellular GPx activity,

which catalyses the reduction of hydroperoxide.<sup>3</sup> GPx4 is another cytosolic GPx isoform, which specifically neutralizes the phospholipid hydroperoxides, the chain initiator of lipid peroxidation process.<sup>3</sup> However, GPx7 is localized in the endoplasmic reticulum and cooperates with PDI in catalysing the oxidative folding of newly synthesized polypeptide chains using hydroperoxides as a cofactor.<sup>4,5</sup> Considering the important functions played by the above enzymes in physiological protection against reactive oxygen species (ROS) and protein folding, it is believed that imitating their functions by using a synthetic molecule will be useful in developing drugs for both antioxidant therapy and protein misfolding induced diseases.<sup>1,2</sup> Anticipating this, much effort has been made in the past few decades on the design and synthesis of functionalized organoselenium compounds to mimic GPx-like enzyme and to assist the oxidative protein folding reaction.<sup>6–9</sup>

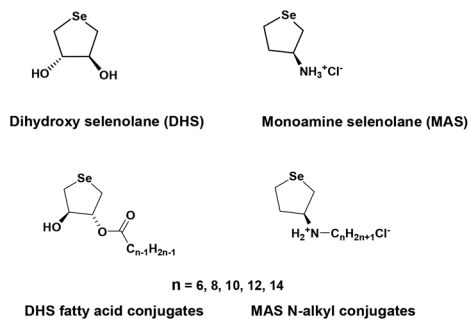
Currently, our group is working on a similar research area and has reported the synthesis of simple water-soluble cyclic organoselenium compounds such as dihydroxy selenolane (DHS) and monoamine selenolane (MAS).<sup>10–13</sup> Both DHS and MAS were shown to exhibit a wide range of biological activities such as free radical scavenging, mimicking the function of GPx1 and catalysing the oxidative protein folding reaction.<sup>10–18</sup>

<sup>a</sup>Radiation and Photochemistry Division, Bhabha Atomic Research Centre, Mumbai - 400085, India. E-mail: kamit@barc.gov.in

<sup>b</sup>Homi Bhabha National Institute, Mumbai - 400085, India

<sup>c</sup>Department of Chemistry, School of Science, Tokai University, Kitakaname, Hiratsuka-shi, Kanagawa 259-1292, Japan

†Electronic supplementary information (ESI) available. See DOI: 10.1039/c5tx00331h



**Scheme 1** Chemical structures of DHS, MAS and their fatty acid/alkyl conjugates.

Interestingly, a number of studies have indicated that conjugation of a drug molecule containing alcohol or amino functional group with a fatty acid/alkyl group to yield an ester and/or amide as a pro-drug can be used as a strategy to take advantage of the metabolic enzymes (like esterase) involved in lipid metabolism to increase the membrane affinity, uptake and bioactivity of active principle or the drug.<sup>19–21</sup> On similar lines, it was hypothesised that incorporating lipophilicity into the structures of DHS and MAS might allow them to localize in the membranes and catalyse the reduction of lipid hydroperoxide as a GPx4 mimic.<sup>17,18</sup> Additionally, such structural modulations can increase their specificity towards the hydrophobic domain of denatured proteins in catalysing oxidative folding reactions like a PDI-GPx7 hybrid system of the cells.<sup>13</sup> Keeping these considerations in view, attaching DHS or MAS to a lipophilic moiety such as fatty acids or alkyl groups of variable chain lengths, hereafter referred as the conjugates of DHS or MAS, appeared to be the right strategy to achieve this.<sup>19–23</sup> Indeed employing cell free systems, we showed that these conjugates of DHS and MAS could inhibit the accumulation of lipid hydroperoxide and catalyse the folding of denatured proteins respectively.<sup>13,17,18</sup> Therefore, such conjugates were projected as better antioxidants compared to the parent compounds such as DHS and MAS.<sup>13,17,18</sup> In continuation to these studies, herein DHS and MAS conjugates were evaluated for cytotoxicity, associated mechanisms and antioxidant effects in cells in order to explore them for future biological applications. The chemical structures of DHS, MAS and their conjugates used in the present study are presented in Scheme 1.

## Materials and methods

### Chemicals

The synthesis and characterisation of parent compounds (DHS and MAS) and their conjugates of varying chain lengths ( $C_{6-14}$ ) were reported previously,<sup>10,13,17,18</sup> except for MAS- $C_6$  conjugate, which was synthesized from MAS and hexanoic acid by following the similar scheme applied for the synthesis of other conjugates of MAS. Spectral data of MAS- $C_6$  are provided as Methods S1.† Butylated hydroxytoluene (BHT), 2,2'-dinitro-

phenyl hydrazine (DNPH), 1,6-diphenyl-1,3,5-hexatriene (DPH), dimethyl sulfoxide (DMSO), glutathione (GSH),  $\beta$ -nicotinamide adenine dinucleotide 2'-phosphate reduced tetrasodium salt hydrate (NADPH), glutathione reductase, cumene hydroperoxide, guanidine hydrochloride, (4,5-dimethylthiazol-2-yl)-2,5-diphenyltetrazolium bromide (MTT), thiobarbituric acid (TBA), trichloroacetic acid (TCA), diethyl pyrocarbonate (DEPC), 2,2'-azobis (2-amidinopropane) dihydrochloride (AAPH), Cellytic M reagent, Tri reagent, 10 $\times$  SYBR green polymerase chain reaction (PCR) mix, thioredoxin reductase (TrxR) assay kit, protease inhibitor cocktail, and amplification grade DNase were purchased from Sigma Chemical Company (St. Louis, MO, USA). 5,5',6,6'-Tetrachloro-1,1',3,3'-tetraethylbenzimidazo-carbocyanine iodide (JC-1) was obtained from Molecular Probes, USA. The lactate dehydrogenase (LDH) assay kit was obtained from Roche, Switzerland. Dulbecco modified Eagle's medium (DMEM), fetal calf serum (FCS), penicillin and streptomycin were purchased from Himedia, India. cDNA synthesis kit was obtained from Thermo Scientific, USA. Annexin-V labeling assay kit was purchased from Abcam, USA. The Bradford protein assay kit was purchased from Bangalore Genei, India. The gene specific primers for RT-PCR were custom synthesized from local agents. All other chemicals with maximum available purity were purchased from reputed local manufacturers/suppliers.

### Cell culture and treatment with selenium compounds

Chinese hamster ovary (CHO) and human breast carcinoma (MCF7) cells obtained from National Centre for Cell Sciences (Pune, India) were cultured in DMEM medium supplemented with 10% fetal calf serum, 100  $\mu\text{g ml}^{-1}$  streptomycin and 100 U  $\text{ml}^{-1}$  penicillin and maintained at 37  $^{\circ}\text{C}$  under 5%  $\text{CO}_2$  and humidified air. The stock solutions of DHS and MAS were prepared in DMEM culture medium and their conjugates in DMSO and then added to the culture medium to obtain the desired concentrations. The hydrolytic stability of the conjugates was confirmed by recording  $^1\text{H}$  NMR spectra of DHS- $C_{14}$  (a representative molecule) in deuterated water as a function of time (Fig. S1†). The concentration of DMSO was kept constant within permissible limits of toxicity (0.25%). The cells treated with selenium compounds were incubated under a humidified atmosphere with 5%  $\text{CO}_2$  for the desired time points prior to assay.

### Cytotoxicity assay

Cytotoxicity was estimated by a colorimetric MTT assay as described previously.<sup>24</sup> Briefly, cells (0.2, 0.5 and 1  $\times 10^4$ ) incubated with increasing concentrations of selenium compounds for 24, 48 and 72 h respectively in triplicates were treated with MTT solution (0.5  $\text{mg ml}^{-1}$  in PBS) for 4 h at 37  $^{\circ}\text{C}$ . The formazan metabolites formed from the reduction of MTT by the living cells were solubilized using 10% SDS in 0.01 N HCl and detected by measuring the absorbance at 550 nm. The percentage (%) cytotoxicity was calculated from the decrease in absorbance of treated samples as compared to that of control cells.

### Cell death characterization

For quantifying the cell death types, cells ( $1 \times 10^5$  cells per ml) treated with selenium compounds for 16 h were labeled using an apoptosis assay kit (Abcam, USA) as per the manufacturer's instructions. The labeled cells were acquired on flow cytometer and characterized using FlowJo® software into four groups: healthy, dead due to loss of membrane integrity, apoptotic and necrotic cells. The following staining criteria were adopted for characterization: cells that did not stain for either Annexin-V or Propidium Iodide (PI) as healthy, which stained only with Annexin-V as apoptotic, both PI and Annexin-V as necrotic and only PI as dead cells with ruptured plasma membrane.<sup>25</sup>

### Mitochondrial membrane potential (MMP) assay

MMP was analyzed using an aggregate-forming lipophilic dye JC-1 as described previously.<sup>26</sup> In brief, cells ( $1 \times 10^4$ ) treated with selenium compounds for 2, 4 and 8 h in quadruplicates were incubated with JC-1 ( $10 \mu\text{g ml}^{-1}$ , final concentration) for 20 min at 37 °C in the dark. Further, the cells were rinsed twice with ice cold PBS and fluorescence emission at 535 and 610 nm was recorded after excitation at 485 and 565 nm respectively using the multimode microplate reader (Synergy H1, BioTek, USA). The representative images showing green emission and red emission were captured using an Olympus fluorescence microscope (Model no. CKX41, Japan) equipped with ProgRes® camera.

### Membrane leakage

Cells ( $1 \times 10^4$ ) cultured in 96-well plates with selenium compounds for 2, 4, 6 and 24 h in quadruplicates were assayed for membrane leakage by determining the activity of LDH leaking out of the cells into the culture medium, according to the manufacturer's instructions (LDH detection kit, Roche, Switzerland).

### Measurement of hemolysis

Blood was collected in heparinised tube by venipuncture from healthy volunteers with strict adherence to the ethical guidelines laid down by the institutional ethics committee of Bhabha Atomic Research Centre. The subject completed the informed consent process prior to participation. The blood samples were processed to obtain a hematocrit or RBCs suspension of 5% in PBS as described previously,<sup>27</sup> stored at 4° C and was used within 6 h. The effect of selenium compounds on hemolysis was evaluated by mixing their varying concentrations with the 5% suspension of RBCs in PBS and incubating this reaction mixture at 37 °C with gentle shaking. The aliquots from this reaction mixture were used in a time course manner for a total time of 2.5 h to determine hemolysis by measuring the absorbance at 540 nm. For reference, RBCs were treated with distilled water and the absorbance of the hemolysate at 540 nm was used as 100% hemolysis.

### Measurement of membrane fluidity

Cell membrane fluidity was measured by estimating the fluorescence anisotropy value of a lipophilic fluorophore, DPH.<sup>28,29</sup> The decrease in anisotropy is indicative of the loss of membrane integrity and/or increase in membrane fluidity.<sup>28–31</sup> In brief cells ( $5 \times 10^6$ ) grown in a culture flask were labeled with DPH at a final concentration of 1  $\mu\text{M}$  at 37 °C for 30 min.<sup>32</sup> Following this, selenium compounds were added to the cells and cultured for 2 and 4 h in a humidified incubator at 37 °C with 5%  $\text{CO}_2$ . Upon incubation, cells were harvested by scraping, washing twice with PBS, and then suspending into 1 ml of PBS. Steady-state fluorescence anisotropy measurements were performed on a Jasco FR-6300 spectrofluorometer equipped with excitation and emission polarizers. The excitation and emission wavelengths were set at 365 and 430 nm, respectively.<sup>32</sup> Fluorescence anisotropy ( $r$ ) was calculated using eqn (1):

$$r = \frac{I_{VV} - GI_{VH}}{I_{VV} + 2GI_{VH}} \quad (1)$$

where  $I_{VV}$  and  $I_{VH}$  are the fluorescence intensities determined at vertical and horizontal orientations of the emission polarizer, respectively, when the excitation polarizer is set in the vertical position. The  $G$  factor, which compensates for differences in detection efficiency for vertically and horizontally polarized light, was calculated from the fluorescence intensity ratio of vertical and horizontal emissions when the excitation polarizer is set in the horizontal position ( $I_{HV}/I_{HH}$ ). The spectral bandwidth of the excitation and emission monochromator was set at 2.5 nm.

### Estimation of selenium incorporation/uptake by cells

Cells ( $5 \times 10^6$ ) in 5 ml of culture medium were treated with selenium compounds (25  $\mu\text{M}$ ) for 1 h and/or 16 h, harvested by scraping, washing three times with PBS, and suspending into one ml of PBS (pH 7.4). The cell lysate was prepared by disrupting cells five times using Branson Sonifier® (Branson Ultrasonics, USA) at 20% amplitude for 2 seconds each. Further the cell lysate was digested with concentrated nitric acid which oxidises selenide ( $\text{Se}^{-2}$ ) to selenite ion  $\text{Se}^{+4}$  and the amount of selenium was estimated by graphite furnace atomic absorption spectrometry (906AA with PAL 3000, GBC Scientific Equipment, Australia) at 197 nm.<sup>33</sup> The total amount (membrane + cellular) of selenium quantified from the cell lysate was normalized with respect to the amount of selenium added to the cells and expressed as percent (%) incorporation/uptake.

### Monitoring interaction of DHS and MAS conjugates with cells

For this, cells ( $5 \times 10^6$ ) in one ml of PBS were labeled with DPH (1  $\mu\text{M}$ , final concentration) as described in previous sections.<sup>32</sup> In order to remove the unbound DPH molecules, the cells were centrifuged at 2000 rpm for 5 min, washed twice with PBS, and resuspended into 1 ml of PBS. To this long chain ( $\text{C}_{14}$ ) conjugates of DHS and MAS were added at desired concentration and their interaction with the plasma mem-

brane of the cells was monitored by following the changes in the fluorescence emission intensity of DPH ( $\lambda_{em} = 430$  nm) as a function of time (0–45 min) on a Jasco FR-6300 spectrofluorometer after excitation at 365 nm. The spectral bandwidth of the excitation and emission monochromator was similar to that of anisotropy studies.

### Measurement of aggregation properties

The aggregation properties of the conjugates of DHS and MAS were studied using fluorescence enhancement<sup>34,35</sup> of DPH. The aqueous solutions of selenium compounds of varying concentrations were incubated with DPH (1  $\mu$ M, final concentration) for 30 min at 37 °C. Following this, fluorescence spectra of the above solutions were recorded. The fluorescence enhancement was calculated as the ratio of the fluorescence emission intensity of DPH at  $\lambda_{em} = 430$  nm in the presence ( $I_r$ ) and absence ( $I_o$ ) of the selenium compounds. The spectral bandwidth of the excitation and emission monochromator was similar to that of anisotropy studies. It should also be noted here that in the above system DPH molecules will be exclusively excited at 365 nm, because selenium compounds used in the study show negligible absorption at this wavelength.

### Measurement of GPx and TrxR activities in cells

Cells ( $5 \times 10^6$ ) in DMEM were treated with selenium compounds for 16 h in a humidified incubator at 37 °C with 5% CO<sub>2</sub>, harvested by trypsinization, washed twice with PBS and lysed in cellytic M® containing protease inhibitors cocktail. The lysate was subjected to centrifugation at 10 000g for 10 min and the supernatant obtained was estimated for TrxR activity using a commercially available kit as per the manufacturer's instructions and GPx activity was estimated according to a method described previously.<sup>36</sup> The protein content in the cell lysate was determined using the Bradford protein assay kit according to the manufacturer's instructions and results are presented as U mg<sup>-1</sup> of protein.

### Gene expression studies

Following treatment with selenium compounds for 16 h as in the case of antioxidant enzyme studies, total RNA was isolated from the cells ( $1 \times 10^6$ ) using TRI reagent (Sigma Chemical Company, St. Louis, MO, USA) according to the manufacturer's instructions. Four micrograms of total RNA was used for the synthesis of cDNA by reverse transcription (cDNA synthesis kit, Thermo Scientific, USA) and real-time PCR was carried out using the template (cDNA), SYBR green master mix and gene specific primers in a Rotor Gene 3000 (Corbett Life Science) machine as described previously. The threshold cycle (CT) values obtained from the above runs were used for calculating the relative expression levels of genes as per the method described previously.<sup>37</sup> The expressions of genes were normalized against a housekeeping gene,  $\beta$ -actin. The primers (forward and reverse) used for cDNA amplification are shown in Table 1.

**Table 1** List of RT-PCR primers used in the gene expression studies

Name of gene	Primer sequence
$\beta$ -actin	5'-GGCTGTATTCCCTCCATCG-3' 5'-CCAGTTGGTAACAATGCCATGT-3'
GPx1	5'-AGTCCACCGTGTATGCCTTCT-3' 5'-GAGACGCGACATTCTCAATGA-3'
GPx4	5'-TGTGCATCCCGGATGATT-3' 5'-CCCTGTACTTATCCAGGCAGA-3'
TrxR1	5'-CCCCTTGCCCCAACTGTT-3' 5'-GGGAGTGTCTTGGAGGGAC-3'

### AAPH induced lipid peroxidation and protein carbonylation

Cells ( $5 \times 10^6$ ) treated with selenium compounds for 16 h were further incubated with AAPH (30 mM) for 6 h in a humidified incubator at 37 °C with 5% CO<sub>2</sub> and the cell lysate was prepared as described in the previous section. Lipid peroxidation and protein carbonylation in the cell lysate were assayed according to TBARS and DNPH methods as described previously.<sup>36</sup> The amount of TBARS was calculated from a standard plot generated using 1,1,3,3-tetraethoxypropane and expressed as nmol of TBARS per mg of protein. The amount of protein carbonyls was calculated using the extinction coefficient of DNPH ( $\epsilon_{370} = 22\,000$  M<sup>-1</sup> cm<sup>-1</sup>) and expressed as nmol carbonyls per mg of protein.

### Statistical analysis

All the experiments were carried out in triplicate and repeated at least two times. The results are presented as means  $\pm$  SEM,  $n = 3$  from an independent experiment. The data were analyzed by one-way ANOVA using Origin (version 6.1) software to confirm the variability of the data. The  $P$  values  $< 0.05$  were considered as statistically significant.

## Results

### Effect of chain length on the cytotoxicity of DHS & MAS conjugates

The cytotoxic effects of DHS, MAS and their conjugates (C<sub>6–14</sub>) in CHO cells evaluated using the MTT assay are shown in Fig. 1. The results indicate that the parent compounds, DHS and MAS in the concentration range (1–50  $\mu$ M) did not exhibit significant cytotoxicity even after 72 hours of their addition into the cells. The shortest chain (C<sub>6</sub>) conjugates of DHS and MAS did not show cytotoxicity up to a treatment concentration of 30  $\mu$ M. Further increase in treatment concentration up to 50  $\mu$ M showed a concentration and time dependent marginal increase (~8–15%) in the cytotoxicity. Longer chain (>C<sub>6</sub>) conjugates of DHS and MAS exhibited significantly higher cytotoxicity compared to the parent compounds or C<sub>6</sub> conjugates at all treatment concentrations and time points (Fig. 1). At an identical treatment concentration, the cytotoxicity effects of DHS conjugates followed the order C<sub>6</sub> < C<sub>8</sub> < C<sub>10</sub> ~ C<sub>12</sub> > C<sub>14</sub>,

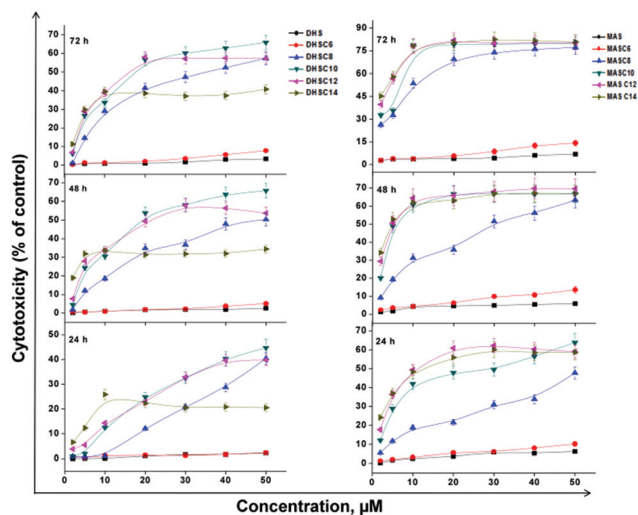


**Fig. 1** Cytotoxic effects of DHS, MAS and their conjugates ( $C_{6-14}$ ) in CHO cells. Cytotoxicity was evaluated by the MTT assay at different time points (24, 48 and 72 h) after the addition of the varying concentrations (1–50  $\mu\text{M}$ ) of DHS, MAS and their conjugates ( $C_{6-14}$ ). Cytotoxicity is expressed as percentage of the control cells (DMSO, 0.25%). Results are presented as mean  $\pm$  SEM,  $n = 3$ .

whereas for MAS conjugates it was seen as  $C_6 < C_8 < C_{10} \sim C_{12} \sim C_{14}$  (Fig. S2A and S2B<sup>†</sup>). The conjugates of intermediate chain lengths ( $C_{8-10}$  of DHS and  $C_8$  of MAS) exhibited a concentration (1–50  $\mu\text{M}$ ) and time (24–72 h) dependent increase in cytotoxicity. However, the conjugates of longer chain lengths ( $C_{12-14}$  of DHS and  $C_{10-14}$  of MAS) showed a saturation effect (Fig. 1). Between the DHS and MAS conjugates, the former showed significantly lesser cytotoxicity than the latter at each chain length, treatment concentration, when evaluated up to 48 h time point (Fig. 1).

In continuation to this study, the cytotoxic effects of the above compounds were also evaluated in a tumor cell type, MCF7. As in the case of CHO cells, the parent compounds DHS and MAS were not toxic to MCF7 cells in the concentration range (1–50  $\mu\text{M}$ ) tested (Fig. S3<sup>†</sup>). However, the conjugates exhibited similar trends of cytotoxicity with respect to the lipophilic chain lengths ( $C_{6-14}$ ), treatment concentrations (1–50  $\mu\text{M}$ ) and time points (24–72 h) (Fig. S3<sup>†</sup>). Additionally at an identical treatment concentration, DHS conjugates exhibited comparable toxicity between the CHO and MCF7 cells, whereas MAS conjugates showed marginally higher toxicity in MCF7 cells compared to CHO cells (Fig. 1, S2 and S3<sup>†</sup>). In a control experiment, treatment with the fatty acids of variable chain lengths ( $C_6$  to  $C_{14}$ ) without any selenide moiety for 72 hours in the 1–50  $\mu\text{M}$  concentration range did not induce significant toxicity in either of the cell types (Fig. S4<sup>†</sup>).

Further to characterize the nature of cell death induced by the conjugates, CHO cells treated with the shortest ( $C_6$ ) and longest ( $C_{14}$ ) chain conjugates of DHS and MAS at an identical concentration of 25  $\mu\text{M}$  were subjected to Annexin-V-PI staining. The representative dot plots and bar graphs are shown in

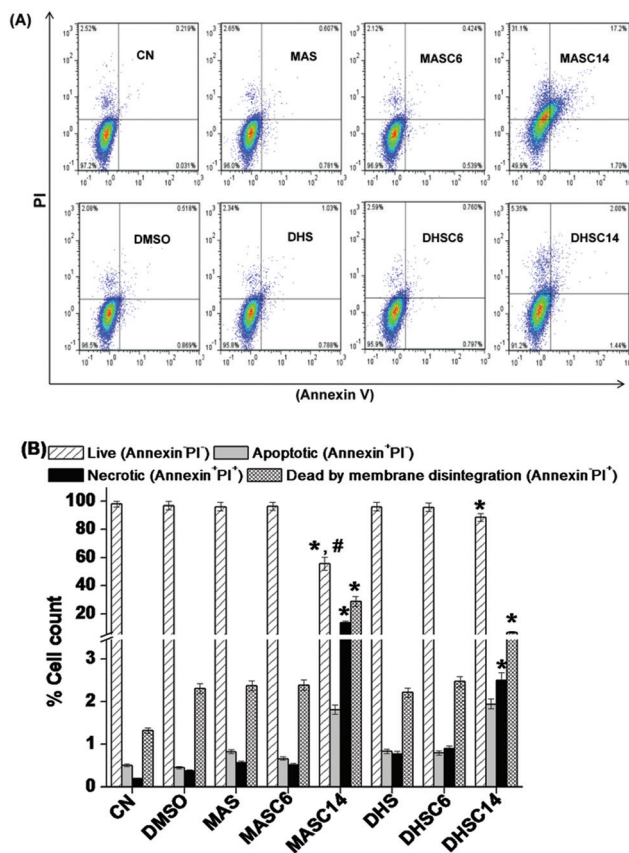


**Fig. 2** Characterization of cell death induced by the conjugates ( $C_6$  and  $C_{14}$ ) of DHS and MAS by Annexin-V and PI staining in CHO cells. The assay was performed at 16 h after addition of the conjugates ( $C_6$  and  $C_{14}$ ) of DHS and MAS to CHO cells at a concentration of 25  $\mu\text{M}$ . (A) Representative dot plots showing distribution of cells under different treatment conditions after flow cytometry acquisition. (B) Bar graph showing percentage (%) live, apoptotic, necrotic and dead cells (membrane disintegration) under different treatment conditions. Results are presented as mean  $\pm$  SEM,  $n = 3$ . \* $p < 0.05$  as compared to the DMSO control group and # $p < 0.05$  as compared to the DHS- $C_{14}$  treated group.

Fig. 2A and B respectively. The results indicated that the parent compounds DHS and MAS and their  $C_6$  conjugates neither induced apoptosis nor necrosis confirming the non-toxic nature of these compounds. However, the  $C_{14}$  conjugates of DHS and MAS showed a significant decrease in the counts of viable cells. The major mechanism of cell death was identified to be membrane disruption leading to necrosis as seen by the significant increase in the number of Annexin<sup>−ve</sup>PI<sup>+ve</sup> and Annexin<sup>+ve</sup>PI<sup>+ve</sup> cells in these groups (Fig. 2A and B). In line with previous results, the number of viable cells was significantly lower in the MAS- $C_{14}$  treated group as compared to DHS- $C_{14}$  suggesting the higher toxicity of former than the latter (Fig. 2A and B).

Since necrosis is also marked by the acute mitochondrial depolarization, the MMP was estimated using a fluorescent probe, JC-1 under similar experimental conditions and the

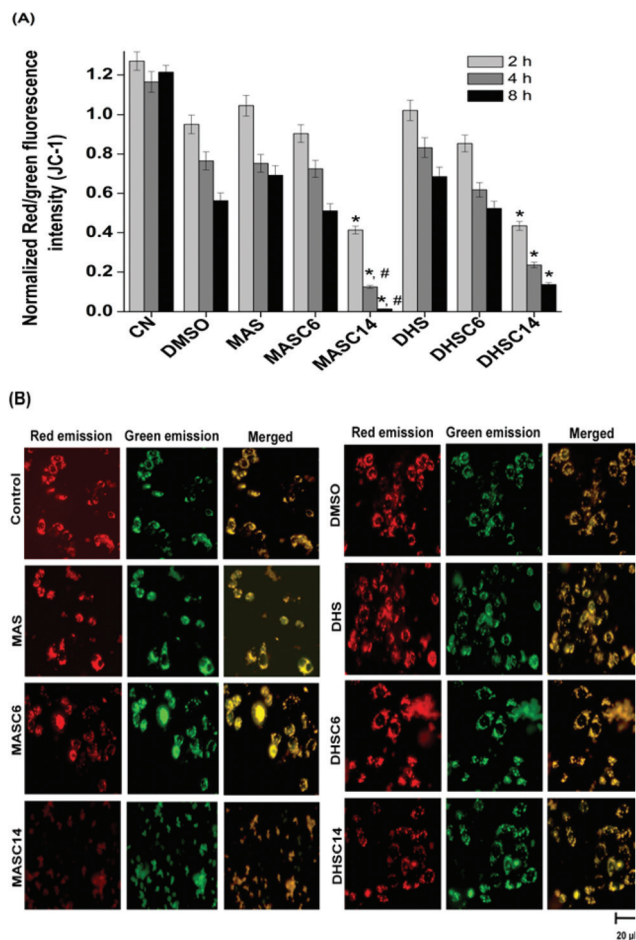


**Fig. 3** Effect of the treatment of 25  $\mu\text{M}$  of the conjugates ( $C_6$  and  $C_{14}$ ) of DHS and MAS on the mitochondrial membrane depolarization in CHO cells. The mitochondrial membrane potential was determined by JC-1 staining in CHO cells: (A) Quantitative analysis of red and green fluorescence intensity ratio at 2, 4 and 8 h after addition of selenium compounds to cells. (B) Representative photographs of red and green fluorescence emission at 8 h after addition of selenium compounds to cells. Results are presented as mean  $\pm$  SEM,  $n = 3$ . \* $p < 0.05$  as compared to the DMSO control group and # $p < 0.05$  as compared to the DHS- $C_{14}$  treated group.

results are shown in Fig. 3A and B. Treatment of cells with  $C_{14}$  conjugates of DHS and MAS showed a much faster decrease in MMP (estimated as the ratio of red and green fluorescence emission of JC-1 at 535 and 610 nm respectively) as a function of time compared to  $C_6$  conjugates or the parent compounds (DHS and MAS) and vehicle (DMSO) control, suggesting acute mitochondrial depolarization by  $C_{14}$  conjugates leading to necrosis (Fig. 3A and B). Here also, MAS- $C_{14}$  in comparison with DHS- $C_{14}$  was more effective in reducing the MMP in a time dependent manner (Fig. 3A and B). For example at the end of 8 h, the ratios of red and green fluorescence emission intensity were observed to be 0.13 and 0.01 respectively for cells treated with  $C_{14}$  conjugates of DHS and MAS as compared to 1.21 of control cells (Fig. 3A).

### Effect of chain length on membrane disruption/integrity by DHS & MAS conjugates

The leakage of the intracellular enzyme LDH from cells is considered as a marker of membrane disruption/toxicity. Organochalcogens are known to inhibit LDH,<sup>38</sup> therefore it is important to know the suitability of LDH assay to be used in the present study. In order to address this, the effect of the treatment with DHS or MAS on the activity of LDH, freshly isolated from the cells, was evaluated. The results indicated that neither DHS nor MAS affected the activity of LDH (Fig. S5†). Based on this, the effect of DHS, MAS and their conjugates on the plasma membrane integrity was evaluated at an identical treatment concentration of 25  $\mu\text{M}$  by monitoring the leakage of an intracellular enzyme LDH from cells to the culture medium. The results are shown in Fig. 4A and B. It can be seen from the figure that parent compounds DHS and MAS did not induce much leakage of LDH from the cells. Treatment with conjugates ( $C_{6-14}$ ) of DHS and MAS led to the time dependent increase in the leakage of LDH from the cells compared to the respective parent compounds, and this effect was significant for conjugates with chain lengths longer than  $C_6$  suggesting their ability to cause plasma membrane disruption (Fig. 4A and B). DHS conjugates showed a biphasic response with regard to the effect of chain length on LDH leakage at each time point. For example, LDH leakage increased with increasing chain lengths from  $C_6$  to  $C_{10}$ , saturated at  $C_{12}$  and then decreased at  $C_{14}$ . In comparison, MAS conjugates exhibi-

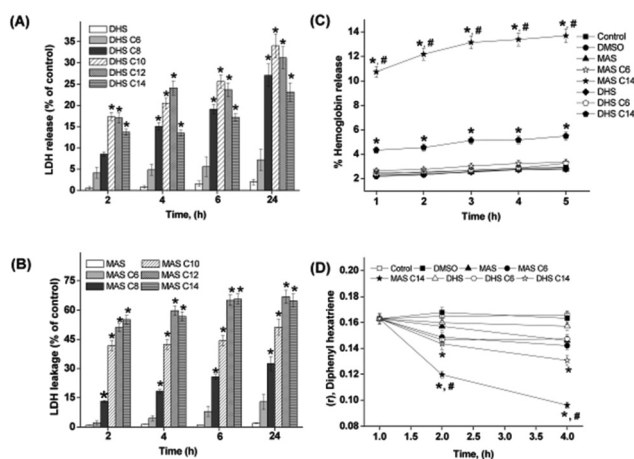


**Fig. 4** Effect of the treatment of DHS, MAS and their conjugates ( $C_{6-14}$ ) on membrane integrity in CHO cells. (A) & (B) Membrane leakage measured as % LDH release induced by the DHS and MAS series of compounds (1–50  $\mu\text{M}$ ) respectively at 2, 4, 6 and 24 h after their addition to the cells. \* $p < 0.05$  as compared to the DHS or MAS treated group (C) percent (%) hemolysis in human RBCs induced under different treatment conditions for a total time of 2.5 h. (D) Plasma membrane fluidity measured as the changes in the anisotropy value of a membrane bound fluorophore, DPH at 2 and 4 h after addition of different selenium compounds at 25  $\mu\text{M}$  to the cells.  $\lambda_{\text{ex}} = 365 \text{ nm}$ ,  $\lambda_{\text{em}} = 430 \text{ nm}$ . Results are presented as mean  $\pm$  SEM,  $n = 3$ . \* $p < 0.05$  as compared to the DMSO control group and # $p < 0.05$  as compared to DHS- $C_{14}$ .

ted a chain length dependent increase in LDH release until  $C_{12}$  and the saturation effect at  $C_{14}$  at each time point.

Among the DHS and MAS conjugates the former was less effective in causing LDH leakage than the latter at each chain length.

The effect of lipophilic chain length on plasma membrane disruption was revalidated using RBC hemolysis as a model system wherein treatments with 25  $\mu\text{M}$  of parent compounds (DHS and MAS) and their  $C_6$  conjugates did not cause hemolysis as time progressed (0.5 to 2.5 h) (Fig. 4C). Whereas treatments with longest conjugates (DHS- $C_{14}$  and MAS- $C_{14}$ ) at identical concentration showed a time dependent increase in hemolysis and this effect was found to be significant for MAS- $C_{14}$  compared to DHS- $C_{14}$  supporting our earlier observations of differential effects by these two compounds (Fig. 4C).

Since plasma membrane disruption is marked by the changes in its fluidity, this parameter was evaluated in CHO cells as an anisotropy value of a fluorophore, DPH is known to be localized in the plasma membrane.<sup>29,32</sup> The results shown in Fig. 4D indicate that the control cells exhibited a maximum anisotropy value of 0.17. Treatments with parent compounds (DHS and MAS) at 25  $\mu\text{M}$  did not affect the anisotropy value of DPH even after 4 h of their addition to cells, suggesting that these compounds did not cause change in fluidity of the plasma membrane (Fig. 4D). Treatments with  $C_6$  and  $C_{14}$  conjugates of DHS and MAS at identical concentration showed a time dependent decrease in anisotropy of DPH and this effect was more prominent at longer chain lengths ( $C_{14}$ ). The anisotropy value of DPH in cells treated with DHS- $C_{14}$  and MAS- $C_{14}$  for 4 h was 0.13 and 0.09 respectively (Fig. 4D). These results thus suggested that the conjugates of DHS and MAS caused membrane disruption resulting in increase in membrane fluidity.

#### Effect of chain length on the incorporation of DHS & MAS conjugates within membranes

From the above studies, it was anticipated that the conjugation of the lipophilic moiety of variable chain lengths ( $C_{6-14}$ ) with DHS and MAS might be affecting their ability to incorporate within membranes and/or cells. In order to address this, the incorporation of DHS, MAS and their conjugates within 1 h after addition to cells (CHO) at a treatment concentration of 25  $\mu\text{M}$  was estimated in terms of the selenium level. The bar graph representing the percent loading under different treatment conditions is shown in Fig. 5A. From the figure, it is clear that the basal selenium level in control cells and those treated with parent compounds such as DHS and MAS was undetectable (<10 ng). Treatment with the conjugates of DHS and MAS led to a significant increase in the percent of selenium incorporated into the cells compared to that of the amount present in the control cells (Fig. 5A). The MAS conjugates showed significantly higher loading compared to the DHS conjugates at each chain length (Fig. 5A). The effect of lipophilic chain length on the cellular incorporation of both DHS and MAS conjugates was observed to be biphasic. For

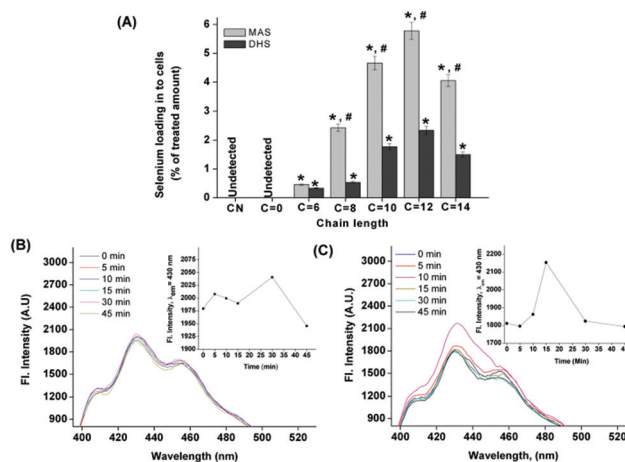


**Fig. 5** Studies on the affinity of DHS, MAS and their conjugates towards plasma membrane in CHO cells. (A) Effect of alkyl chain length on the incorporation/uptake of selenium into membranes/cells following treatment with DHS, MAS and their conjugates ( $C_{6-14}$ ) at 25  $\mu\text{M}$  for an hour. The amount of selenium in the cells was determined as described in the materials and methods section and normalized with respect to the treated amount of selenium. Results are presented as mean  $\pm$  SEM,  $n = 3$ . CN – untreated control cells. \* $p < 0.05$  as compared to the DMSO control group and # $p < 0.05$  as compared to the DHS conjugates at each chain length. (B) & (C) Overlapped fluorescence spectra of CHO cells stained with a membrane bound fluorophore, DPH recorded soon after the addition of DHS- $C_{14}$  and MAS- $C_{14}$  respectively to the cell suspension in a time course manner (0–45 min). The excitation was performed at 365 nm. Insets of (B) & (C) show the interaction/binding of DHS- $C_{14}$  and MAS- $C_{14}$  respectively with the plasma membrane monitored in terms of the changes in the fluorescence emission ( $\lambda_{em} = 430$  nm) intensity of DPH.

example the percent incorporation increased with increasing chain length up to  $C_{12}$  and a further increase in chain length to  $C_{14}$  led to the decrease in loading. The uptake studies performed at an early time point (1 h) may be indicative of the incorporation of conjugates mainly into the plasma membrane of cells. Therefore, the above studies suggested that between DHS and MAS conjugates the latter exhibited greater affinity for cellular membranes and for each of these two series of compounds, such affinity increased up to a length of  $C_{12}$ .

In order to revalidate the above conclusion, the binding/interaction of the longest  $C_{14}$  conjugates of DHS and MAS to the plasma membrane of CHO cells was studied employing DPH as a probe. The fluorescence of DPH is highly sensitive to the changes in polarity of the membrane microenvironment.<sup>28,29,32</sup> Earlier it has been shown that time resolved changes in the fluorescence intensity of DPH can be used as a means to understand the binding of a hydrophobic drug to the plasma membrane of cells.<sup>39</sup> In the present study, addition of DHS- $C_{14}$  to the cells at 25  $\mu\text{M}$  did not cause much change in the fluorescence intensity of DPH during the initial 30 min of interaction but decreased at later time points (Fig. 5B). Whereas treatment with MAS- $C_{14}$  at identical concentration led to a sharp increase in DPH fluorescence by 15 min and then decreased in a time dependent manner (Fig. 5C).

The binding of a lipophilic conjugate to plasma membrane is expected to increase the hydrophobic environment around the DPH molecules resulting in the increase in its fluorescence intensity. However, membrane disruption by the conjugates can cause a decrease in DPH fluorescence. Therefore, our results confirmed that DHS-C<sub>14</sub> exhibited lesser affinity towards cells membranes compared to MAS-C<sub>14</sub>.

### Effect of chain length on the self-aggregation properties of DHS and MAS conjugates

The self-aggregation behaviour of the conjugates (C<sub>6–14</sub>) of DHS and MAS was monitored by measuring the fluorescence intensity ( $\lambda_{em} = 430$  nm) of DPH as a function of their increasing concentrations (2–50  $\mu$ M) in aqueous solution. DPH shows weak fluorescence in aqueous solution, however incorporation of this molecule into micellar structure or the aggregates, causes a significant increase in the fluorescence intensity.<sup>32</sup> The representative emission spectrum and fluorescence enhancement ratio of DPH under different treatment conditions are shown in Fig. 6A–D.

Our results indicated that the fluorescence intensity of DPH did not change much as a function of concentration of DHS or MAS conjugates up to a chain length of C<sub>8</sub> and C<sub>10</sub> respectively (Fig. 6A–D). However, C<sub>10–14</sub> conjugates of DHS and C<sub>12–14</sub> conjugates of MAS exhibited a concentration and chain length dependent increase in the fluorescence intensity of DPH suggesting formation of aggregates by the long chain conjugates at higher concentrations (Fig. 6A–D). Between the longer

conjugates ( $\geq C_{10}$ ) of DHS and MAS of identical chain length and concentration, the former showed significantly higher enhancement in the fluorescence emission of DPH compared to the latter. For example at a concentration of 25  $\mu$ M, the longest chain conjugates, DHS-C<sub>14</sub> and MAS-C<sub>14</sub> showed enhancement in the fluorescence intensity of DPH by  $\sim 20$  and  $\sim 8$  folds respectively (Fig. 6A–D). This confirmed that longer chain ( $\geq C_{10}$ ) conjugates of DHS exhibited higher tendency of forming aggregates compared to MAS conjugates of identical chain length.

### Effect of chain length on the antioxidant activity of DHS & MAS conjugates in the cells

The nontoxic C<sub>6</sub> conjugates of DHS and MAS screened from the above experiments were further evaluated for antioxidant effects in CHO cells in terms of their ability to modulate the expression of important antioxidant selenoenzymes (such as GPx1, GPx4 and TrxR1) and also to protect the cells from AAPH induced oxidative damage like lipid peroxidation and protein carbonylation. The results were compared with those of the parent compounds (DHS and MAS). Since the incorporation/uptake of parent compounds into cells was undetectable for a treatment time of 1 h, we increased the treatment time to 16 h and then estimated the uptake. The results indicated that the uptake of DHS and MAS increased only in nanograms, which corresponded to  $0.15 \pm 0.01\%$  and  $0.23 \pm 0.01\%$  respectively. The uptake of C<sub>6</sub> conjugates of DHS and MAS at 16 h was higher in comparison with parent compounds and showed a saturation effect with respect to early detection (1 h). Furthermore, the results on the antioxidant activities as shown in Fig. 7A revealed that treatments with DHS and MAS at a concentration of 25  $\mu$ M led to a moderate increase in TrxR activity but a significant increase in GPx activity. The compound MAS was more effective than DHS in inducing the GPx activity. In agreement with the above results, DHS and MAS showed significantly higher induction in the expressions of GPx isoforms (GPx1 and GPx4) than TrxR1 at the mRNA level (Fig. 7B). Whereas the expression of GPx1 was higher in MAS treated cells, another important isoform GPx4 was induced more with DHS (Fig. 7B). The C<sub>6</sub> conjugates of DHS and MAS showed even higher induction in the expressions of GPx and TrxR both at mRNA and activity levels compared to their respective parent compounds (Fig. 7A and B). Further, pretreatment of cells with DHS or MAS caused significant reduction in the levels of malondialdehyde in cells exposed to AAPH indicating their ability to protect from the lipid peroxidation (Fig. 7C). The C<sub>6</sub> conjugates of DHS and MAS showed an increase in the protection of cells from AAPH induced lipid peroxidation and protein carbonylation compared to the respective parent compounds (Fig. 7C). With regard to the antioxidant enzymes, the exposure of cells to AAPH did not affect the activity of GPx, but led to a significant increase in the activity of TrxR (Fig. 7D). The pretreatment with DHS or MAS did not show much change in the activities of GPx and TrxR compared to the AAPH group (Fig. 7D). On contrary pretreatment with C<sub>6</sub> conjugates of DHS and MAS showed significantly elevated GPx

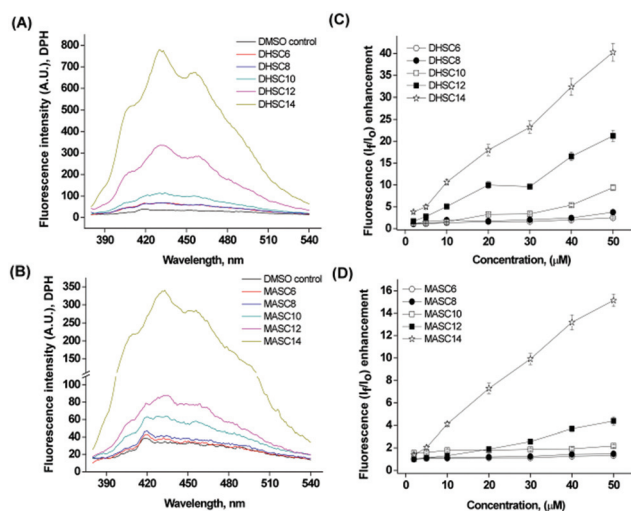


**Fig. 6** Aggregation studies of DHS, MAS and their conjugates (C<sub>6–14</sub>) using fluorescence enhancement of a lipophilic fluorophore DPH. (A) & (B) Overlapped fluorescence spectra of DPH in aqueous solutions of the increasing concentrations (2–50  $\mu$ M) of DHS and MAS series of compounds respectively containing 0.25% DMSO. (C) & (D) Enhancement in the fluorescence intensity of DPH induced by DHS and MAS series of compounds respectively.  $I_f$  – Fluorescence intensity in the presence of selenium compounds.  $I_o$  – Fluorescence intensity in the absence of selenium compounds.  $\lambda_{ex} = 365$  nm,  $\lambda_{em} = 430$  nm. Results are presented as mean  $\pm$  SEM,  $n = 3$ .

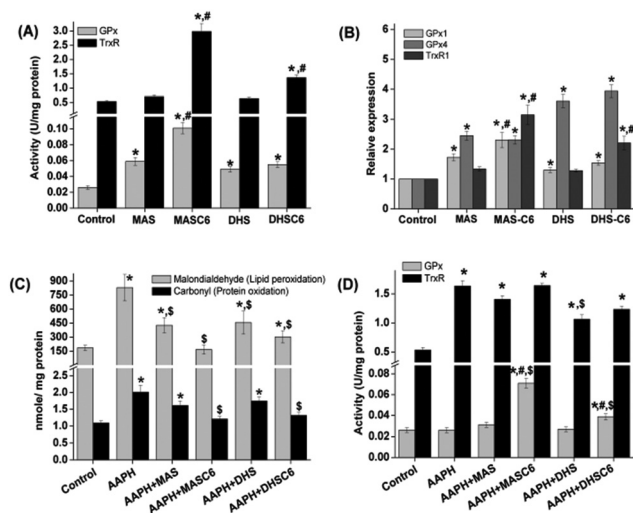


**Fig. 7** Antioxidant effects of 25  $\mu\text{M}$  of DHS, MAS and their  $\text{C}_6$  conjugates in CHO cells. (A) Modulation in the activities of GPx and TrxR at 16 h after addition of the compounds. (B) Modulation in the expression of genes such as *GPx1*, *GPx4*, and *TrxR1* at 16 h after addition of the compounds. The expressions of above genes in different treatment groups were normalized against the control group and the relative expression changes have been plotted. Actin expression was used as internal control for all the genes. (C) Protective effect of the pretreatment with compounds against the AAPH (30 mM) induced lipid peroxidation and protein carbonylation estimated at 6 h post exposure by TBARS and DNPH assays respectively. (D) Effect of the pretreatment with compounds on activities of GPx and TrxR at 6 h post exposure of AAPH (30 mM). Results are presented as means  $\pm$  SEM,  $n = 3$ . \* $p < 0.05$  as compared to the control group, # $p < 0.05$  as compared to respective parent compounds DHS and/or MAS, \$  $p < 0.05$  as compared to the AAPH alone group.

activity and no change in TrxR activity compared to the AAPH group (Fig. 7D). Taken together, these results suggested that  $\text{C}_6$  conjugates are better than the parent compounds in exhibiting antioxidant effects in the cell.

## Discussion

With an aim of designing new selenium based antioxidants we had earlier established that combining the fatty acid/alkyl group as a lipophilic unit with the redox active hydrophilic selenide moiety such as DHS and MAS is an effective approach.<sup>13,17,18</sup> For example, the amphiphilic fatty acid conjugates of DHS were shown to inhibit the lipid peroxidation in the liposomal model system through the GPx4 like catalytic mechanism involving  $2e^-$  reduction, whereas the *N*-alkylated conjugates of MAS catalysed the oxidative folding of misfolded/denatured proteins like a PDI-GPx7 hybrid model.<sup>13,17,18</sup> These different activities of the conjugates of DHS and MAS were also reported to be dependent on the chain length of the lipophilic moiety. Since the lipophilicity of a compound is often associated with biological functions as

well as the toxicity,<sup>40–43</sup> the first parameter that is necessary to be evaluated prior to biological application of the conjugates of DHS and MAS as GPx4 and PDI-GPx7 mimics respectively is their toxicity to the cells.

In order to address this, in the present study, we used two different cell lines CHO and MCF7 representing the normal model and tumor cell type respectively for the cytotoxicity evaluation.<sup>40–44</sup> Our results indicated that neither the parent compounds (DHS and MAS) nor the free fatty acids ( $\text{C}_6$  to  $\text{C}_{14}$ ) in the concentration range of 1–50  $\mu\text{M}$  were toxic to CHO and MCF7 cells. However, the conjugates ( $\geq \text{C}_8$ ) of DHS and MAS in a similar concentration range were significantly toxic to both the cell types. This prompted us to believe that the amphipathic character resulting from the combination of a hydrophilic head as selenide and lipophilic tail as a fatty acid/alkyl group makes the conjugates membrane active, which finally dictates the cytotoxicity.<sup>41,45–48</sup> Interestingly, the fatty acid conjugates of similar chain length containing oxygen in place of selenium in the ring structure (furan fatty acids) have been reported to be antioxidants and non-toxic to cells, confirming that the observed cytotoxicity is indeed due to the selenium moiety.<sup>49,50</sup> Further, a recent report indicated that the polarity of the hydrophilic head group affects the surface properties of the amphipathic surfactants.<sup>51</sup> Taken together, it can be inferred that selenium by influencing the polarity of the hydrophilic head might be controlling the surface properties and in turn the cytotoxicity of DHS and MAS conjugates. As expected the affinity of the conjugates of DHS and MAS for the plasma membrane was evidenced in terms of their ability to enhance the incorporation of selenium in the membranes per cell within 1 h of the treatment. The nature of cell death induced by the conjugates of DHS and MAS was identified to be necrosis as supported by the increase in the number of  $\text{PI}^{+ve}\text{AnninV}^{+ve}$  stained cells through flow cytometry.<sup>25</sup> The plausible mechanisms of cytotoxicity could be the vertical insertion of the conjugates of DHS and MAS into plasma membrane with their selenide and fatty acid/alkyl chain groups facing towards the polar head and hydrophobic tail of lipid bilayer respectively.<sup>46,48</sup> Since the lipophilic chains in conjugates are saturated, it may further allow them to pack together with the hydrophobic tails of the lipids in membrane through hydrophobic interactions to form microcluster or aggregates.<sup>46,48,49</sup> Such aggregates can finally cause local disturbance in the dynamics and packing order of lipids and proteins in the membrane resulting in disintegration or pore formation followed by leakage of intracellular constituents, acute depolarisation of mitochondria (the power house of cell) and necrosis.<sup>47,48,52–54</sup> Supporting this hypothesis, the conjugates of DHS and MAS were observed to cause an increase in the fluidity (as a drop in anisotropy value of DPH) of plasma membrane, leakage of intracellular proteins like LDH in CHO cells and haemoglobin in RBCs and finally membrane disintegration ( $\text{PI}^{+ve}$  cells). These findings are also in agreement with the previous studies wherein similar mechanism of membrane disintegration and subsequent cytotoxicity has been proposed for surface active amphipathic drugs like *N*-alkylated imino

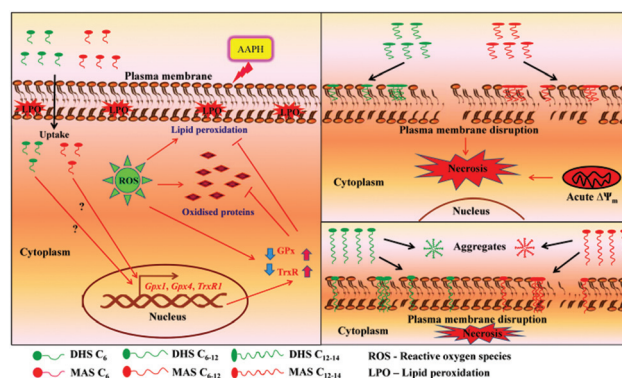
sugars and antimicrobial peptides such as magainin and cecepins.<sup>41,47,48</sup>

Further, MAS conjugates exhibited significantly higher toxicity than DHS conjugates at each chain length. Additionally, the effect of chain length ( $C_{6-14}$ ) on the cytotoxic effect of the conjugates of DHS and MAS were observed to be nonlinear, where the maximum toxicity was seen at  $C_{10}$ . It is well known that the plasma membranes of the mammalian cells are negatively charged.<sup>55</sup> Since the conjugates of MAS and DHS are cationic and neutral in nature respectively, the insertion of the former into the plasma membranes is expected to be higher compared to the latter and thus accounting for their differential toxicity. This is in concurrence with previous reports wherein cationic surface active drugs have been shown to be more toxic than the neutral ones.<sup>48,56</sup> Moreover, the membranes of transformed (tumor) cells have been shown to be more negatively charged than that of normal cells<sup>55</sup> and that is why we observed MAS conjugates but not the DHS conjugates exhibiting higher toxicity in MCF7 compared to CHO cells. In addition to the charge differences, DHS and MAS conjugates being amphiphilic in nature may also differ in their surface properties contributing to their differential cytotoxicity.<sup>47,48</sup> In line with this, our results on fluorescence enhancement of DPH indicated that the long chain ( $\geq C_{10}$ ) conjugates of DHS and MAS formed aggregates as a function of concentration and this effect was prominent in the case of the DHS conjugates. Such differences can be justified by the explanation that the aggregation of MAS conjugates being cationic in nature would be less favorable due to repulsive forces. Since DHS conjugates showed higher aggregation behavior, it can be understood that due to this supramolecular formation there would be lesser availability of free molecules to interact with the cell membrane causing lesser cytotoxicity.<sup>46</sup> This was indeed supported by the fact that in all our studies, the  $C_{14}$  conjugates of DHS and MAS exhibited most notable differences in terms of cellular effects (such as cytotoxicity, membrane disruption, incorporation). Further, the nonlinear relationship observed between the cytotoxicity and chain length ( $C_{6-14}$ ) of the lipophilic moiety of DHS and MAS conjugates could also be attributed to their self-aggregation properties.<sup>23</sup> It is important to note here that the conjugates of DHS and MAS in the concentration range of 1–50  $\mu\text{M}$  did not exhibit the point of inflection (concentration of the compound at which a dramatic increase in DPH fluorescence occurred) suggesting that concentrations at which these compounds evoked significant toxicity were much lower than their critical micelle concentrations (CMCs).<sup>33,35,41</sup> This is in agreement with our observation on the mechanism of cell death induced by these compounds through necrosis as amphiphilic compounds at concentrations higher than the CMC cause solubilization of cellular lipids and proteins instead of membrane disintegration.<sup>41</sup>

The results of the present study and those of our previous studies are in agreement that increasing the lipophilicity of DHS and MAS through long chain alkylation increased their affinity for the membrane beyond any doubt.<sup>13,17,18</sup> In these studies, increased membrane affinity was attributed to be

reason for the ability of the conjugates of DHS and MAS to mimic the functionality of GPx4 and PDI-GPx7 respectively in a cell free system.<sup>13,17,18</sup> However, the same very reason of membrane affinity became the cause of toxicity and thus a major concern in the biological applications of long chain conjugates of DHS and MAS. Taken together, the cytotoxic effects of DHS and MAS conjugates appear to be independent of their abilities to act as GPx4 and PDI-GPx7 mimics in cell free systems. It is also important to note here that the toxicity of DHS, MAS and their  $C_6$  conjugate is extremely low when compared to other known organochalcogens,<sup>57</sup> making them suitable prototypes for new drug design.

At this stage it was felt necessary to evaluate the antioxidant effect of parent compounds and the nontoxic  $C_6$  conjugates in normal CHO cells. We restricted our study to the estimation of the levels of selenoproteins exhibiting antioxidant activities in the cells such as GPx1, GPx4 and TrxR1. Like the above GPx isoforms, TrxR1 is also an important cytosolic selenoenzyme that is required to maintain thioredoxin (endogenous antioxidant) in the reduced state.<sup>58</sup> In this study parent compounds DHS and MAS significantly induced the expressions of all the above antioxidant selenoenzymes both at mRNA and activity levels and also provided protection against AAPH induced lipid peroxidation.<sup>27,36</sup> Interestingly, the  $C_6$  conjugates of DHS and MAS were even better than the respective parent compounds in imparting the above activities confirming the role of HLB in improving the antioxidant activity. The mechanisms by which DHS and MAS led to the induction of selenoproteins remain to be understood. Interestingly, the antioxidant genes like *GPx1*, *GPx4* and *TrxR1* are the transcriptional targets of a redox sensitive transcription factor, Nrf2 (nuclear factor-E2-related factor 2), which has been shown to be induced by organochalcogens including ebselen and diphenyl diselenide.<sup>59–61</sup> Therefore similar mechanisms may also account for the antioxidant activity of DHS, MAS and their  $C_6$  conjugates in cells. It is also worth mentioning here that DHS- $C_6$  was less active than MAS- $C_6$  in inducing the selenoenzymes and in protecting from AAPH mediated oxidative stress. The reason for this could be the probable cleavage of DHS- $C_6$  (which contains an



**Scheme 2** Schematic representation of the cellular effects of the conjugates of DHS and MAS.

ester linkage) into the parent compound by the esterase present in the plasma membrane of the cells. In the absence of any evidence for this cleavage, we can conclude based on the fact that DHS-C<sub>6</sub> could significantly increase the incorporation of selenium into the membranes per cell justifies its application as a pro-drug.<sup>19–21</sup> In contrast MAS-C<sub>6</sub>, which contains an amide linkage may be a model compound for fine-tuning the toxicity and other biological application. The observed cellular effects of the conjugates of DHS and MAS are summarized in Scheme 2.

## Conclusions

In conclusion the amphiphilic conjugates of DHS and MAS mimicked surface active compounds in causing cytotoxicity through membrane disintegration and necrosis. Conjugating a fatty acid/alkyl group as a lipophilic unit with a hydrophilic antioxidant moiety has been an effective approach to enhance the antioxidant activities. However, HLB is the important consideration in converting a nontoxic compound to a toxic one. Among DHS and MAS conjugates of varying chain lengths, C<sub>6</sub> conjugates appear to be the appropriate bioinspired prototypes of selenium antioxidants.

## Acknowledgements

Miss Prachi Verma acknowledges Homi Bhabha National Institute for financial assistance in the form of senior research fellowship. The authors also wish to thank Dr (Smt) S. Suvarna, Analytical Chemistry Division, Chemistry Group, BARC for providing help in the selenium estimation in the cells.

## References

- D. Bhowmick, S. Srivasstava, P. D'Silva and G. Mugesh, *Angew. Chem., Int. Ed.*, 2015, **54**, 8449–8453.
- E. A. Kersteen and R. T. Raines, *Antioxid. Redox Signaling*, 2003, **5**, 413–424.
- R. B. Flohe and M. Maiorino, *Biochim. Biophys. Acta*, 2013, **1830**, 3289–3303.
- V. Bosello-Travain, M. Conrad, G. Cozza, A. Negro, S. Quartesan, M. Rossetto, *et al.*, *Biochim. Biophys. Acta*, 2013, **1830**, 3846–3857.
- L. Wang, L. Zhang, Y. Niu, R. Sitia and C. Wang, *Antioxid. Redox Signaling*, 2014, **20**, 545–556.
- W. J. Lees, *Curr. Opin. Chem. Biol.*, 2008, **12**, 740–745.
- J. Beld, K. J. Woycechowsky and D. Hilvert, *Biochemistry*, 2008, **47**, 6985–6987.
- G. Mugesh and H. B. Singh, *Chem. Soc. Rev.*, 2000, **29**, 347–357.
- K. P. Bhabak and G. Mugesh, *Acc. Chem. Res.*, 2010, **43**, 1408–1419.
- M. Iwaoka, T. Takahashi and S. Tomoda, *Heteroat. Chem.*, 2001, **12**, 293–299.
- F. Kumakura, B. Mishra, K. I. Priyadarsini and M. Iwaoka, *Eur. J. Org. Chem.*, 2010, 440–445.
- K. Arai, K. Dedachi and M. Iwaoka, *Chem. – Eur. J.*, 2011, **17**, 481–485.
- K. Arai, K. Moriai, A. Ogawa and M. Iwaoka, *Chem. – Asian J.*, 2014, **12**, 3464–3471.
- B. G. Singh, E. Thomas, F. Kumakura, K. Dedachi, M. Iwaoka and K. I. Priyadarsini, *J. Phys. Chem. A*, 2010, **114**, 8271–8277.
- S. Chakraborty, S. K. Yadav, M. Subramanian, K. I. Priyadarsini, M. Iwaoka and S. Chattopadhyay, *Free Radical Res.*, 2012, **46**, 1378–1386.
- K. Arai, F. Kumakura, M. Takahira, N. Sekiyama, N. Kuroda, T. Suzuki, *et al.*, *J. Org. Chem.*, 2015, **80**, 5633–5642.
- M. Iwaoka, N. Sano, Y. Y. Lin, A. Katakura, M. Noguchi, K. Takahashi, *et al.*, *ChemBioChem*, 2015, **16**, 1226–1234.
- M. Iwaoka, A. Katakura, J. Mishima, Y. Ishihara, A. Kunwar and K. I. Priyadarsini, *Molecules*, 2015, **20**, 12364–12375.
- M. Laguerre, C. Bayrasy, J. Lecomte, B. Chabi, E. A. Decker, C. Wrutniak-Cabello, G. Cabello and P. Villeneuve, *Biochimie*, 2013, **95**, 20–26.
- C. Bayrasy, B. Chabi, M. Laguerre, J. Lecomte, E. Jublanc, P. Villeneuve, C. Wrutniak-Cabello and G. Cabello, *Pharma Res.*, 2013, **30**, 1979–1989.
- D. M. Lambert, *Eur. J. Pharm. Sci.*, 2000, (Suppl 2), S15–S27.
- H. R. Mellor, J. Nolan, L. Pickering, M. R. Wormald, F. M. Platt, R. A. Dwek, *et al.*, *Biochem. J.*, 2002, **366**, 225–233.
- R. Lucas, F. Comelles, D. Alcantara, O. S. Maldonado, M. Curcuroze, J. L. Parra, *et al.*, *J. Agric. Food Chem.*, 2010, **58**, 8021–8026.
- T. Mosmann, *J. Immunol. Methods*, 1983, **65**, 55–63.
- M. Van Engeland, F. C. Ramaekers, B. Schutte and C. P. Reutelingsperger, *Cytometry*, 1996, **24**, 131–139.
- A. Cossarizza, M. Baccaranicontri, G. Kalashnikova and C. Franceschi, *Biochem. Biophys. Res. Commun.*, 1993, **197**, 40–45.
- A. Kunwar, B. Mishra, A. Barik, L. B. Kumbhare, R. Pandey, V. K. Jain, *et al.*, *Chem. Res. Toxicol.*, 2007, **20**, 1482–1487.
- M. Shinitzky and Y. Barenholzb, *Biochim. Biophys. Acta*, 1978, **515**, 367–394.
- L. A. Royce, P. Liu, M. J. Stebbins, B. C. Hanson and L. R. Jarboe, *Appl. Microbiol. Biotechnol.*, 2013, **97**, 8317–8327.
- M. B. Lande, J. M. Donovan and M. L. Zeidel, *J. Gen. Physiol.*, 1995, **106**, 67–84.
- D. B. Goldstein, *Annu. Rev. Pharmacol. Toxicol.*, 1984, **24**, 43–64.
- J. Plasek and P. Jarolim, *Gen. Physiol. Biophys.*, 1987, **6**, 425–437.
- R. K. Chaurasia, S. Balakrishnana, A. Kunwar, U. Yadav, N. Bhata, K. Anjariaa, *et al.*, *Mutat. Res.*, 2014, **774**, 8–16.
- M. C. A. Stuart, J. C. van de Pas and J. B. F. N. Engberts, *J. Phys. Org. Chem.*, 2005, **18**, 929–934.

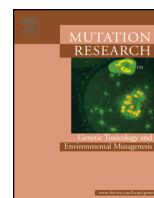
- 35 M. Wolszczak and J. Miller, *J. Photochem. Photobiol.*, 2002, **147**, 45–54.
- 36 A. Kunwar, H. Narang, K. I. Priyadarsini, M. Krishna, R. Pandey and K. B. Sainis, *J. Cell. Biochem.*, 2007, **102**, 1214–1224.
- 37 K. J. Livak and T. D. Schmittgen, *Methods*, 2001, **25**, 402–408.
- 38 T. H. Lugokenski, L. G. Müller, P. S. Taube, J. B. Rocha and M. E. Pereira, *Drug Chem. Toxicol.*, 2011, **34**, 66–76.
- 39 M. A. Carfagna and B. B. Muhoberac, *Mol. Pharmacol.*, 1993, **44**, 129–141.
- 40 S. C. Mckarns, C. Hansch, W. Caldwell, W. T. Morgan, S. K. Moore and A. D. J. Doolite, *Fundam. Appl. Toxicol.*, 1997, **36**, 62–70.
- 41 H. J. Mellor, F. M. Platt, R. A. Dwek and T. D. Butters, *Biochem. J.*, 2003, **374**, 307–314.
- 42 M. A. Gauthier, P. Simard, Z. Zhang and X. X. Zhu, *J. R. Soc., Interface*, 2007, **4**, 1145–1150.
- 43 S. Matsunaga, M. Jimbo, M. B. Gill, L. L. L. Wyhe, M. Murata, K. Nonomura, *et al.*, *ChemBioChem*, 2011, **12**, 2191–2200.
- 44 D. L. Holliday and V. Speirs, *Breast Cancer Res.*, 2011, **13**, 215.
- 45 M. Dymond, G. Attard and A. D. Postle, *J. R. Soc., Interface*, 2008, **5**, 1371–1386.
- 46 A. S. Inacio, K. A. Mesquita, M. Baptista, J. R. Santos, W. L. C. Vaz and O. V. Vieira, *PLoS One*, 2011, **6**, 1–15.
- 47 S. Schreier, S. V. P. Malheiros and E. Paula, *Biochim. Biophys. Acta*, 2000, **1508**, 210–234.
- 48 B. Bechinger and K. Lohner, *Biochim. Biophys. Acta*, 2006, **1758**, 1529–1539.
- 49 I. Lengler, T. Buhrke, E. Scharmach and A. Lampen, *Lipids*, 2012, **47**, 1085–1097.
- 50 A. Teixeira, R. C. Cox and M. R. Egmond, *Food Funct.*, 2013, **4**, 1209–1215.
- 51 M. Borse, V. Sharma, V. K. Aswal, P. S. Goyal and S. Devi, *J. Colloid Interface Sci.*, 2005, **284**, 282–288.
- 52 D. A. Brown and E. London, *J. Biol. Chem.*, 2000, **275**, 17221–17224.
- 53 T. M. Lima, M. F. Cury, G. Giannocco, M. T. Nunes and R. Curi, *Clin. Sci.*, 2006, **111**, 307–317.
- 54 W. X. Zong and C. B. Thompson, *Genes Dev.*, 2006, **20**, 1–15.
- 55 E. J. Ambrose, D. M. Easty and P. C. T. Jones, *Br. J. Cancer*, 1958, **12**, 439–447.
- 56 C. E. Carpenter and J. R. Broadbent, *J. Food Sci.*, 2009, **74**, R12–R15.
- 57 D. B. Caeran, D. F. Meinerz, J. Allebrandt, E. P. Waczuk, D. B. dos Santos, D. O. Mariano and J. B. Rocha, *Biomed. Res. Int.*, 2013, **2013**, 537279.
- 58 D. Mustacich and G. Powis, *Biochem. J.*, 2000, **346**, 1–8.
- 59 V. Tamasi, J. M. Jeffries, G. E. Arteel and K. C. Falkner, *Arch. Biochem. Biophys.*, 2004, **431**, 161–168.
- 60 A. F. de Bem, B. Fiuza, P. Calcerrada, P. M. Brito, G. Peluffo, T. C. Dinis, M. Trujillo, J. B. Rocha, R. Radi and L. M. Almeida, *Nitric Oxide*, 2013, **31**, 20–30.
- 61 G. Zhang, V. Nitteranon, S. Guo, P. Qiu, X. Wu, F. Li, H. Xiao, Q. Hu and K. L. Parkin, *Chem. Res. Toxicol.*, 2013, **26**, 456–464.



Contents lists available at [ScienceDirect](http://www.sciencedirect.com)

## Mutation Research/Genetic Toxicology and Environmental Mutagenesis

journal homepage: [www.elsevier.com/locate/gen tox](http://www.elsevier.com/locate/gen tox)  
Community address: [www.elsevier.com/locate/mutres](http://www.elsevier.com/locate/mutres)



# Dihydroxyselenolane (DHS) supplementation improves survival following whole-body irradiation (WBI) by suppressing tissue-specific inflammatory responses



Amit Kunwar<sup>a,\*</sup>, Prachi Verma<sup>a,b,1</sup>, H.N. Bhilwade<sup>c</sup>, Michio Iwaoka<sup>d</sup>,  
K. Indira Priyadarsini<sup>a,b,\*</sup>

<sup>a</sup> Radiation and Photochemistry Division, Bhabha Atomic Research Centre, Mumbai 400085, India

<sup>b</sup> Homi Bhabha National Institute, Bhabha Atomic Research Centre, Mumbai 400094, India

<sup>c</sup> Radiation Biology & Health Sciences Division, Bhabha Atomic Research Centre, Mumbai 400085, India

<sup>d</sup> Department of Chemistry, Tokai University, Kitakaname, Hiratsuka-shi, Kanagawa 259-1292, Japan

## ARTICLE INFO

### Article history:

Received 2 May 2016

Received in revised form 24 June 2016

Accepted 5 July 2016

Available online 22 July 2016

### Keywords:

Dihydroxyselenolane

Radioprotector

Glutathione peroxidase

Inflammation

Selenomethionine

## ABSTRACT

Dihydroxyselenolane (DHS), a simple water-soluble organoselenium compound, was evaluated for radio-protection in BALB/c mice after whole-body irradiation (WBI) (8 Gy <sup>60</sup>Co, 1 Gy/min), by monitoring 30-d post-irradiation survival and biochemical/histological changes in radiosensitive organs. Intraperitoneal administration of DHS at 2 mg/kg for five consecutive days before irradiation and three times per week during the post-irradiation period showed maximum benefit (40% improvement in 30 d post-irradiation survival). DHS treatment, despite inducing expression of glutathione peroxidases (*GPx1*, *GPx2*, and *GPx4*) in spleen and intestine, did not protect against radiation-induced acute (10-day) haematopoietic and gastrointestinal toxicities. DHS treatment significantly reduced radiation-induced DNA damage in peripheral leukocytes and inflammatory responses in intestine, lung, and circulation. The anti-inflammatory effect of DHS was associated with reductions in lipid peroxidation, expression of pro-inflammatory genes such as *Icam-1*, *Ccl-2*, and *iNos-2*, and subsequent infiltration of inflammatory cells. Irradiated mice treated with DHS survived until day 30 post-irradiation and showed restoration of spleen cellularity and intestinal villi, but had moderately increased systemic and tissue-specific inflammatory responses. Another organoselenium compound, selenomethionine, evaluated in parallel with DHS at the same dose and treatment schedule, showed comparable radioprotective effects. The mechanism of radioprotection by DHS is mainly via suppression of inflammatory responses.

© 2016 Elsevier B.V. All rights reserved.

## 1. Introduction

The application of ionizing radiation in industry, defense, medicine, and agriculture presents the risk of unwanted exposure [1,2] leading to mutations, cell death, and acute syndromes involving the hematopoietic and gastrointestinal systems [3–7]. Radioprotectors are agents that can provide a survival advantage against high-dose acute radiation injury, in cases of radiation emergency and also to protect normal cells during cancer radiotherapy. The search for an ideal radioprotector started soon after World War II. However, the only compound available for clinical

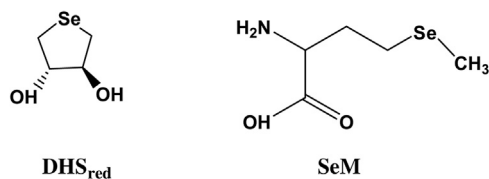
use is amifostine, a sulfhydryl agent discovered by screening almost 4000 sulphur compounds [8–10]. Amifostine is approved for treatment of mucositis and xerostomia in head-and-neck cancer patients undergoing radiotherapy but not for use in cases of radiation emergency [10,11]. Furthermore, amifostine can cause behavioural toxicity and other side effects, including nausea and vomiting. Therefore, development of new radioprotectors is desirable [8–11].

Considering the similarities in the properties of sulphur and selenium, it was anticipated that selenium compounds act as radioprotectors [12]. Selenium is a micronutrient and a constituent of important antioxidant enzymes, including glutathione peroxidase (GPx), thioredoxin reductase (TrxR), and selenoprotein P (SeP) [13–16]. Several selenium compounds (organic and inorganic) have been evaluated [17–21] and induction of GPx has been considered to be the mechanism of action of such com-

\* Corresponding authors.

E-mail addresses: [kamit@barc.gov.in](mailto:kamit@barc.gov.in) (A. Kunwar), [kindira@barc.gov.in](mailto:kindira@barc.gov.in) (K.I. Priyadarsini).

<sup>1</sup> Should be regarded as joint first authors.



**Scheme 1.** Chemical structures of dihydroxy selenolane and selenomethionine.

pounds. We have been screening organoselenium compounds for *in vivo* radioprotective activity [22–26] and have initiated studies on a simple water-soluble organoselenium compound, dihydroxy-selenolane (DHS) [27]. DHS exhibits a wide range of biological activities, such as free radical scavenging, mimicking the function of GPx, and catalysing the oxidative folding of misfolded and/or denatured proteins [27–29]. DHS induces GPx and accelerates the healing of indomethacin-induced stomach ulceration in mice, by modulating arginine metabolism and anti-inflammatory pathways [30–32]. Encouraged by these results, in the present study, DHS has been evaluated for radioprotection in a mouse model, by monitoring the improvement in 30-d post-irradiation survival and biochemical, histological, and inflammatory changes in radiosensitive organs, such as spleen, intestine and lung, after whole-body irradiation (WBI) at a lethal absorbed dose of 8 Gy. We also studied the effect of DHS administration on radiation-induced DNA damage in peripheral leukocytes and on tissue-specific expression of GPx and pro-inflammatory genes such as *Icam-1*, *CCl-2*, and *iNOS-2*. The radioprotective effect of DHS was compared with selenomethionine (SeM), a dietary selenium supplement (18,33). The chemical structures of DHS and SeM are presented in [Scheme 1](#).

## 2. Materials and methods

### 2.1. Chemicals

DHS was synthesized and purified as reported previously [30]. Diethyl pyrocarbonate (DEPC), SeM, SYBR Green-II dye, Trizol reagent, cell lysis M, dimethyl sulfoxide (DMSO), glutathione (GSH), NADPH, glutathione reductase, cumene hydroperoxide, NaCl,  $\text{KH}_2\text{PO}_4$ ,  $\text{K}_2\text{HPO}_4$ , formaldehyde, triton X-100, phenyl-methylsulphonyl fluoride (PMSF), protease inhibitor cocktail (1X), high- and low-melting-point agarose, thiobarbituric acid (TBA), butylated hydroxytoluene (BHT), trichloroacetic acid (TCA), ethylenediaminetetraacetic acid (EDTA), and amplification grade DNase (Sigma Chemical Co., St. Louis, MO, USA) were purchased from local suppliers. SYBR green polymerase chain reaction (PCR) mix (2X) from Roche (Indianapolis, IN, USA) and cDNA synthesis kit from Thermo Scientific, (Waltham, MA, USA) were also purchased from local suppliers. Culture medium (RPMI-1640), fetal calf serum, and tris base were purchased from Himedia, India. Cytokine ELISA kits were obtained from Abcam (Cambridge, MA, USA) through the local supplier. Gene-specific primers were custom synthesized by local suppliers. The protein estimation kit was purchased from M/s Bangalore Genei, India. All other chemicals, of highest purity, were procured from local manufacturers/suppliers.

### 2.2. Animals

Male BALB/c mice (7–8 weeks old, 20–25 g) were maintained under standard conditions ( $20 \pm 2^\circ\text{C}$ , 65–70% humidity, 12 h/12 h day/night cycle, balanced laboratory diet, and tap water *ad libitum*) in the animal house facility of Bhabha Atomic Research Centre, Mumbai. The experiments were conducted according to the guidelines of the Institutional Animal Ethics Committee.

### 2.3. Experimental design and WBI

DHS and SeM solutions were prepared in sterile phosphate-buffered saline (PBS) immediately before the experiment. DHS dose was selected based on previous studies [31,32]. Mice were randomized into four groups: sham control, drug control, radiation control, and drug + radiation. The irradiated groups received PBS (control) or drug (DHS or SeM) intraperitoneally (i.p.) for five consecutive days prior to irradiation, and dosing was continued during the post-irradiation period, three times weekly until the end of the experiment. The sham and drug control mice were not irradiated and received treatment either with PBS or drug (DHS or SeM), similar to the irradiated groups, until they were sacrificed at the desired time point (day 30 post-irradiation). For irradiation, mice were placed in ventilated perspex containers and subjected to WBI, absorbed dose 8 Gy, using a  $^{60}\text{Co}$  Bhabhatron  $\gamma$ -source (Department of Atomic Energy, India) at dose rate 1 Gy/min and source-to-sample distance = 60 cm. After irradiation, the mice were housed under normal laboratory conditions and monitored daily for 30 d by recording body weights on regular interval and mortality (if any). Kaplan-Meier survival curves were drawn using GraphPad Prism<sup>®</sup> (version 3.2). For mechanistic study, irradiated mice were housed under normal laboratory conditions and euthanized by cervical dislocation 10 or 30 d post-irradiation; only the drug-treated mice survived to 30 d. In order to study survival or 30-d post-irradiation parameters, ten mice per group were analysed; for the early data point (10 d), five mice per group were analysed. Results are presented as mean  $\pm$  SEM ( $n = 3-5$ ).

### 2.4. Bronchoalveolar lavage fluid (BALF) and serum analysis

Prior to sacrifice, mice were paralysed with an overdose of chloroform, a tracheotomy was performed, and a cannula was inserted and tied. The lungs were infused with 1 ml PBS, and then the infusate was aspirated back, collected into a sterile eppendorf tube and centrifuged at  $400 \times g$  for 5 min at  $4^\circ\text{C}$ . Cell-free supernatant or BALF was used for protein concentration determination using a protein assay kit (Bangalore Genei, India). The cell pellet was resuspended in 0.25 ml PBS, total cell numbers were counted using a haemocytometer, and cytopins were prepared ( $5 \times 10^4$  cells/slide). Following BALF collection, blood was collected in the centrifuge vials by intracardiac puncture, incubated at  $4^\circ\text{C}$  overnight and centrifuged at  $1,000 \times g$  for 5 min to furnish serum as supernatant. The serum was stored at  $-20^\circ\text{C}$  until analysed for cytokines using ELISA kits according to manufacturer's instruction.

### 2.5. Estimation of hematopoietic parameters

The spleen was removed immediately after sacrificing animal and the spleen parameters like index (spleen weight/body weight), cellularity and colony forming units (CFU) were determined as described previously [23,34]. The splenocytes ( $5 \times 10^6$ ) were homogenized in 1 ml Trizol reagent using a tissue disruptor (Qiagen, Germany) and stored at  $-70^\circ\text{C}$  until used for mRNA expression analysis by quantitative real-time PCR. Similarly splenocytes ( $10 \times 10^6$ ) were lysed in 10 mM tris buffer, pH 7.4, containing 0.5% Triton X-100, 5 mM BHT and  $100 \mu\text{M}$  PMSF and  $100 \mu\text{g}$  of protein equivalent was for determination of GPx activity. The hematocrit in each group was performed by an auto analyzer using peripheral blood ( $50 \mu\text{l}$ ), collected in heparinised tubes from the mice tails.

### 2.6. Estimation of intestinal and lung toxicity parameters

Upon euthanasia, a portion of jejunum and right lung was excised, washed thrice with ice cold PBS, fixed in 10% buffered for-

malin, dehydrated by passing through a graded series of alcohol, embedded into paraffin blocks, and sections of 5  $\mu\text{m}$  thickness were cut. The tissue sections stained with hematoxylin and eosin and imaged using an inverted microscope (Olympus CKX41) attached to ProgRes<sup>®</sup> digital camera. Lung inflammatory response was scored on a scale of 0–6; 0 being clear lung and 6 being extremely inflamed (characterized by excessive thickening of the alveolar walls with cellular infiltrate and exudates present in the alveolar space of the entire lung section) [35]. Another small portion of the jejunum and the left lung was homogenized in 1 ml Trizol reagent using a tissue disruptor and stored at  $-70^\circ\text{C}$  until used for gene expression assessment by quantitative real-time PCR. The remainder of jejunum and left lung tissue perfused thrice each with 1 ml cold PBS to wash out any trapped blood volume and edema fluid, homogenized (10% weight/volume) in 10 mM tris buffer, pH 7.4, containing 0.5% Triton X-100, 5 mM BHT and 100  $\mu\text{M}$  PMSF using a tissue disruptor, centrifuged at  $10,000 \times g$  for 5 min and the supernatant (tissue extract) was used for the estimation of lipid peroxidation as thiobarbituric acid reactive substances (TBARS) and GPx activity analysis [30,36]. The protein content in the tissue homogenate was estimated using protein assay kit (Bangalore Genei, India).

### 2.7. BALF cellular analysis

The cytopins were stained with hematoxylin and eosin and viewed under Olympus fluorescence microscope CKX41, Japan attached to ProgRes<sup>®</sup> digital camera and differential cell counts were reported as the percentage of 500 cells counted from one cytospin per mouse [25].

### 2.8. Gene expression studies

Trizol homogenates were processed to isoate the mRNA according to manufacturer's instruction. About 2  $\mu\text{g}$  total RNA was reverse transcribed using cDNA synthesis kit (Thermo Scientific, USA). The real time PCR was carried out in a 10  $\mu\text{l}$  reaction mixture containing 5  $\mu\text{l}$  2X SYBR green PCR master mix, 1  $\mu\text{l}$  forward and reverse primer and 4  $\mu\text{l}$  diluted (10 x) cDNA, using the Rotor Gene Q (Qiagen, Germany) machine. The amplification steps were: denaturation at  $95^\circ\text{C}$  for 5 min; denaturation at  $95^\circ\text{C}$  for 15 s; annealing at  $58^\circ\text{C}$  for 15 s; extension at  $72^\circ\text{C}$  for 20 s; and melt curve analysis. Steps 2–4 were repeated for 35 cycles. The relative expression levels of genes was calculated using the threshold cycle (CT) values obtained from above runs as per the method described previously [37]. The expressions of genes were normalized against the house-keeping gene  $\beta$ -actin. The sequences of the primers (forward and reverse) used for cDNA amplification are included in Table 1.

### 2.9. Estimation of hepatic parameters

Upon euthanasia hepatic tissue perfused with cold PBS, a portion homogenized in Trizol reagent using a tissue ruptor (Qiagen, Germany) and gene expression analysis was performed as described in previous section. The remainder of hepatic tissue was fixed in to 10% buffered formalin and used for histopathology as described previously.

### 2.10. Alkaline single cell gel electrophoresis

Mice were randomized, grouped ( $n=5$ ) as described in the previous section, administered with PBS or drugs (DHS or SeM) and irradiated at 5 Gy ( $^{60}\text{Co}$ , 1 Gy/min). The blood samples were taken from the tail vein 15 and 60 min post-irradiation and processed for the alkaline single-cell gel electrophoresis (comet) assay, as described previously [38]. Two microscope slides were prepared from each mouse and fifty images were grabbed per slide using a

**Table 1**

List of primers used in gene expression analysis by RT-PCR is presented.

Name of gene	Primer sequence	Gene Bank Accession No.
$\beta$ Actin	GGCTGTATCCCCTCCATCG CCAGTTGGTAAACAATGCCATGT	NM.007393
Icam 1	GTGATGCTCAGGTATCCATCCA CACAGTTCTCAAAGCACAGCG	NM.010493
Ccl2	TAAAAACCTGGATCGGAACAAA GCATTAGCTTCAGATTTACGGGT	NM.011333
Csf3	ATGGCTCAACTTTCGCCACG CTGACAGTGACCAGGGGAAC	NM.009971
Nos2	GTTCTCAGCCCAACAATAACAAGA GTGGACGGGTCGATGTCAC	NM.010927
Selp1	AGCTCTGCTGTTACAAAGCC CAGGTCTTCCAATCTGGATGC	NM.001042613
GPx1	AGTCCACCGTGTATGCCTTCT GAGACGGACATTCTCAATGA	NM.008160
GPx2	GCCTCAAGTATGTCGGACCTG GGAGAACGGGTCATCATAAGGG	NM.030677
GPx4	TGTGCATCCCGCATGATT CCCTGTACTTATCCAGGCAGA	NM.008162

Carl Zeiss Axioplan fluorescent microscope (Germany). The images were analysed using CASP software version 1.2.0 ([www.Casplab.com](http://www.Casplab.com)) to calculate percent (%) DNA in tail, tail length (TL), tail moment (TM), and olive tail moment (OTM). The results are presented as mean  $\pm$  SEM ( $n=5$ ).

### 2.11. Statistical analysis

Statistical significance ( $p < 0.05$ ) of the difference between the means of treatment groups was determined by one way ANOVA. A two-tailed Student's *t*-test was used for the comparisons between the means of two groups and  $p$  values  $< 0.05$  were considered as statistically significant. Kaplan-Meier survival curves were analysed for statistical significance ( $p < 0.05$ ) using Mantel-Cox log-rank test of Graph Pad Prism<sup>®</sup> (version 3.02).

## 3. Results

### 3.1. DHS dose optimization

The radioprotective effect of DHS against the lethal dose (8 Gy) of WBI was evaluated in terms of enhancement of 30-d post-irradiation survival. For this, single i.p. doses of DHS, 2–50 mg/kg body weight, were administered 30 min before radiation exposure; following this, survival of animals was monitored for 30 d. Irradiation induced symptoms of radiation sickness in the mice: loss of appetite, irritability, lethargy, ruffling of hair, weight loss, and diarrhea. The radiation control group showed median survival of 10 d and complete mortality by 12 d (Fig. 1A & B). Pre-administration of DHS at a single i.p. dose 2–50 mg/kg body weight did not show any protection from radiation-induced mortality (data not shown). Increasing the administration of DHS to 5 consecutive days in a similar dose range showed better protection. Although DHS at 2, 25, and 50 mg/kg body weight significantly increased median survival time (to 13, 21 and 24 d, respectively), its ability to improve survival to 30 d was seen only at 50 mg/kg body weight (by 20%) (Fig. 1A). This suggested that DHS may work better if administered as a supplement. Accordingly, in another experiment, DHS was administered not only for five consecutive days prior to radiation exposure but also during the post-irradiation period, for three days per week until the end of the experiment, and survival of the mice was monitored. Interestingly, our results indicated that under above treatment regime, DHS provided significant radioprotection; 30-d survival was improved by 40% even at the lowest dose (2 mg/kg) tested (Fig. 1B). Increasing the dose to 50 mg/kg did not

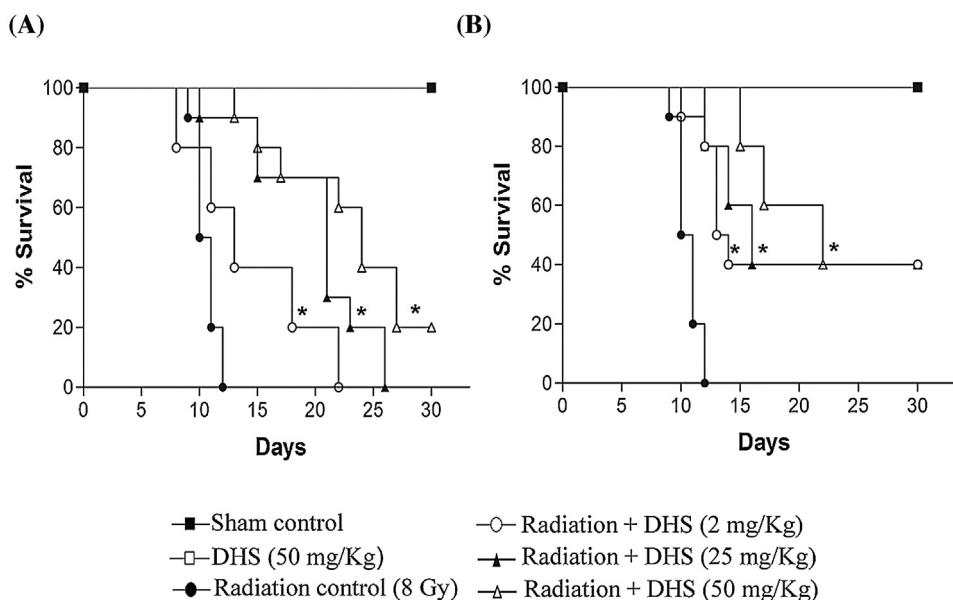


**Fig. 1.** Effect of DHS (2–50 mg/kg) administration (ip) on the 30 days survival of mice exposed to WBI at an absorbed dose of 8 Gy. The mice survival data as a function of post-irradiation time (30 days) was plotted using Graph Pad Prism® to obtain Kaplan-Meier survival curves (A) DHS was administered for five consecutive days and 30 min after the last dose, mice were irradiated (B) DHS was administered for five consecutive days prior to irradiation and continued during the post irradiation period for three times a week till end of experiment. \* $p < 0.05$  as compared to the radiation control.

increase protection (Fig. 1B). The DHS control group did not show mortality or any other visible toxicity symptoms throughout the experiment (30 d), suggesting the low toxicity of DHS (Fig. 1A & B). In all of our further studies, DHS was administered at 2 mg/kg in the combined treatment regime of pre- (5 d) and post- (3 d per week) irradiation. The radioprotective effect of DHS was compared with SeM at an identical dose (2 mg/kg) and treatment schedule.

### 3.2. Effect of DHS and SeM on 30-d post-irradiation survival

The 30-d survival curves following WBI are shown in Fig. 2A. SeM significantly improved survival, by 30%, comparable to the effect of DHS (40%). The improvement by both DHS and SeM was also supported by their abilities to increase relative body weights as compared to the radiation control group (Fig. 2B). As with DHS, the SeM control group too did not show mortality or any other visible toxicity symptoms throughout the experiment (30 d) (Fig. 2A & B).

### 3.3. Effect of DHS and SeM on radiation induced genotoxicity

Radiation-induced genotoxicity was evaluated in peripheral lymphocytes by the comet assay as a function of time (15 and 60 min) following radiation exposure. DNA damage parameters are shown in Fig. 3A. Representative fluorescence images are shown in Fig. 3B. As expected, irradiation led to a significant increase in DNA damage at 15 min post-irradiation. At 60 min post-irradiation, radiation-induced DNA damage was reduced considerably in the radiation control group, suggesting the normal repair process. The treatments with DHS and SeM showed significant reductions in the extent of radiation-induced DNA damage. Levels of residual DNA damage in DHS- and SeM-treated groups 60 min after radiation exposure were significantly higher than control levels. The efficacies of both DHS and SeM were comparable. The drug control groups (DHS and SeM) did not show any induction of DNA damage at 2 mg/kg.

### 3.4. Effect of DHS and SeM on the radiation induced hematopoietic toxicity

The abilities of DHS and SeM to protect the hematopoietic system were evaluated by monitoring the spleen parameters and hematocount in peripheral circulation. The changes in spleen markers such as index and cellularity under the radiation- and drug-treated conditions are shown in Fig. 4A. Exposure to radiation led to a significant decrease in spleen index and cellularity by d 10, suggesting acute hematopoietic damage/syndrome. Treatment with either DHS or SeM did not show any significant improvement. However, these parameters remarkably increased in irradiated mice treated with DHS or SeM and surviving until 30 d post-irradiation. The renewal of hematopoietic system also depends on the proliferation of clonogenic stem cells in the spleen. Therefore, effects of DHS and SeM on such proliferation were investigated by the spleen CFU assay and by monitoring the expression of colony stimulating factor *Csf-3* at mRNA level. As shown in Figs. 4B and C, irradiation induced the proliferation of clonogenic stem cells, as evidenced by the increase in the number of CFU in the radiation control group compared to the sham control group on d 10 post-irradiation. Treatment with DHS or SeM in irradiated mice did not alter this parameter significantly compared to the radiation control. In agreement with above results, DHS or SeM treated groups, although did not show any significant change in the expression of *Csf-3* on d 10, increased significantly on d 30 in the surviving mice (Fig. 4D).

In addition to spleen parameters, the counts of various cell types in peripheral circulation also constitute the hematopoietic system. The effects of radiation and treatments with DHS and SeM on hematocount are presented in Table 2. As expected, irradiation led to significant decrease in counts of neutrophils, lymphocytes, platelets, and total white blood cells (WBC) by d 10 post-irradiation as compared to the sham control group. Treatment with DHS or SeM in irradiated mice did not show any improvement in hematocount on d 10 post irradiation as compared to the radiation control. However, these parameters improved, close to sham control levels, on d 30 post-irradiation in the surviving mice treated with

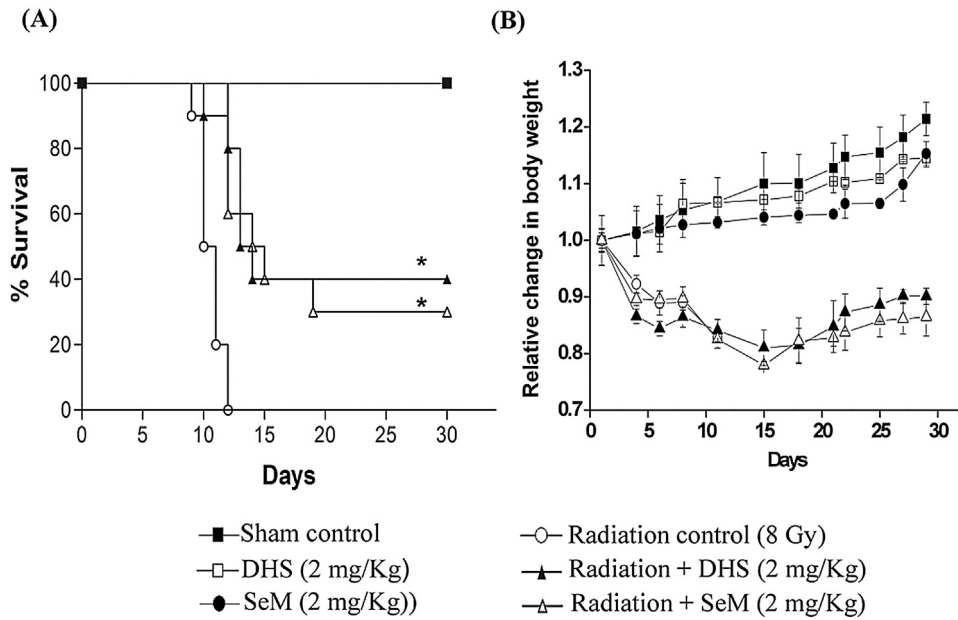


**Fig. 2.** Comparative effect of DHS (2 mg/kg) and SeM (2 mg/kg) administration (ip) on the 30 days survival of mice exposed to WBI at an absorbed dose of 8 Gy. Both drugs were administered for five consecutive days prior to irradiation and continued during the post irradiation period for three times a week till the end of experiment. (A) The mice survival data as a function of post-irradiation time (30 days) was plotted using Graph Pad Prism® to obtain Kaplan-Meier survival curves. The survival data sets of sham control, DHS control, radiation control and radiation+DHS groups have been repeated to show the comparative effect. \**p* < 0.05 as compared to the radiation control. (B) Relative change in body weight for different treatment groups plotted as a function of time in days. The results are presented as mean ± SEM (n = 4–10).

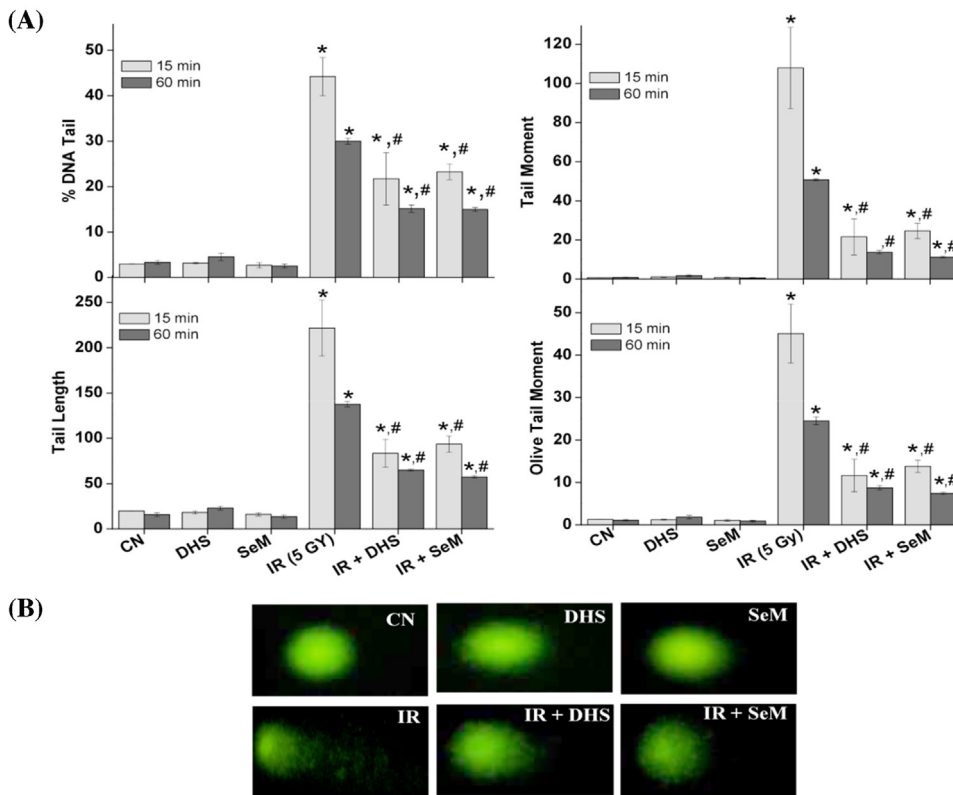


**Fig. 3.** Effect of DHS (2 mg/kg) and SeM (2 mg/kg) administration (ip) on the radiation (5 Gy) induced DNA strand breaks as assayed by comet assay. The drugs were given for five consecutive days prior to irradiation and peripheral blood was drawn at 15 and 60 min post irradiation from the tail vein of mice. The blood containing peripheral leukocytes were subjected to single cell gel electrophoresis. (A) Bar graphs showing DNA damage parameters in various treatment groups. The results are presented as mean ± SEM (n = 5). \**p* < 0.05 as compared to the sham control group. #*p* < 0.05 as compared to the radiation control group. (B) Representative fluorescent images showing the nuclei stained with SYBR Green-II from the different treatment groups following electrophoresis. CN – Sham control, IR - Irradiation.

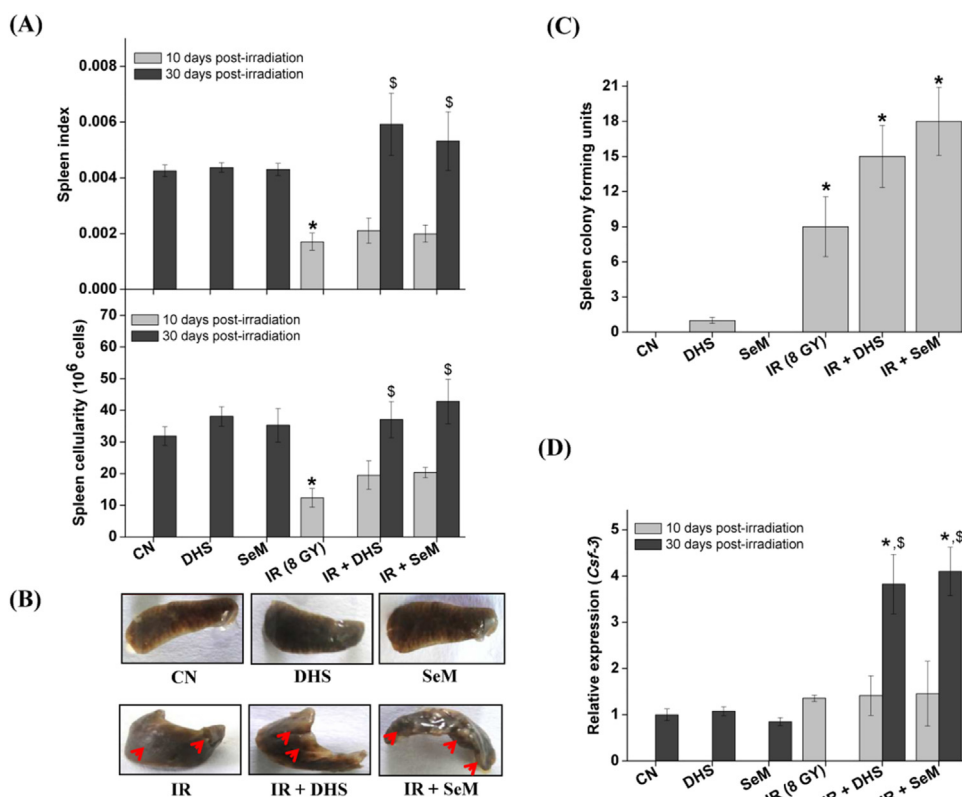


**Fig. 4.** Effect of DHS (2 mg/kg) and SeM (2 mg/kg) supplementation (ip) on the radiation (8 Gy) induced hematopoietic toxicity. (A) Bar graph showing spleen index (spleen weight/body weight) and cellularity under different treatment conditions. (B) & (C) Images and counts respectively of spleen colonies under different treatment conditions. The spleen colony forming assay was performed only on 10th day post irradiation. (D) mRNA expression of *Csf-3* as monitored by RT-PCR. The expression of above gene in different treatment groups was normalized against the sham control group and the relative expression changes have been plotted. Actin expression was used as internal control. The results are presented as mean  $\pm$  SEM (n = 3–5). \*p < 0.05 as compared to the sham control group <sup>§</sup>p < 0.05 as compared to respective drug (DHS or SeM) plus radiation treated group evaluated on 10th day post irradiation. CN – Sham control, IR - Irradiation.

**Table 2**

Hematocount under different treatment conditions is presented. The results are presented as mean  $\pm$  SEM (3–5 mice). \* p < 0.05 as compared to the sham control group. # p < 0.05 as compared to the radiation control group. <sup>§</sup>p < 0.05 as compared to respective drug (DHS or SeM) plus radiation treated group evaluated on 10th day post irradiation.

Treatment groups	Total WBC ( $10^3/\mu\text{l}$ )	Neutrophile ( $10^3/\mu\text{l}$ )	Lymphocytes ( $10^3/\mu\text{l}$ )	Platlets ( $10^3/\mu\text{l}$ )	Haemoglobin (% gm)
Sham control	4.35 $\pm$ 0.50	0.83 $\pm$ 0.02	3.33 $\pm$ 0.56	447 $\pm$ 58	14.45 $\pm$ 0.55
DHS control	3.55 $\pm$ 0.65	0.71 $\pm$ 0.04	2.59 $\pm$ 0.51	375 $\pm$ 35	13.55 $\pm$ 0.55
SeM control	3.25 $\pm$ 0.35	0.69 $\pm$ 0.15	2.32 $\pm$ 0.55	295 $\pm$ 6	14.5 $\pm$ 1.5
Radiation (8 Gy) (~10 days post irradiation)	0.30 $\pm$ 0.02 <sup>*</sup>	0.03 $\pm$ 0.01 <sup>*</sup>	0.22 $\pm$ 0.02 <sup>*</sup>	48 $\pm$ 21 <sup>*</sup>	9.4 $\pm$ 1.35 <sup>*</sup>
Radiation + DHS (~10 days post-irradiation)	0.31 $\pm$ 0.08	0.07 $\pm$ 0.04	0.23 $\pm$ 0.04	85 $\pm$ 46	8.25 $\pm$ 0.92
Radiation + DHS (30 days post irradiation)	2.60 $\pm$ 0.90 <sup>§</sup>	1.11 $\pm$ 0.42 <sup>§</sup>	1.28 $\pm$ 0.39 <sup>§</sup>	305 $\pm$ 55 <sup>§</sup>	14.2 $\pm$ 2
Radiation + SeM (~10 days post-irradiation)	0.42 $\pm$ 0.11 <sup>#</sup>	0.10 $\pm$ 0.06	0.28 $\pm$ 0.05	99 $\pm$ 37	8.97 $\pm$ 0.79
Radiation + SeM (30 days post irradiation)	3.05 $\pm$ 1.15 <sup>§</sup>	1.13 $\pm$ 0.33 <sup>§</sup>	1.80 $\pm$ 0.75 <sup>§</sup>	289 $\pm$ 19 <sup>§</sup>	14.15 $\pm$ 0.85 <sup>§</sup>

drug DHS or SeM and irradiated. The compounds DHS and SeM did not show any significant difference in affecting the radiation-induced hematopoietic changes. DHS and SeM control groups showed spleen parameters such as spleen index, spleen cellularity, CFU, and the expression of *Csf-3* and hematocount in peripheral circulation similar to those of the sham control (Fig. 4A–D, Table 2).

### 3.5. Radiation-induced intestinal toxicity and inflammatory responses

The small intestine is also an important radiosensitive organ. The protective effects of DHS and SeM on radiation-induced intestinal toxicity and inflammatory responses were evaluated through histological examination and by monitoring the levels of lipid peroxidation and mRNA of pro-inflammatory genes (*Icam-1*, *CCl-2* and *iNOS-2*). As shown in Figs. 5 and 6 A, irradiation led to acute intesti-

nal toxicity characterized by shortening and destruction of the villi structure and increase in the level of oxidative damage marker lipid peroxidation on d 10 post-irradiation. Further, the radiation control group showed an increase in expression of pro-inflammatory genes (*Icam-1*, *CCl-2* and *iNOS-2*) (Fig. 6B–D). The treatments with DHS and SeM in irradiated mice did not result in any significant protection with respect to villi structure but significantly reduced the levels of lipid peroxidation and pro-inflammatory genes (*Icam-1*, *CCl-2* and *iNOS-2*) as compared to radiation control at the common time point (d 10 post-irradiation) (Fig. 5 and Fig. 6A–D). Interestingly, mice surviving to d 30 showed maintenance in villi structure and unaltered levels of lipid peroxidation and pro-inflammatory genes (*Icam-1*, *CCl-2* and *iNOS-2*) as compared to those evaluated on d 10 (Fig. 5 and Fig. 6A–D). Both DHS and SeM were comparable in protecting the intestine from radiation-induced toxicities. DHS and SeM control groups did not show any adverse effect with respect

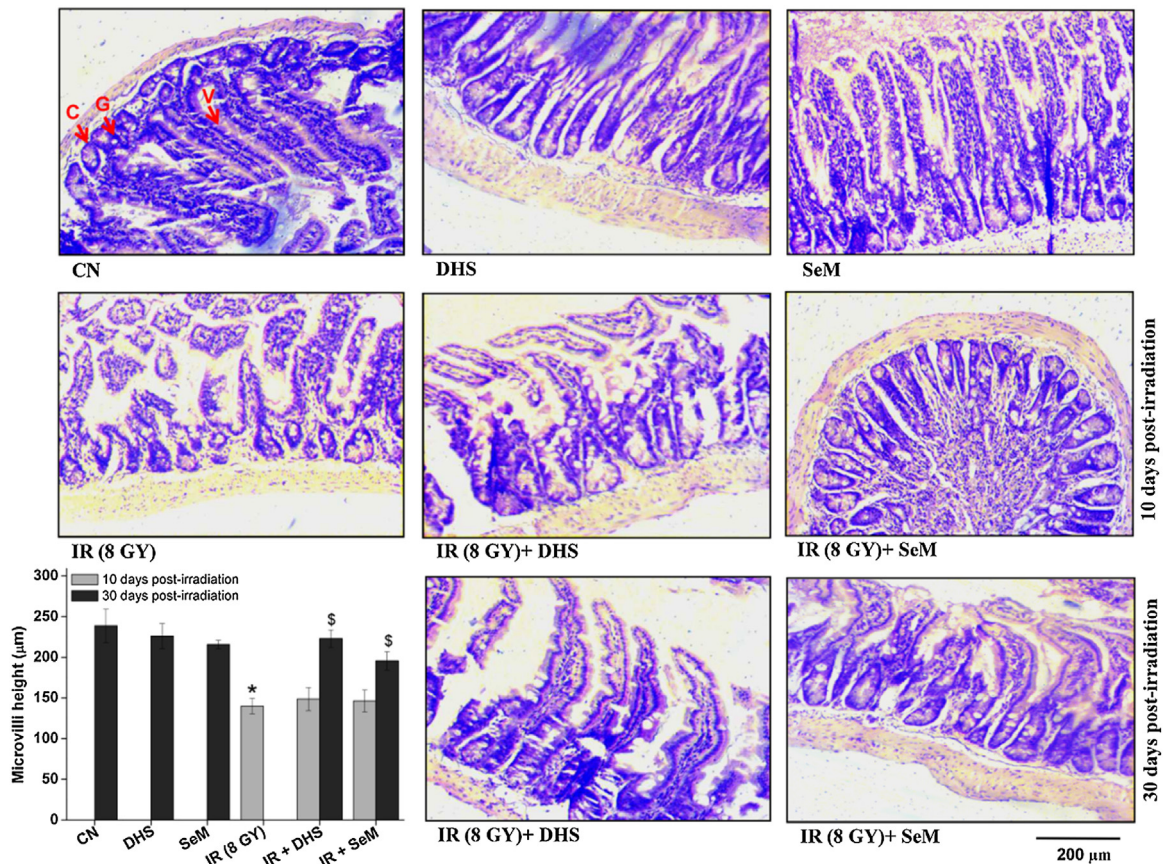


**Fig. 5.** Effect of DHS (2 mg/kg) and SeM (2 mg/kg) supplementation (ip) on the radiation (8 Gy) induced intestinal toxicity. Images of representative tissue section of jejunum excised from the mice of the various groups and stained with hematoxylin and eosin are presented. Magnification – 10 $\times$ . The inset of the figure shows the length of villi under different treatment conditions. The results are presented as mean  $\pm$  SEM (n = 3–5). \*p < 0.05 as compared to the sham control group  $^{\S}$ p < 0.05 as compared to respective drug (DHS or SeM) plus radiation treated group evaluated on 10th day post irradiation. CN – Sham control, IR – Irradiation, C - Cryptic cell, G - Goblet cell, V - Villi.

to intestinal structure or pro-inflammatory gene expression (Fig. 5 and Fig. 6A–D).

### 3.6. Radiation-induced inflammatory responses in the lung

The effects of DHS and SeM on radiation-induced inflammatory responses in lung were evaluated by histologically assessing the infiltration of inflammatory cells in lung tissue and BAL. The representative lung tissue sections from different groups stained with hematoxylin and eosin and the inflammatory scores based on the semi quantitative examination are shown in Fig. 7 and the BAL cell differentials are presented in Table 3. These results indicate that WBI led to acute inflammatory response in the lung, as evidenced by the presence of inflammatory cell infiltrates in lung parenchyma and BAL and the thickening of alveolar wall as compared to the sham control group on d 10. WBI significantly increased total BAL cellularity but did not alter the cell differentials (percentage of macrophages, neutrophils, lymphocytes and ciliary epithelial cells), compared to the sham control group (Table 3). Treatments with DHS and SeM in irradiated mice showed significant protection from radiation-induced inflammatory response as evidenced by the clear lung parenchyma and decrease in the BAL cellularity at the common time point (d 10). We also analysed the lung tissue for lipid peroxidation and BAL fluid for leaked proteins as indications of lung damage (Fig. 8A and B). In agreement with the above results, treatments with DHS and SeM showed significant reduction in radiation-induced lipid peroxidation in lung tissue and protein leakage in BAL on d 10 (Fig. 8A and B). Irradiation caused an

increase in pulmonary expressions of the *Icam-1* and *CCl-2* genes involved in the recruitment of inflammatory cells to the damaged tissues (Fig. 8C and D). Treatments with DHS and SeM in irradiated mice caused reduction in the expression of the above genes on d 10 compared to the radiation control group (Fig. 8C and D). Notably, mice from this group showed marginal elevation in lung inflammatory response marked by the influx of inflammatory cells in to lung and BAL, lung damage parameters (like lipid peroxidation and BAL protein content) and the expression of pro-inflammatory genes (*Icam-1* and *CCl-2*) on d 30 as compared to those evaluated on d 10 (Fig. 7, Fig. 8 and Table 3). All the above results suggest the role of DHS and SeM in suppressing inflammatory response in the lung by inhibiting oxidative damage and subsequent influx of inflammatory cells. Both DHS and SeM did not differ significantly in affecting the radiation induced inflammatory response in the lung (Fig. 7, Fig. 8 and Table 3). DHS and SeM control groups did not show any adverse effect with respect to the lung toxicity parameters such as histological changes, BAL cellularity, lipid peroxidation, BAL protein content and gene expression (Fig. 7, Fig. 8 and Table 3).

### 3.7. Radiation-induced systemic inflammation

The effects of DHS and SeM on radiation-induced systemic inflammation were examined by monitoring the circulatory levels of pro-inflammatory cytokines like TNF $\alpha$  and IL6 in the serum on d 10. The results presented in Fig. 9 indicate that WBI led to significant increase in the levels of TNF $\alpha$  and IL6 in circulation. Treatments with DHS and SeM in irradiated mice showed signif-

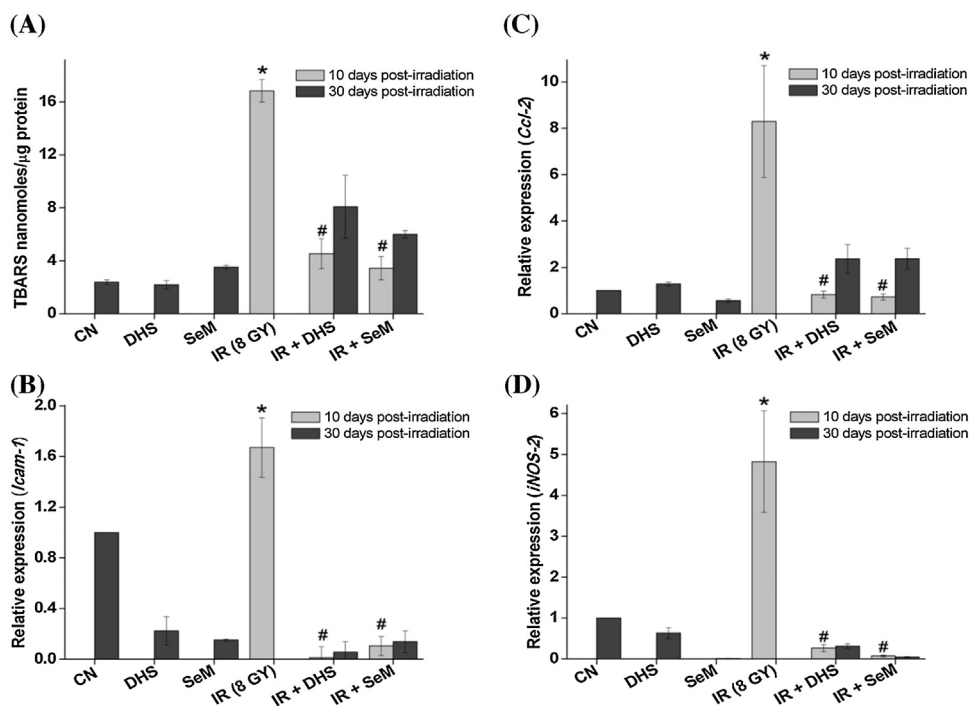


**Fig. 6.** Effect of DHS (2 mg/kg) and SeM (2 mg/kg) supplementation (ip) on the radiation (8 Gy) induced intestinal inflammatory responses. (A) Level of lipid peroxidation in the jejunum excised from the mice of various groups. (B), (C) and (D) mRNA expressions of *Icam1*, *CCL2*, and *iNOS-2* as monitored by RT-PCR. The results are presented as mean  $\pm$  SEM ( $n = 3-5$ ). The expression of above genes in different treatment groups was normalized against the sham control group and the relative expression changes have been plotted. Actin expression was used as internal control. \* $p < 0.05$  as compared to the sham control group, # $p < 0.05$  as compared to the radiation control group. CN – Sham control, IR – Irradiation.

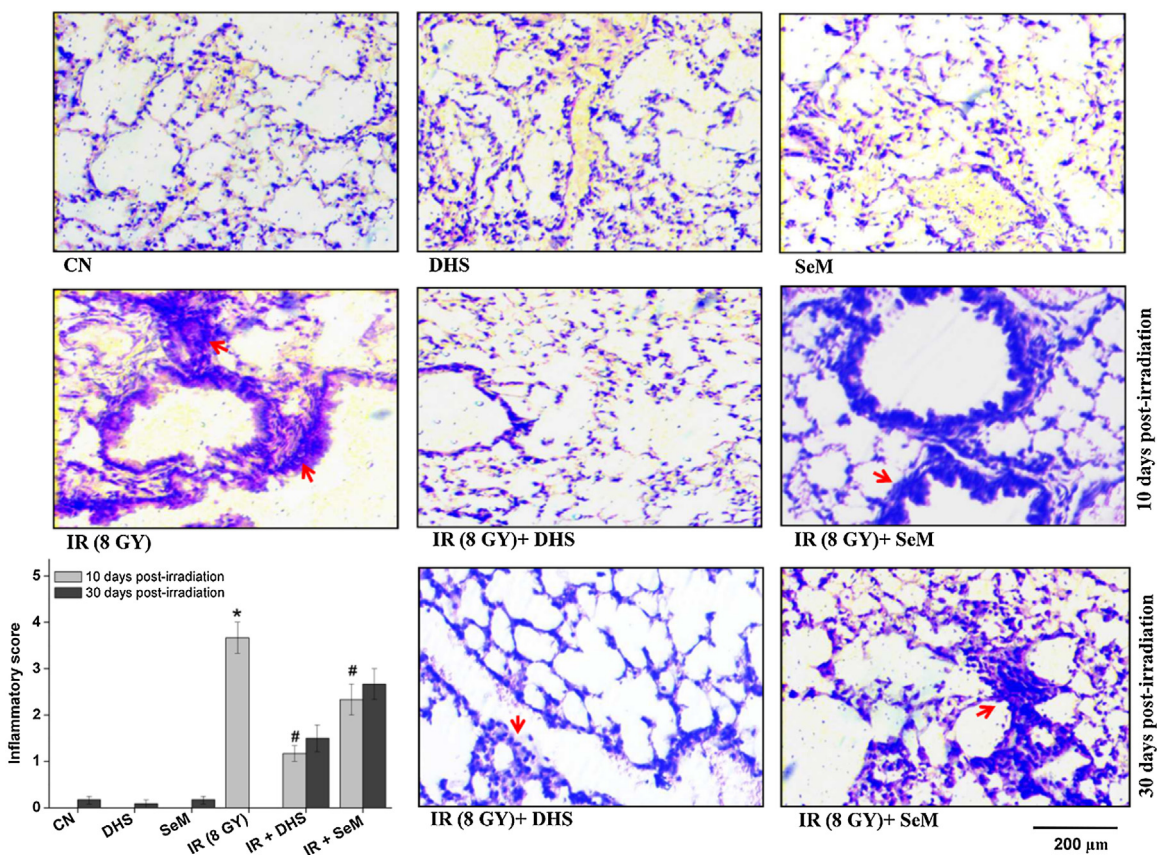


**Fig. 7.** Effect of DHS (2 mg/kg) and SeM (2 mg/kg) supplementation (ip) on the radiation (8 Gy) induced lung inflammatory responses. Images of representative tissue section of right lung excised from the mice of the various groups and stained with hematoxylin and eosin are presented. Magnification – 10 $\times$ . The inset of the figure shows the inflammatory scores under different treatment conditions. The results are presented as mean  $\pm$  SEM ( $n = 3-5$ ). \* $p < 0.05$  as compared to the sham control group, # $p < 0.05$  as compared to the radiation control group. CN – Sham control, IR – Irradiation.

**Table 3**

BAL cell differential under different treatment conditions is presented. The results are presented as mean  $\pm$  SEM (3–5 mice). \*  $p < 0.05$  as compared to the sham control group. #  $p < 0.05$  as compared to the radiation control group.  $^{\$}p < 0.05$  as compared to respective drug (DHS or SeM) plus radiation treated group evaluated on 10th day post irradiation.

Treatment groups	Total BAL cellularity (10 <sup>3</sup> /ml)	BAL macrophages (% of total cells)	BAL lymphocytes (% of total cells)	BAL ciliary epithelial (% of total cells)	BAL neutrophils (% of total cells)
Sham control	74.72 $\pm$ 14.44	89.00 $\pm$ 0.60	6.80 $\pm$ 2.0	4.20 $\pm$ 1.40	–
DHS control	63.50 $\pm$ 6.50	85.00 $\pm$ 2.30	9.60 $\pm$ 1.20	5.40 $\pm$ 0.81	–
SeM control	66.35 $\pm$ 20.12	88.36 $\pm$ 1.50	7.46 $\pm$ 1.89	4.18 $\pm$ 01.20	–
Radiation (8 Gy) (~10 days post irradiation)	149 $\pm$ 14.97 <sup>*</sup>	86.99 $\pm$ 3.91	10.20 $\pm$ 3.17	3.20 $\pm$ 1.07	0.38 $\pm$ 0.11
Radiation + DHS (~10 days post-irradiation)	68.75 $\pm$ 21.25 <sup>#</sup>	84.90 $\pm$ 1.7	11.3 $\pm$ 1.70	3.00 $\pm$ 0.20	0.80 $\pm$ 0.20
Radiation + DHS (30 days post irradiation)	167.50 $\pm$ 26.16 <sup>§</sup>	80.37 $\pm$ 3.74	14.98 $\pm$ 2.67	4.40 $\pm$ 2.83	0.20 $\pm$ 0.05
Radiation + SeM (~10 days post-irradiation)	108.75 $\pm$ 13.65	80.9 $\pm$ 3.6	12.33 $\pm$ 2.10	6.27 $\pm$ 1.30	0.50 $\pm$ 0.20
Radiation + SeM (30 days post irradiation)	202.77 $\pm$ 80.53 <sup>§</sup>	77.53 $\pm$ 1.87	15.27 $\pm$ 3.20	7.00 $\pm$ 1.62	0.20 $\pm$ 0.10

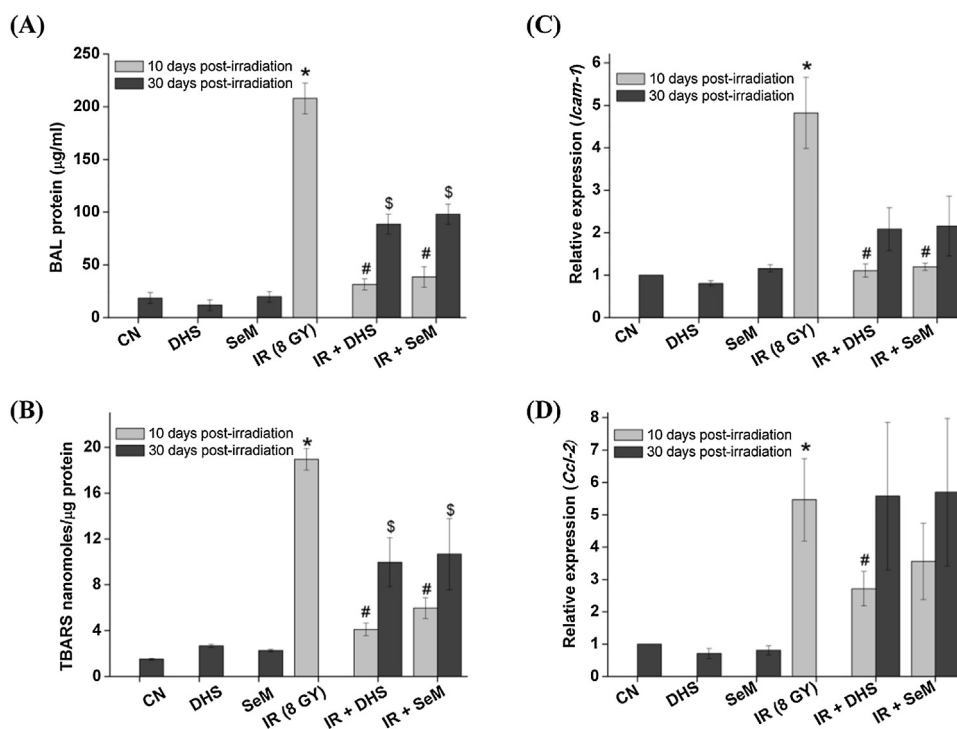


**Fig. 8.** Effect of DHS (2 mg/kg) and SeM (2 mg/kg) supplementation (ip) on the radiation (8 Gy) induced oxidative damage and pro-inflammatory gene expression in the left lung. (A) Level of BAL protein (B) Level of lipid peroxidation (C) and (D) mRNA expressions of *Icam-1* and *Ccl-2* respectively as monitored by RT-PCR. The results are presented as mean  $\pm$  SEM (n = 3–5). The expression of above gene in different treatment groups was normalized against the sham control group and the relative expression changes have been plotted. Actin expression was used as internal control. \*  $p < 0.05$  as compared to the sham control group, #  $p < 0.05$  as compared to the radiation control group,  $^{\$}p < 0.05$  as compared to respective drug (DHS or SeM) plus radiation treated group evaluated on 10th day post irradiation. CN – Sham control, IR – Irradiation.

icant reduction in the levels of TNF $\alpha$  and IL6 as compared to the radiation control. The mice that survived from this group to d 30 showed a marginal increase in the levels of the above cytokines as compared to those evaluated on d 10. The drug and sham control groups showed comparable levels of TNF $\alpha$  and IL6 in serum.

### 3.8. Seleoprotein P (*SelP*) production in the liver

The antioxidant effects of DHS and SeM in response to radiation exposure were evaluated in terms of the mRNA expression of *SelP-1* in the liver. The result shown in Fig. 10A clearly indicates that irradiation led to significant induction of *SelP-1* in the liver on d 10 as compared to the sham control. DHS and SeM control groups also showed significant induction in *SelP-1* level as compared to

the sham control. Treatments with DHS and SeM in irradiated mice showed higher levels of *SelP-1* in liver than the radiation control on d 10 and on d 30; the levels were comparable to those of the respective drug control groups. DHS was better than SeM in inducing *SelP-1*, both under irradiated and unirradiated conditions. Liver was also evaluated histologically to determine hepatotoxicity, if any, associated with DHS or SeM. Fig. 10B, showing representative liver tissue sections, indicates that although there were significant increases in the numbers of binucleate cells following irradiation or drug (DHS and SeM) treatments, neither of these treatments altered hepatic architecture as compared to the sham control at any time points. DHS induced higher numbers of binucleate cells than SeM, under irradiated and unirradiated conditions.

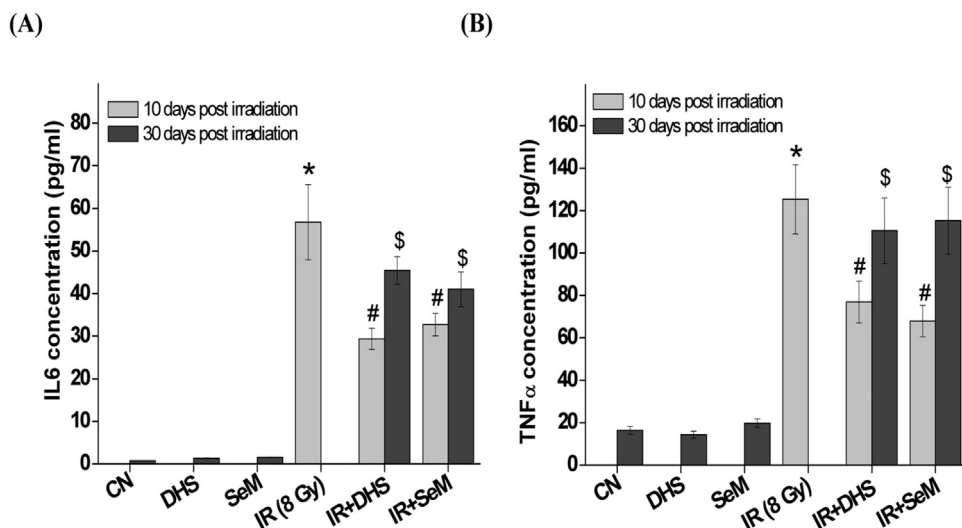


**Fig. 9.** Effect of DHS (2 mg/kg) and SeM (2 mg/kg) supplementation (ip) on the radiation (8 Gy) induced systemic inflammation. (A) & (B) Levels of IL6 and TNF $\alpha$  monitored in the serum using ELISA kit. The results are presented as mean  $\pm$  SEM (n = 3–5). \*p < 0.05 as compared to the sham control group, #p < 0.05 as compared to the radiation control group, \$p < 0.05 as compared to respective drug (DHS or SeM) plus radiation treated group evaluated on 10th day post irradiation. CN – Sham control, IR – Irradiation.

### 3.9. Tissue-specific expression of GPx enzymes

DHS has been reported to affect the expression of another important antioxidant selenoprotein, GPx. Thus, total activities and mRNA expressions of different enzymes, GPx1, GPx2, and GPx4, were monitored in lung, intestine and spleen. The results are presented in Fig. 11. Irradiation led to significant increase in total GPx activity in spleen and lung (Fig. 11A). DHS and SeM showed comparable induction in GPx activity in all three organs under irradiated and un-irradiated conditions (Fig. 11A). With regard to mRNA expressions, irradiation led to induction of all three GPx isoforms in spleen, GPx2 and GPx4 in the intestine, and only GPx1 in the lung on d 10 (Fig. 11B). DHS or SeM control groups also showed induction of all three GPx isoforms. However, they differed in their tissue-specific expressions. For example, the DHS control group showed a significant increase in expression of GPx1 and GPx4 in the spleen and intestine and that of GPx2 only in the intestine (Fig. 11B). On the other hand, SeM control group showed increased expression of GPx1 in the intestine and of GPx2 in spleen and intestine and did not alter the level of GPx4 in any of the three tissues investigated (Fig. 11B). In line with these results, treatments with DHS and SeM in irradiated mice, although distinct in their responses, significantly augmented the radiation-induced expression of GPx enzymes in different tissues on d 10, d 30, or both time points. DHS significantly increased the radiation-induced expression of GPx1 in all three organs and of GPx2 and GPx4 in intestine and spleen, respectively (Fig. 11B). SeM treatment increased radiation-induced expression of GPx1 in intestine, GPx2 in spleen and intestine, and did not affect expression of GPx4 (Fig. 11B). Together, these results confirm the abilities of DHS and SeM to induce expressions of GPx1, GPx2, and GPx4 in radiosensitive organs spleen, intestine and lung leading to an increase in total GPx activity, which might favor protection from radiation-induced oxidative damage and subsequent inflammatory response.

## 4. Discussion

Exposure of animals to a lethal dose of radiation (>6 Gy) induces hematopoietic and gastrointestinal syndromes accompanied with systemic as well as organ-specific inflammatory responses leading to multi-organ failure and death [4–7,39]. Here, a water-soluble selenium compound, DHS, was evaluated as a radioprotector. Our

results indicate that five consecutive days of administration of DHS before radiation exposure in mice significantly prevented radiation-induced DNA damage but did not provide a significant improvement in 30 d survival. Supplementation with DHS at a similar dose continued for three times weekly during the post-irradiation period showed significant improvement in survival. These results suggest that the availability of DHS during the post-irradiation period (when organ toxicity is induced) is important [25]. In subsequent studies, we focused on examining the effect of DHS supplementation (pre and post-irradiation) on organ-specific toxicity and inflammatory responses.

Radiation-induced hematopoietic syndrome in mice is characterized by acute loss of hematopoietic cells in the circulation and spleen [5,40]. Protection from hematopoietic syndrome by an agent depends not only on its ability to protect hematopoietic cells from undergoing radiation-induced cell death or apoptosis but also to renew the hematopoietic system by inducing proliferation of surviving stem cells [40,41]. Treatment with DHS, although did not show any protection from radiation-induced acute hematopoietic toxicity, delayed the proliferation of clonogenic stem cells, as evidenced by the remarkable increase in hematocount in circulation and the expression of Csf-3 in spleens of animals surviving to irradiation until d 30. Like the hematopoietic system, the small intestine is also a highly radiosensitive organ [6,24]; epithelial cells undergo oxidative damages and cell death resulting in disruption of villi and mounting of inflammatory responses. The lung is another radiosensitive organ, shown to be the target of radiation-induced oxidative damages and inflammatory responses [25,39]. Treatment with DHS showed delayed restoration of villi structure and significantly prevented radiation induced acute infiltration of inflammatory cells. The inhibition of inflammatory responses in intestine and lung by DHS was associated with its ability to prevent lipid peroxidation, an initiator of inflammatory responses, and to reduce the expression of genes involved in the recruitment of inflammatory cells to the damaged tissues [42–44]. Treatment with DHS also prevented systemic inflammation [24].

Further, DHS was evaluated for its ability to modulate tissue-specific expression of antioxidant genes [18–20,23,25,30,45–48]. Of seven GPx enzymes known, GPx1, GPx2, and GPx4 have established antioxidant and anti-inflammatory roles [49–52]. GPx1 is the major cytosolic enzyme accounting for GPx activity and catalyses the reduction of hydroperoxides [49]. GPx2 performs the same

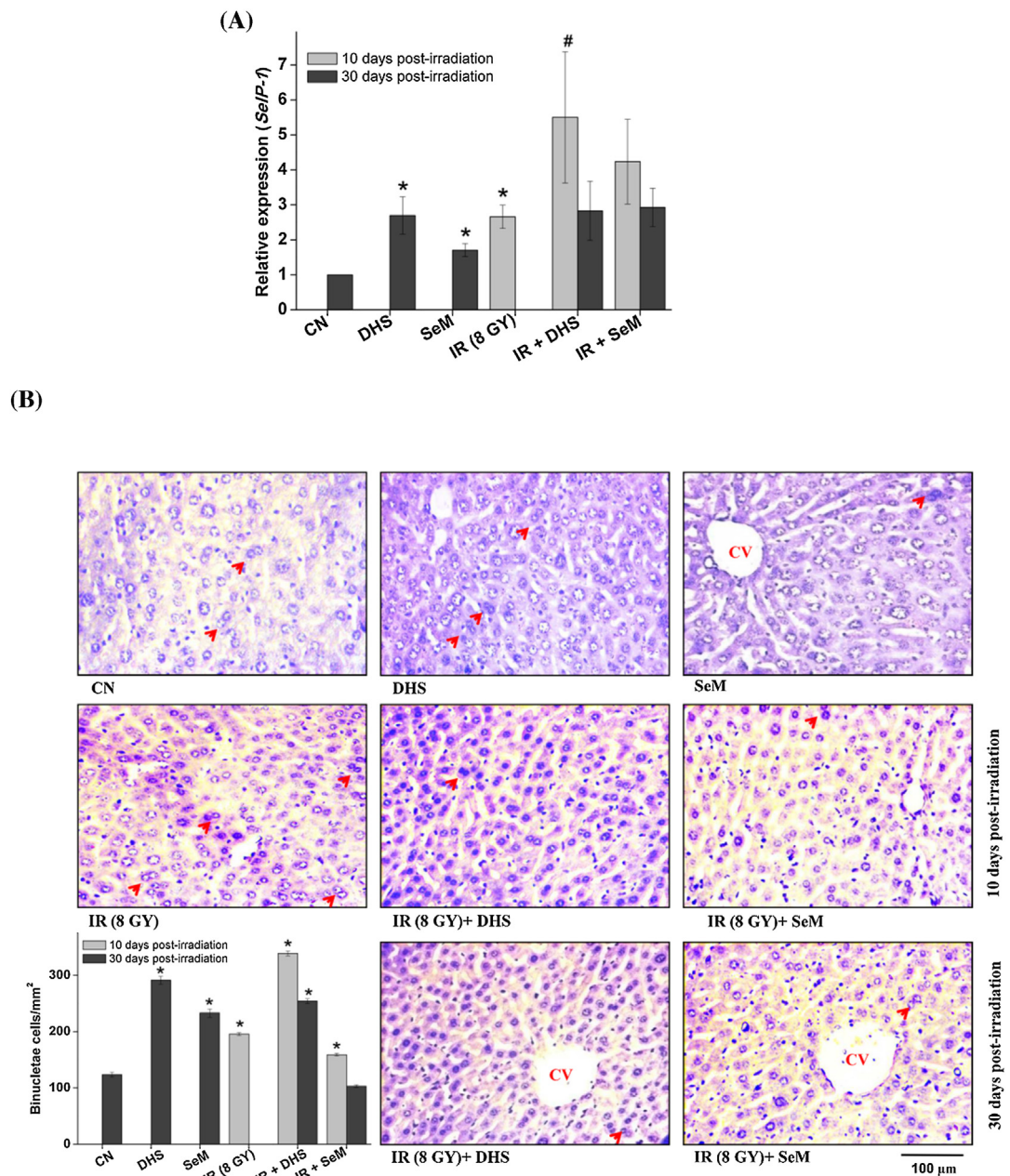


**Fig. 10.** Effect of DHS (2 mg/kg) and SeM (2 mg/kg) supplementation (ip) on the radiation (8 Gy) induced changes in hepatic parameters. (A) mRNA expression level of *SelP-1* in hepatic tissue under different treatment conditions. The results are presented as mean  $\pm$  SEM (n=3–5). The expression of above gene in different treatment groups was normalized against the sham control group and the relative expression changes have been plotted. Actin expression was used as internal control. (B) Images of representative hepatic tissue section from various groups stained with hematoxylin and eosin are presented. Magnification – 20 $\times$ . The inset of the figure shows the counts of binucleate cells under different treatment conditions. CV- Central vein. Arrow indicates binucleate cells. \*p < 0.05 as compared to the sham control group, #p < 0.05 as compared to the radiation control group. CN – Sham control, IR – Irradiation.

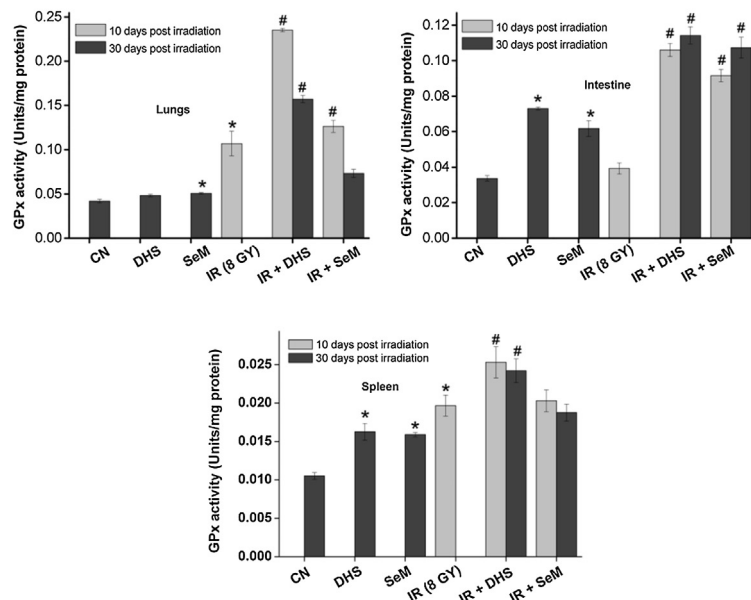
function but is expressed mainly in the gastrointestinal system [49]. GPx4 has substrate specificity towards phospholipid hydroperoxides and plays a role in preventing lipid peroxidation [49]. Thus one of the mechanisms responsible for the ability of DHS to inhibit radiation-induced lipid peroxidation might be the induction of GPx [45,46,50–52,53]. Further, it is also possible that GPx may play a tissue-specific role in protection. Another important antioxidant selenoprotein, SelP, is synthesized mainly in the liver in response to intracellular selenium status and is secreted in the plasma [47,48]. The ability of DHS to reduce the systemic inflammation could be attributed to the increase in the expression of *SelP-1*. Increase in intracellular GPx level does not contribute much to the protection of lymphocytes against radiation-induced apoptosis [54,55] and

this could be the reason for the observed effect of DHS on spleen parameters.

Histological and biochemical analysis revealed an increase in inflammatory responses in the intestine, lung and circulation of DHS and radiation treated group by d 30. The delayed increase in spleen cellularity and hematocounts in circulation of these mice could also occur because of the inflammatory responses. These results thus suggest that the survival advantage offered by DHS was mainly due to suppression of radiation-induced inflammatory responses at early time point (d 10) in the radiosensitive organs. The mechanisms of action of DHS are summarized in Scheme 2.

Interestingly, radioprotective effect of DHS is comparable to SeM [18,26,33]. Our results indicate that DHS is as good as SeM,

(A)



(B)

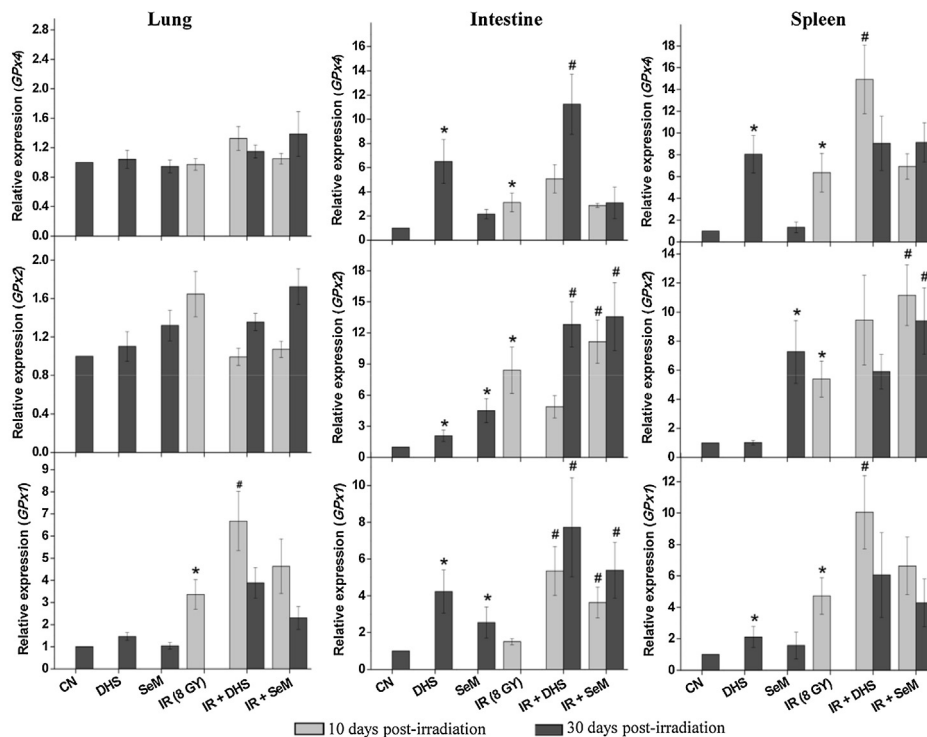
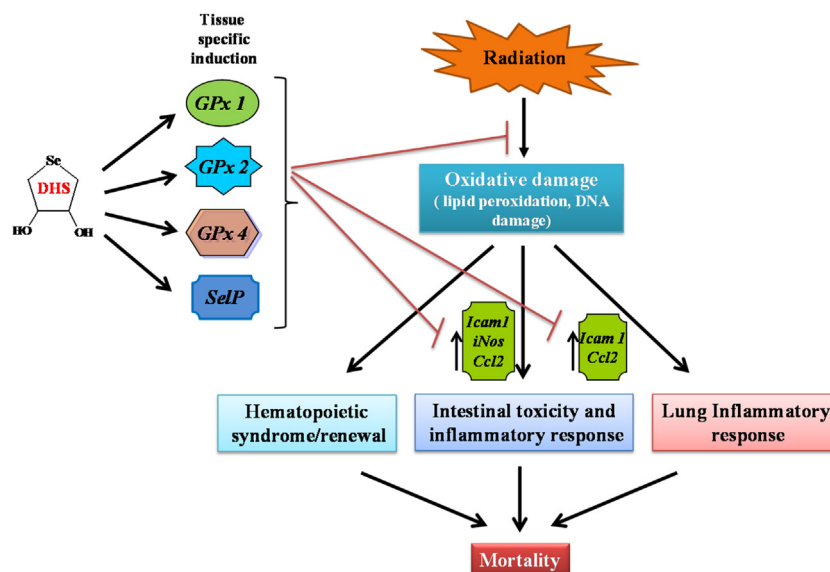


**Fig. 11.** Effect of DHS (2 mg/kg) and SeM (2 mg/kg) supplementation (ip) on the radiation (8 Gy) induced changes in (A) total GPx activity in lung, intestine and spleen (B) mRNA expression of *GPx1*, *GPx2* and *GPx4* in lung, intestine and spleen. The results are presented as mean  $\pm$  SEM (n = 3–5). The expression of above genes in different treatment groups was normalized against the sham control group and the relative expression changes have been plotted. Actin expression was used as internal control. \*p < 0.05 as compared to the sham control group, #p < 0.05 as compared to the radiation control group. CN – Sham control, IR – Irradiation.

or marginally better in improving survival. Most of the biochemical and histological parameters were comparable, except that SeM did not alter the expression of *GPx4*. We and others have evaluated many organic and inorganic selenium compounds for *in vivo* radioprotection and the survival advantages reported in those studies are similar to that of DHS [17,18,20,23]. Thus, both DHS

and SeM, showing remarkable protection against the radiation-induced inflammatory response, warrant evaluation as agents for treatments of radiotherapy-associated inflammatory side effects. Designing selenium compounds to induce intracellular GPx may not be the only strategy to find better radioprotectors. It would be interesting to design new selenium compounds which could help



**Scheme 2.** Proposed activities of DHS in mice model against WBI.

in haematopoietic and gastrointestinal renewal by stimulating the proliferation of stem cells [40].

## 5. Conclusions

DHS and SeM showed comparable effects on survival following WBI. The protective effects of both compounds appear to be mediated through induction of GPx, reduction of lipid peroxidation, and inhibition of infiltration of inflammatory cells in radiosensitive organs, leading to suppression of the inflammatory response. Compounds like DHS should be explored for use as selenium supplements.

## Conflict of interest

None.

## Acknowledgment

Prachi Verma acknowledges Homi Bhabha National Institute for financial assistance in the form of a senior research fellowship.

## References

- [1] B.M. Moores, D. Regulla, A review of the scientific basis for radiation protection of the patients, *Radiat. Prot. Dosim.* 147 (2011) 22–29.
- [2] J.F. Weiss, M.G. Simic, Introduction: perspectives in radioprotection, *Pharmacol. Ther.* 39 (1988) 1–2.
- [3] P.A. Riley, Free radicals in biology: oxidative stress and the effects of ionizing radiation, *Int. J. Radiat. Biol.* 65 (1994) 27–33.
- [4] I.V. Mavragani, D.A. Laskaritou, B. Frey, S.M. Candéias, U.S. Gaipf, K. Lumnitzky, A.G. Georgakilas, Key mechanisms involved in ionizing radiation induced systemic effects: a current review, *Toxicol. Res.* 5 (2016) 12–33.
- [5] A.L. Carsten, Acute lethality: the hematopoietic syndrome in different species, In: Response of different species to total body irradiation, (1984), 59–86.
- [6] K.E. Carr, S.P., Hume, R., Ettarh, E.A., Carr, S. McCollough, Radiation-induced changes to epithelial and non-epithelial tissue, In: Radiation and the Gastrointestinal Tract, (1995), 113–128.
- [7] J.W. Denham, M. Hauer-Jensen, The radiotherapeutic injury—a complex wound, *Radiother. Oncol.* 63 (2002) 129–145.
- [8] T.R. Sweeney, Survey of Compounds from the Antiradiation Drug Development Program of the U.S. Army Medical Research and Development Command, U.S. Government Printing Office, Washington, DC, 1979.
- [9] P.E. Brown, Mechanism of action of aminothiol radioprotectors, *Nature* 213 (1967) 363–364.
- [10] C.N. Andreassen, C. Grau, J.C. Lindegaard, Chemical radioprotection: a critical review of amifostine as a cytoprotector in radiotherapy, *Semin. Radiat. Oncol.* 13 (2008) 62–72.
- [11] J. Gul, S. Zhu, X. Li, H. Wu, Y. Li, F. Hua, Effect of amifostine in head and neck cancer patients treated with radiotherapy: a systematic review and meta-analysis based on randomized controlled trials, *PLoS One* 9 (2014) e95968.
- [12] L.A. Wessjohann, A. Schneider, M. Abbas, W. Brandt, Selenium in chemistry and biochemistry in comparison to sulfur, *Biol. Chem.* 388 (2007) 997–1006.
- [13] I. Rosenfield, O.A. Beath, Selenium: Genotoxicity, Biochemistry, Toxicity and Nutrition, Academic Press, New York, 1964.
- [14] P. Brenneisen, H. Steinbrenner, H. Sies, Selenium oxidative stress, and health aspects, *Mol. Aspects Med.* 26 (2005) 256–267.
- [15] M.P. Rayman, The importance of selenium to human health, *Lancet* 356 (2000) 233–241.
- [16] L.V. Papp, J. Lu, A. Holmgren, K.K. Khanna, From selenium to selenoproteins: synthesis, identity, and their role in human health, *Antioxid. Redox. Signal.* 9 (2007) 775–806.
- [17] H.D. Hurt, E.E. Cary, W.H. Allaway, W.J. Visek, Effect of dietary selenium on the survival of rats exposed to chronic whole body irradiation, *J. Nutr.* 101 (1971) 363–366.
- [18] J.F. Weiss, V. Srinivasan, K.S. Kumar, M.R. Landauer, M.L. Patchen, Radioprotection by selenium compounds, in: Trace Elements and Free Radicals in Oxidative Diseases, AOCS Press, Champaign, 1994, pp. 211–222.
- [19] A.M. Diamond, J.L. Murray, P. Dale, R. Tritz, D.J. Grdina, The effects of selenium on glutathione peroxidase activity and radioprotection in mammalian cells, *Radiat. Oncol. Invest.* 3 (1995) 383–386.
- [20] J.K. Tak, J.W. Park, The use of ebselen for radioprotection in cultured cells and mice, *Free Radic. Biol. Med.* 46 (2009) 1177–1185.
- [21] F. Sieber, S.A. Muira, E.P. Cohen, P.E. North, B.L. Fish, A.A. Irving, M. Mader, J.E. Moulder, High-dose selenium for the mitigation of radiation injury: a pilot study in a rat model, *Radiat. Res.* 171 (2009) 368–373.
- [22] A. Kunwar, S. Jayakumar, H.N. Bhilwade, P.P. Bag, H. Bhatt, R.C. Chaubey, K.I. Priyadarsini, Protective effects of selenocystine against  $\gamma$ -radiation-induced genotoxicity in Swiss albino mice, *Radiat. Environ. Biophys.* 50 (2011) 271–280.
- [23] A. Kunwar, P. Bansal, S.J. Kumar, P.P. Bag, P. Paul, N. Reddy, L.B. Kumbhare, V.K. Jain, R.C. Chaubey, M.K. Unnikrishnan, K.I. Priyadarsini, In vivo radioprotection studies of 3,3'-diselenodipropionic acid, a selenocystine derivative, *Free Radic. Biol. Med.* 48 (2010) 399–410.
- [24] A. Kunwar, P.P. Bag, S. Chattopadhyay, V.K. Jain, K.I. Priyadarsini, Anti-apoptotic anti-inflammatory, and immunomodulatory activities of 3,3'-diselenodipropionic acid in mice exposed to whole body  $\gamma$ -radiation, *Arch. Toxicol.* 85 (2011) 1395–1405.
- [25] A. Kunwar, V.K. Jain, K.I. Priyadarsini, C.K. Haston, A selenocystine derivative therapy affects radiation-induced pneumonitis in the mouse, *Am. J. Respir. Cell Mol. Biol.* 49 (2013) 654–661.
- [26] R.K. Chaurasia, S. Balakrishna, A. Kunwar, U. Yadav, N. Bhata, K. Anjariaa, R. Nairy, B.K. Sapra, V.K. Jain, K.I. Priyadarsini, Cytogenotoxicity assessment of potential radioprotector, 3-diselenodipropionic acid (DSePA) in Chinese Hamster Ovary (CHO) cells and human peripheral blood lymphocytes, *Mutat. Res.* 774 (2014) 8–16.
- [27] M. Iwaoka, T. Takahashi, S. Tomoda, Synthesis and structural characterization of water-soluble selenium reagents for the redox control of protein disulfide bonds, *Heteroat. Chem.* 12 (2001) 293–299.

- [28] F. Kumakura, B. Mishra, K.I. Priyadarsini, M. Iwaoka, A water-soluble cyclic selenide with enhanced glutathione peroxidase-like catalytic activities, *Eur. J. Org. Chem.* 44 (2010) 440–445.
- [29] B.G. Singh, E. Thomas, F. Kumakura, K. Dedachi, M. Iwaoka, K.I. Priyadarsini, One-electron redox processes in a cyclic selenide and a selenoxide: a pulse radiolysis study, *J. Phys. Chem. A* 114 (2010) 8271–8277.
- [30] P. Verma, A. Kunwar, K. Arai, M. Iwaoka, K.I. Priyadarsini, Alkyl chain modulated cytotoxicity and antioxidant activity of bioinspired amphiphilic selenolanes, *Toxicol. Res.* 5 (2016) 434–445.
- [31] S. Chakraborty, S.K. Yadav, M. Subramanian, K.I. Priyadarsini, M. Iwaoka, S. Chattopadhyay, (DL-trans-3,4-dihydroxy-1-selenolane (DHS(red) accelerates healing of indomethacin-induced stomach ulceration in mice, *Free Radic. Res.* 46 (2012) 1378–1386.
- [32] S. Chakraborty, S.K. Yadav, M. Subramanian, M. Iwaoka, S. Chattopadhyay, DL-trans-3,4-Dihydroxy-1-selenolane (DHSred) heals indomethacin-mediated gastric ulcer in mice by modulating arginine metabolism, *Biochim. Biophys. Acta* 1840 (2014) 3385–3392.
- [33] E.N. Bermingham, J.E. Hesketh, B.R. Sinclair, J.P. Koolgaard, N.C. Roy, Selenium-enriched foods are more effective at increasing glutathione peroxidase (GPx) activity compared with selenomethionine: a meta-analysis, *Nutrients* 6 (2014) 4002–4031.
- [34] P.U. Devi, P.G.S. Prasanna, Comparative radioprotection of mouse hemopoietic study by some thiols and a polysaccharide, *Proc. Natl. Acad. Sci. Lett.* 65B (1995) 89–92.
- [35] J. Sharplin, A.J. Franko, Quantitative histological study of strain-dependent differences in the effects of irradiation on mouse lung during the early phase, *Radiat. Res.* 119 (1989) 1–14.
- [36] H. Ohkawa, N. Ohishi, K. Yagi, Assay for lipid peroxides in animal tissues by thiobarbituric acid reaction, *Anal. Biochem.* 95 (1979) 351–358.
- [37] K.J. Livak, T.D. Schmittgen, Analysis of relative gene expression data using real-time quantitative PCR and the 2(-Delta C(T)) method, *Methods* 25 (2001) 402–408.
- [38] T. Sandhya, K.M. Lathika, B.N. Pandey, H.N. Bhilwade, R.C. Chaubey, K.I. Priyadarsini, K.P. Mishra, Protection against radiation oxidative damage in mice by Triphala, *Mutat. Res.* 609 (2006) 17–25.
- [39] L.B. Marks, X. Yu, Z. Vujaskovic, W.Jr. Small, R. Folz, M.S. Anscher, Radiation-induced lung injury, *Semin. Radiat. Oncol.* 13 (2003) 333–345.
- [40] S. Suryavanshi, D. Sharma, R. Checker, M. Thoh, V. Gota, S.K. Sandur, Amelioration of radiation-induced hematopoietic syndrome by an antioxidant chlorophyllin through increased stem cell activity and modulation of hematopoiesis, *Free Radic. Biol. Med.* 85 (2015) 56–70.
- [41] R.J. Hauke, S.R. Tarantolo, Hematopoietic growth factors, *Lab. Med.* 31 (2000) 613–615.
- [42] S.L. Freeman, W.K. MacNaughton, Ionizing radiation induces iNOS-mediated epithelial dysfunction in the absence of an inflammatory response, *Am. J. Physiol.* 275 (2000) G1353–G1360.
- [43] M. Molla, M. Gironella, R. Miquel, V. Tovar, P. Engel, A. Biete, J.M. Pique, J. Panes, Relative roles of ICAM-1 and VCAM-1 in the pathogenesis of experimental radiation-induced intestinal inflammation, *Int. J. Radiat. Oncol. Biol. Phys.* 57 (2003) 264–273.
- [44] D.E. Hallahan, S. Virudachalam, Intercellular adhesion molecule 1 knockout abrogates radiation induced pulmonary inflammation, *Proc. Natl. Acad. Sci.* 94 (1997) 6432–6437.
- [45] H. Tapiero, D.M. Townsend, K.D. Tew, The antioxidant role of selenium and selenol-compounds, *Biomed. Pharmacother.* 57 (2003) 134–144.
- [46] D. Bhowmick, S. Srivasstava, P. D'silva, G. Mughes, Highly efficient glutathione peroxidase and peroxiredoxin mimetics protect mammalian cells against oxidative damage, *Angew. Chem. Int. Ed.* 54 (2015) 8449–8453.
- [47] F.B. Raymond, E.H. Kristina, Selenoprotein P – expression functions, and roles in mammals, *Biochim. Biophys. Acta* 1790 (2009) 1441–1447.
- [48] Y. Saito, T. Hayashi, A. Tanaka, Y. Watanabe, M. Suzuki, E. Saito, Selenoprotein P in human plasma as an extracellular phospholipid hydroperoxide glutathione peroxidase: isolation and enzymatic characterization of human selenoprotein P, *J. Biol. Chem.* 274 (1999) 2866–2871.
- [49] R.B. Flohe, M. Maiorino, Glutathione peroxidases, *Biochim. Biophys. Acta* 1830 (2013) 3289–3303.
- [50] P. Geraghty, A.A. Hardigan, A.M. Wallace, O. Mirochnitchenko, J. Thankachen, L. Arellanos, V. Thompson, J.M. D'Armiento, R.F. Foronjy, The glutathione peroxidase 1-protein tyrosine phosphatase 1B-protein phosphatase 2A axis. A key determinant of airway inflammation and alveolar destruction, *Am. J. Respir. Cell Mol. Biol.* 49 (2013) 721–730.
- [51] A.M. Dittrich, H.A. Meyer, M. Krokowski, D. Quarcoo, B. Ahrens, S.M. Kube, M. Witznath, R.S. Esworthy, F.F. Chu, E. Hamelmann, Glutathione peroxidase-2 protects from allergen-induced airway inflammation in mice, *Eur. Respir. J.* 35 (2010) 1148–1154.
- [52] C. Duong, H. Seow, S. Bozinovski, P.J. Crack, G.P. Anderson, R. Vlahos, Glutathione peroxidase-1 protects against cigarette smoke-induced lung inflammation in mice, *Am. J. Physiol. Lung Cell. Mol. Physiol.* 299 (2010) L425–L433.
- [53] S.A. Mattmiller, B.A. Carlson, L.M. Sordillo, Regulation of inflammation by selenium and selenoproteins: impact on eicosanoid biosynthesis, *J. Nutr. Sci.* 2 (2013) 1–13.
- [54] J. Sun, Y. Chen, M. Li, Z. Ge, Role of antioxidant enzymes on ionizing radiation resistance, *Free Radic. Biol. Med.* 24 (1998) 586–593.
- [55] D.B. Mansur, Y. Kataoka, D.J. Grdinab, A.M. Diamond, Radiosensitivity of mammalian Cell lines engineered to overexpress cytosolic glutathione peroxidase, *Radiat. Res.* 155 (2001) 536–542.